DETERMINATION OF DISEASE PROGRESSION WITH EARLY TOXIN-INDUCED NEUROPATHOLOGY IN THE AGEING MUTANT SOD MOUSE MODEL OF AMYOTROPHIC LATERAL SCLEROSIS

by

Grace Lee Kam

M.Sc., University of Edinburgh, 2004

A THESIS SUBMITTED IN PARTIAL FULFILLMENT OF
THE REQUIREMENTS FOR THE DEGREE OF

Doctor of Philosophy

in

The Faculty of Graduate Studies

(Experimental Medicine)

THE UNIVERSITY OF BRITISH COLUMBIA
(Vancouver)

December 2011

Abstract

Adult onset amyotrophic lateral sclerosis (ALS) poses progressive and irreversible functional deficits to the central nervous system due to loss of motor neurons, caused by some poorly characterized, multifactorial etiology. Research focused on sporadic ALS cases with vastly greater incidence than hereditary ALS describes the potential causes to be of environmental origin. The discovery of endemic ALS in the native Chamorro population of Guam during the 1950s and the co-occurence of Parkinsonism and dementia led to searches for an environmental cause. To determine whether a genetic predisposition to adult-onset ALS could be exacerbated by atoxin that is known to produce a similar phenotype, I combined genetic and environmental models of ALS and tested a known neurotoxin (steryl glucosides) for its potential synergistic properties in combination with the genetic defect. Transgenic SOD1 G37R mice were treated with 42 mg toxin per kilogram of body weight daily in their daily diet. Results showedan additive effect of toxinonspinal motor neuron death, and caused decreases in average soma diameter on surviving motor neurons. The presence of the transgene alone resulted insmaller diameter ventral root axons.Toxin exposure alone resulted in a bimodal configuration of the ventral root size histogram resembling a more immature state of motor axons.The transgene alone markedly increased the amount of GFAP- and Iba1-positive glial cells in the spinal cord grey matter, with a heterogeneous expression of ramified (resting) and activated morphology. The transgene in combination with toxindid not significantly change glial numbers, but caused all glial cells to become extensively activated. Although the mechanism of cycad toxin-induced neurodegeneration remains uncertain, these results showed that dietary exposure to environmental toxin alone was sufficient to produce a disease phenotype, and when implemented in conjunction to a genetic predisposition to ALS was sufficient to produce a more severe disease phenotype. In conclusion, the environmental agent studied here has direct cytotoxic effects, contributes to disease progression in ALS, and indicate an additive effect of dietary neurotoxin in combination with genetic mutations leading to familial ALS.

Preface

All procedures involving animals were approved by UBC Animal Care Committee with regards to breeding (Certificate #A07-0018) and experimentation (Certificate #A07-0026).

Table of Contents

List of Tables

Chapter 3

Appendix C

List of Figures

Chapter 1

Chapter 3

Chapter 4

Abbreviations

AD	Alzheimer's disease
ALS	amyotrophic lateral sclerosis
ALS-PDC	amyotrophic lateral sclerosis Parkinsonism dementia complex
AMPA	amino-3-hydroxy-5-methyl-4-isoxazole propionic acid
APC	antigen presenting cell
BMAA	β-N-methylamino-L-alanine
BOAA	β-N-oxalylamino-L-alanine
BSSG	β-sitosterol β-D-glucoside
CCS	copper chaperone for SOD
ChAT	choline acetyltransferase
CNS	central nervous system
CST	corticospinal tract
Cu	copper
D-AP5	D-2-amino-5-phosphonopentanoic acid
FALS	familial amyotrophic lateral sclerosis
G37R	substitution of glycine to arginine at position 37
G93A	substitution of glycine to alanine at position 93
GFAP	glial fibrillary acidic protein
Iba1	ionized calcium binding adaptor molecule 1
MAM	methylazoxymethanol
MHC	major histocompatibility complex
MN	motor neuron
mSOD1	mutant superoxide dismutase 1
NF	neurofilament
NMDA	N-methyl-D-aspartate
PD	Parkinson's disease
PBS	phosphate buffered saline
ROS	reactive oxygen species
SALS	sporadic amyotrophic lateral sclerosis
SG	stigmasterol β-D-glucoside

SOD1	Cu/Zn superoxide dismutase 1 (intracellular)
TBS	tris buffered saline
TUNEL	terminal deoxynucleotidyl transferase (TdT)-mediated urine triphosphate-biotin nick end labelling
WT	wild type
Zinc	Zn

Acknowledgements

I offer my sincerest gratitude to the people who have contributed their helpful expertise in this work, provided moral support, and showed patience to me during strenuous times. Indeed, the efforts – intentional or unbeknownst – of so many people who have been involved in my graduate student life have transformed my graduate experience to a more endurable and less arduous endeavour. My heart is thankful to infinite proportions.

I would like to begin my thanking Dr. Christopher Shaw for allowing me to have a piece of this pie and for trusting me and believing in me. His optimism has been encouraging and his tireless enthusiasm for community issues opened my eyes to the big picture. Thanks too to my colleagues of the Shaw lab, some with whom (Pierre Zwiegers) I have been working with since the beginning. Pierre, I feel sentimental about the memories we have together going through the changes in our lab's technology and personnel. I feel fortunate to have had the opportunity to work with such a fabulous and friendly group of people.

I would be remiss if I failed to acknowledge the members of my committee who had an invaluable part of my scientific development: Drs. Andrew Eisen, Ian MacKenzie, and Chun Seow. Their professional expertise and enthusiasm about research have helped me develop my skills as a young researcher. I am grateful to have had the opportunity be mentored by such a brilliant committee.

Special thanks to the staff of Jack Bell Research Institute who accommodated my requests and made my time there go smoothly. Thanks also to the lab of Dr. Neil Cashman generously providing of all the breeding animals necessary to complete my research and for sharing the use of important equipment and research space. Thank you to the members of the Scottish Rite Charitable Association who have awarded me with a Graduate Student Award to fund my work. This work has also received financial support from the National Institutes of Health, ALS Association, and Pacific Alzheimer Research Foundation.

The greatest and most important support I have received came from outside the academic realm: my friends, family, and my husband. My friends have been brilliantly encouraging and I completely forgive them for the annoyance of repeatedly asking me when I will graduate. My family includes my parents-in-law and sister-in-law who have always been fully behind my efforts and show

their tireless love in the most creative ways. I am grateful how Mum and Dad have shown genuine interest in my life and my work and Janice has taught me so much about being more carefree. I thank my greatest support, my husband Arthur Kam, who has done so much in great proportions to facilitate my progress. Arthur has been so patient, understanding, unwaveringly encouraging, and humorously entertaining. I feel honoured to have had the wonderful experience of getting engaged, buying a place, planning a wedding, getting married and seeing more of the world all in 2009 and then completing my PhD. Arthur has been a powerful influence in my graduate student life, but most importantly in my personal life. This thesis is dedicated to him.

Dedication

To my husband, Arthur

Chapter 1. General Introduction

1.1 Amyotrophic Lateral Sclerosis

Jean-Martin Charcot (born 1825) was the first to identify amyotrophic lateral sclerosis (ALS) at La Salpêtrière Hospital in Paris while describing patients amongst a heterogeneous group of individuals with spinal muscular atrophies. His clinical and pathological studies set the foundation for distinguishing between upper and lower motor neurons and the role of the corticospinal tract between them. He was the first to describe ALS anatomically, involving the loss of anterior horn cells correlated to muscle atrophy and weakness, and lateral sclerosis (hardening) of the spinal cord corresponding to contractures of the joints and spasticity (Goetz, 2005). His observation of sclerosis in the lateral columns of the spinal cord that correspond to the pyramidal tracts were important in our current understanding of functional loss due to pathology of the motor and descending efferent pathways involved in voluntary movement. A description of two separate but related cases between 1865 and 1869 led to his hypothesis of the division of the spinal cord between the lateral columns and anterior horn, each causing a different clinical presentation (Goetz, 2000). In an era before diagnostic medical equipment, Charcot presented a method of precise anatomical diagnosis by studying direct relationships between clinical and anatomically pathological states (Goetz, 2002).

The early studies of Charcot marked the beginning of developing an understanding of motor neuron disease. Charcot conceived the term "amyotrophic lateral sclerosis" in 1874 following his first diagnosis in a patient exhibiting signs of both weakness and atrophy (lower motor neuron signs) coupled with spasticity and contracture (upper motor neuron signs) (Goetz, 2000). The term contained appropriate anatomical references, with amyotrophy referring to spinal gray matter involvement and hence muscle weakness, and lateral sclerosis referring to the hardening of the lateral white matter funiculus in spinal cord that corresponds to degeneration of the corticospinal tract.

Classical (Charcot) ALS is currently described as a progressive neurodegenerative disorder that primarily affects upper and lower motor neurons. ALS is still referred to in the literature as Charcot's disease, but Lou Gehrig's disease is the more colloquial name in North America referring to the famous baseball player who died in 1941 with the disease. By any name, it is a progressive paralytic disorder due to the degeneration of the large motor neurons in the brain and spinal cord. In addition, there is associated degeneration of the corticalspinal tracts at the level of the spinal cord in a gradient of increasing severity in the rostral to caudal direction. Sensory involvement seldom

occurs, and the brain stem motor nuclei are involved with the exception of oculomotor neurons. Diagnosis is based on clinical features and neuropathological findings. The disease invariably leads to paralysis and to respiratory failure and death. About 10% of all ALS cases are familial (FALS) and inherited in an autosomal dominant manner while the remainder are sporadic with no known cause, but are suspected to be of environmental origin. The average age of onset differs between familial and sporadic ALS, and variable ages of onset have also been found within countries and between countries (Chio et al., 2009; Gil et al., 2008; Goldacre et al., 2010; Testa et al., 2004). The overall trend is that ALS is rare before age 40 and increases with age with men being at greater risk than women (1.3 men to 1 woman) between 50 to 60 years of age. An earlier age at onset and shorter survival are generally associated with SOD1-related familial ALS (Cudkowicz et al., 1997). The overall trend for mean age at onset for sporadic ALS is about a decade later than familial ALS and appears to have a wider range, between 40 and 60 years of age (Fang et al., 2009).

The causes of ALS unrelated to familial inheritance have been the subject of much debate. These sporadic cases make up the majority of ALS cases for which no effective treatments have been found. Numerous studies proposed several risk factors, including increased physical activity (Harwood et al., 2009; Valenti et al., 2005), deficiencies in nutrition (Okamoto et al., 2007), trauma (Armon, 2007), exposure to agricultural chemicals (Furby et al., 2010), and viral infections including HIV and herpes (Cermelli et al., 2003; Zuniga Ramirez et al., 2006). Some studies have suggested that certain environmental determinants during early childhood including adequate domestic amenities, over-crowdedness, and frequent relocation were potential risk factors for ALS (Martyn et al., 1992). Other studies have identified an increased risk of ALS in persons who served in the military, including the 1991Gulf War (Kasarskis et al., 2009; Weisskopf et al., 2004; Weisskopf et al., 2005; Weisskopf et al., 2005), although an increased risk of ALS in veterans was also reported for military service unrelated to the Gulf War (Pastula et al., 2009). Other less well defined risk factors that have been considered and still investigated in case-control studies include smoking (Kamel et al., 1999) and exposure to chemicals such as those in pesticides, paint, and cleaning agents (Fang et al., 2009; Sutedja et al., 2009). The problem with these case-control studies is that they involve patient questionnaires that are susceptible to recall bias and discrepancies between similar studies of ALS risk factors. A positive family history and increasing age have been identified as consistent risk factors in numerous studies.

Interest in finding proven environmental causes for sporadic ALS prevails since purely genetic causal factors for ALS account for only a small fraction of all disease cases. As the causes for sporadic ALS have not been identified, focus has been concentrated on the mechanisms of motor neuron diseases of genetic origin with the hope that findings can be applied to sporadic cases. While studies that focus on environmental causative agents are relatively few, studies that seek to find the link between environmental causation and genetic susceptibility are even scarcer(Shaw et al., 2008).

1.2 ALS and the anatomy of the motor system

The human motor system is a complex and highly specialized 2-tiered organization consisting of upper motor neuron and lower motor neuron levels in a 3-dimensional anatomy. Voluntary movement is a complex multifaceted process that involves many areas of the brain, namely control sites located in the cortex such as the primary motor, premotor, and supplementary motor cortices of the frontal and parietal lobe. The neurons of the frontal and parietal lobes work cooperatively through the primary motor cortex via the corticospinal system to influence the activity of neurons in the brainstem and spinal cord. The term upper motor neuron is applied to corticospinal neuron cell bodies in the cortex and their axons. Damage to upper motor neurons results in muscles that are initially weak but eventually become spastic, exhibit increased muscle tone (hypertonia), and show an increase in deep tendon reflexes (hyperreflexia). Muscles that are no longer under the control of upper motor neurons show spasticity. The clinical presentation is an increased resistance to passive movement by an examiner. Lesions to upper motor neurons affect groups of muscles, resulting in the clinical presentation of abnormal reflexes. For example, the Babinski sign is one of the most common pathological reflex indicating upper motor lesions and involves dorsiflexion of the big toe in response to firm stroking of the lateral part of the sole. These upper motor neuron signs are diagnostic criteria for some forms of ALS.

The spinal cord is the final coordinator of voluntary movement and is connected to our brain by highly organized ascending and descending tracts modulated by inter-neuronal feedback circuits. Spinal motor neurons that are specifically vulnerable in ALS are of the somatic type and are located in the anterior horn of the spinal cord. Omission of the term somatic is common in the ALS literature, and references to motor neurons or anterior horn cells discussed previously are directed at somatic motor neurons. The two main populations of spinal motor neurons are (1) the large anterior horn cells (α motor neurons) that innervate extrafusal skeletal muscle cells and are

involved in direct motor control and (2) the smaller γ motor neurons that innervate intrafusal fibres of the muscle spindles, the inner sensory component of muscles that primarily detect changes in muscle length. Alpha motor neurons are stacked into columns in the brainstem motor nuclei and spinal cord anterior horns, and are organized somatotopically rostral to caudal. Both cell populations are collectively referred to as lower motor neurons, and their axons leave the spinal cord via the anterior (ventral) roots and run distally in their final common path to link the nervous system and skeletal muscles.

Upper and lower motor neurons are functionally connected by convergence and divergence through many specialized networks or tracts. The concept of convergence indicates the aspect of the motor system where many upper motor neurons can innervate one lower motor neuron, and divergence is the opposite – one upper motor neuron innervating many lower motor neurons. ALS is a disease that is highly selective for this motor system, although other CNS areas are also affected in some ALS cases (discussed in Chapter 2). Fibrillations, fasciculations (twitches reflecting contraction of single motor units), and muscle weakness followed by paralysis are characteristic signs of damage to lower motor neurons or their axons. Lower motor neuron degeneration accompanied by an observed paucity of anterior horn cells is a hallmark feature of ALS, along with corticospinal tract demyelination. This presents evidence of lower motor neuron deficits, which produce the predictable clinical signs. Muscle spasticity, with associated hypertonia and hyperreflexia observed in ALS is a feature of lower motor neuron damage. Anatomically, it is the result of a loss of descending inhibitory control on the γ motor neurons(EnterzariTaher et al., 1997). This leads to increased activity of γ motor neurons and therefore increased activity of muscle spindle sensory components, resulting in an increased activation of the associated α motor neurons.

The corticospinal tract is the great voluntary motor pathway, and is classified as a descending pathway along with the reticulospinal and vestibulospinal tracts. Most of its fibres originate in the pyramidal neurons located in layer five of the primary motor cortex of the precentral gyrus. A small portion of these pyramidal cells are called Betz cells, named after Vladimir Betz who first described them, which also give rise to corticospinal axons. The giant Betz cells spread as laminar sheets in layer five of the primary motor cortex (also called Brodmann area 4), and are organized somatotopically laterally to medially. The corticospinal fibres descend through the corona radiata and converge to pass through the internal capsule where the fibres are somatotopically organized

such that the axons that terminate in the high cord levels are located most rostrally (Figure 1-2). It continues through the mid portion of the midbrain crus cerebri where fibres from the upper limb areas of the motor cortex are located medially and those from lower limbs are located laterally.

From the midbrain, fibres continue though the basilar pons and aggregate on the anterior surface of the brainstem upon reaching the medulla oblongata. Here the aggregationforms the pyramid where fibres that terminate in cervical levels are located medially and those projecting to lower cord levels are more lateral. Collaterals of these axons that descend through the brainstem (called corticonuclear or corticobulbar fibres) innervate various motor cranial nerve nuclei, namely those that serve muscles of the face. At the spinomedullary junction, about 85% to 90% of the corticospinal fibres cross the midline in the motor pyramidal decussation, still maintaining a somatotopic organization. These crossing fibres descend in the lateral funiculus on the contralateral side of the spinal cord to form the lateral corticospinal tract. The minority of fibres that do not cross form the anterior corticospinal tract and continue down the ipsilateral anterior funiculus of the spinal cord. Bilateral weakness observed in ALS is indicative of corticospinal tract involvement.

In the anterior horn of the spinal cord, lateral corticospinal tract axons synapse upon the dendrites of α and γ motor neurons of various spinal cord levels. At their level of termination, corticospinal fibres synapse on different populations of neurons: (1) excitatory and inhibitory interneurons (Renshaw cells) that influence flexor and extensor motor neurons, respectively, and (2) alpha motor neurons that innervate distal flexor muscles. For simplicity, Figure 1-2 shows only synapses onto alpha motor neurons. Clonus is a repetitive and sequential contraction of muscle flexors and extensors as observed in some cases of ALS. This clinical symptom is caused by upper motor neuron lesions resulting in cortical fibre loss and subsequent loss of Renshaw cell inhibition of antagonistic muscle extensors.

The axon of an alpha motor neuron reaches a muscle to form specialized synapses called neuromuscular junctions or motor end plates. A motor unit comprises a motor neuron in the spinal cord or brainstem together with the group of muscle fibres it innervates. The neurotransmitter for alpha motor neurons is acetylcholine, which is synthesized in the neuronal cell body in a reaction catalyzed by the choline acetyltransferase (ChAT) enzyme. Following a depolarizing action potential, voltage-dependent sodium channels along the axon cause an influx of calcium into the cell causing acetylcholine release into the synaptic cleft via synaptic vesicles. Acetylcholine binds to

specific receptors on the postsynaptic membrane and opens ion channels causing a depolarizing end plate potential that spreads over the surface of the muscle fibre. This potential triggers the release of calcium ions from the muscle, which elicits the movement of actin and myosin filaments resulting in muscle movement.

Figure 1-1. Ascending and descending pathways

The pyramidal tract (anterior and lateral corticospinal tract) and posterior column pathway involved in ALS. *Note:* Motor components are not drawn to scale and collateral innervations are not included.

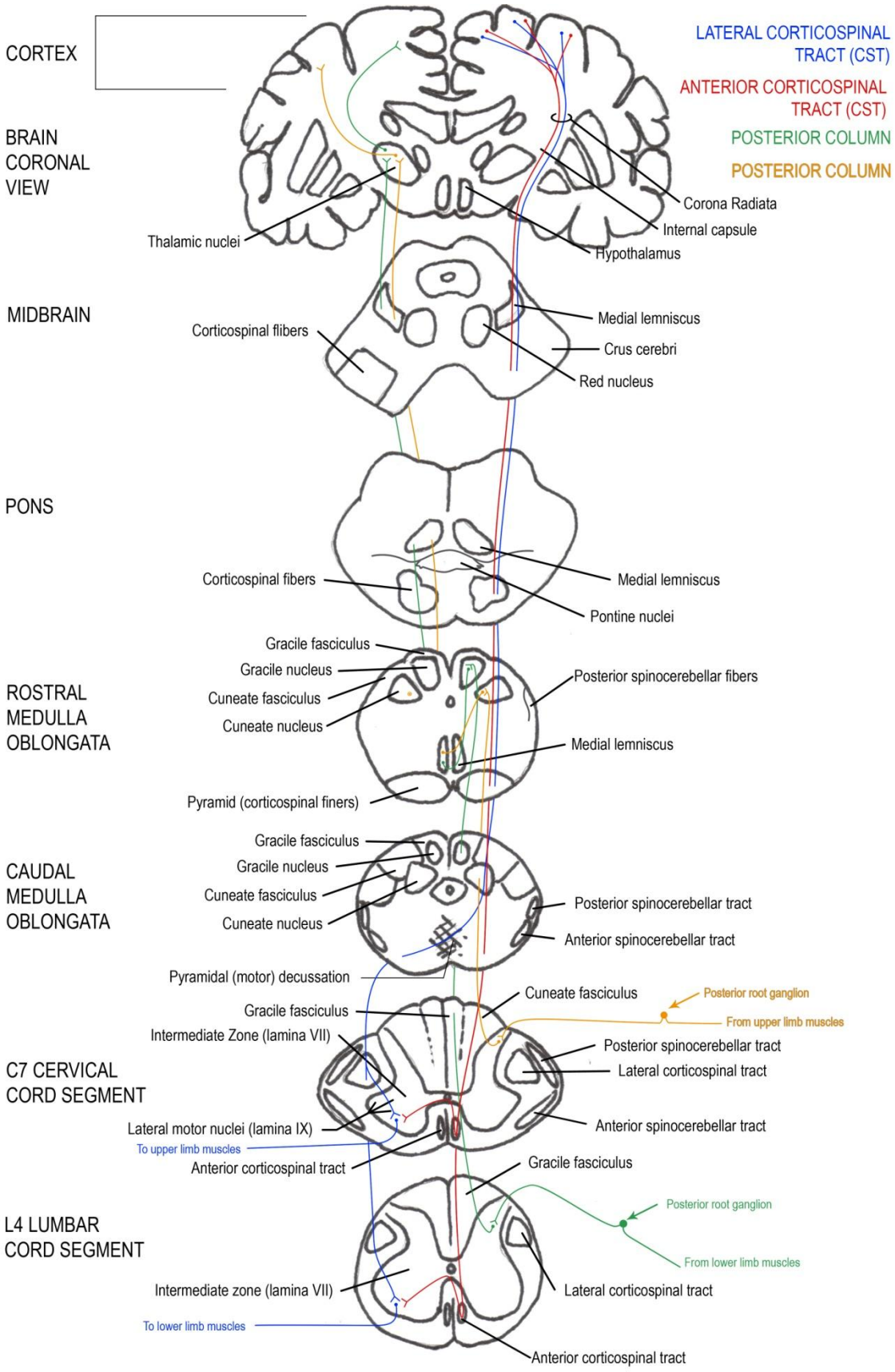
CORTEX
BRAIN
CORONAL
VIEW
LATERAL CORTICOSPINAL
TRACT (CST)
ANTERIOR CORTICOSPINAL
TRACT (CST)
POSTERIOR COLUMN
POSTERIOR COLUMN
Corona Radiata
Internal capsule
Hypothalamus
Thalamic nuclei
MIDBRAIN
Medial lemniscus
Crus cerebri
Red nucleus
Corticospinal flibers
PONS
Medial lemniscus
Pontine nuclei
Corticospinal fibers
Gracile fasciculus
Gracile nucleus
Cuneate fasciculus
Cuneate nucleus
Posterior spinocerebellar fibers
Medial lemniscus
ROSTRAL
MEDULLA
OBLONGATA
Pyramid (corticospinal finers)
Gracile fasciculus
Gracile nucleus
Cuneate fasciculus
Cuneate nucleus
Posterior spinocerebellar tract
Anterior spinocerebellar tract
CAUDAL
MEDULLA
OBLONGATA
Pyramidal (motor) decussation
Cuneate fasciculus
Posterior root ganglion
Gracile fasciculus
From upper limb muscles
Intermediate Zone (lamina VII)
Posterior spinocerebellar tract
Lateral corticospinal tract
C7 CERVICAL
CORD SEGMENT
Lateral motor nuclei (lamina IX)
Anterior spinocerebellar tract
To upper limb muscles
Anterior corticospinal tract
Gracile fasciculus
Posterior root ganglion
From lower limb muscles
L4 LUMBAR
CORD SEGMENT
Intermediate zone (lamina VII)
Lateral corticospinal tract
To lower limb muscles
Anterior corticospinal tract

1.3 Signs and symptoms of ALS

The most common and characteristic presenting feature of ALS are symptoms related to progressive muscle weakness without signs of sensory loss. Muscle cramping and wasting are also among the signs and symptoms noticed by patients. Typically the muscles that control eye movement, bowel and bladder function are preserved. These include preservation of the oculomotor nucleus in the midbrain and Onuf's nucleus in the sacral spinal cord, respectively.However, a recent study observed neuron loss in Onuf's nucleus in some patients showing prolonged disease duration with artificial respiratory support and patients with hereditary ALS with a Gly72Ser mutation in the copper/zinc (Cu/Zn) superoxide dismutase gene (Kobayashi et al., 2011). Cognitive abnormalities under the category of dementia are rare at disease onset. Exceptions include patients diagnosed with the ALS-dementia syndrome. Multisystem involvement is more evident later during the course of the disease. Generally, these include upper motor neuron dysfunction, which exhibits as spasticity and brisk tendon reflexes including the Babinski sign in adults (infants will show an extensor Babinski response in the absence of neurological disease). Loss of lower motor neurons is the hallmark of ALS and inevitably results in progressive muscle weakness, muscle atrophy, and loss of tendon reflexes. The symptoms for limb onset ALS start in the arms or legs, usually with the loss of distal limb function.

For patients with bulbar onset ALS, the first symptom is usually dysarthria followed by dysphagia. Onsets symptoms are bulbar in about 20% of ALS patients (Testa et al., 2004). Disease progression is faster in ALS patients with bulbar onset and a shorter time period between onset of symptoms and diagnosis (Qureshi et al., 2006). Bulbar onset is associated with advanced age and female sex, with the highest risk in individuals greater than 75 years of age (Testa et al., 2004). Bulbar onset patients(Zoccolella et al., 2006; Shoesmith et al., 2007)frequently present with pseudobulbar symptoms such as lower facial weakness, slurred speech, brisk jaw reflexes, and emotional lability(Zoccolella et al., 2006; Shoesmith et al., 2007). Limb weakness originating from either the arms or legs develops either with dysarthria or after several months or years. Wasting of tongue and neck muscles occurs later in bulbar onset ALS.

With disease progression, a majority of ALS cases will develop both upper and lower motor neuron signs that affect bulbar and limb muscles, respectively. Bulbar signs involve pathology of muscles supplied by the motor nerves of the brain stem and are observed as difficulty in swallowing, breathing, speech, and other functions of the pharynx. Percent survival from ALS onset decreases

exponentially with disease progression: 93% after one year, 48% after three years, and 24% after five years (Testa et al., 2004). The prognosis of classic ALS is fatal, with respiratory muscle involvement causing death between 3 and 5 years after onset of symptoms. Respirator assistance is documented to prolong survival between 4 and 8 years with continued use (Nishihira et al., 2009). Patients with respirator-assisted survival were reported to show evidence of widespread multisystem degenerative features that were not observed during the natural course of ALS, even while clinical signs are limited to the upper and lower motor neurons (Mizutani et al., 1992; Ono et al., 1997). However, the neuropathological heterogeneity of ALS with respiratory support is controversial. A more recent study described a case of sporadic ALS in a 48 year old man with a short disease course of 12 months, showing prominent multiple system degeneration involving the substantia nigra without respiratory support (Machida et al., 1999).

1.4 Directionality of degeneration in ALS

Charcot offered the term amyotrophic lateral sclerosis on the basis of observing discoloured plaques (sclerosis) in the lateral columns of the spinal cord in a few patients showing upper and lower motor neuron signs (Goetz, 2000). He believed that the sclerosis of the lateral columns resulted in anterior horn cell loss, a hypothesis postulating upper motor neurons as the initial site of disease (anterograde degeneration). The debate between upper motor neuron and lower motor neuron primacy (retrograde degeneration) still continues, as neuropathologic and neurophysiology studies search for correlations between upper and lower motor neurons. If clinical upper and lower motor neuron signs could be detected in the same muscle upon ALS onset, determining the site of initial degeneration would be straightforward. However, the reality is that lower motor neuron signs often overpower the clinical representation and upper motor neuron involvement may be absent or scarce (Leigh, 2007; Shaw et al., 2007). The reverse situation may also occur in that upper motor neuron signs may be detectable while muscle weakness or atrophy is either absent or delayed (Leigh, 2007; Shaw et al., 2007). This clinical dissociation between upper and lower motor neuron signs have raised the fascinating question whether the upper and lower motor neuron involvement occur independently from one another.

Numerous studies have failed to find a correlation between upper and lower motor neuron dysfunction (Pamphlett et al., 1995; J. Ravits et al., 2007; Attarian et al., 2008; van der Graaff et al., 2009), implicating a third hypothesis that upper and motor neurons degenerate independently from one anotherdue to fundamentally different disease processes and that degeneration of either one

alone is sufficient to lead to progressive deterioration.Clinical studies of patients with ALS showed that lower motor neuron involvement was more severe ipsilateral to the more prominent upper motor neuron signs (Ravits et al., 2007). These studies did not support initiation of ALS in either the upper or lower motor neuron. Kiernan and Hudson observed that cortical and lower motor neurons were significantly smaller in ALS patients, but with no correlation between the numbers of surviving lower motor neurons and the mean sizes of pyramidal (layer 5) cells of the precentral gyri (Kiernan & Hudson, 1991). They concluded in their study that functionally related upper and lower motor neurons likely degenerate independently rather than from a trans-synaptic effect (Kiernan & Hudson, 1991).

There is a general acceptance by researchers that clinical weakness in ALS is a direct consequence of spinal motor neuron death. Studies supporting the retrograde "dying back" degeneration demonstrate marked neuropathology in the spinal cord compared to the motor cortex, as measured by increased frequency of intracellular inclusions (Ince et al., 1998), pathological motor neuron morphology, (Schiffer et al., 1994)or astrocytic gliosis (Schiffer et al., 2004) in the spinal cord. Using stereological methods, Gredal and colleagues report no differences in the number of neurons in the neocortex upon comparing ALS patients with controls (Gredal et al., 2000). Studies using diffusion tensor imaging demonstrated increasing measures of diffusion coefficient and fractional anisotropy in a rostral to caudal direction along the corticospinal tract, supporting a dying back mechanism of ALS (Karlsborg et al., 2004; Nair et al., 2010). Furthermore, a recent study suggested that mitochondrial dysfunction due to aberrant axonal transport along microtubules supports the dying back axonopathy model of ALS (Shi et al., 2010). These studies employed a limited view on upper motor neuron pathology and assigned a retrograde degenerative mechanism after observation of a more severe phenotype in the spinal cord with only minimal changes in the motor cortex. In contrast to considerable research dedicated to spinal motor neurons in mutant SOD1 G93A mice and other models (Chiu et al., 1995), relatively little neuropathological studies are devoted to the motor cortex and its adjacent areas. Using a timeline study to illustrate the spatiotemporal progression of motor neuron pathology in SOD1G93A mice, Fischer and colleagues demonstrated a distal dying back axonopathy as observed by loss of marked neuromuscular junction denervation at day 47, followed by severe loss of motor axons from the ventral root by day 80, and loss of alpha motor neurons after day 80 (Fischer et al., 2004). In this mutant SOD1G93A model, transgenic mice became noticeably impaired by 121± 23 days of age and moribund by 169± 16 days

(Gurney et al., 1994). This study provided the first spatiotemporal study of axonopathy, although it did not include the upper motor neuron.

Hegedus et al. (2007) recorded whole muscle and motor unit isometric contractile forces from both fast and slow twitch muscles in the SOD1G93A mouse to explore the time course of functional motor unit loss and to see whether a differentiation in the loss of fast versus slow twitch muscle occurs. They found a significant decline in both the whole muscle contractile force and the number of functional motor units from fast but not from slow twitch muscle at 40 days of age. There was a biphasic decline in motor unit numbers, where the loss of motor units from fast twitch muscles was initially quick and then reached a plateau in the symptomatic phase of the disease. These findings indicated that there was abnormal sprouting capacity of intact motor units to reinnervate denervated muscle fibres to sustain muscle force. Further recordings from fast twitch muscles of asymptomatic 60-day-old SOD1G93A mice demonstrated preferential loss of the most forceful large motor units, and activity-dependent conversion of motor units to smaller fibres (Hegedus et al., 2008). Their results supported immunohistochemical evidence indicating that denervation commences during the asymptomatic stage and proceeds in a muscle fibre type-specific manner.

Frey et al. (2000) reported that fast-type neuromuscular synapses are selectively vulnerable very early on before the onset of clinical deficits and fail to exhibit terminal sprouting, whereas slow-type synapses retain sprouting ability and are particularly resistant. They reported early and selective loss of fast-type neuromuscular synapses with low sprouting competence in different genetic mouse models of neuromuscular disease, including SOD1G93A mice andprogressive motoneuropathy (pmn) mice. They proposed a dying-back hypothesis where the clinical features of motor neuron diseases are determined by how sensitive peripheral neuromuscular synapses are to neuronal dysfunction. The authors proposed that under conditions of partial dysfunction, differential sprouting in the target region may ensure that essential muscle functions associated with posture and coordination are conserved at the expense of muscle force (Frey et al., 2000). Expanding on these findings, Pun et al. (2006) provided insights into the mechanisms of selective vulnerability in ALS. The authors proposed that selective axonal vulnerabilities might involve selective primary damage to axon subtypes or failure of vulnerable axons to compensate for disease-related burdens. Their results showed that in SOD1G93A mice, fast-type axons in the hind limb were affected synchronously early on before symptom onset, leading to an abrupt loss of their peripheral synapses.

In contrast, slow-type axons were particularly resistant to disease and compensated efficiently by maintaining expanded motor units up to the final phase of disease. Although slow motor neuron axons were resistant, the authors reported a slowly progressing reduction late in the disease, indicating that slow axons were also vulnerable but to a much smaller extent. Their study provided evidence that the onset of the clinical phase coincides with the weakening and loss of fast synapses, and the progressive weakening of slow motor neuron axons determines clinical progression during the end phase of disease (Pun et al., 2006).

There are relatively fewer studies that conclude with a reformulation of Charcot's view of upper motor neuron primacy in ALS. Several observations led to proposing the hypothesis of an anterograde degeneration process. Eisen and colleagues postulated that ALS is a disease of cortico-motor neurons in which the upper motor neuron drives the lower motor neuron to degeneration (Eisen et al., 1992; Eisen et al., 2001). They presented evidence from numerous studies that, when combined, implicated an anterograde excitotoxicity of lower motor neuron degeneration induced by a sufficient number of live but dysfunctional cortico-motor neurons in the primary cortex. Furthermore, they proposed that cortico-motor neurons are hyperexcitable (due to loss of cortical inhibitory interneurons) and drive the lower motor neurons into a metabolic deficit (Eisen et al., 2001). Cortical hyperexcitability is an early feature of disease that persists throughout the disease process (Vucic et al., 2006). Vucic and colleagues showed in pre-symptomatic familial ALS patients that cortical hyperexcitability preceded the development of clinical signs of disease, pointing to a cortical onset for ALS (Vucic et al., 2008). In support of the view that cortical hyperexcitability mediates anterograde degeneration in ALS, Vucic and colleagues reported in ALS patients a uniform reduction in intracortical inhibition combined with a reduction in the resting motor threshold (Vucic et al., 2009). These findings indicate that a loss of inhibitory intracortical circuits work together with excessive excitation of lowered threshold intracortical pathways to mediate cortical hyperexcitability. However, another study of pyramidal tract pathology challenged the dying back hypothesis with an observation of marked axon loss in the brainstem corticospinal tract in conjunction with spinal cord demyelination (Nakano, 2001). The paucity of studies supporting anterograde degeneration in ALS reveals a general bias towards retrograde degeneration, and urges greater devotion to more detailed studies of the motor cortex in ALS.

Chapter 2. Amyotrophic Lateral Sclerosis and the disease spectrum

2.1 Familial ALS

Familial forms of ALS comprise only 10% of patients and are clinically and pathologically similarto sporadic ALS (SALS; discussed later below). Familial ALS (FALS) is inherited following Mendelian ratios, and isassociated with various genetic loci including mutations of the genes encoding Cu/Zn superoxide dismutase (SOD1), alsin (ALS2), senataxin, vesicle associated membrane protein B (VAPB); (Shaw et al., 2007), and the more recently discovered valosin-containing protein (VCP); (Johnson et al., 2010). Autosomal dominant forms of FALS are adult-onset while autosomal recessive FALS are usually juvenile onset with a slower progression and longer survival (Orban et al., 2007). Neuropathologically, two general phenotypes are recognized for FALS. The first shows degeneration limited to the upper and lower motor neuron systems and identified as classical ALS (Leigh, 2007). The second shows multisystem involvement with degeneration of the posterior column, spinocerebellar tracts, and Clarke's column, a group of cell bodies in the intermediate zone of the lumbar to thoracic spinal cord whose axons relay proprioceptive information to the cerebellar cortex via the spinocerebellar tract (Ince et al., 2007).

Upper motor neuron pathology in classical ALS is demonstrated by changes in the motor cortex and the corticospinal tract (CST) as well as the descending pyramidal motor pathway. Ultrastructural studies of the large pyramidal Betz cells in the fifth layer of the primary motor cortex appropriately determine motor cortex involvement in ALS. The Betz cell is particularly affected in the degenerative process of ALS whereas its neighboring pyramidal cells are generally spared (Hammer et al., 1979). However, Gredal and colleagues reported that the total neuron number of Betz cells remained unchanged in ALS (Gredal et al., 2000). A recent study showed no signs of reduced nuclear volume or perikaryon volume in the motor cortex, raising suspicions of possible metabolic changes (Toft et al., 2005). Another study using a different technique involving immunoreactivity of non-phosphorylated neurofilament protein showed depletion of the Betz population in ALS (Nihei et al., 1993). This finding is in agreement with earlier studies showing a paucity of Betz cells even when no involvement of the pyramidal tract was noted (Brownell et al., 1970). While studies of Betz cell death in ALS were contradictory, Sasaki and colleagues reported a greater ease of staining Betz cells with antibodies against neurofilament protein in ALS brains compared to healthy controls (Sasaki et al., 1994), validating this detection method over other conventional staining methods. Studies using this method of visualizing Betz cells also observed the presence of Bunina bodies, Lewy body-like inclusions, and skein-like inclusions (discussed

laterbelow in SALS) as well as constricted bundles of thick neurofilament in this cell population (Sasaki et al., 1994). Age-related degenerative changes were observed in Betz cells characterized by the detection of dense inclusion bodies in neurologically healthy controls (Sasaki et al., 2001). Betz cell involvement and cortical spinal tract degeneration were shown to be invariably observed between individual ALS patients, supporting the generally accepted description of ALS as a heterogeneous disease (Sasaki et al., 1999a). Still others have observed fragmentation of the Golgi apparatus of Betz cells in a fraction of FALS patients that resembled the fragmentation in spinal cord motor neurons (Fujita et al., 1999).

Characteristics of upper motor neuron pathology include astrocytic gliosis and corticospinal tract (CST) degeneration, as observed by myelin pallor in lateral portions of spinal cord white matter. Astrogliosis occurs invariably in the motor cortex and adjacent subcortical white matter (Sasaki et al., 1994). Astrocyte gliosis also occurs with microglial activation in the motor cortex with significant correlation to the burden of clinical upper motor neuron signs (Turner et al., 2004). Apart from focal astroglial reactions and the more widespread microglial activation, only minor histopathological lesions are present in the motor cortex in a majority of ALS cases (Troost et al., 1992). Senile plaques, Alzheimer's neurofibrillary changes, and granulovacuolar bodies are usually absent in the cortex and other parts of the CNS. Pallor of myelin in the white matter of anterior and lateral corticospinal tract associated with axonal loss is a consistent feature of almost all cases of ALS (Rafalowska et al., 1998) and is usually most severe in the brain stem and cervical cord (Brownell et al., 1970). This is expected since the CST projection to the cervical enlargement is greater because it also contains the axons projecting to the lumbar enlargement.

Lower motor neuron loss and intracytoplasmic pathology is a cardinal feature of classical ALS. Hirano and colleagues first described cytoplasmic hyaline inclusion resembling Lewy bodies in the anterior horn cells of FALS patients (Hirano et al., 1967b), which are currently termed Lewy body-like hyaline inclusions for their resemblance to Lewy bodies. These inclusions are confined to motor neurons, and not observed in brain motor nuclei or glial cells. They appear as eosiniphilic cores with peripheral halos in the perikarya of lower motor neurons (Murayama et al., 1990), and were later identified to be a network of 10nm neurofilament granules (Hirano, 1998). These inclusions are spherical conglomerations of material that do not involve aggregation of phosphorylated neurofilament (tau) or α-synuclein.

ALS is by definition a neurodegenerative disease that selectively affects both upper and lower motor neurons. Hence the pathology described above is consistent with clinical aspects of the classical type of ALS as they are restricted to the motor system. However, with a greater understanding of ALS and the advancement of diagnostic equipment since the era of Charcot, it is currently accepted that ALS can demonstrate clinical signs consistent with the degeneration of extra motor systems. These exceptional cases are defined as ALS with multisystem involvement, and were first identified with an observation of pallor of posterior column accompanied by demyelination in a majority of FALS cases and in 10% of SALS cases (Brownell et al., 1970), althoughmost ALS cases with multisystem pathology were initially found in sporadic ALS. In particular, demyelination is observed in the cuneate fasciculi of the poster columns from the lumbar through to cervical segments in addition to CST degeneration (Tanaka et al., 1984). Cell loss in Clarke's column may be extreme, with surviving neurons filled with hyaline inclusions. However, earlier reports showed that only patients with FALS with a long survival of over 5 years had pathological findings consistent with posterior column and Clarke's column involvement (Tsuchiya et al., 2000).

A growing number of research studies in the literature are dedicated to describing changes in the patterns of intracortical inhibition and the contribution of inhibition loss in ALS. The imbalance between inhibitory and excitatory control may play a critical role in motor neuron degeneration in ALS, since excitatory signalling and/or their dis-inhibition will increase Ca^{2+} influx and lead to depolarization. Evidence of these events supports the excitotoxicity hypothesis, as discussed later in this Chapter. Alterations in inhibitory neurotransmission have been reported in both ALS patients and mutant SOD1 mice (EnterzariTaher et al., 1997; Sasabe et al., 2010; Sunico et al., 2011). Furthermore, a loss of inhibitory control in ALS patients has been supported by studies showing abnormal levels of inhibitory neurotransmitters in serum of ALS patients (Niebroj-Dobosz et al., 1999), impaired intracortical inhibition in ALS patients (Zanette et al., 2002), and reduced expression of inhibitory neurotransmitter receptors in the cortex and spinal cord of ALS patients (Petri et al., 2003; Petri et al., 2006). Other studies on inhibitory neurotransmitter expression in the cortex of ALS patients demonstrated extramotor dysfunction, with involvement of temporal and prefrontal regions (Lloyd et al., 2000; Petri et al., 2006). It was then proposed that loss of inhibition might contribute to the development of cortical hyperexcitability in ALS, since most of the transcranial magnetic stimulation (TMS) studies performed on ALS patients reported a decrease in the effectiveness of the intracortical inhibitory processes (Ziemann et al., 1997; Salerno et al., 1998;

Zanette et al., 2002; Vucic et al., 2006). A magnetic stimulus applied to the motor cortex is known to transiently depress the electromyographic activity in target muscles due to cortical inhibitory mechanisms. In these studies, the magnetic stimulus was applied using paired-pulse methods and revealed a decrease in TMS-induced inhibition in ALS patients. However, while these studies point to the occurrence of a loss of intracortical inhibition as part of the pathogenic process in ALS, Attarian and colleagues described increased inhibitory responses in single motor unit studies of ALS patients throughout the disease course and stronger inhibition during the first year after disease onset (Attarian et al., 2009). Schmied and Attarian noted that the enhanced inhibitory effects of TMS in their studies were designed on patients performing voluntary contractions, while the decrease in inhibition were reported in TMS paired-pulse studies on resting patients (Schmied et al., 2008). The tonic activity of the cortical afferents is likely to differ between subjects at rest and subjects performing voluntary movement. The authors also argued that the first pulse in TMS paired-pulse studies reflects only the fast corticomotoneuronal pathway only, while the single TMS pulses in their studies included fast and slow corticomotoneuronal pathways as well as non-monosynaptic pathways (Schmied et al., 2008). Despite the contradicting evidence possibly brought about by differing methodologies, aberrant inhibitory changes may contribute to the eventual demise of the corticomotoneuron.

Ubiquitinated intracytoplasmic inclusions as described in the SALS cases (discussed later below) are not a part of FALS pathology, with the exception of FALS cases related to SOD1 where ubiquitinated inclusions are detectable. (FALS related to SOD1 is discussed below.) Anterior horn cells of ALS patients with multisystem degeneration show Lewy body-like hyaline inclusions (Hirano et al., 1967b) and Bunina bodies indistinguishable from the neuropathology of sporadic ALS (discussed below). The large neurons of the brain stem reticular formation were observed to show chromatolysis and Lewy body-like inclusions in a subset of extra-motor dysfunction ALS cases (Kato et al., 1992). A most surprising finding in an ALS patient was that the spinocerebellar tract was severely demyelinated while the CST was intact (Li et al., 1988), illustrating the heterogeneic nature of ALS disease (Strong et al., 2003).

2.1.1 Causes of ALS

2.1.1.1 Cu/Zn superoxide dismutase

Research in the early 1990s evaluating FALS patients localized the gene causing FALS to chromosome 21 (Siddique et al., 1991). In 1993, a large collaborative effort contributing a milestone to the understanding of ALS was made with the discovery that about 20% of the FALS cases are associated with 60 possible mutations so far of the gene encoding the cytosolic (intracellular) Cu/Zn-binding superoxide dismutase (Rosen et al., 1993). SOD1 mutations in animals were also an extremely interesting model to study selective neuronal vulnerability in ALS because SOD1 is a ubiquitous enzyme that is expressed predominantly in the neurons of the brain and spinal cord (Pardo et al., 1995; Bergeron et al., 1996).

The signs and symptoms of lower motor involvementin SOD1 FALS are essentially similar to non-SOD1 FALS as described above. Upper motor neuron involvement is either mild or absent despite pronounced lower motor neuron degeneration (Hirano, 1998). In addition, variations in involvement of the poster column, spinocerebellar tracts and other extra motor systems are observable among different mutant SOD1 subtypes. Symptoms can commence in the limbs or the bulbar region just as in non-SOD1 cases, although there is a propensity for limb onset in SOD1 FALS. The individual mutations in SOD1 do not predict disease severity, and it is very difficult to give a prognosis based on the mutations (Orrell et al., 1999). Neuropathology of SOD1 ALS has some resemblance to non-SOD1 cases. Ubiquitinated cytoplasmic neuronal inclusions and hyaline conglomerate inclusions have been described in only some cases of SOD1 FALS (Ince et al., 1998). However, different SOD1 mutations exhibit varying expressions of cellular pathology and neuropathological characterization of SOD1 FALS is incomplete. Furthermore, evidence of genetic heterogeneity in SOD1 FALS is observed in studies reporting that the genetic background of SOD1 FALS differs between different populations, countries, and regions (van Es et al., 2010). The most distinguishing neuropathological features of SOD1 FALS are the observation of SOD1-positive Lewy-body like hyaline inclusions (Watanabe et al., 2001), SOD1 misfolding and aggregation (discussed below), and the absence of TDP-43 positive inclusions that are typical in non-SOD1 ALS (discussed below).

It is important to note that the family of SOD metalloenzymes in yeast and mammals also includes a manganese-containing mitochondrial matrix enzyme (SOD2) and an extracellular Cu/Zn-

binding enzyme (SOD3), all of which are free radical scavengers that catalyze superoxide radicals (Fridovich, 1995). Of these, intracellular SOD1 is important in the research literature because of its physiological function in superoxide dismutation and therapeutic potential. Mammalian SOD1 is mainly expressed in the cytosol with a lesser extent in the intermembrane space of the mitochondria. SOD1 is highly expressed in liver and kidney and is also abundant in motor neurons (Culotta et al., 2006b). The strongest link between human disease and mutant SOD enzymes is found in the Cu/Zn SOD forms, mutations of which are implicated in causing FALS (Rosen et al., 1993). SOD1 requires Cu and zinc ions as redox active transition metals at the active site to carry out its enzymatic activity, and the loss of these ions results in various disease expressions, such as ALS in the case for SOD1 mutations and disruptions in mitochondria homeostasis in the case for SOD2 mutations (Culotta et al., 2006b). The primary role of SOD1 is to catalyze the conversion of unwanted superoxide radicals, or reactive oxygen species (ROS), to $H_2O_2$and molecular oxygen (Yim et al., 1993). These ROS are natural products generated from oxidative metabolism in all aerobic organisms and include the superoxide anion ($O_2\cdot^-$), the hydroxyl radical (OH·), and peroxide anions (O_2^{2-}). In the absence of normal production and detoxification of superoxide radicals, cell injury will occur (Cookson et al., 2002). Damage from ROS induces oxidation of proteins, mutations in DNA, and cell death.

The enzymatic structure of SOD1 was described as a dimer of two identical subunits with a signature β-barrel structure positioning its active site on opposite ends of the dimer (Culotta et al., 2006b). Mutations occur in the backbone, the β-barrel structure, and the dimer interface (Deng et al., 1993). Over 100 mutations have been identified in SOD1 FALS with the majority of mutations being missense mutations that involve one animo acid being substituted for another (Orrell, 2000). The active site of Cu/Zn SOD has a deep location at the centre of each homodimer and surrounded with positively charged residues along the walls to attract its superoxide anion substrate in a copper-dependent manner. The enzymatic activity depends on the cyclic reduction and oxidation of the copper catalytic centre (Gurney, 1997). Furthermore, mutations in SOD1 were implicatedin a fraction of apparent SALS cases (Jones et al., 1993; Naini et al., 2007), and recently three novel SOD1 variants were detected in SALS patients (Luquin et al., 2008). The most common SOD1 mutations found in apparent SALS cases are the D90A (substitution of aspartic acid for alanine at position 90) and I113T (substitution of isoleucine for threonine at position 113) mutations, and can be inherited as a recessive trait slowly progressing ALS, a dominant trait with reduced penetrance, or

de novo mutation in an unaffected carrier (Andersen et al., 2004). Although these reports are exciting for research focused at finding common FALS to SALS disease mechanisms, the relationship between mutant SOD1 and sporadic ALS is unclear and must be taken with caution because a true diagnosis of FALS may be difficult with the low penetrance of mutant SOD. In addition, findings of commonalities between FALS and SALS are controversial since it is still not known whether misfolded SOD1 may be causative for all types of ALS, and other studies demonstrate that aberrant SOD1 misfolding is unique to SOD1-related FALS cases suggesting a separate disease pathway for SALS (Liu et al., 2009).

Shortly following the discovery of SOD1 mutations in FALS, Cleveland and colleagues showed that only some SOD1 mutations caused diminished SOD1 enzyme activity, thereby possibly increasing oxidative damage due to free radicals, while most SOD1 mutants showed minimal loss of enzyme activity (Borchelt et al., 1994). FALS patients heterozygous for SOD1 mutations still have between 50% and 60% normal SOD1 activity in the brain (Deng et al., 1993). SOD1 mutant-mediated disease occurred independently despite elimination or elevation of wild type SOD1 in transgenic mice (Bruijn et al., 1998). These findings led to a generally accepted hypothesis that the deleterious effects of the mutated SOD1 are caused by a "toxic gain of function" of the enzyme (Yim et al., 1996). Furthermore, growing research into SOD1 mutations demonstrated SOD1 misfolding, resulting in an abnormal capacity to react with free radicals or disruptive misfolded protein aggregation (Kang et al., 1996; Cleveland et al., 2000). Most importantly, SOD1 mutant mice were reported to have normal levels of wild type mouse SOD1, further supporting the hypothesis of a toxic gain of function of mutant SOD1 triggering selective motor neuron death (Gurney et al., 1994; Dalcanto et al., 1995). The strongest evidence for a toxic gain of function of mutant SOD1 were the studies showing that expression of human mutant Cu/Zn SOD1 in transgenic mice caused motor neuron disease, while expression of wild type Cu/Zn SOD1 at similar levels does not result in any observable phenotype (Gurney et al., 1994; Wong et al., 1995).

2.1.1.2 Transgenic mouse models

Following theimportant discovery of SOD1, genetic mutations quickly became a valuable (and preferred) model of ALS motor neuron death because of the implications of a common pathway to motor neuron loss between FALS and SALS (Li et al., 1988). With the efficiency of generating SOD1 mutants in experimental animals, the mechanisms underlying motor neuron death in the presence of SOD1 mutations have been studied extensively. Gurney and colleagues generated

the first transgenic model of human motor neuron disease (Gurney et al., 1994). In their studies, Gurney and colleagues produced transgenic mice that express mutant forms of human SOD with a substitution of glycine to alanine at position 93 (G93A). These were the pioneer *in vivo* investigations of SOD1-mediated motor neuron cell death, reported to cause a progressive paralytic disease and death at four to five months of age with little effect on enzyme activity. Disease started with tremors and ended in complete paralysis of one or two limbs. The transgenic mice provided a striking demonstration of selective vulnerability of anterior horn neurons while neurons of the posterior column and dorsal root ganglia were mostly spared (Dalcanto & Gurney, 1994a). The pathophysiology of motor neuron death was further investigated in multiple lines of transgenic mice and demonstrated a progressive motor neuron disease with cytoskeletal pathology similar to FALS (Dalcanto et al., 1995; Tu et al., 1996). It was hoped that a better understanding of pathogenetic mechanisms involved in FALS might provide an understanding of SALS.

Transgenic mouse models have been widely used to study the familial forms of ALS, Parkinson's disease, and Alzheimer's disease. In addition to the SOD1 models of FALS, other models of motor neuron disease have been described. These include the wobbler mice caused by a spontaneous mutation in the wobbler gene, *wr* (Duchen et al., 1968), the motor neuron degeneration (MND) in mice that are homozygous for mutations in motor neuron degeneration gene, *mnd* (Callahan et al., 1991), and the autosomal recessive mouse mutant with progressive motor neuronopathy (Schmalbruch et al., 1991). In regard to ALS, mice carrying human SOD1 mutations are currently the most widely used models.

2.1.1.3 mSOD1G37R (line 29) mouse model

Selective spinal motor cell death is a widely appreciated hallmark feature of human ALS (Ravits et al., 2009). The mechanism(s) governing selective spinal motor neuron vulnerability in the presenceof SOD1 mutations are believed to cause motor neuron disease through an acquisition of an adverse property by the mutant enzyme. This expanded on the hypothesis of free radical damage as a mechanism of motor neuron degeneration in FALS, and fuelled further genetic studies of mutant SOD1 activity and its specific role in mediating neuronal cell death.

The precise activity of mutant SOD1 is not uniform across the various missense mutations identified in FALS. However, most but not all SOD1 mutants do not completely lose their enzymatic activity. FALS mutations show different intrinsic effects on enzymatic activity.

Alterations in the overall enzymatic activity are as a result of mutant SOD1 subunits acting in a dominant manner, since heterodimerization with mutant subunits does not appreciably alter the activity of wild type subunits (Deng et al., 1993). SOD1 mutations showing surprisingly modest losses in enzyme activity can still yield motor neuron death (Borchelt et al., 1994), which calls into question aberrant ROS metabolism as the mechanism of neuronal injury. The research group led by Gurney made the first mSOD1G93A mice available to the research community via Jackon Laboratories (Gurney et al., 1994). Through a natural (and serendipitous) unequal crossover within the transgene locus during meiosis, various lines of transgenic mice were bred that differed in transgene copy number. In all these lines of mice, expression of the mutant human SOD1 is proportional to transgene copy number (Gurney et al., 1994). Lines of mSOD1G93A mice that produce greater amounts of mutant SOD1 in the brain have an earlier age of onset and death than those that produce lesser amounts (Dalcanto et al., 1995). In addition, the mice that were more severely affected were the high expressers of the mutated gene, illustrating a clear difference in the age-dependent penetrance of motor neuron disease. In addition to earlier clinical onset and faster disease pace, these animals also showed Wallerian degeneration of the axons of the white matter in anterior and lateral columns as well as posterior columns of the spinal cord (Dalcanto et al., 1995). This finding of multisystem disorder in transgenic mice was an important contribution to research in the development of more accurate models for studying human motor neuron disease. Thus clinical disease onset and severity in multiple mouse lines correlates with the number of transgene copies rather than the insertion site. These experiments were vital in demonstrating that transgene expression levels correspond to neurotoxicity.

Assays of various missense mutations in human mutant SOD1 measuring enzyme activity were demonstrated to show a continuum of activity, with some missense mutations causing inactivity and the mutation of glycine substitution to arginine at position 37 (mSOD1G37R) retaining full activity (Borchelt et al., 1994). Shortly following this finding, mutant lines of transgenic G37R mutant SOD1 mice were produced through a collaborative effort of researchers at Johns Hopkins and the Ludwig Institute (Wong et al., 1995). These mice were produced to analyze the mechanisms for mutant SOD1 causing disease *in vivo* and the levels of G37R product were between the ranges of 5 – 12 times the endogenous SOD1 in the spinal cord. All mouse lines accumulating G37R mutations developed a severe progressive motor neuron disease resembling the G93A mutation.

The G37R mutation in the SOD1 gene did not affect the enzyme activity of superoxide dismutase. In addition, progressive pathology of line 29 animals was slower than other lines with higher G37R copy numbers. For example, vacuoles were conspicuous in the ventral horn of line 29 mice by 15 weeks of age and marked motor neuron loss was detectable by 20 weeks of age. G37R lines expressing much higher copy numbers showed vacuolation by 11 weeks of age and reduced motor neuron numbers by 15 weeks of age (Wong et al., 1995). Moreover, the dying cells were associated with degenerating axons, thereby demonstrating more severe spinal cord pathology as well as widespread degenerative changes reflecting a gene-dosage relationship. It is unclear what triggers the death of these cells and whether the axonal degeneration is directly responsible for it. Ventral root degeneration and demyelination was observed in the ventral root exit zone (the ventral portion of the spinal cord at which the ventral roots emerge) and motor nerve roots at 35 weeks of age for line 29 mice, and 18 weeks of age for higher expressers (Wong et al., 1995). In summary, in mice expressing mutant G37R SOD1, vacuolar pathology in the motor neurons precedes axonal degeneration, muscle atrophy, and motor neuron death. A study in presymptomatic SOD1 G37R transgenic mice showed early axonal abnormalities including SOD1 accumulation and vacuolation. In addition, the study reported anterograde transport of mutant SOD G37R in motor axons, indicating that mutant SOD1 may act locally to damage motor axons (Borchelt et al., 1998).

As discussed previously, research on the G93A mutation suggested that mutant SOD1 causes cell death by means of a toxic gain of function rather than a loss of function. But what is the mechanism by which mutant SOD1 G37R exerts its toxicity? Mutant SOD1 G37R retains full enzyme activity while the G85R mutation has no enzymatic activity (Borchelt et al., 1994), demonstrating that enzymatic activity is not a determining factor on the ability of the mutant protein to cause FALS. Therefore, it is possible that the presence or absence of enzymatic activity may affect the onset or phenotype of the disease. Wang and colleagues, in a study comparing G85R with G37R knockdown mice, reported that G85R knockdown in microglia induced a prolonged early and late disease phase (Wang et al., 2009) while G37R knockdown in the same cells only prolonged the late phase and to a much greater extent (Boillee et al., 2006). These results point to a possible role of mutant enzyme activity in influencing the deleterious effects of mutant SOD1 expression in microglia. The finding of a prolongation in early disease following G85R and not G37R knockdown is particularly noteworthy since early disease in G37R mice is about four times longer than in G85R mice (Bruijn et al., 1997). Epidemiology studies on families of dominantly inherited ALS also

showed that the presence of the G37R mutation predicted an earlier age at onset and a longer survival (Cudkowicz et al., 1997). Wang and colleagues hypothesized that the dismutase-active G37R has both a neurotoxic and neuroprotective effect in microglia that contrasts with a purely neurotoxic effect of the dismutase-inactive G85R mutant SOD1. In addition, they suggested that the notably decreased lifespan (due to a more severe disease phenotype) in G85R compared to G37R mice does not allow sufficient time for a more prominent effect to be observed from the knockdown (Wang et al., 2009). Therefore, the G85R mutation leads to a more rapidly progressive symptomatic late disease that leads to death earlier than the G37R mutation, thus making the G85R phenotype more difficult to ameliorate. Furthermore, the G37R transgenic mouse is also a low expressor line compared to the more popular G93A mouse carrying mutant SOD1.

When compared alongside different mutant SOD1 mouse models of ALS, transgenic mice with the G37R mutation develop the disease with a longer course, with highest mutant accumulation reaching end-stage disease most rapidly between 8.5 and 11 months of age, accompanied by the death of 55% of spinal motor neurons (Boillee et al., 2006). The particular C57/BL6 SOD1G37R (line 29) mice used in this study have a life span of 10–12 months (Nguyen et al., 2000). This lengthy disease course consists mostly of an extended early disease phase in which mice are pre-symptomatic but possibly exhibiting sub-threshold degenerative CNS changes. Research in G37R mice has shown that pathological changes in the spinal cord were detectable as early as 5 months before disease onset (Farah et al., 2003). Nguyen and colleagues demonstrated how the neurodegenerative process could be modified by chronic early (presymptomatic) exposure to environmental factors in the G37R mouse model (Nguyen et al., 2004). In this *in vivo* study, the authors exposed presymptomatic G37R mice with intraperitoneal administration of lipopolysaccharide, a potent activator of microglia, as early as 3 months of age (Nguyen et al., 2004). G37R mice showed accelerated disease progression, motor axon degeneration, and a shortened life span when treated chronically starting at 6 months of age. These results supported the hypothesis that environmental/immunological challenges may be an etiological factor in sporadic ALS (Nguyen et al., 2004).

When taken together, the lengthy disease course of line 29 G37R mice would allow more time during the presymptomatic stage to observeenvironmental factor modulation on disease onset and progression. The current study addresses the effects of chronic administration of steryl glucoside, a neurotoxin in the seeds of cycad palm, in a genetic model of neurodegeneration. The

toxins in cycad are slow acting, and the cumulative effect of chronic dietary exposure is responsible for a disease phenotype involving motor system degeneration in humans and mice (Spencer et al., 1991; Wilson et al., 2002). G37R transgenic mice have a longer life span of up to one year and reliably reproduce the stereotypical disease phenotype reminiscent of other more popular SOD1 mouse models of ALS. Hence this transgenic G37R mouse line is ideal for the current study, allowing more flexibility in experimental design concerning the timing of toxin exposure to allow sufficient time for a more prominent effect to be observed from the toxin. Timing is important for gene-environment interaction studies, since sufficient evidence is available for early neuropathology at various levels of the CNS before disease symptom onset. The effects of the environmental factor may be negligible if administered when the neurodegeneration is already well underway due to the transgene. Presymptomatic chronic exposure to the environmental factor ensures interaction with the sub-threshold degenerative genetic effects. Furthermore, the choice of this G37R mouse line for this study is justified by their inclusion in previous gene-environment studies using different lines of G37R mice (Nguyen et al., 2004).

2.1.1.4 SOD1-mediated motor neuron degeneration

Evidence for increased oxidative stress as the pathological basis of motor neuron disease has been described for transgenic SOD1G93A mice. Mutant enzymes showed increased catalysis of the hydrogen peroxide reaction with enzyme-bound copper (Cu) to generate hydroxyl radicals via the Fenton reaction (Yim et al., 1996). The enhancement of Fenton catalysis by SOD1 mutations in FALS can also function to produce secondary radicals. Consistent with this, administration of Cu chelators that prevent Cu loading into the enzyme active site delays disease onset in transgenic mice (Gurney et al., 1998). The hydroxyl radicals produced by mutant Cu/Zn SOD may react with membrane lipids to trigger oxidative injury to motor neuron lipids (lipid peroxidation) and proteins, an event preceding the onset of clinical motor neuron disease (Hall et al., 1998). Presymptomatic accumulation of cholesterol esters indicative of altered membrane metabolism was observed, consistent with a role for oxidative stress in spinal motor neurons (Cutler et al., 2002). Furthermore, evidence of lipid peroxidation was associated with an accumulation of vitamin E in the spinal cord, indicative of protective antioxidant mechanisms. In the SOD1G93A mouse model of ALS, vitamin E supplementation had no effect on survival, but it did significantly delay symptom onset and slow disease progression as assessed by wheel activity (Gurney et al., 1998). Vitamin E appeared to delay

symptoms in ALS patients as observed by an extended period in the milder state of ALS compared to placebo recipients, but did not exend life span (Butterfield et al., 2002).

In spite of suspicions of the role of oxidative stress in ALS pathology, treatment strategies aimed at reducing oxidative success had mixed success. Neuroprotective strategies such as Cu chelation and vitamin E therapy that inhibit oxidative mechanisms served to delay disease onset without affecting disease onset or survival (Gurney et al., 1998). Therapeutic strategies that interfere with disease propagation, on the other hand, have been successful at increasing the duration of symptomatic disease although with no effect on disease onset. The most recognized strategy was treatment with riluzole, a presynaptic inhibitor of glutamatergic neurotransmission, which was successful at extending survival in SOD1G93A transgenic mice (Gurney et al., 1996). However, in population based studies and clinical trials, riluzole failed to show an effect on disease onset and had minimal efficacy in prolonging survival (3 – 6 months) (Miller et al., 2007). Furthermore, the effect of riluzole was limited more to an early stage of disease in an ALS sub-population of bulbar-onset and elderly patients (Zoccolella et al., 2007).

Another proposed mechanism for SOD1-mediated motor neuron vulnerability involves metal ion dysregulation and the subsequent induction of homeostatic defence mechanisms. Olsen and colleagues (Olsen et al., 2001), reported a prominent activation of genes involved in Cu and iron (Fe) ion regulation after the onset of paralysis. Low levels of intracellular copper are seen in healthy spinal cords where the copper chaperone of SOD (CCS) loads copper into Cu/Zn SOD1. The reported activation of genes involved in Cu homeostasis may be an adaptive response to stress in late disease (Olsen et al., 2001). The progressive mitochondrial pathology common to mutant SOD1 serves as a rich Fe reservoir that is released into the cytoplasm (Dalcanto & Gurney, 1994a; Dalcanto & Gurney, 1994b; Wong et al., 1995; Olsen et al., 2001). Free Cu and Fe metal ions are thus increasingly available in motor neurons to catalyze the formation of harmful hydroxyl radicals via the Fenton reaction (Olsen et al., 2001). Again, the production of hydroxyl radicals from hydrogen peroxide during the Fenton reaction increases protein susceptibility to oxidation. Mutant SOD1 was also observed by other groups to be depleted of zinc (Zn), a condition sufficient to induce nitric oxide-dependent apoptosis selectively in cultured motor neurons (Estevez et al., 1999).

The past decade was marked by increased attention towards mutant SOD1 misfolding as a possible mechanism in disease pathogenesis. An antioxidant role for SOD1 *in vivo* incurs a greater

risk of oxidative stress that, once accumulated, could promote its misfolding and aggregation. This shift in focus was accompanied by a growing list of new discoveries of different missense mutations in FALS since the 90s. Aggregates of mutant SOD1 were observed in motor neurons and astrocytes corresponding to disease onset and increased in abundance with disease progression in transgenic mice expressing a SOD1 mutation with glycine substituted to arginine at position 85 (Bruijn et al., 1997; Bruijn et al., 1998). However, monomeric misfolded SOD1 in 3 ALS mouse models with G37R, G85R, and G93A mutations was expressed predominantly in the motor neurons and motor axons of mSOD1 mice and its accumulation correlated with disease onset and disappeared with motor neuron degeneration (Rakhit et al., 2007). These mutant SOD1 aggregates are purported to inhibit normal neuronal function by various mechanisms. Mutant SOD1 A4V, D90A, and G93A readily formed misfolded aggregates upon oxidation of amino acid residues in the active site (Rakhit et al., 2002), and this discovery became a reliable *in vitro* model of SOD1-misfolding. Monomer/misfolded SOD1 was not detected in human sporadic ALS cases or in non-SOD1 FALS cases (Liu et al., 2009), although both mutant and WT SOD1 were shown to be monomeric intermediates prior to misfolding under oxidative stress (Rakhit et al., 2004). However, Bosco and colleagues recently described aberrant misfolded wild type SOD1 in a subset of sporadic ALS cases, which supports a common SOD1-dependent pathogenic mechanism in both SALS and FALS (Bosco et al., 2010b). Batulan and colleagues showed that motor neurons in mSOD1G93A mice had an abnormally high threshold compared to glial cells for induction of heat shock protein (Batulan et al., 2003), suggesting that this impaired ability to activate this stress response was due to saturation of the heat shock chaperones by mutant SOD1 aggregates. Mutant SOD1 aggregates also inhibited normal organelle function via accumulation of aggregates inside that organelle. In addition, aggregation of these damaged proteins may inhibit the ubiquitin-proteasome pathway. Misfolded and aggregated SOD1 (wild type, A4V, G85R, and G93A) selectively induced proteasomal inhibition in motor neurons while non-motor neurons were spared (Urushitani et al., 2002). Abnormal protein aggregates may have sequestered proteins required for proteasome function, thereby inhibiting their normal degradation processes.

Furthermore, neuronal and glial aggregates stain intensely for both SOD1 and ubiquitin (Bruijn et al., 1997). Prominent neurofilament accumulations are a component of cytoplasmic inclusions (Hirano et al., 1967a; Hirano, 1991; Williamson et al., 1998). Lewy-body like inclusions were described in the perikarya of neurons and astrocytes from transgenic mice (DalCanto et al.,

1997). In particular, motor neurons were observed to undergo a triphasic response following introduction of mutant human SOD1. Initial pathological changes in the anterior horn cells showed filamentous mutant SOD1 aggregates in cell processes during the early presymptomatic stages (Stieber et al., 2000). Coincidental to disease onset, motor neurons showed peroxidative damage to lipid membranes as evidenced by Golgi fragmentation, vacuolation of mitochondria and endoplasmic reticulum (DalCanto et al., 1996; Mourelatos et al., 1996) and SOD1 aggregation within neuronal perikarya (Stieber et al., 2000). Later in the disease process, the appearance of neurofilament inclusions then ubiquinated cytoplasmic inclusions and mutant SOD1 aggregates were observed more prominently (Tu et al., 1996; Bruijn et al., 1997; Bruijn et al., 1998; Williamson et al., 1998) with only variable fragmentation of Golgi apparatus (Stieber et al., 2000). There is variable evidence of motor neuron loss, but demyelination of descending spinal tracts and motor endplate denervation is apparent (Olsen et al., 2001; Fischer et al., 2004). This is followed by a delayed response of cellular changes in the spinal cord marked by post-symptomatic microglial and astrocyte activation and ultimate motor neuron loss (Chiu et al., 1995; Hall et al., 1998) that was described to coincide with the onset of paralysis (Olsen et al., 2001). The death of motor neurons is associated with degenerating axons of the motor type while dorsal ganglia are relatively spared.

The human SOD1 mutations introduced into experimental mice induced a consistentand progressive phenotype of motor neuron disease exquisitely localized to spinal motor neurons with relative sparing of the cells of somatic tissues. At lower expression levels, the pathological changes more closely resemble human FALS with motor neuron loss, gliosis, and filamentous pathology with ubiquinated Lewy bodies in ventral horn motor neurons (Dalcanto et al., 1995; Tu et al., 1996). Dismutase activity in mutant SOD1 was observed to be preserved in the presence of other cellular ROS regulators. The functional consequence of this phenomenon is unknown, but challenges the hypothesis that free radical damage underlies motor neuron disease in this model. In short, little is known about the mechanisms underlying mutant SOD1-induced motor neuron death.

2.1.2 Other causes of ALS

2.1.2.1 TDP-43

Identification of disease-linked proteinssuch as TDP-43 and FUS in ALS is an important step for understanding the neurodegenerative mechanism targeted to motor neurons correlating with the consistent observation of intraneuronal inclusions causal to disease. Disease proteins are

known for other neurodegenerative diseases in which dominant mutations in the genes encoding for the neuronally deposited protein account for some of the disease cases. For example, mutations in the amyloid precursor protein gene encoding Aβ peptide are responsible for the signature amyloid plaques in Alzheimer's disease (Tamaoka et al., 1994; Small, 1998). The major disease protein component of Lewy body deposits in Parkinson's disease were linked to mutations in the gene encoding α-synuclein, a protein primarily found in neural tissue with purported functions of microtubule association and vesicle trafficking (Alim et al., 2004; Cooper et al., 2006). The microtubule-associated protein tau (MAPT) gene encodes tau. Tau proteinis abundant in CNS neurons, acting to stabilize axonal microtubules and promote tubulin assembly into microtubules. Mutations in MAPT are observed in a subset of neurodegenerative diseases known as tauopathies, with the distinguishing feature of abnormal aggregates of hyperphosphorylated tau (also known as paired helical filaments) in the form of neurofibrillary tangles. Alzheimer's disease, frontotemporal dementia without ubiquitinated inclusions, progressive supranuclear palsy, and Guam ALS-parkinsonism dementia complex are examples of tauopathies (Roberts, 1988; Hof et al., 1994; Williams et al., 2009).

Efforts to identify disease proteins in motor neuron disease led to the characterization of the cellular protein transactivationresponsive (TAR)-DNA-binding protein with a molecular mass of 43 kDa (TDP-43). TDP-43 was originally identified as a transcriptional repressor that binds to chromosomally integrated HIV-1 TAR DNA and represses viral transcription (Ignatius et al., 1995). TDP-43 is ubiquitously expressed, highly conserved, localized primarily in the nucleus under normal conditions (Ayala et al., 2005). It was later discovered that TDP-43 was the major protein component of round and skein-like cytoplasmicubiquitin inclusions specific to sporadic ALS and frontotemporal dementia with ubiquitin inclusions (Neumann et al., 2006; Tan et al., 2007). However, mutant SOD1 transgenic mice did not show relocation of TDP-43 to the cytosol that is characteristic of human ALS, indicating that TDP-43 was functional and did not cause the ALS-like disease in this mouse model (Moisse et al., 2009a). The role of TDP-43 in the CNS is uncertain, but mutations in the gene encoding TDP-43 are associated with neurodegenerative disorders including ALS and frontotemporal lobar degeneration (Kwong et al., 2007), and is observed to assume a cytoplasmic skein-like or round distribution under these pathological conditions (Neumann et al., 2006). A recent study showed an increase in cytosolic TDP-43 expression in lumbar spinal cord

motor neurons after axotomy, indicating a role for TDP-43 in the molecular response to neuronal injury and that this response is perturbed in ALS (Moisse et al., 2009b).

Strong and colleagues demonstrated that TDP-43 interacted with human light molecular weight neurofilament (NFL) and suggested its potential to bind to nuclear NFL mRNA and regulate its translocation to the cytosol for translation (Strong et al., 2007). The observation that TDP-43 is predominantly non-nuclear in its localization in ALS motor neurons, and the finding that TDP-43 has both DNA and RNA-binding properties compelled Strong and colleagues to suggest that TDP-43 was post-translationally modified in ALS to give rise to skein formation and ubiquitination (Strong et al., 2007). Their study in human ALS spinal cords showed cytosolic skeins of TDP-43 aggregates, mostly in the absence of ubiquitin colocalization. In addition, they observed 3 isoforms of TDP-43 in spinal cord homogenates that are not due simiply to enhanced phosphorylation, suggesting alternative post-translational modifications. Strong and colleagues proposed that under normal conditions, TDP-43 acts to stabilize NFL mRNA within the nucleus, and that TDP-43 is post-translationally modificed in ALS in a manner that gives rise to isoform phosphorylation and skein formation (Strong et al., 2007). More specifically, TDP-43 has the potential to bind to nuclear NFL mRNA forming a RNA/protein complex, regulate its translocation to the cytosol, and then regulate its site-specific translation once the RNA/protein complex is anchored to the cytoskeleton (Strong et al., 2007).

Although TDP-43 positive inclusions are not associated with tau immunoreactivity, TDP-43 was demonstrated to show abnormal phosphorylation and accumulation in glial cells (Arai et al., 2006; Zhang et al., 2008a). The involvement of TDP-43 in ubiquitinated neuronal and glial inclusions are specific to human cases of sporadic ALS and non-SOD1 FALS (Mackenzie et al., 2007) illustrating pathological heterogeneity among familial ALS subtypes. However, the presence of abnormal TDP-43 features in SOD1-related human ALS or mutant SOD1 mice remains controversial. Some studies have confirmed the absence of TDP-43 pathology in SOD1 ALS (Robertson et al., 2007; Turner et al., 2008), while others studies have reported contradictory findings (Shan et al., 2009). These conflicting reports represent the two extremes of studies that show that TDP-43, although co-localized with ubiquitin, is not the major ubiquinated target, and that TDP-43 positive skeins are not necessarily ubiquitinated (Sanelli et al., 2007; Strong et al., 2007). Nevertheless, it is generally accepted that ubiquitinated TDP-43 in skein-like and round neuronal inclusions are neuropathological features of SALS as well as FALS to a more limited degree.

Pathogenic mutations in the TARDBP gene encoding TDP-43 are active mediators of neurodegeneration in autosomal dominant familial ALS that are placed in a class of disorders known as TDP-43 proteinopathies (Van Deerlin et al., 2008). Mutations in TARDBP occur much less frequently than SOD1 mutations, and comprise 1% of ALS cases or 5% of patients with non-SOD1 familial ALS (Van Deerlin et al., 2008). The mutations of TARDBP affect the highly conserved amino acid residues in the C-terminal glycine-rich part of TDP-43, which regulates gene expression and mediates protein-protein interactions (Rutherford et al., 2008; Van Deerlin et al., 2008). Mutations in TDP-43 that affects its RNA binding region responsible for the interaction of TDP-43 with NFL mRNA has been identified in ALS, pointing to a mechanism of aberrant TDP-43-mediated mRNA trafficking in neurodgeneration (Kabashi et al., 2008).

The pathologic mechanism of TDP-43 remains unclear, but several hypotheses have been suggested. A loss of function mechanism for TDP-43 may result in transcriptional deregulation or aberrant RNA splicing, in light of its known role in exon skipping and splicing inhibition (Wang et al., 2004; Buratti et al., 2005). A recent study has suggested that TARDBP mutations that impair TDP-43 function were pathogenic by a gain-of-function mechanism by inducing toxicity through mislocalization or elevated concentrations of TDP-43 (Barmada et al., 2010). This hypothesis was supported by experiments showing that over-expression of mutant human TDP-43 in mice showed progressive motor weakness leading to paralysis with TDP-43 redistribution and fragmentation (Stallings et al., 2010). In addition, cytoplasmic TDP-43 accumulation in neurons implicates a potential undefined toxic function associated with disruption of normal cell function. It has been proposed that hyperphosphorylation of TDP-43 may disrupt important signalling pathways that lead to neuronal dysfunction (Forman et al., 2007).

2.1.2.2 FUS related amyotrophic lateral sclerosis

Research has been advanced through the recent identification of over 30 (mostly missense) mutations of the gene Fused in sarcoma/translated in liposarcoma (FUS/TLS) in individuals with familial ALS(Kwiatkowski et al., 2009; Lagier-Tourenne & Cleveland, 2009) and sporadic ALS to a lesser degree (Belzil et al., 2009; Corrado et al., 2010). FUS/TLS mutations are estimated to comprise about 5% of FALS, which is comparable to the frequency of TDP-43 gene mutations in ALS but less than that for SOD1. This gene is involved in the regulation of transcription, splicing and RNA transport, binding RNA through its C-terminus (Vance et al., 2009). It has ubiquitous expression and is normally located in both nucleus and cytoplasm, but nuclear expression

predominates in neurons (Aman et al., 1996). It has functional homology to another ALS gene, TARDBP, which indicates that a common mechanism may underlie motor neuron degeneration (Vance et al., 2009). Furthermore, mutant forms of FUS/TLS accumulate in the cytoplasm of neurons in a manner comparable to TDP-43 pathology (Kwiatkowski et al., 2009). This cytoplasmic redistribution leads to recruitment of FUS/TLS into perinuclear stress granules in proportion to their cytoplasmic expression levels that co-localize with inclusions in FALS patients, implicating stress granule formation in the pathogenesis of disease (Bosco et al., 2010a; Dormann et al., 2010). Stress granules contain characteristic RNA-binding proteins that serve as markers and are observed under conditions of cellular stress such as heat shock.

The neuropathology of ALS causes involving mutant FUS/TLS is comparable to those involved in familial ALS, including myelin pallor in the corticospinal tracts, degeneration of the Betz cells in the motor cortex, and prominent ubiquitin cytoplasmic inclusions (Kwiatkowski et al., 2009). However, FUS/TLS immunoreactivity within the nuclei of neurons and non-neural cells is observed in both disease and healthy cases, although more pronounced in disease. Identification of stress granules implicate two disease mechanisms including a defect in nuclear import of mutant FUS/TLS and cellular (environmental) stress, each capable of initiating eventually larger cytoplasmic inclusions of FUS (Dormann et al., 2010).

The pathogenic mechanism of FUL/TLS mutations remains unclear, but recent studies offer several hypotheses. Missense mutations in FUL/TLS may lead to aberrant trafficking with subsequent cytoplasmic retention of the mutant protein (Kwiatkowski et al., 2009). A loss of function may be the pathogenic mechanism for mutant FUS/TLS, where the protein loses its ability to transport mRNA encoding actin-stabilizing proteins (Munoz et al., 2009). FUS/TLS can modulate the stability of neurofilament mRNA with its RNA binding capabilities and hence aberrant mRNA binding may lead to altered RNA metabolism (Strong, 2010).

2.1.2.3 Optineurin

The OPTN gene encodes for optineurin, a protein that plays a role in glaucoma, a neurodegenerative eye disease that can lead to blindness. Pathogenesis of glaucoma by mutations in the optineurin-coding region of OPTN is not clearly understood, but aberrant endocytic trafficking has been suggested (Nagabhushana et al., 2010). Optineurin plays a role in the maintenance of the

Golgi complex, in membrane trafficking, and post-Golgi trafficking to lysosomes (Sahlender et al., 2005).

Optineurin has most recently been included as a causative factor for familial and sporadic ALS. Ubiquitinated intracytoplasmic skein-like inclusions in SALS and Lewy body-like hyaline inclusions in FALS co-localize with optineurin (Maruyama et al., 2010). SOD1-immunoreactive Lewy body-like hyaline inclusions from SOD1 FALS as well as TDP-43 inclusions are also positive for OPTN (Maruyama et al., 2010). The mechanism of optineurin pathogenesis is unclear, but one hypothesis suggests an aberrant feedback loop between optineurin and up-regulation of nuclear factor kappa B (NF-κB), a cell death inhibitor (Maruyama et al., 2010; Swarup et al., 2010). The affect of ALS-associated mutations of optineurin on vesicle trafficking is not known.

2.2 Sporadic ALS

Similar to FALS, the essential feature of sporadic amyotrophic lateral sclerosis (SALS) is also marked by degeneration of both the upper and lower motor neuron systems. Unlike the FALS cases, sporadic forms have preserved posterior columns and spinocerebellar tract. However, pyramidal tract degeneration is observed in a fraction of SALS cases (Brownell et al., 1970; Piao et al., 2003). SALS comprises the majority of all ALS cases and do not have an identified causal gene linkage. At the cellular level, SALS pathology is defined by the presence of cytoplasmic inclusions termed Bunina bodies in the lower motor neuron, some of which are also common to FALS (Nakano et al., 1993). Bunina bodies are 4 to 5 μm homogeneous inclusions found in a majority of SALS cases in lower motor neurons and occasionally in upper motor neurons (Murayama et al., 1990). These cytoplasmic inclusions are defined as small round eosinophilic granular inclusions with tubules or vesicular structures. They are composed of bundles of unconstructed filaments about 20-25 nm in diameter and have been described as a pathologic hallmark of ALS due to their consistent association exclusively with ALS (Sasaki et al., 1993). They have been detected with cystatin C, a proteinase inhibitor, and invariably with ubiquitin (Okamoto et al., 1993). Disease duration for cases exhibiting Bunina bodies was significantly shorter than for those without them, while the age of onset was not affected (Piao et al., 2003). CNS pathology of typical SALS includes neuronal loss and astrocytic gliosis in the motor cortex and spinal anterior horn, and myelin pallor in the CST.

Ubiquitinated neural inclusions in the surviving lower motor neurons are associated with essentially all SALS cases (Lowe et al., 1988; Piao et al., 2003). These inclusions are skein-like that appear as spherical structures in the neuronal cytoplasm and are observed at much higher frequencies than Bunina bodies in motor neurons. Mizusawa and colleagues first described their unique morphology as thread-like linear or tubular structures often surrounded by pale areas (Mizusawa et al., 1991). Upon aggregation, these inclusions appear as dense collections of thick filaments that are randomly and loosely arranged (Mizusawa et al., 1991). They are faintly eosinophilic spherical aggregates containing 15-25 nm bundles of unconstricted filaments that appear thread-like and occur with high frequency in SALS (Piao et al., 2003). They are not detectable with SOD1, phosphorylated neurofilament (tau), or α-synuclein staining and are usually isolated to SALS cases. It has been suggested that skein-like inclusions may be involved with autolysosomal processing due to their resemblance to early stage autolysosomes (Nakano et al., 1993). Ubiquitin immunoreactive cytoplasmic inclusions are also observed in cerebral small neurons including those of the caudate nucleus and/or putamen and in the temporal lobe. Ubiquinated neurites in the neostriatum and temporal lobe were found to be associated with the bulbar onset form of ALS. The inclusions of the neostriatum are rarer and exhibit a crescent or circular shape, but the pathology of the neostriatum as a whole is unremarkable without obvious neuronal loss or astrogliosis. These inclusions are generally indistinguishable from the ones in the temporal lobe.

Hyaline conglomerate inclusions are also features of neuronal pathology in SALS. These lesions are observed at a much lower frequency than ubiquitinated inclusions, and at an even lower frequency in SALS compared to SOD1-related FALS cases (Ince et al., 1998). They demonstrate immunoreactivity for both phosphorylated and non-phosphorylated heavy and medium chain neurofilament protein, and also to ubiquitin (Ince et al., 1998). They are eosinophilic spheroids containing 15-20 nm randomly oriented fibrils, and have been shown to be immunoreactive to SOD1, even in SALS cases (Chou et al., 1996). This observation suggests a possibility of wild type SOD1-mediated neuronal pathology.

2.2.1 Guam ALS (Marianas/Western Pacific ALS)

The incidence of amyotrophic lateral sclerosis (ALS) among the indigenous Chamorro people of Guam during the 1950s was exceedingly high.The earliest epidemiologic investigations involved detailed tours of duty in which investigators traveled to Guam to observe the affected

patients and to survey the general population. The socio-economic impact of this disease to individuals, their families, and to their society was well understood and attempts at determination of a possible etiologic factor were strongly pursued. Although investigators were granted access to local hospital records and death certificates while in Guam, hospital records were not informative or limited to late disease stages while death certificates were either lost or unreliable. The population of Guam was relatively small and the prevalence of ALS was easily inviting as an unusual opportunity to study epidemiology. The unusually high occurrence of people diagnosed with ALS in this isolated geographical area classified Guam as a disease cluster (Koerner, 1952; Kurland et al., 1954; Mulder et al., 1954). Subsequent epidemiological, clinical, and pathological studies of Guam ALS confirmed earlier suspicions that the Guam condition met the criteria for classical ALS. A clinical diagnosis of ALS was based on the observation of the major presenting symptoms of muscular weakness and atrophy in almost all cases, bulbar palsy in 75% - 80% of cases usually in later disease stages, and lateral sclerosis in combination with other symptoms (Mulder, 1957; Hirano et al., 1966; Hirano et al., 1967a). These cases usually showed signs of upper and lower motor neuron lesions of pseudo-bulbar, bulbar, and spinal areas developing invariably during the course of the illness, with no signs of dementia or extrapyramidal dysfunction (Stanhope et al., 1972; Brody et al., 1975). The presenting symptom was muscle atrophy in about half of the patients while spasticity appeared first in a minority of cases (Mulder, 1957; Hirano et al., 1961a; Hirano et al., 1967a; Brody et al., 1975). In the smallest number of cases, muscle atrophy at the bulbar or spinal level in the absence of spasticity was the only clinical sign while histological evidence of upper motor neuron involvement was invariably present (Hirano et al., 1966). Extraocular muscle weakness, loss of bowel and bladder control, and objective sensory deficits were absent in all cases (Brody et al., 1975). However, these cases also showed especially unique features including: (1) the presence of Alzheimer's neurofibrillary tangles widely distributed in cortical and subcortical areas while senile plaques were absent (Hirano et al., 1966; Brody et al., 1975;); (2) atrophy and pallor of the substantia nigra resembling Parkinsonism cases(Hirano et al., 1966; Hirano et al., 1967a); and (3) progressive dementia in a subset of the affected population accompanied with Parkinsonism (discussed below).

The affected population observed in this disease cluster were the Chamorro people who were native to Guam. Although the history of motor neuron disease in Guam has not been well documented prior to World War II, the first known death certificate with the diagnosis of amyotrophic lateral sclerosis was reported in 1931 (Kurland et al., 1954). Death records in Guam

during the early 1900s were not usually kept by physicians in most cases and the causes of death categories listed as either due to paralysis, progressive muscular atrophy, or other non-neurologic causes (Mulder et al., 1954). Pioneer investigators of Guam ALS inevitably observed poor or variable quality of health reports and thus had to rely heavily on interviews to survey the family history (Arnold et al., 1953; Kurland et al., 1954). When more stringent clinical diagnosis criteria were applied, it was found that for many of the deaths listed as due to paralysis, there was evidence that ALS was the cause of death. The Chamorros recognized this illness and called it *lytico*, derivedfrom the Spanish word 'paralytico' for paralyzed.

Attempts by Arnold and colleagues failed to find any obvious cause for the high incidence after evaluating family history, alcohol, malnutrition, potential toxins in food, water and soil, trauma, head injury, and encephalitis (Arnold et al., 1953). The syndrome in Guam was observed to have no identifiable etiologic factor, affecting individuals between the ages of 30 and 65 with predominance in males (Koerner, 1952; Arnold et al., 1953; Kurland et al., 1954). In addition, their survey also showed that ALS was seldom, if ever, found either in the large transient Filipino population or US-born military personnel on the island (Stanhope et al., 1972). These earliest investigations estimated that the incidence of ALS in Guam between 1953 and 1954 was 100 times greater than the estimated rate of occurrence in the United States (Arnold et al., 1953; Kurland et al., 1954; Mulder et al., 1954). For a more detailed historical account on Guam, the author refers the reader to Appendix A.

2.2.2 Guam PDC

A form of Parkinsonism with dementia as a second neurological disorder was also uniquely endemic in this population. This disorder was less widely recognized by the Chamorros who called it *bodig* with reference to a person developing senility during normal aging. The first observation of some signs and symptoms of Parkinsonism coupled with Guamanian ALS was observed in two patients in 1954, but was dismissed as occurring by chance (Kurland et al., 1954). Mulder and Kurland reported these symptoms and serologic findings most compatible with a postencephalitic type of Parkinsonism following a previous Japanese B encephalitis outbreak (Mulder et al., 1954).

In general, patients were described as having a striking akinesia, shuffling gait, expressionless face and muscle rigidity while coarse tremor was variable and comparatively minimal among the outstanding characteristics of the disease (Hirano et al., 1961a). Extrapyramidal postural abnormalities and slowing of gait occurred early, while muscle rigidity prominently in the trunk,

neck, and upper limbs became more obvious as the disease progressed. Late stages showed generalized rigidity and pronounced immobility (Steele, 2005). In over one third of patients, extrapyramidal features preceded the development of ALS or full syndrome parkinsonism-dementia patients developed motor neuron disease (Hirano et al., 1961a). The distinguishing feature apart from these Parkinsonism signs was the presence of marked mental deterioration with memory impairment and disorientation (Koerner, 1952). The large majority of patients with Guamanian Parkinsonism presented with a combination of a severe progressive dementia with extrapyramidal signs (Brody et al., 1975). In 25% of the patients, dementia was the only feature of the disease for a variable period, while in 38% of cases, it was the dominant feature of the illness (Steele, 2005). Guamanian dementia was indistinguishable fromdementia with Parkinsonism, and both exhibited cognitive deficits resembling Alzheimer's disease (Galasko et al., 2002). It was concluded that the Parkinsonism and dementia syndrome of Chamorros was clinically and pathologically distinct, and the name parkinsonism-dementia complex (PDC) of Guam was given (Elizan et al., 1966). The features of PDC were consistent with Parkinson plus syndromes, a group of neurodegenerative diseases with the classical Parkinson's disease features (tremor, rigidity, akinesia/bradykinesia) with additional features that distinguish them from idiopathic Parkinson's disease. Parkinson plus syndromes were difficult to differentiate from Parkinson's disease and from each other. Of particular interest is progressive supranuclear palsy (PSP), a rare degenerative disease involving progressive deterioration and death of selected areas of the CNS such as the basal ganglia, frontal lobes, brainstem (namely the midbrain portion controlling eye movement), and the spinal cord. PSP is clinically characterized by Parkinsonism features, dementia, and neurofibrillary tangles of hyperphosphorylated tau aggregates in certain nuclei of the basal ganglia, brain stem, and cerebellum common to PDC. However, the characteristics of PSP distinguishing it from PDC include pseudobulbar signs (slurred speech, difficulty swallowing, jaw jerks), dystonia of neck muscles resulting in an upturned resting head posture, impaired voluntary eye movements, and the appearance of Lewy bodies and senile plaques (Steele et al., 1964; Uchikado et al., 2006; Keith-Rokosh et al., 2008).

The distribution of cases of PDC was similar to that for ALS on Guam, with greater prevalence in the southern villages where the economy is predominantly agricultural (Kurland et al., 1954; Hirano et al., 1961a). Case studies of PDC on Guam between 1956 and 1960 revealed an early age of onset, a preponderance of males, and minimal evidence of familial aggregation (Hirano et al.,

1961a; Stanhope et al., 1972). These findings contrasted those for idiopathic Parkinson's disease in U.S. populations at the time where age of onset was much later, the clinical disease duration was much longer, and there was essentially no difference by sex (Kurland et al., 1958). The relation between the *lytico* and *bodig* aspects was unclear, although patients were observed for ALS, PDC, or both disorders.

2.2.3 Guam ALS-PDC

Pathological changes to the spinal cord similar to those of ALS were reported in cases whose primary symptoms were those of PDC (A. Hirano et al., 1966). The spectrum of neurological diseases described in Guam was termed ALS-PDC since its phenotypes included classic ALS, PDC, Parkinsonism without dementia, and just dementia. It was usual for just one phenotype (ALS, Parkinsonism, or dementia) to dominate, but overlap also occured between them. In spite of distinct clinical and pathological features differentiating PDC from ALS, the two disorders had similar age range of onset (20 to 72), sex ratio (2.5-3 men to 1 woman), duration (3.7-4.1 years for men and 4.3-4.7 years for women with younger age of onset corresponding invariably to longer survival), high incidence in a single small population, and familial pattern (Reed et al., 1966). The clinical presentation of ALS-PDC fell into three patterns: (1) simultaneous presentation of both features; (2) initial onset of PDC followed by amyotrophy and spasticity; and (3) onset of ALS features followed by dementia or PDC (Hoffman et al., 1976; Kakulas et al., 1980). These clinical and neuropathologic commonalities led researchers to hypothesize that ALS and PDC were different manifestations of a single disease entity over a broad clinical spectrum (Hirano et al., 1966).

The neuropathological features of ALS-PDC were first described in the course of post mortem examinations of patients from Guam in the late 1950s (Hirano et al., 1961b). In summary, macroscopic examination showed variable atrophy of frontal and temporal lobes and loss of pigment in substantia nigra resembling idiopathic Parkinson's disease. The most prominent features were abundant neurofibrillary tangles formed by pathological tau in the motor cortex, substantia nigra, hippocampus, and brainstem motor neurons (Oyanagi et al., 1994a; Oyanagi et al., 1999; Yamazaki, Hasegawa et al., 2005). Neurofibrillary changes were rare in the basal ganglia and senile plaques or Lewy bodies were not observed. Intracytoplasmic granulovacuolar bodies were also prominent features of the affected neurons in these areas, described as round, argyrophilic inclusions with a peripheral halo that resemble round hyaline inclusions in sporadic ALS. Ubiquitinated

inclusions and Bunina bodies in the lower motor neurons were found, similar to sporadic ALS (Oyanagi et al., 1994a; Wada et al., 1999). These ubiquitinated inclusions were found to be either tau-positive, or TDP-43 positive, but TDP-43 and tau pathology was not observed to co-localize (Hasegawa et al., 2007; Geser et al., 2008). TDP-43 pathology was also observed to be mislocalized and abnormally phosphorylated (Hasegawa et al., 2007). Motor neurons in the brainstem were observed to show swollen cytoplasm with eccentric nuclei and thickened neurofibrils. Astrocyte gliosis and reactive microgliosis were commonly observed in the involved cortex and substantia nigra. Neuronal cell loss was most apparent in the substantia nigra and globus pallidus (Oyanagi et al., 1994b). There was bilateral demyelination of pyramidal tracts and degeneration of the anterior cells of the spinal cord. Most importantly, the neuropathologic changes in the spinal cord of the Guam ALS cases are virtually identical to those classically described in the disease (Perl et al., 1997).

The Guam disorders were most commonly thought to be of genetic origin due to observations in family clusters. However, geographic patterns of occurrence, and the absence of a definite pattern of inheritance supported the hypothesis of environmental causal factors over genetic causation (Reed et al., 1966; Reed et al., 1975; Stanhope et al., 1972). A decline in the incidence of ALS (Garruto et al., 1985) and PDC (Zhang et al., 1990) on Guam after 1965 was observed in the absence of significant changes in age-specific death rates. Specifically, the incidence of ALS for Guamanian males and females peaked in 1950-1954 and declined steadily for both sexes starting in the late 1950s until the early 1980s when the rates for both sexes were for the first time comparable. The incidence of PDC started to decrease in the early 1960s for males and in the late 1970s in females to comparable rates in males and females by 1980 (Plato et al., 2003). These observations led to a hypothesis that the etiologic factors were still present in Guam despite a decline in incidence, indicating that an exposure early in life is involved (Brody et al., 1975). Reed and Brody reported that environmental factors associated with some aspect of the traditional way of life, involving either a cumulative or a long latent period, seemed to be causally involved (Reed et al., 1975). Whiting (Whiting, 1963) established a firm link between ALS-PDC and the consumption of the seeds of *Cycas circinalis*, the indigenous cycad palm of Guam which had been an important source of carbohydrates for the Chamorros especially during World War II. Hill later reported the misapplication of the scientific nomenclature *Cycas circinalis*and correctly identified the taxa in the western pacific region as *C.micronesica* (Hill 1994). The name *C. micronesica* will be used from here, as Marler and colleagues have suggested (Marler et al., 2005a). Four critical observations supported the

proposal for a toxin in *C.micronesica* playing a significant role in the etiology of ALS-PDC: (1) the extreme prominence of the disease to Charmorros and some others who also shared their culture (Brody et al., 1975); (2) the heavy Chamorro reliance oncycad seed consumption during World War II and the post-war high prevalence of this neurodegenerative disease (Reed et al., 1975); (3) the historically low incidence of ALS-PDC in the island of Saipan where cycad was scarce (Kurland et al., 1954); and (4) the direct relation between the decline of incidence of ALS-PDC and decreased traditional cycad consumption as a result of increased westernization (Garruto et al., 1985).

2.2.4 Comparing ALS-PDC and ALS

ALS-PDC exhibits certain clinical similarities to ALS. Both disorders present with a comparable combination of both upper and lower motor neuron involvement. The development, in some cases, of dementia and extrapyramidal features are characteristics of both disorders although at a higher frequency for ALS-PDC. Decreased disease duration after the onset of bulbar symptoms and preponderance in males are common to both subtypes. The features of cellular pathology in motor neurons common to both ALS-PDC and sporadic ALS, such as Bunina bodies, ubiquitinated TDP-43 positive inclusions, and round hyaline inclusions, have received much attention, supporting the hypothesis that similar disease mechanisms may affect the motor neurons in both disorders. In terms of cerebral pathology, both diseases show a predominance of degeneration in the motor cortex, in addition to some pathological changes in the hippocampus.

The difference in incidence and geographic cluster is clear as would be expected on the basis of the previously discussed epidemiological studies. Furthermore, among the Guamanian ALS-PDC patients, while familial aggregation was quite common, only a fraction of classic ALS cases were hereditary. Other differences include the occurrence of ALS-PDC among younger patients and a longer survival in Guam despite similar ages at death (Hirano et al., 1967a). Neuropathologically, the presence of filamentous aggregates of hyperphosphorylated tau in the spinal cord and brain is a typical neuropathological finding of Guam ALS-PDC, but non-Guamanian ALS was not associated with tau pathology (Okamoto et al., 2001; Jimenez-Jimenez et al., 2005).

Considerations on similarities and differences in clinical and pathological aspects are important for elucidating the characteristic disease features of the commonly affected areas in ALS-PDC and non-Guamanian ALS. Differential expression of neuronal pathology would indicate that the mechanisms involved in the onset of neuronal degeneration and the subsequent clinical

presentation are different in ALS-PDC and non-Guamanian ALS. Current neuropathological findings in Guamanian and non-Guamanian ALS suggest that the pathology of ALS-PDC may be an unusual tau-mediated tangle disorder, while non-Guamanian ALS has features of typical motor neuron disease characterized by ubiquitinated intracytoplasmic neuronal inclusions.

2.2.5 Cycad hypothesis and modeling ALS-PDC

The Chamorros were an aboriginal group that have resided in Guam for many centuries. Several studies have investigated genetic risk factors in an effort to elucidate the cause of Guamanian ALS or PDC. For example, shortly following the important discovery of mutations of the Cu/Zn superoxide dismutase (SOD1) gene in some familial cases of ALS (discussed below), researchers reported that no mutations were found in Chamorros with ALS or PD (Figlewicz et al., 1994). The possible relationship between apolipoprotein E (Apo E, a genetic risk factor for Alzheimer's disease) alleles and neuropathological alterations in ALS-PDC were also analyzed. Although Apo E was observed in neurofibrillary tangles and the rare amyloid deposits in ALS-PDC cases (Buee et al., 1996), no Apo E alleles were over-represented (Chen et al., 1996). Similarly, no alleles of CYP2D6 gene associated with idiopathic Parkinson's disease were over-represented in Chamorros with PDC (Chen et al., 1996). Furthermore, no tau mutations were found in Guam ALS or PDC cases despite the prevalent feature of neurofibrillary tangles containing tau in both disorders (Poorkaj et al., 2001; Kowalska et al., 2003). In light of these genetic causality studies, the unique complexity of ALS-PDC was not attributable a hereditary causation. The etiology of this disease was elusive, but the environmental cycad hypothesis has prevailed and indicates a powerful but unexplained interaction between the genes of Chamorro people and the Guamanian environment.

The earliest suspicion of toxicity by consumption of cycad was a suggestion by Felipe de la Corte in 1875 dissuading Chamorros from eating federico nuts (de la Corte, 1875). Federico is a type of cycad palm – called *fadang* in Chamorro – with resemblance to a fern tree bearing large nut-like seeds that are poisonous. Historical Chamorro subsistence on cycad made use of the gametophyte tissue of cycad (Whiting, 1963). Their traditional process of preparation involved extracting the gametophyte, slicing it and washing it to remove acute toxins. Then the cycad was dried overnight and pulverised into flour for use in their various recipes. The people of Guam detoxified the nuts by soaking for several days and sometimes boiling them, then grinding them into flour after sun drying to make starch for a variety of cooked dishes (Whiting, 1963; Rogers, 1995).

The Chamorros believed their traditional practices of repeated washing removed toxins and enabled safe consumption. The green outer husks of *Cycas micronesica* seeds were chewed to relieve thirst and used as a treatment for tropical ulcers (Whiting, 1963). De la Corte recommended that federico nuts not be eaten because he believed they cause "endemic illnesses which have become hereditary and produce the elephanteasis illness, often causing premature aging and short life (de la Corte, 1875)." The seeds of the cycad palm were a food staple in Guam during Japanese colonization and World War II when food was scarce. Consumption of cycad remains the strongest epidemiological link to ALS-PDC of Guam since the birth of the cycad hypothesis.

Cycads are spermatophytes resembling palms or ferns with a large crown of compound leaves and restricted to tropical and subtropical regions of the world (Whiting, 1963). The unusual toxic properties of cycad led to various efforts to identify a constituent in cycad which might be of etiologic importance in the occurrence of ALS-PDC. Early investigations on cycad revealed several water soluble molecules in the seeds and stem, notably the water soluble amino glycoside (sugar moiety) cycasin (Nishida et al., 1955; Riggs, 1956) that is joined via a β-glucoside linkage to methylazoxymethanol (MAM). This aglycone MAM without its sugar was a candidate causative factor for the disorder (Matsumoto et al., 1966; Smith, 1966). Cycasin was toxic when the sugar moiety was cleaved in a deglycosylation process by the enzyme β-D glucosidase following ingestion (Spatz, 1969). The resultant free MAM, minus its innocuous sugar group, was a mutagenic, hepatotoxic, and carcinogenic compound due to its ability to increase nucleic acid methylation (Matsumoto et al., 1966; Smith, 1966). Despite its potential neurotoxic properties, the relationship of MAM to Guamanian ALS and Parkinsonism-dementia was only conjectural. Animal tests suggested that MAM was a hepatic carcinogen and teratogen, but neuropathology in animals did not correlate to the abnormalities assocated with ALS-PDC (Smith, 1966; Seawright et al., 1999; Lu et al., 2000). However, the possibility that cycad was still of etiologic importance with regard to ALS on Guam remained.

In addition to the acutely toxic compound MAM, early studies revealed that β-N-methylamino-L-alanine (BMAA) was a potential slow neurotoxin in the food sources derived from the seeds of cycad (Vega et al., 1967; Spencer, 1987) that was associated with the development of more chronic and long term illnesses. BMAA, a non-protein amino acid, is an N-methyl-D-aspartate (NMDA) and AMPA receptor agonist that can impact neurons following some routes of

administration. BMAA induced cell death *in vitro* by excitotoxic action on different glutamate subtypes (Weiss et al., 1989), and induced neurological symptoms and some pathological changes in the motor neurons of the brain and spinal cord of cynomolgus monkeys (Spencer et al., 1987). The monkeys developed corticomotorneuronal dysfunction after 2-12 weeks, as well as motor neuron degeneration reminiscent of ALS. However, the results with BMAA feeding failed to be reproduced in primates by other groups, showing no delayed, chronic neurotoxic effect of cycad feeding (Garruto et al., 1988). Furthermore, the doses of BMAA administered were so high that it was unlikely that such quantities were ever consumed during World War II, when food was scarce in Guam (Duncan et al., 1988).

Similar BMAA studies in rodents also reported administering doses orders of magnitude higher than Chamorros would consume for dietary or medicinal use of cycads (Perry et al., 1989; Duncan et al., 1991), but did not produce any behavioural or neuropathological abnormalities that would be expected of ALS or PD (Perry et al., 1989). Consistent with these negative findings in rodents, oral administration of BMAA at doses thought to be reflective of human consumption were also unsuccessful at influencing any behavioural or neuropathological effects when signs of motor neuron loss, apoptosis, astrocytosis and microglia activation were examined (Cruz-Aguado et al., 2006). Furthermore, BMAA did not cross the blood brain barrier (Duncan et al., 1991), a finding that was confirmed by other studies that were unable to detect BMAA in the brains of Chamorro PDC patients or mice fed BMAA despite using more sensitive and modern techniques (Montine et al., 2005; Snyder et al., 2009a; Snyder et al., 2009b). There were conflicting results about BMAA permeability through the blood brain barrier, as other studies reported detectable BMAA accumulation in the brains of ALS patients and rodents fed BMAA (Mash et al., 2008; Karlsson et al., 2009). A recent *in vitro* study showed that BMAA was a very weak glutamate receptor agonist with a toxicity that was comparable with the nutritional supplement β-alanine (Lee et al., 2011). Overall, the possibility of BMAA as a latent neurotoxin linked to ALS-PDC on Guam or neurological diseases elsewhere is not strong.

While unwashed cycad flour contained cycasin and BMAA, the extensive washing procedures adopted by the Chamorros in cycad preparation removed substantial amounts of these toxins from cycad seed flour (Dastur et al., 1966; Duncan et al., 1990; Khabazian et al., 2002). An early study on rhesus monkeys showed that consumption of washed cycad flour from Guam induced behavioural and histopathological features of ALS-PDC (Dastur, 1964). More recent

studies in rodents also demonstrated that neurological deficits resembling features of human ALS-PDC were induced in adult mice following *in vivo* feeding of cycad flour that had been washed according to traditional Chamorro practices (Wilson et al., 2002; Schulz et al., 2003). These chronic neurotoxic effects were induced by a then unidentified toxin that was not water soluble since the cycad flour was shown not to contain significant amounts of cycasin/MAM or BMAA. Khabazian et al. identified three steryl glucosides in the cycad seed as campesterol glucoside, stigmasterol β-D-glucoside (SG), and β-sitosterol β-D-glucoside (BSSG) that were shown to remain in cycad seed after traditional washing methods, while levels of cycasin and BMAA were undetectable and very minimal, respectively (Khabazian et al., 2002). A detailed study by Marler et al. (2005a) reported BSSG as comprising the largest fraction of isolated steryl glucosidesfrom cycad seeds. The author refers the reader to Appendix B for a review on plant steryls and recent cycad studies.

Environmental models concerning neurotoxin exposure present a challenge to study as there may be a long latency period following exposure. However, *in vivo* feeding of washed cycad seed flour (which does not contain BMAA or MAM) to mice showed that many of the behavioural and pathological features of ALS-PDC could be reproduced in a mouse model. Daily dietary exposure to cycad was neurotoxic in rodents, causing progressive spinal motor neuron death by apoptosis as measured using caspase-3 labeling in the ventral spinal cord, cortex, and substantia nigra (Wilson et al., 2002). Apoptotic motor neurons in the ventrolateral grey matter appeared to be associated with increased cell death despite the absence of degenerating axons or neuromuscular junctions (Lee et al., 2009). In addition, apoptotic spinal motor neurons in lumbar and thoracic sections of animals fed cycad showed evidence of abnormal morphological features and neurofibrillary tangles (Wilson et al., 2002; Tabata et al., 2008). In regard to Parkinsonism features, Shaw et al. (2003) reported a significant loss of striatal dopamine terminals and dopamine transporters. Motor coordination deficits were detectable following two weeks of daily cycad feeding, followed by memory deficits, both of which progressed even after cessation of feeding (Wilson et al., 2004). The most pronounced neurological effects of cycad toxicity arose from cycad seeds shown to contain higher concentrations of steryl glucosides (Wilson et al., 2002).

In vivo dietary exposure to synthetic BSSG induces behavioural motor deficits, loss of motor neurons in spinal cord, decreased tyrosine hydroxylase labeling, and increased caspase-3 and astrocytosisin mice (Tabata et al., 2008). These mice were fed BSSG daily for 15 weeks and the neuropathological effects were observed 17 weeks after cessation of toxin exposure. Following

washed cycad exposure *in vivo*, the CNS environment consistently showed insidious astroglial activation and proliferation (Tabata et al., 2008; Tabata et al., 2008; Lee et al., 2009). Following *in vivo* exposure to synthetic BSSG exposure, a robust astrocytic response occured in the absence of microglial activation (Tabata et al., 2008), indicating that the CNS astrocytic response to neural insult was an early event compared to phagocytosis. *In vitro* studies in a mouse derived motor neuron-like cell line that was vulnerable to BSSG exposure observed a dose-dependent toxicity (Ly et al., 2007; Tabata et al., 2008).

Further studies using cortical slice preparations showed that isolated compounds from cycad seeds as well as synthetic BSSG were capable of inducing depolarizing field potentials, lactate dehydrogenase release, and calcium-dependent glutamate release which were reversible by the NMDA antagonist D-2-amino-5-phosphonopentanoic acid (Khabazian et al., 2002). The NMDA antagonist effectively blocks the effects of NMDA, thereby decreasing glutamate release. Exposure to cycad-derived and synthetic phytosterols also induced alterations in the activity of specific protein kinases in cortical slices (Khabazian et al., 2002). Congruently, spinal cord tissue from cycad-fed mice showed generalized decrease in glutamate transporters, decreased excitatory amino acid receptor levels, and increased GABA-A receptor levels that may reflect an early overall glutamate-mediated excitotoxicity (Wilson et al., 2003). Down regulation of glial glutamate transporter variants of the GLT-1 subtype around blood vessels of the spinal grey matter was the late disease phenotype in these animal studies (Wilson et al., 2007). These findings, in addition to observations of decreased glutamate transporter levels, strongly supported an excitotoxic mechanism of neuronal cell loss (Wilson et al., 2003). When taken together, studies demonstrating the neurotoxicity of steryl glucosides may have important etiological implications, and strengthen the speculation cycad seeds were primarily responsible for the motor deficits and neuropathology in cycad-fed mice and hence human ALS-PDC.

2.3 Unresolved issues of selective vulnerability of motor neurons

The most distinctive aspects of motor neurons are their asymmetry, large size, and enormously elongated and thick axons. These characteristics may also contribute to their vulnerability in ALS.The mechanisms of selective motor neuron injury in ALS are complex, multifactorial and incompletely understood. Genetic mutations in SOD1 exhibit several mechanisms leading to motor neuron-targeted toxicity, as discussed before. But SOD1 FALS is

only a very limited disease subtype among a large group of neurodegenerative disorders. To date, many mechanisms have been proposed as important contributors to motor neuron injury. More commonly studied mechanisms include excitotoxicity, mitochondrial dysfunction, endoplasmic reticulum dysfunction, aberrant axonal transport, abnormal protein aggregation, altered RNA processing, insufficient growth factor signalling, inflammation, and the involvement of non-neural cells mediating injury. The following discussion will review the recent developments of some mechanisms.

2.3.1 Non-cell autonomous toxicity

The role of non-neuronal neighbouring cells in the selective susceptibility of neuronal subtypes in ALS has begun to receive much attention recently (reviewed by Ilieva et al., 2009). Non-cell autonomy is an alternate model of ALS pathogenesis that challenges the previously assumed cell autonomous mechanism that proposes disease production caused by damage within a selective population of affect neurons alone. Initial efforts focused primarily on mutant SOD1 expression to study ALS pathogenesis. However, neuron-specific expression of mutant SOD1 did not produce disease in mice (Pramatarova et al., 2001; Lino et al., 2002), indicating a role for non-neuronal cells in disease pathogenesis. Supporting this notion is the study by Clement and colleagues in chimeric mice that are mixtures of normal and mutant SOD1 (Clement et al., 2003), which clearly demonstrates that normal motor neurons develop aspects of ALS pathology when in the vicinity of mutant SOD1 non-neural cells. Furthermore, selective excision of mutant SOD1 synthesis in motor neurons in the CNS delayed disease onset but did not alter the rate of disease progression (Boillee et al., 2006). These results indicate a role of mutant SOD1 within different cell types in the initiating phase of disease caused by mutant SOD1 damage with motor neurons, and link the later disease phase to the inflammatory response of microglia and mutant SOD1 toxicity within these cells.

Since the inception of a non-cell autonomy hypothesis, numerous studies focused on delineating the identities of non-neural cells whose mutant SOD1 synthesis contributes to disease. Studies involved observing the influence of specific non-neural cells expressing mutant SOD1 on disease pathogenesis in normal or mutant SOD1 motor neurons. As expected, primary glial cells carrying mutant SOD1 mutation induced neurodegenerative properties in normal and mutant motor neurons *in vitro* (Di Giorgio et al., 2007; Nagai et al., 2007; Marchetto et al., 2008). The mechanism of mutant glial-mediated neurodegeneration may be related to excitotoxic damage, as mutant SOD1 expression in astrocytes were shown to lose their normal GluR2 regulating ability, thereby rendering

cells vulnerable to excitotoxicity (Van Damme et al., 2007). Whereas diminished mutant SOD1 expression in motor neurons results in delayed disease onset, diminished mutant expression in astrocytes sharply slowed later disease progression (Yamanaka et al., 2008) in a manner that is independent of astrocyte proliferation (Lepore et al., 2008). In addition to astrocytes, mutant-expressing microglial cells are key to rapid disease progression. Selective deletion of mutant SOD1 in microglia had the most profound effect on slowing later disease progression (Boillee et al., 2006; Yamanaka et al., 2006) in a manner that is also independent of astrocyte proliferation (Gowing et al., 2008).

The recent developments outlined thus far provide collective evidence for mutant SOD1-mediated ALS in a disease process that is non-cell autonomous. It is now known that mutant SOD1 synthesis in motor neurons has a primary role in driving disease onset. Neighbouring non-neural cells, namely astrocytes and microglia, also develop SOD1 mutant damage and cause accelerated disease progression. It is possible that non-cell autonomous toxicity works in conjunction with other mechanisms of motor neuron degeneration, and the contributions of multiple mechanisms work together to involve multiple cell types in disease onset and progression. Ilieva and colleagues suggested that selective vulnerability of motor neurons to toxicity from the ubiquitously expression of mutant SOD1 may be the result of "accidental convergence of the motor neuron's own inherent functional properties and the combination of mutant damage developed within it and its multiple cell partners" (Ilieva et al., 2009). In this proposed model, damage is initiated in the motor neuron by SOD1-mediated microglia dysfunction and is perpetuated by generalized inflammation in the CNS. Misfolded mutant SOD1 perpetuates the disease by initiating endoplasmic reticulum stress in the motor neuron and possibly in astrocytes also, as evidenced by loss of glutamate reuptake. These events continue to drive the cell into an excitotoxically vulnerable state, and the resultant increases in intracellular calcium accelerate further damage within the motor neuron. Finally, misfolded mutant SOD1 in microglia induces toxic levels of extracellular superoxide following activation and migration to become motor neuron neighbouring cells.

Although studies of non-cell autonomy are predominantly in SOD1 FALS cases, it may also be involved in other disease subtypes that involve ubiquitous expression of causative proteins. As discussed previously, dominant mutations in TDP-43 and FUS/TLS have been reported as causative genes for sporadic and non-SOD1 FALS. The observation of TDP-43 and FUS/TLS inclusions in neuronal cells and glia is a feature of sporadic ALS and non-SOD1 FALS (Neumann et al., 2006;

Kwiatkowski et al., 2009), and supports a hypothesis of non-cell autonomy being a universal feature in ALS.

2.3.2 Excitotoxicity

Glutamate is the major excitatory neurotransmitter in the CNS and binds to either ionotropic ion channels or metabotropic G protein-coupled receptors. Its action is terminated by glutamate reuptake mainly in astrocytes surrounding the synapse that convert it into glutamine. Glutamate toxicity is primarily mediated through AMPA receptors, an ionotropic receptor classified as such due to its affinity to the agonist amino-3-hydroxy-5-methyl-4-isoxazole propionic acid). Physiologically, AMPA receptors are impermeable to calcium ions at rest, but once missing the GluR2 subunit, they have been shown to be calcium permeable (Isaac et al., 2007). More importantly, deficient RNA editing of GluR2 in ALS motor neurons have been demonstrated and the resulting calcium-permeable AMPA receptors have been implicated in excitotoxic degeneration (Kawahara et al., 2003; Kwak et al., 2005). Restoration of the GluR2 subunit resulted in AMPA receptors with a low calcium permeability and motor neurons that were less vulnerable to excitotoxicity (Bogaert et al., 2010b).

Neuronal death results from glutamate-induced excitotoxicity, characterized by increased intracellular free calcium via calcium-permeable ionotropic receptors in combination with a low calcium buffering capacity (Bogaert et al., 2010a). The cellular result is an excessive influx of calcium that is unable to be balanced by the mitochondria buffering capabilities of the cell. Failure of the mitochondria buffering system causes the cell to be highly vulnerable to mitochondria-mediated apoptosis (programmed cell death, discussed in the next section on mitochondrial pathobiology), and reactive oxygen species (Emerit et al., 2004). In addition, intracellular calcium can activate catabolic enzymes such as proteases that cause cell damage. In summary, permeable ionotropic AMPA receptors when persistently activated cause a self-perpetuating calcium dysregulation with toxic properties to motor neurons.

A role for the dysregulation of glutamate in ALS-mediated neurodegeneration has been established. Recent advances have contributed to a more comprehensive understanding of how glutamate signalling goes awry in ALS. Increased plasma levels of glutamate have been recently documented in ALS patients (Andreadou et al., 2008), supporting the glutamate excitotoxicity hypothesis along with earlier studies showing decreased glutamate uptake, altered glutamine

synthetase, and decreased expression levels of the glial glutamine transporter EAAT2 (Rothstein et al., 1992; Plaitakis et al., 1993; Rothstein et al., 1995).

2.3.3 Mitochondrial pathobiology

The roles of mitochondria are providing energy for the cell in the form of ATP, buffering intracellular calcium, and regulation of apoptotic cell death, all of which are critical for cell survival. As discussed previously, early signs of pathological mitochondria are observed as organelle swelling, broken outer membranes, vacuolar degeneration, and abnormal cristae (Wong et al., 1995; Sasaki et al., 2007). Recent studies have focused on the ALS-related functional disruptions in mitochondria. In sporadic ALS, progressive alterations in mitochondrial function were observed as a decrease in complex IV of the electron transport chain alterations in oxidative phosphorylation capacity (Echaniz-Laguna et al., 2006). Other studies suggested an increased production of reactive oxygen species as a result of calcium overload following excitotoxic stimulation of AMPA receptor (Carriedo et al., 2000), a model that links the hypotheses of excitotoxicity and oxidative damage due to mitochondrial dysfunction. This model has been demonstrated a more recent study showing mitochondria vulnerability by impaired intracellular calcium regulation and disruption of mitochondrial electrochemical potential (Jaiswal et al., 2009).

In SOD1 FALS, mitochondrial dysfunction is demonstrated by SOD1-mediated induction of morphological changes by binding to Bcl-2 and releasing cytochrome C (Pedrini et al., 2010). Mutant SOD1 was demonstrated to show preferred aggregation in the mitochondrial intermembrane space, causing neuronal toxicity and impaired mitochondrial dynamics (Magrane et al., 2009). In mutant SOD1 transgenic mice, decreases in the enzyme activities of the mitochondria electron transport chain have been demonstrated in the spinal cord at early ALS stages (Jung et al., 2002; Mattiazzi et al., 2002), implicating defective mitochondrial respiration and ATP synthesis and a cellular environment conducive to oxidative damage.

2.4 Insights from ALS-PDC on ALS heterogeneity

The clinicopathology of FALS shows remarkable heterogeneity. The recognizable motor phenotypes of ALS are heterogeneous, and consideration of them requires careful delineation of the body region of onset, the relative amount of upper to lower motor neuron involvement, and the rate of progression of disease. The body region of ALS onset is unpredictable but classifiable between limb onset and bulbar onset. The rate of disease progression is different for the ALS subtypes, with

bulbar onset showing the shortest disease duration to death. The relative mix of upper and lower motor neurons involvement is heterogeneous, and non-motor manifestations must be considered in some ALS cases, producing clinically overlapping combined disorders such as ALS with dementia or ALS without dementia but showing temporal lobe pathology compatible with ALS with dementia (Tsnchiya et al., 2002). One study described clinicopathological findings of SALS in a 60 year old man with upper limb onset, but post mortem analysis revealed predominant upper motor neuron involvement resembling primary lateral sclerosis with preservation of anterior horn cells (Tsuchiya et al., 1999). This finding is consistent with another study of eight atypical ALS patients with confined upper limb atrophy showing degeneration of the Betz cells of the motor cortex and spinal and brainstem motor neuron loss consistent with ALS (Sasaki et al., 1999b). However, some of the patients in this latter study showed anterior horn cell loss while the motor cortex and brainstem motor neurons were preserved, further supporting the view of ALS heterogeneity. Furthermore, while motor neuron loss is a consistent feature, clinical symptoms and post-mortem neuropathology can reveal variable outcomes even among the same family (Tanaka et al., 1984). The absence of an effective treatment can be explained in part by the complex and heterogeneous genetic, biochemical, and clinical features of ALS, and by the usually late onset of treatment. A better understanding of the possible common key features underlying the heterogeneity, namely concerning the focal process of motor neuron degeneration, may lead to further clarification of the neuropathology between individual ALS patients belonging to different ALS subtypes. Knowledge of the primary locus of disease expression may lead to more focused therapeutic trials and treatments.

While ALS is one of the more common motor neuron diseases, the recognition of disease variants and mimic syndromes may lead to further insights into possible causes for the general ALS syndrome. From a biochemical perspective, the mechanisms underlying motor neuron degeneration arenot yet completely understood and the multifactorial nature of ALS should be assessed in consideration of the clinical heterogeneity of ALS. As already discussed, several genes and environmental influences have been suggested as possible risk factors for ALS. It is possible that genetic causes of susceptibility to environmental toxins are responsible for heterogeneous expression of clinical symptoms. A better understanding of interactions between these suspected genetic causes and environmental risk factors and their influence (alone and in combination) on producing heterogeneous clinical features may lead to more clearly defined pathological profiles among individuals or groups of ALS patients and in turn lead to more focused therapeutic trials.

Guam ALS-PDC is a unique class amongst ALS variants, because the motor neuron disease component is clinically and neuropathologically identical to ALS. In summary, its features resembling ALS include demyelination of the lateral tracts, degeneration and loss of anterior horn cells, variable degeneration in the neurons of motor cortex, its recent identification as a TDP-43 proteinopathy, and the appearance of intracytoplasmic round hyaline inclusions. ALS-PDC has, to varying degrees, added clinical and neuropathological features of Parkinson's disease and Alzheimer's disease. Parkinson's disease features of ALS-PDC include common clinical manifestations of bradykinesia, rigidity, and shuffling gait, and the common neuropathological features are loss of pigmentation in substantia nigra and atrophy of the frontal and temporal lobes. Alzheimer's disease features of ALS-PDC include dementia, granuvacuolar degeneration of ganglion cells, and neurofibrillary tangles that are ultrastructurally, immunohistochemically, and biochemically identical to those of Alzheimer's disease. Since Guam ALS-PDC is characterized by numerous clinical and neuropathologic similarities to ALS, Parkinson's disease and Alzheimer's disease, this disorder provides a unique opportunity for a multi-level approach in determining dysfunction and degeneration of neurons in the related diseases.

Guam ALS-PDC may be seen as avaluable model for the major age-related neurodegenerative diseases and insights gained through the study of this disease will provide a valuable understanding of the analogous conditions encountered elsewhere. The interest in studying ALS-PDC lies in its expression of clinical correlations to other neurodegenerative diseases without a demonstrable genetic component or responsible gene mutation. In addition, its appearance in a concentrated disease cluster is also a valuable characteristic that make ALS-PDC an optimal research focus for gaining insight into the etiology of neurodegenerative diseases.Any detailed studies on gene and environment interactions must distinguish between susceptibility and variables that modify the phenotype. These may not be identical, that is, a factor that contributes to disease initiation may not necessarily modify the disease course. The study presented here establishes a structure and groundwork for further epidemiological and gene-environment research to determine the plausibility of an interaction between ALS genetic susceptibility and prognostic (environmental) variables.

Chapter 3. Motor Dysfunction and Spinal Motor Neuron Pathology

3.1 Introduction

Familial amyotrophic lateral sclerosis (FALS) is a progressivemotor neuron diseaseof premature degeneration of motor neurons invariably leading to death by respiratory failure. About 10% of all ALS cases are familial and ~20% of FALS cases are caused by mutations in SOD1 (Rosen et al., 1993) while the remainder are sporadic with no known cause. Motor neuron injury and cell death are unique and critical aspects common to both sporadic and familial ALS. In studies of SOD1G93A transgenic mice that model SOD1 FALS, functional deficits from vulnerable motor axon injuryoccurred early on during the presymptomatic period of disease (Frey et al., 2000; Fischer et al., 2004; Pun et al., 2006; Hegedus et al., 2007; Hegedus et al., 2008). Similar data have been observed in other lines of SOD1 ALS mice, with motor neuron injury causing significant motor unit loss during a presymptomatic window of time (Frey et al., 2000; Pun et al., 2006). However, purely genetic causal factors for ALS account for only a small fraction of all disease cases. As the causes for sporadic ALS have not been clearly identified, focus has been concentrated on the mechanisms of motor neuron diseases of genetic origin with the hope that findings can be applied to sporadic cases(Leigh, 2007; Shaw et al., 2007),but the link for translating FALS findings to sporadic ALS is controversial (Rakhit et al., 2004; Kwong et al., 2007; Mackenzie et al., 2007; Robertson et al., 2007).

While studies that focus on environmental causative agents are relatively few, studies that seek to find the link between environmental causation and genetic susceptibility are even scarcer (Shaw et al., 2008). Studies of the ALS disease cluster among the Chamorro people of Guam shortly after World War II provided evidence of environmental causation (Koerner, 1952; Kurland et al., 1954; Mulder et al., 1954). Similar to classical ALS, these Guamanian cases usually showed signs of upper and lower motor neuron lesions developing invariably during the course of the illness while extraocular muscle weakness and objective sensory deficits were absent (Stanhope et al., 1972; Brody et al., 1975). An atypical form of Parkinsonism that presented with dementia emerged also with high incidence, and all cases showed widespread expression of abnormal tau protein (Hirano et al., 1966). Consistent with environmental causation, consumption of flour made from cycad seeds has been a recognized feature of Chamorro culture for generations (Whiting, 1963), and active neurotoxins in the form of steryl glucoside variants contained in cycad seeds has have been identified (Khabazian et al., 2002; Shaw et al., 2006; Ly et al., 2007; Tabata et al., 2008). The cycad steryl glucosides are neurotoxic to primary neuronal and astroglial cultures (Khabazian et al., 2002) as well as to motor neuron-derived cell lines (Ly et al., 2007). Moreover, synthetic steryl glucosides fed to mice causes

motor deficits consistent with an ALS phenotype with progressive motor neuron loss in spinal cord and later cell loss in the striatum (Wilson et al., 2006a; Tabata et al., 2008). Collectively, these studies indicate a neurotoxic etiology to human disease in its various forms.

Although the foregoing evidence is compelling, it is still uncertain whether steryl glucosides are alone responsible for all the pathological outcomes or whether it works in conjunction with genetic susceptibility factors. Motor neuron loss in animal models is demonstrable by the cycad neurotoxins linked to Guamanian ALS and Parkinsonism (Wilson et al., 2002; Wilson et al., 2004). *In vivo* studies in adult CD-1 mice exhibited dramatic motor deficits followed by progressive cognitive dysfunction after 30 days of exposure to cycad flour (Wilson et al., 2002). Following 70 days of cycad feeding, quantitative magnetic resonance imaging in adult CD-1 mice showed decreased volumes in lumbar cord grey matter, substantia nigra, striatum, motor cortex, and basal nuclei (Wilson et al., 2004). Similar data has been reported for SOD1G93A mice without cycad exposure, where the primary difference involved decreases in spinal cord white matter volume in transgenic animals (Petrik et al., 2007). Based on these observations, I reasoned that the enhancement of an ALS-parkinsonism phenotype in an animal model of neurotoxin etiology could modify the onset and progression of disease symptoms in SOD1 transgenic mice affecting, in turn, the spinal microenvironment and neuronal morphology. The idea of genetic and environmental interplay has been an established focus for numerous studies, and is not limited to neurodegenerative diseases (Wang et al., 2000; Seltzer et al., 2004; van Dellen et al., 2005; Coppede et al., 2006; McOmish et al., 2007). To explore this possibility, I assessed the progressive changes in motor function in SOD1G37R mice and wild type littermates, noting neurobehavioural changes with synthetic cycad toxin exposure. The degree of lower motor neuron loss and the surviving motor neuron morphology were then evaluated by quantitatively measuring soma diameter in anterior horn cells of the lumbar spinal cord. In a variant experiment, I repeated this experiment in a cohort of the more widely studied mutant SOD1G93A mouse model of ALS. The results from this latter experiment are presented in Appendix C and contribute to the overall picture of gene-toxin interactions as will be discussed in the final chapter in relation to the main findings of this dissertation.

Genetic models of neurodegenerative disease are attractive in their reproducibility and predictability such that models of mutant SOD1 have quickly become the 'gold standard' in studying ALS. However, the clinical phenotype of ALS is heterogeneous, and mutant SOD1 mouse models

of ALS show unpredictably different phenotypes depending on transgene expression levels (Dalcanto et al., 1995), background strain and gender (Heiman-Patterson et al., 2005). Here I exploitedtransgenic mice harbouring SOD1G37R mutations akin to human FALS to examine neurotoxin interactions with a genetic causal factor. This low expressor line of mutant SOD1 mice develop a disease with a longer course, with disease onset at approximately 11 months of age (DalCanto et al., 1997). This lengthy disease course would allow more time for observation of cycad steryl glucoside toxicity. The cycad toxin used was a synthetic stigmasterol β-D-glucoside (SG) to ensure uniformity of toxicity as variances of SG concentration in cycad tissue and differential SG concentrations with cycad seed age have been reported (Marler et al., 2005a; Marler et al., 2009a). Using synthetic SG is an appropriate alternative to cycad from Guam and SG has been demonstrated to be an active toxin in cycad seeds (Wilson et al., 2002; Wilson et al., 2003; Tabata et al., 2008) and hence a valid reproduction to the environmental model of ALS-PDC.

3.2 Methods

3.2.1 Animals

A colony of mice heterozygous for the G37R mutation (line 29) of the human gene for SOD1, were obtained from the laboratory of Dr. Neil Cashman (Vancouver, BC, Canada). The original breeder mice were produced by Dr. D.W. Cleveland by microinjecting a plasmid encoding wild type human SOD1 contained within 12 kb genomic DNA fragment into hybrid (C57BL/6J x C3H/HeJ)F2 mouse embryos. The G37R mutation was introduced into the human SOD1 gene by PCR using a mutagenic primer (Wong et al., 1995). Transgenic mice from this founder line (line 29) express a moderate (7-fold) increase in SOD1 activity in spinal cord, with pathology restricted to motor neurons in the spinal cord and brainstem (Wong et al., 1995). The laboratory of Dr. Cashman maintained the transgene by breeding male hemizygotes to naive C57BL/6 dams, and continued until all progeny were on a pure C57BL/6 background. In this study, C57BL/6 +/+ female mice were paired with C57BL/6 $SOD1^{G37R}$/+ male hemizygous carriers and the progeny from the breeding were ear punched for genotyping at Transnetyx, Inc (Cordova, TN, USA). Non-transgenic littermates were used as controls. Animals were weaned at 3 weeks of age and housed individually at Jack Bell Research Centre (Vancouver, BC, Canada) at a constant temperature of 21 – 22°C and a 12-hour light/dark cycle. All procedures such as animal husbandry, treatment, and euthanasia were carried out in accordance with the regulations and guidelines of the Canadian

Council on Animal Care and National Institute of Health and approved UBC Animal Care protocols. For analysis of disease progression in a toxic-induced nervous system, transgenic animals and non-transgenic littermates at 10 weeks of age were started on a daily diet containing 42 mg of steryl glucoside per kilogram of body weight. The 10 week starting point for SG feeding allowed time for sufficient baseline motor behavioural testing after weaning at 3 weeks. The 42 mg/kg body weight dose of SG corresponds approximately to those reported in Tabata et al. (2008). However, in this study, toxin exposure was set at a fixed concentration and began at 5 months of age. The weight adjustment in this study was administered to ensure a consistent dosage corresponding to the size of the animal at specific ages, since animals in this study were followed up to 13 months of age. It is important to note that the pellet containing steryl glucoside was only a part of the overall diet, with the other part consisting of regular mouse chow. In the comparative study, age-matched transgenic animals and wild type littermates not receiving steryl glucoside but rather a placebo flour pellet were used. These control animals were maintained on a regular mouse chow diet of daily proportions equal in weight (and caloric value) to the diet containing toxin. Mice were considered at end stage of the disease when they were severely paralyzed and were unable to right themselves within 30 seconds when placed on their side.

3.2.2 Behavioural assessment

Animals were observed daily for development of tremor, weakness, and loss of weight. At regular 3 week intervals, starting at 4 weeks of age when no signs of disease symptoms were present and up to 51 weeks of age, animals were monitored for onset of disease phenotype.

The inverted wire hang test, used to evaluate grip endurance, was performed as described previously (McDonald et al., 2001). The task was performed by placing the mouse on a wire mesh, allowing the mouse to obtain its grip and then swiftly inverting the lid over an empty mouse cage to avoid injury. Latency to fall into the empty cage was measured with a stopwatch over a 120-second maximum test session, recorded in two separate trials with the average used in analyses. A clean wire mesh was used for each mouse. The trained experimenter was uninformed of genotypes.

Motor performance was monitored by Rotarod testing using an IITC Rotarod (IITC Life Science Inc., Woodland Hills, CA; #755). The rotarod is a suitable test for motor skill learning and general motor performance (Lalonde et al., 1995). Mice were placed on a partitioned rotating rod 1.25 inches in diameter and tested at a constant speed of 30 RPM. A non-accelerating rotarod has

been described previously to emphasize the test for motor skill learning and minimize the other factors (Shiotsuki et al., 2010). Animals fell onto a platform that is sensed by magnetic switches and the time that the animal remains on the rod (up to a maximum of 180 seconds) is displayed and recorded. Rotarod testing was performed on the same day as grip endurance testing.

An extension reflex of the hindlimbs is normally observed when a mouse is suspended in the air by the tail. In mice with motor neuron disease, a retraction of the hindlimb is more commonly observed (Barneoud et al., 1999). Scores for hind limb clasping reflex were recorded as described previously (Tabata et al., 2008). A perfect score of 4 was awarded when mice displayed normal bilateral hind limb extension. A score of 3 indicated one hind limb extended while the other limb showed tremors or quivers. Bilateral hind limb tremors or quivering was awarded a score of two. A score of 1 describes one hind limb fully retracted while the other shows tremors. Bilateral limb retraction indicates a score of zero. This method of scoring leg extension was more sensitive to subtle deficits with cycad feeding (Wilson et al., 2005), and was our modification of the more traditional two-point test.

Spontaneous locomotor activity and emotionality were evaluated by placing the animals in a circular open field arena for 5 minutes while monitored by an overhead CCD camera connected to a computer. The mice were placed individually into the centre of the arena and activity was recorded for a 5-minute period. Differences in exploratory behaviour were quantified by measuring the time spent in inner and outer zones of the open field (Spink et al., 2001). The signal was composed of a series of frames that were then digitalized, sent to the computer, detected, and several parameters were calculated from the resulting data. The signal was analyzed using Ethovision software (Noldus Information Technology, Leesburg, VA), a video tracking and movement analysis system. The parameters recorded were: distance moved, time in central zone, number of crossings to centre zone, and time in movement. Data were collected in one testing session at 5, 7, 9, and 12 months of age to compare activity prior to symptom onset, at the initial disease onset, and at end stage.

Detailed gait analysis was facilitated with a digital video camera mounted below an illuminated testing chamber that enclosed the animal on a clear treadmill (Mouse Specifics, Inc., Boston, MA). Digital recording image acquisition software was used to capture the raw video images and then exported to a gait analysis program (DigiGait 9.9, Mouse Specifics, Inc., Boston, MA). The animals were placed inside the illuminated testing chamber and the treadmill was started

at a walking pace. The speed of the treadmill was gradually increased to a maximum of 25 cm/sor the speed at which the mouse was still running consistently (i.e., straight line and at a fixed position relative to the camera), which was then the speed at which the mice were recorded for 450 frames. Therefore, the speeds used were between 10 cm/s and 25 cm/s. From this video clip, a portion of the video was selected in which the animal consistently stayed in the same position relative to the camera for at least 5 strides per paw. Locomotor speed can act as a confounder for the interpretation of gait data, and walking speeds have been reported as critical when evaluating hindlimb kinematics during gait (Costa et al., 2010). Therefore, the speeds used were between 10 cm/s and 25 cm/s. From preliminary experimentation of Bl6 mice, the slowest speed at which consistent running activity was obtained was 10cm/s and the fastest was 25 cm/s.

Mice were placed on a stationary treadmill, which was then accelerated to a maximum test speed of 25 cm/s for data collection. Each mouse was allowed 3 trials on the treadmill, and successful trials were ones in which the animal was able to maintain treadmill speed for greater than 3 seconds. The successful trials were recorded with digital video and analyzed. The analysis software outputs several parameters based on when individual paws are in contact with the treadmill: stride time, swing duration, stride length, stance duration, stance width, brake duration, stride frequency, and paw placement angles. Stride length is the distance between successive strides of the same paw and should be nearly equivalent between each paw of an animal in the absence of disease affecting gait. Stance width is the distance between both fore limbs or both hind limbs during stance. This distance was measured during peak stance while the animals were running on the treadmill. Paw angle measurements were useful to determine neuromuscular dysfunction, as a larger angle of the hind paws was associated with ataxia and demyelinating disease (Powell et al., 1999). Stride duration is the time for one paw to make a complete stride and is dependent on stride frequency. Swing duration is the length of time for one paw in swing phase (no contact with treadmill belt). A greater stride frequency corresponds to lower stride duration. Ventral plane videography was used to generate digital paw prints while the animals were in motion and to quantify temporal and spatial indices of gait dynamics in all experimental groups at the ages of 5, 7, 9, and 12 months. These time points were chosen to compare gait difference prior to disease onset, at the initial disease onset, and at end stage. Testing was less frequent to avoid habituation to the treadmill.

When progression of muscle weakness in these animals became prominent, behavioural testing was arrested and food was placed at the bottom of their cages together with transgel to provide hydration. Transgel was provided by the animal unit and contained approximately 70% water and contains hydrocolloids, potassium sorbate, phosphoric acid and a mixture of carbohydrates. Onset of the clinical disease was determined by the first appearance of hind limb tremors when lifted by the tail. At disease end stage, animals were monitored daily. A similar experimental end point was used for all animals (including non-transgenic animals for comparison), defined by the observation of one of the following criteria: 1. inability of the mouse to right themselves within 30 seconds when placed on their side; 2. loss of more than 20% of body weight; 3. complete paralysis of both hind limbs. Mice that have reached this end point were euthanized and scored as 'dead'. Hence when an animal has met the euthanasia criteria, its age at sacrifice was considered the survival time.

3.2.3 Synthesis of SG

Gram quantities of SG were purchasedfromNeurodyn Inc. (Charlottetown, PEI). In short, a multistep process converted non-glycosylated β-sitosterol into β-sitosterol glucopyranosyl. Fractions were screened for SG using thin layer chromatography to confirm its presence and purity. The compound was lyophilized with methanol and 0.5 M sodium methoxide for 24 hours at 85°C using a silica bath with an attached reflux condenser under nitrogen to deprotect the sugar hydroxyls. The next day, the solution was cooled to 4°C on ice. After adding cold methanol, the solution was filtered and the precipitate was collected in a round bottom flask. SG was purified by adding distilled deionized water, boiling to 120°C, cooling to room temperature, filtering, and washing again with deionized water. The precipitate was collected again, heated to 135°C in pyridine, cooled, and placed in the fridge overnight in deionized water. The next day, the precipitate was filtered with cold water followed by cold acetone, transferred into a scintillation vial and lyophilized using a vacuum desiccator overnight. Synthesized compounds were characterized using NMR analysis, and purity was confirmed by HPLC.

3.2.4 Tissue processing

All transgenic and non-transgenic animals were sacrificed at disease end-stage or experimental end stage, as described above. Animals were sacrificed by intracardial perfusion with phosphate buffered saline (PBS), pH 7.4, followed by fixation with cold 4% paraformaldehyde in PBS. Prior to perfusion, mice were anaesthetized with a sub lethal dose of halothane by inhalation.

The central nervous system (CNS), ventral roots, and gastrocnemius muscle were dissected out and post-fixed for 1 hour in fresh 4% paraformaldehyde. Tissues were cryoprotected in increasing concentrations of sucrose in PBS (5%, 10%, and 25%) for 1 hour at the first two concentrations and overnight at 4°C at the final concentration. Tissues were then frozen in OCT (Tissue Tek; Somagen Diagnostics, Edmonton, AB, Canada; #4583) compound in isopentane cooled on dry ice. Frozen tissues were stored at -80°C until cryosectioned at -20°C on a Leica cryostat (model CM3050 S). Serial sections (10 μm and 35 μm thick) were subsequently collected in 10 parallel sets onto Superfrost Plus microscope slides (Fisher Scientific, Ottawa, ON, Canada; #12-550-15), air dried and stored at -80°C until stained. Each set was stained with a different marker, and adjacent sets corresponded to adjacent sections.

3.2.5 CNS Immunohistochemistry

To determine disease progression in the mouse central nervous system, immunofluorescence with cell-specific antibodies in conjunction with Hoechst (Sigma; #33258) or Nissl staining was used. Table 1-1 lists the antibodies used in visualizing the CNS and Table 1-2 lists the secondary antibodies.

Table 3-1. Primary antibodies used in studying CNS.

Primary antibody	Detected antigen	Host	Concentration used	Source	Catalogue number
Polyclonal anti-ChAT	Motor neurons	Goat	1:100	Millipore, Billerica, MA	AB144P
Polyclonal anti-Iba1	Reactive microglia	Rabbit	1:200	Wako Chemicals, Richmond, VA	019-19741
Monoclonal anti-GFAP	Astrocytes	Mouse	1:100	Cell Signalling Technologies, Boston, MA	3670

Abbreviations used above: ChAT (Choline acetyltransferase), Iba1 (ionized calcium binding adapter molecule 1), GFAP (glial fibrillary acidic protein)

Table 3-2. Secondary antibodies used in this study.

Secondary antibody	Concentration used	Source	Catalogue number
FITC Goat anti-mouse	1:200	Jackson ImmunoResearch	115-096-003
FITC Rabbit anti-goat	1:150	Jackson ImmunoResearch	305-096-003
Alexa 488 Goat anti-rabbit	1:100	Invitrogen	A11008

In general, sections for immunofluorescence were initially air dried then washed 3 times in PBS (5 minutes per wash) at room temperature. Sections were then blocked in PBS containing 1% BSA, 0.1% Triton X-100, 0.05% Tween-20, and 10% normal goat serum (NGS; Vector Labs, Burlingame, CA #S-1000) or normal rabbit serum (Vector Labs, Burlingame, CA, #S-5000) for one hour at room temperature. When necessary, sections were also blocked in PBS containing 1:100 mouse IgG Fab fragments (Jackson ImmunoResearch; #015-000-007) following two PBS washes (2 minutes per wash). Sections were then washed two times again and incubated overnight at 4°C with the primary antibody diluted in PBS containing 1% BSA and 0.05% sodium azide. Sections were then rinsed 3 times in PBS and incubated for one hour at room temperature with the appropriate secondary antibody diluted in PBS. Following 3 PBS rinses, sections were stained in 4 μg/ml Hoechst 33258 for 10 minutes, rinsed in PBS, and mounted in 0.2% DABCO-glycerol. In negative controls, the primary antibody was omitted.

Sections for Nissl staining were initially air dried, fixed in 80% acetone for 2 minutes, and hydrated briefly in descending ethanol concentrations (95%, 70% and 50%). Sections were rinsed briefly in two changes of dH_2O, and then stained in 0.5% cresyl violet for 5 minutes at room temperature. Sections were rinsed briefly in dH_2O followed by 50% ethanol, then dehydrated in increasing ethanol concentrations (70% with 1% acetic acid, 90% and 100%) for 30 seconds each. Sections were then placed in xylene until clear and coverslipped with Permount mounting medium (Fischer Scientific, CAS 108-88-3).

3.2.6 Cell Quantification and Imaging

To quantify the amount of pathological marker labelling in the CNS, every tenth transverse section of lumbar cord between L3 and L5 was assessed. Quantification after immunohistochemistry was performed blind with respect to treatment and genotype using Adobe Photoshop CS3 (Version 10.0) on images captured on a Zeiss microscope (Axiovert 200M inverted;

Carl Zeiss, Thornwood, NY). Motor neurons in the ventral horn of lumbar cord were identified as ChAT-positive cells with Hoechst staining. All motor neurons were counted in the ventral horns of every tenth cord section. Motor neuron counts of ChAT-positive cells for each group were presented as a percentage of motor neuron numbers in controls. Motor neurons counts between groups were compared by the Student *t* test using Prism 5.0 (GraphPad Software, Inc.).

Soma measurements and morphological observations of Nissl-stained ventral horn cells were conducted in Motic software (Motic Images Advanced 3.2) on images captured on a Motic B5 Professional Series light microscope. Nissl-stained neurons were identified by the presence of an identifiable nucleolus and somata. Neurons in the ventrolateral and ventromedial quadrants of the ventral horn were classified as presumed motor neurons using the following criteria (Stephens et al., 2006): a single prominent nucleolus, coarse Nissl granules in the cytoplasm, and possessing 1–5 processes in the plane of section. This describes the morphology of a normal healthy cell. Anterior horn cells undergoing chromatolysis were studied and identified as cells appearing swollen with a pale cytoplasm and an eccentric nucleus.

Motor neuron diameters were measured by calculating the average length of two lines spanning the diameter of the cell and intersecting like crosshairs with the intersection point on the centre of the nucleus. Data were recorded in Microsoft Excel and statistical analysis was performed using Statistica 8.0 (StatSoft Inc., Tulsa, OK, USA). Statistics were calculated from 5 sections from each tissue examined per animal.

Quantification of astrocytes and microglia were recorded in the ventral horn of the lumbar enlargement at disease end-stage. Every tenth transverse section of lumbar cord between L3 and L5 was assessed. Quantification after immunohistochemistry was performed blind with respect to treatment and genotype using Adobe Photoshop CS3 (Version 10.0) on images captured on a Zeiss microscope (Axiovert 200M inverted; Carl Zeiss, Thornwood, NY). Astrocytes and microglia in the lumbar cord were identified as GFAP- and Iba1-positive cells with Hoechst staining, respectively. In brief, all astrocytes and microglia were counted as the number of fluorescent pixels in the standardized field of interest. Green or red pixels of GFAP- and Iba-positive cells, respectively, for each group were presented as a percentage of the total pixels, or the percent of fluorescent labelling. Motor neurons counts between groups were compared by the Student's *t* test using Prism 5.0 (GraphPad Software, Inc.).

3.2.7 Statistics

Data are presented as means ± standard error of the means (S.E.M.) as indicated.Statistical significance between groups on rotarod performance, wire hang test, leg extension test, and body weight measures were analyzed using a repeated measures ANOVA via Statistica8.0 statistical software (StatSoft Inc., Tulsa, OK) and graphed usingPrism 5 (GraphPad Software Inc., San Diego, CA). All results were analyzed to determine the effect of SG alone, G37R mutation alone, or the interaction between these two variables by ANOVA. Statistical significance between experimental and control groups for all other behavioural and histological assessments were calculated using a Student *t*-test. The *t* test was used when only two groups and one condition were compared, as in the case of the quantitative histological data. Distributions of Nissl stained soma diameters were tested for normality using a one-sample Kolmogorov-Smirnov test, and differences between groups for each sex and cell morphology were detected using one-way ANOVA. Following that, a post hoc test using multiple comparison Tukey HSD test was used to find out which groups were significantly different from controls. The analysis and graphs of distribution functions were computed by SPSS version 17.0 (New York, USA). Differences were considered statistically significant at $p < 0.05$. P values were expressed as exact values except in cases where $p < 0.0001$. The statistical content and methodology was reviewed by a statistician.

3.3 Results

3.3.1 Disease phenotype

The disease phenotype developed and progressed in a stereotyped fashion in SOD1G37R mice as described previously (Wong et al., 1995; DalCanto et al., 1997). The first consistent sign of disease was a fine consistent tremor that is observable in one or both hind limbs. This develops at around 11 months of age and is more obvious when mice are suspended by the tail. Proximal muscle weakness was observed although not pronounced in mice with tremor. Passive movement of the hind limbs in mice with tremor reveals wobbling and instability during locomotion. At this stage, the micewere still able to raise their pelvis from the cage surface to reach food and water during exploration.

As the disease progresses further, proximal muscle weakness and marked atrophy developed. Weakness and atrophy was more evident in the hind limbs usually than in the fore limbs. Mice were unable to raise their pelvis from the cage floor and any attempted forward movement occurs with

their forelimbs dragging their bodies across the floor. Transgenic mice appeared thin along their flanks while their coats developed a thick and coarse appearance due to impaired grooming. These mice extended their hind limbs less than normal during locomotion or when lifted by the tail. Once paresis was evident, animals were fed with food pellets and transgel placed on the floor of their cage.

At end stage disease, transgenic mice were severely paralyzed and lie slightly tilted towards one side. They were generally alert, but do not move in response to tapping on their cage or when gently prodded. When placed onto their side, the mice were unable to actively right themselves. Mice were euthanized when no longer able to right themselves within 30 seconds of being placed on their side. Paralysed hind limbs remained permanently extended both at rest and during limited locomotion. The degree of stiffness between paralysed hind limbs varied between animals. Within the last two weeks of their illness, the hind limb tremors became less apparent and another tremor of the distal joints of the toes developed that occurred in the absence of hind foot movement. In addition, some animals developed whole body tremors at rest. Roughly 30% of transgenic mice developed infections in one or more eyes, which was an indication of forelimb weakness restricting them from grooming their face. The mean age at which G37R mice reached end stage disease was 395 ± 10 days.

Clinical disease was observed only in mice expressing mutant SOD1G37R. Wild type SOD1 littermates remained free of clinical disease at 1 year of age.

3.3.2 Demonstrated motor deficits in motor behaviour

Significant motor deficits were observed in the behaviour tests that were performed, but the severity and onset of motor deficits differed between males and females. In all variables of motor behaviour under study, male and female animals were analyzed separately. The number of animals used in the analysis of behavioural studies is outlined in the following table.

Table 3-3. The number of animals used in behavioural analysis.

	Control-fed		SG-fed	
	Males	Females	Males	Females
mSOD1G37R	10	19	7	10
wt littermate	18	17	12	10

A greater number of female transgenic mice survived longer than their male counterparts, which allowed a longer duration of behaviour analysis for females without compromising the numbers of subjects in each group. Males were also tested until 51 weeks of age, but the diminished numbers of subjects in the mutant SOD1 groups and SG-fed wild type group resulted in animal numbers much less than those in the corresponding female groups. The numbers of surviving males in the experimental groups were insufficient for statistical analysis. Hence the data sets for male behavioural analysis were formulated to include only up to 30 weeks of age.

The performance on the rotarod of G37R transgenic mice was almost identical to wild type littermates for both sexes during the baseline testing between 4 to 10 weeks of age before commencement of SG treatment (Fig. 3-1). Motor coordination deficits on the rotarod began appearing in wild type mice 2 weeks after beginning SG treatment in males (Fig. 3-1A) and 8 weeks in females (Fig. 3-1B), reaching significance by 8 weeks of SG treatment in males ($p < 0.0001$) and 18 weeks in females ($p = 0.008$). Control-fed males showed a similar level of rotarod performance throughout the study, as demonstrated by a minimal decline in performance with increasing age (Fig. 3-1A). Significant main effects of SG diet ($F = 6.58$, $DF = 1$, $p = 0.01$) were observed in male mice while genotype effects were not yet significant ($F = 0.84$, $DF = 1$, $p = 0.36$) during the time points studied. In addition, there was an interaction between SG diet and G37R genotype ($F = 645.81$, $DF = 1$, $p < 0.0001$). In contrast, significant main effects of the G37R mutation were observed in female mice (Fig. 3-1B; $F = 13.03$, $DF = 1$, $p = 0.0004$). While SG-fed female wild types showed a decline in latency to fall compared to controls, this effect started after 40 weeks of age and was not significant ($F = 1.86$, $DF = 1$, $p = 0.17$). Similar to the male counterparts, an interaction between SG and SOD1G37R genotype was also observed in females ($F = 1699.02$, $DF = 1$, $p < 0.0001$).

The performance on the wire hang of G37R transgenic mice was almost identical to wild type littermates for both sexes during the baseline testing between 4 to 10 weeks of age before commencement of SG treatment (Fig. 3-2). Grip endurance deficits on the wire hang began appearing in wild type mice 2 weeks after beginning SG treatment in males (Fig. 3-2A) and 17 weeks in females (Fig. 3-2B), reaching significance by 8 weeks of SG treatment in males ($p < 0.0001$) and 38 weeks in females ($p = 0.002$). Male mice exposed to SG were significantly impaired compared with controls (Fig. 3-2A; $F = 4.75$, $DF = 1$, $p = 0.03$). A significant genotype × diet interaction was detected in males ($F = 804.5$, $DF = 1$, $p < 0.0001$). However, genotype effects were not significant ($F = 2.14$, $DF = 1$, $p = 0.14$). In female mice, significant main effects of SG diet ($F = 11.47$, $DF =$

1, p = 0.0008) and G37R genotype (F = 5.69, DF = 1, p = 0.02) were observed (Fig. 3-2B). Similar to males, there was a significant genotype ×diet interaction (F = 2224.18, DF = 1, p < 0.0001). Although the effect of SGfeeding in male wild type mice was evident earlier than females, the diet effects in females achieved greater statistical significance. Wire hang performance in male wild type controls was almost identical to G37R controls after 20 weeks (Fig. 3-2A), while female wild type controls showed little impairment throughout the behavioural study (Fig. 3-2B). This sex difference between wild type controls affects the degree of significance measured in experimental groups.

Leg extension reflexes of G37R transgenic mice were almost identical to wild type littermates for both sexes during the baseline testing between 4 to 10 weeks of age before commencement of SG treatment (Fig. 3-3). The ability of G37R and SG-fed mice to demonstrate the extension of hindlimbs decreased as a function of age. The muscle endurance and motor coordination impairments described above were accompanied by a loss of the extension reflex (Fig. 3-3). Extension reflex deficits began appearing in wild type mice 2 weeks after beginning SG treatment in males (Fig. 3-3A) and 20 weeks in females (Fig. 3-2B), reaching significance only in females by 26 weeks of SG treatment (p = 0.048). Unlike the behavioural performances described above for male mice, significant effects of both SG diet (F = 22.54, DF = 1, p < 0.0001) and G37R genotype (F = 28.13, DF = 1, p < 0.0001) were observed (Fig. 3-3A). In addition, males showed a significant interaction between genotype and diet (F = 1180.49, DF = 1, p < 0.0001). Similar data was observed for female mice (Fig. 3-3B), with significant main effects of both SG diet (F = 17.79, DF = 1, p < 0.0001) and G37R genotype (F = 18.51, DF = 1, p < 0.0001). Females also showed significant interaction between genotype and SG diet (p < 0.0001). Continued SG exposure in male and female wild type mice resulted in a decreased leg extension score similar to control-fed G37R groups.

Changes in body weight are a common feature of ageing. Body weight of G37R transgenic mice were almost identical to wild type littermates for both sexes during the baseline testing between 4 to 10 weeks of age (Fig. 3-3). Body weight in male mice showed a significant overall difference in G37R mice (Fig. 3-4A; F = 36.73, DF = 1, p < 0.0001). However, SG-fed males did not show significant body weight changes (F = 0.36, DF = 1, p = 0.55) although a significant interaction between genotype and diet was detected (p < 0.0001). Female mice showed similar data, with a significant main effect of genotype (F = 9.08, DF = 1, p = 0.003) and a significant genotype × diet interaction (p < 0.0001). Female mice also showed a significant main effect of diet (F = 18.0, DF =

1, $p < 0.0001$). All animals gained weight steadily over time as expected and weights were comparable between sexes and conditions.

Figure 3-1. Rotarod performance at 30 rpm and the effects of mutant SOD1 and SG diet. The effect of G37R transgene and SG exposure on the average time to fall off the rotarod in male (A) and female (B) mice. SG-fed males showed significant performance deficits while the performance of SG-fed females was not significantly different from controls. A significant effect of the G37R genotype was evident only in females. A significant genotype × diet interaction was observed in both sexes. Data are reported up to 30 weeks of age for male mice and 51 weeks for females. Note maximum time is 180 seconds and weeks 4 to 10 represent baseline performance before SG feeding in all animals. See Table 3-3 for the number of animals per group. Data are expressed as mean ± S.D. *Significant motor coordination deficits in SG-fed wild types compared to wild type controls.

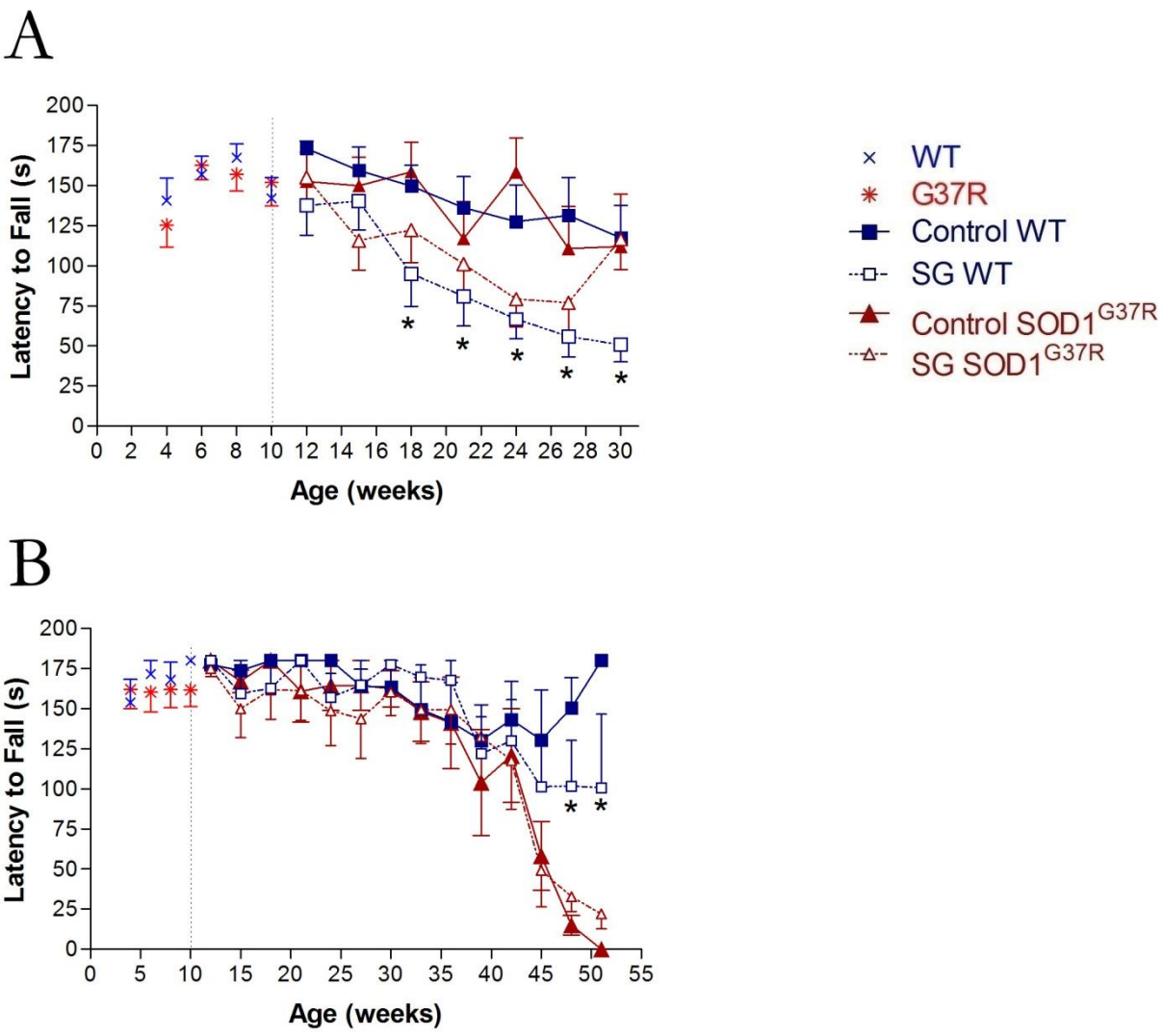

Figure 3-2. Wire hang performance for G37R and SG-fed mice.

The effect of G37R transgene and SG exposure on the ability to hang by all four limbs from a suspended wire mesh for male (A) and female (B) mice. SG-fed males and females showed significant performance deficits compared from controls. A significant effect of the G37R genotype was evident only in females. A significant genotype × diet interaction was observed in both sexes.Data are reported up to 30 weeks of age for male mice and 51 weeks for females. Note maximum time is 120 seconds and weeks 4 to 10 represent baseline performance before SG feeding in all animals. See Table 3-3 for the number of animals per group. Data are expressed as mean ± S.D. *Significant motor coordination deficits in SG-fed wild types compared to wild type controls.

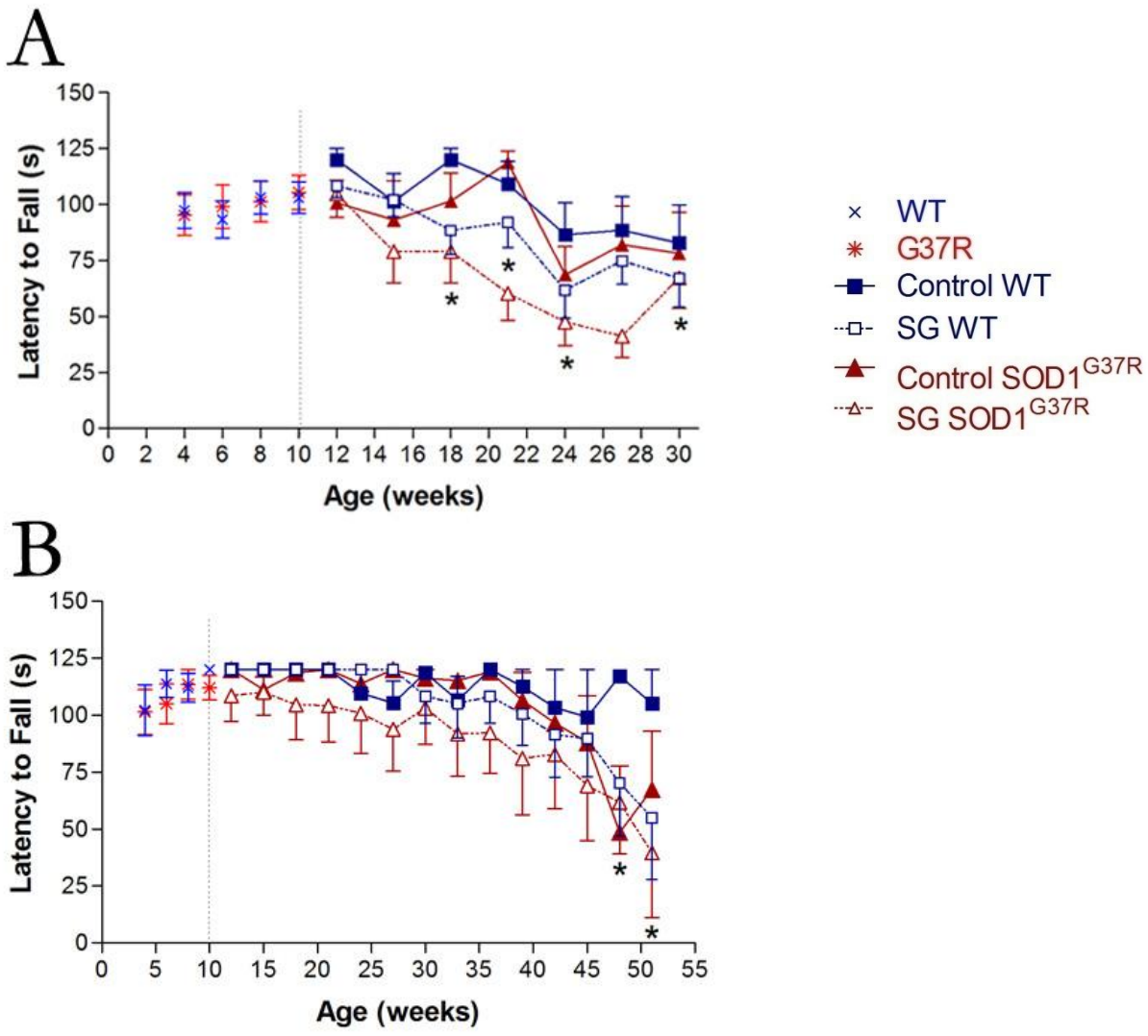

Figure 3-3. Evaluation of the extension reflex in the different experimental groups.

The effect of G37R transgene and SG exposure on the progressive loss of reflex as a function of age for male (A) and female (B) mice. Significant main effects of SG exposure and G37R genotype was observed in both sexes. A significant genotype × diet interaction was also observed in both sexes. Data are reported up to 30 weeks of age for male mice and 51 weeks for females. Note weeks 4 to 10 represent baseline performance before SG feeding in all animals. See Table 3-3 for the number of animals per group. Data are expressed as mean ± S.D. *Significant motor coordination deficits in SG-fed wild types compared to wild type controls.

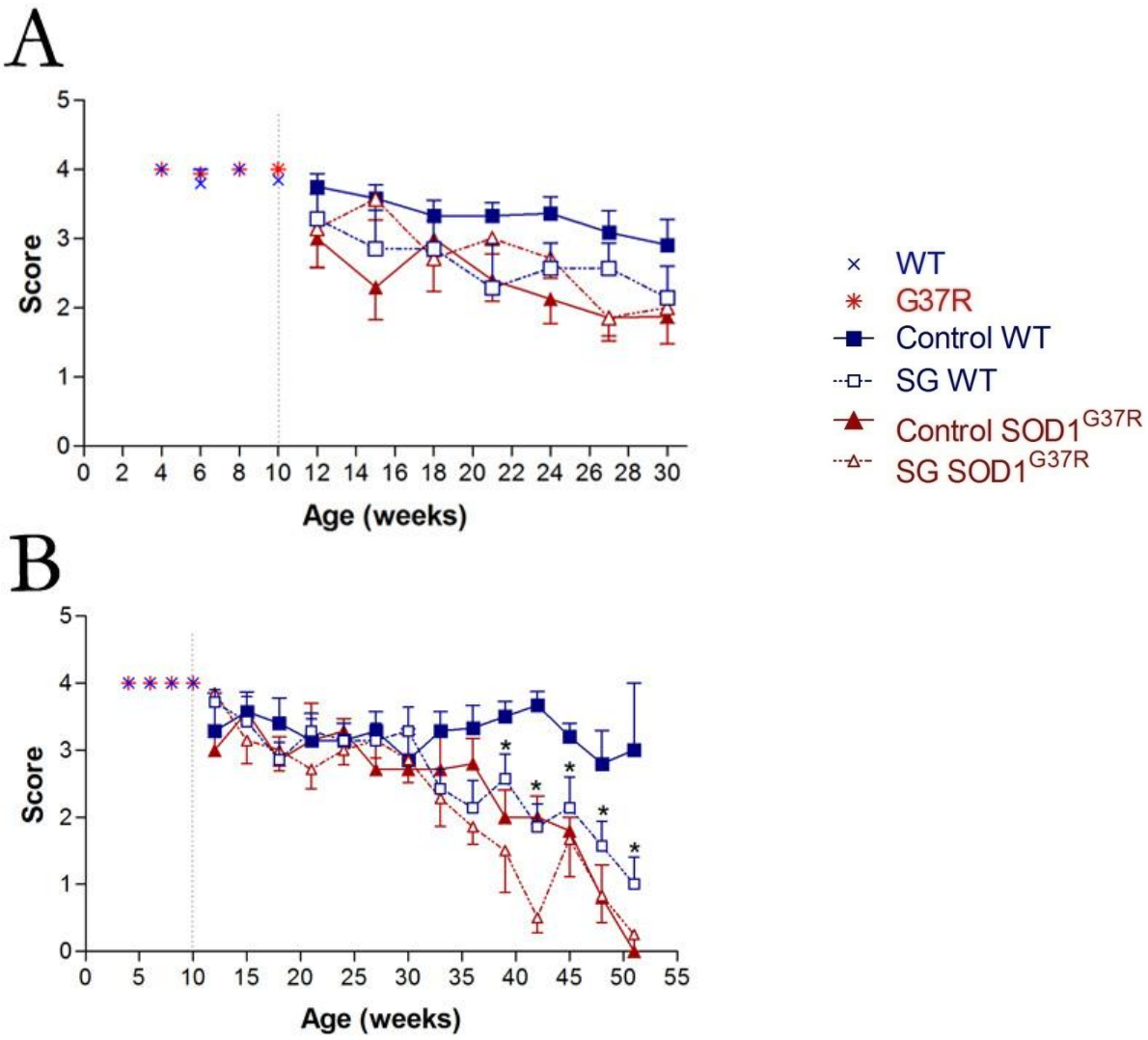

Figure 3-4. Measures of body weight changes over time in male and female mice.

Body weight as a function of age for male (A) and female (B) mice. Significant main effects of genotype and a significant genotype × diet interaction was observed in both sexes. Female mice also showed a significant SG diet effect. Data are reported up to 30 weeks of age for male mice and 51 weeks for females. Note weeks 4 to 10 represent baseline performance before SG feeding in all animals. See Table 3-3 for the number of animals per group. Data are expressed as mean ± S.D.

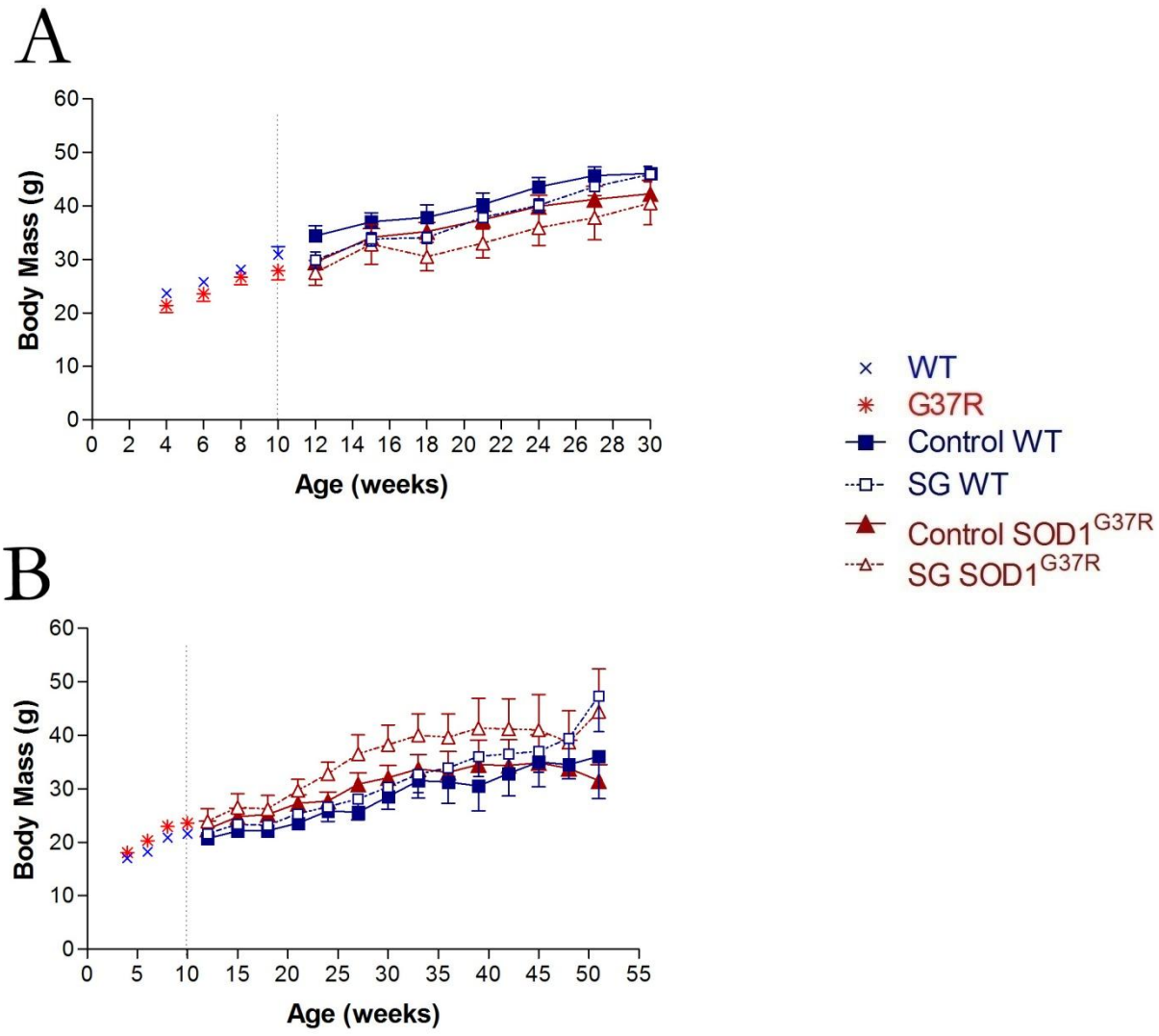

3.3.3 Detailed gait analysis

Changes in gait indices as measured by ventral plane videography were reported in various mouse models of Parkinson's disease (Amende et al., 2005) and gait deterioration was observed at disease onset as a consequence of nerve injury in the mSOD1G93A mouse model of ALS (Wooley et al., 2005). However, gait dynamics have not been described for environmental mouse models of motor neuron disease, or genetic mouse models of ALS involving gene-environment interactions.

Gait dynamics were comparable between G37R and wild type littermates. Animals received their first exposure to the gait testing equipment at 5 months of age before onset of symptoms. However, a majority of the animals were uncooperative to perform on the treadmill. At 9 months and especially at 12 months of age, a majority of mSOD1G37R animals were either unable to run at speeds as low as 10 cm/second or simply uncooperative to perform on the treadmill. As a result, subject numbers were lacking in the experimental groups at the 5 month, 9 month and 12 month testing age. Hence the data collected for mice at this age were not included in the study. Results from gait analyses at 7 months of age were analyzed in detail.

Impairment of the stride length appeared in wild type ($p = 0.002$) and G37R ($p = 0.003$) males with SG exposure (Fig. 3-5A and Table 3-4). A significant main effect for SG diet was observed in male mice ($p = 0.0006$), but the interaction between diet and genotype was not significant ($p = 0.23$). In addition, significant stride length impairment was observed in SG-fed G37R males compared to their control-fed counterparts ($p = 0.003$). Data in female mice showed a significant interaction between diet and genotype ($p = 0.03$), although stride length measurements of G37R and SG-fed female mice were comparable to control-fed wild type littermates ($p = 0.62$ and $p = 0.29$, respectively). Overall measures of stride length were greater in females than in males (Table 3-5). Impairments in stride frequency showed similar patterns as stride length impairments for both sexes (Fig. 3-5B). Significant stride frequency impairment was observed in SG-fed G37R males and SG-fed wild types compared to wild type controls ($p = 0.02$ and $p = 0.0001$, respectively). Significant main effects for SG diet ($p < 0.0001$) and G37R genotype ($p = 0.043$) were observed for stride frequency in male mice, but with no significant diet × genotype interaction ($p = 0.89$). Data in female mice showed no differences in stride frequency measurements of G37R or SG-fed mice compared to control wild types ($p = 0.1$ and $p = 0.51$, respectively). The diet and genotype interaction for stride frequency was also not significant in females ($p = 0.18$). Male mice exhibited

an overall shorter stride length and lower stride frequency than female mice and exposure to SG increased these gait indices to levels comparable to the average values of all female groups.

Changes in stance width were minimal and occurred in male mice only (Fig. 3-6 and Table 3-4). Average stance width measurements between front and rear paws for female experimental groups were comparable to control-fed wild types. The changes in stance width for male mice were minimal, with a trend towards an increased stance width in the forelimbs of SG-fed G37R males. Although a Student's *t* test indicated a significant increase in stance width for this group ($p = 0.04$), it is likely due to the relatively small standard error and not reflective of a true difference. As expected, the stance width of the fore limbs was less than the hind limbs for both sexes.

Splay angles were measured from the digital paw prints to define and quantify fore limb and hind limb orientation in degrees (Fig. 3-7). Splay angle, otherwise known as paw placement angle, is defined as the angle the paw makes with the long axis of the direction of motion. Paw placement angles were not significantly different between the genotypes or with exposure to SG. In male mice, all three groups exhibited similar front and hind paw angles during locomotion (Fig. 3-7 and Table 3-4). In addition, there was no interaction between diet and genotype for paw angle measurements in the fore limbs or hind limbs ($F = 0.9$, $DF = 1$, $p = 0.35$). Similar data for female mice were observed in both front and hind limbs during locomotion (Fig. 3-7 and Table 3-5). Paw angle measurements in female mice also did not show a significant interaction between diet and genotype ($F = 0.23$, $DF = 1$, $p = 0.63$).

The duration of time spent in the stride, stance, and swing phases of hind limbs during locomotion is a sensitive measurement to evaluate gait abnormalities. An effect of SG diet was observed in stride duration in male mice (Fig. 3-8 and Table 3-4; $F = 18.2$, $DF = 1$, $p < 0.0001$) while genotype effects were not significant ($F = 3.55$, $DF = 1$, $p = 0.06$). No interaction between diet and genotype was observed ($F = 0.13$, $DF = 1$, $p = 0.72$). Data for stance duration in male mice was similar, with a significant SG effect ($F = 15.2$, $DF = 1$, $p = 0.0002$) in the absence of diet genotype interaction ($F = 1.51$, $DF = 1$, $p = 0.22$). Swing duration in male mice showed a significant main effect of diet ($F = 10.15$, $DF = 1$, $p = 0.002$) and genotype ($F = 6.87$, $DF = 1$, $p = 0.01$). However, the diet × genotype interaction was not significant ($F = 0.66$, $DF = 1$, $p = 0.42$). These changes were expected since male groups exposed to SG showed significant increases in stride frequency (Figure 3-5B). The corresponding female groups showed only significant genotype

effects in stride ($F = 4.0$, $DF = 1$, $p = 0.05$) and stance ($F = 4.51$, $DF = 1$, $p = 0.04$) durations (Fig. 3-8 and Table 3-5). Swing duration in female mice did not show any diet ($F = 0.07$, $DF = 1$, $p = 0.8$) or genotype effects ($F = 1.0$, $DF = 1$, $p = 0.31$). Similar to male mice, data in females did not show a significant diet genotype interaction in any of these parameters ($p = 0.32$ for stride, $p = 0.58$ for stance, and $p = 0.1$ for swing duration). In addition, when compared to G37R controls, G37R female mice receiving toxin showed a significant increase in stride and stance duration ($p = 0.01$ and $p = 0.04$, respectively), resulting in a duration comparable to control-fed wild types. Although this increase in stride length may suggest that SG rescued the G37R phenotype, female mice showed no other changes in gait dynamics. Control-fed mutant females showed a slightly longer stride length (Fig. 3-5A) with no changes in stride frequence (Fig. 3-5B) compared to wild types, and hence these mice compensate by decreasing stride and stance duration. Therefore, the data observed in Fig. 3-8 for female mice point out significant decreases in durations for control-fed mutants due to a compensatory mechanism, resulting in significant differences compared to their SG-fed counterparts.

Quantitative summaries and comparisons of gait parameter outputs from the analysis program are represented in Table 3-4 for male mice and Table 3-5 for female mice. When front paw and hind paw gait parameters were averaged together several of the measures exhibited significant differences in male mice. These differences were chiefly in SG-fed male groups, and included stride frequency, stride duration, stance duration, and swing duration. Brake duration, stance width, and paw placement angle were not different between groups.

Figure 3-5. Stride length and stride frequencyat age 7 months for G37R and wild type mice. The effect of G37R transgene and SG exposure on stride length (A) and stride frequency (B) was measured by ventral plane videography using Digigait software and technology. Significant main effects of SG exposure on stride length were observed in male mice only. Similar data was observed for stride frequency in male mice. No significant changes in stride length or frequency were observed between different female groups. See Table 3-3 for the number of animals per group. Data are expressed as mean ± SEM.

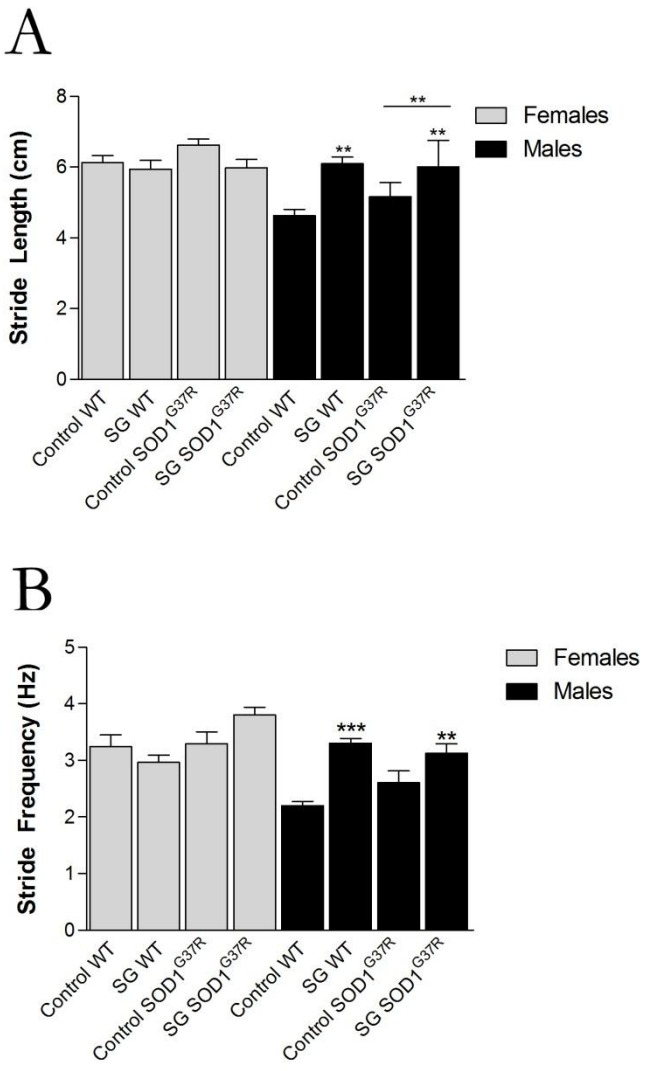

Figure 3-6. Effect of SG exposure and G37R transgene on forelimb and hindlimb stance width. Changes in forelimb and hindlimb stance width was measured by ventral plane videography using Digigait software and technology. No significant changes in stance width were observed between different male and female groups. See Table 3-3 for the number of animals per group. Data are expressed as mean ± SEM.

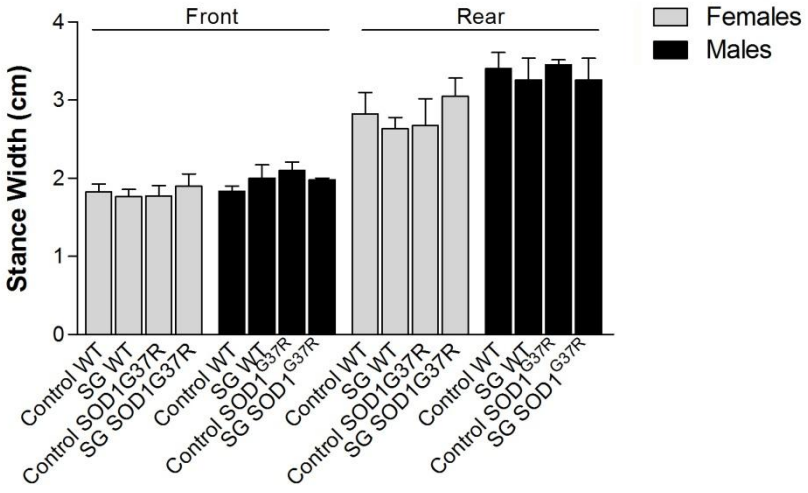

Figure 3-7. Effect of SG exposure and G37R transgene on forelimb and hindlimb angles. Placement angles between forelimbs and hindlimbs were measured by ventral plane videography using Digigait software and technology. No significant changes in paw placement angle were observed between different groups of both sexes. No significant interaction between diet and genotype was found in the fore limbs or hind limbs. See Table 3-3 for the number of animals per group. Data are expressed as mean ± SEM.

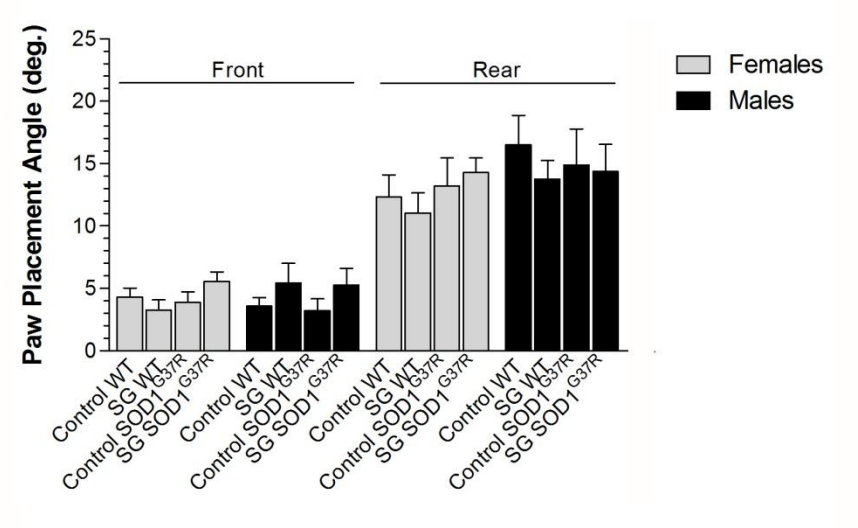

Figure 3-8. Effect of SG exposure and G37R transgene on gait parameters at age 7 months. Significant main effects of SG exposure were observed for stride and stance duration. Significant main effects of both SG and G37R transgene were observed for swing duration in males. Significant main effects of genotype were observed only for stride and stance duration in female mice. SG-fed G37R females also showed significant increases in stride duration and stance duration when compared to control fed G37R counterparts. No significant interaction between diet and genotype was observed for these parameters in both sexes. See Table 3-3 for the number of animals per group. Data are expressed as mean ± SEM.

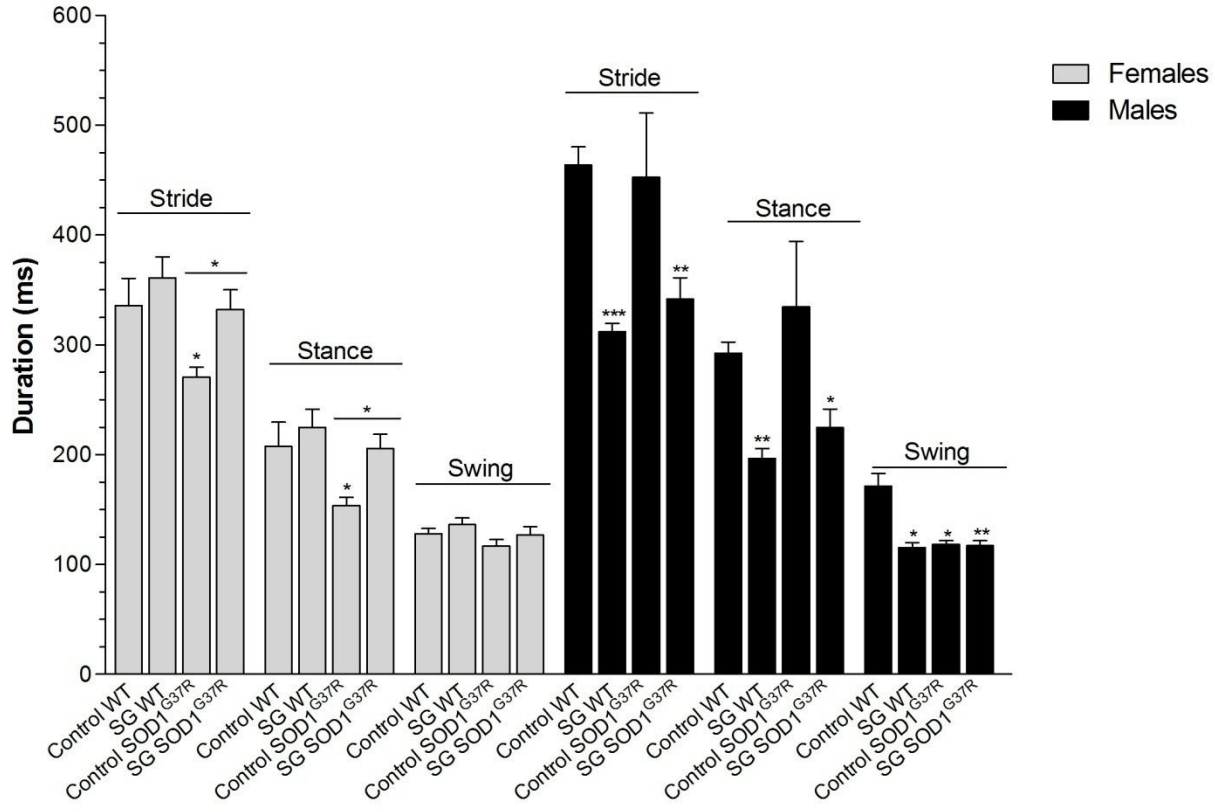

Table 3-4. Gait parameters in male mice walking at a maximum speed of 25 cm/s.

Male Mice	Control treated			SG-fed			
	Wild type (n = 5)	G37R (n = 5)	p value	Wild type (n = 5)	p value	G37R (n = 5)	p value
Stride length (cm)	4.6 ± 0.2	5.2 ± 0.4	0.3	6.1 ± 0.2	**0.002**	6.0 ± 0.7	**0.003**
Stride Frequency (steps/s)	2.2 ± 0.1	2.6 ± 0.2	0.4	3.3 ± 0.1	**0.0001**	3.1 ± 0.1	**0.02**
Stride Duration (ms)	464 ± 17	453 ± 58	0.8	312 ± 8	**0.0002**	342 ± 19	**0.01**
Stance Duration (ms)	292 ± 10	335 ± 59	0.5	197 ± 9	**0.001**	225 ± 17	**0.01**
Swing Duration (ms)	171 ± 12	118 ± 4	**0.01**	115 ± 4	**0.01**	117 ± 5	**0.005**
% Brake Duration in Stride	10.8 ± 1.5	18.2 ± 4.7	0.2	10.2 ± 1.4	0.8	13.3 ± 1.2	0.2
% Brake Duration in Stance	17.3 ± 2.0	25.5 ± 5.2	0.2	17.1 ± 2.8	0.9	20.8 ± 2.2	0.3
Forelimb Stance Width (cm)	1.8 ± 0.1	2.1 ± 0.1	0.1	2.0 ± 0.2	0.5	2.0 ± 0.1	**0.04**
Hind limb Stance Width (cm)	3.4 ± 0.2	3.5 ± 0.1	0.8	3.3 ± 0.3	0.7	3.3 ± 0.3	0.7
Forelimb Paw Placement Angle (deg.)	3.6 ± 0.7	3.2 ± 0.9	0.8	5.4 ± 0.6	0.4	5.3 ± 1.3	0.4
Hind limb Paw Placement Angle (deg.)	16.5 ± 2.3	14.9 ± 2.9	0.7	13.8 ± 1.5	0.3	14.4 ± 2.2	0.5

Means ± SEM. P values as compared to control-fed wild type mice; values in bold are significant.

Table 3-5. Gait parameters in female mice walking at a maximum speed of 25 cm/s.

FemaleMice	Control treated			SG-fed			
	Wild type (n = 5)	G37R (n = 5)	p value	Wild type (n = 6)	p value	G37R (n = 6)	p value
Stride length (cm)	6.1 ± 0.2	6.6 ± 0.2	0.2	5.9 ± 0.2	0.6	5.9 ± 0.2	0.8
Stride Frequency (steps/s)	3.2 ± 0.2	3.3 ± 0.2	0.1	3.0 ± 0.1	0.5	3.8 ± 0.1	0.9
Stride Duration (ms)	336 ± 25	271 ± 9	**0.01**	362 ± 19	0.5	332 ± 18	0.9
Stance Duration (ms)	208 ± 22	154 ± 7	**0.04**	225 ± 17	0.5	205 ± 13	0.8
Swing Duration (ms)	128 ± 5	117 ± 6	0.2	136 ± 6	0.9	127 ± 8	0.6
% Brake Duration in Stride	18.5 ± 2.6	14.5 ± 1.8	0.2	14.4 ± 1.8	0.2	18.8 ± 2.7	0.9
% Brake Duration in Stance	31.7 ± 4.5	26.0 ± 3.2	0.3	22.5 ± 2.1	0.05	29.5 ± 3.5	0.7
Forelimb Stance Width (cm)	1.8 ± 0.1	1.8 ± 0.1	0.8	1.7 ± 0.1	0.7	1.8 ± 0.1	0.7
Hind limb Stance Width (cm)	2.8 ± 0.3	2.7 ± 0.3	0.7	2.6 ± 0.1	0.5	3.0 ± 0.2	0.5
Forelimb Paw Placement Angle (deg.)	4.2 ± 0.7	3.9 ± 0.8	0.7	3.3 ± 0.8	0.4	5.5 ± 0.7	0.3
Hind limb Paw Placement Angle (deg.)	12.3 ± 1.7	13.1 ± 2.2	0.8	11.0 ± 1.6	0.6	14.2 ± 1.1	0.4

Mean ± SEM. P values as compared to control-fed wild type mice; values in bold are significant.

3.3.4 Open field and central zone activity

The open field activity (Fig. 3-9A) showed reduced locomotion in G37R male fed control ($p = 0.001$) and SG diet ($p = 0.01$) at age 7 months compared to wild type controls. Significant main effects of genotype were observed in male mice ($F = 5.17$, $DF = 1$, $p = 0.03$), but the interaction between diet and genotype was not significant ($F = 0.2$, $DF = 1$, $p = 0.64$). The total distance traveled was not significantly different between female groups (Fig. 3-9A). No significant effects of SG ($F = 0.04$, $DF = 1$, $p = 0.84$) or genotype ($F = 0.37$, $DF = 1$, $p = 0.55$) were observed in female mice, and the diet genotype interaction was also not significant ($F = 0.03$, $DF = 1$, $p = 0.87$).

In the open field, a decrease in the amount of time spent in the center of the arena was observed for G37R male mice with SG exposure (Fig. 3-9B; $p = 0.03$), but the treatment with SG did not influence the time spent in central zone for wild type males ($p = 0.94$). A significant diet × genotype interaction was observed for males ($F = 4.7$, $DF = 1$, $p = 0.038$). In contrast, each factor alone, genotype ($F = 0.07$, $DF = 1$, $p = 0.79$) and diet ($F = 0.23$, $DF = 1$, $p = 0.63$), does not affect the center zone duration in males. Control-fed mutant females spent less time in the central zone compared to all other groups, but this difference was not significant ($p = 0.68$). Female groups showed no interaction between diet and genotype ($F = 0.57$, $DF = 1$, $p = 0.46$). Similarly, each factor alone, genotype ($F = 0.05$, $DF = 1$, $p = 0.82$) and diet ($F = 0.04$, $DF = 1$, $p = 0.84$) does not affect the center zone duration in females.

The number of crossings into the center of the open field was analyzed in the same way as for the time spent in the center. Exposure to SG did not influence the number of entries into the central arena for female mice (Figure 3-9C). SG-fed female groups showed a slight increase in the number of centre crossings, but this change was not significant ($p = 0.37$). SG-fed G37R females also showed a slight increase in number of entries to the central zone, but this change was also not significant ($p = 0.82$). The SG diet ($F = 0.21$, $DF = 1$, $p = 0.65$) and G37R genotype ($F = 0.2$, $DF = 1$, $p = 0.66$) did not affect the number of entries into the central arena in female groups; interaction between these two variables was not significant ($p = 0.99$).

Male experimental groups made overall fewer passes to the centre arena overall compared to female mice (Fig. 3-9C). SG-fed wild type males showed a non-significant trend towards decreased crossing into the centre zone compared to wild type controls ($p = 0.09$). G37R control males showed decreased passes to the centre of the arena ($p = 0.03$), and this effect was less pronounced

in SG-fed G37R males ($p = 0.03$). No main effects on the number of central zone crossings were found for the SG diet ($F = 0.14$, $DF = 1$, $p = 0.71$) or the genotype ($F = 1.8$, $DF = 1$, $p = 0.18$); interaction between these two variables was also not significant ($F = 0.35$, $DF = 1$, $p = 0.56$).

In summary, male mutants spend less time in locomotion and make less passes to the centre arena. Exposure of SG toxin to male G37R mice gives similar results, in addition to a significantly less time spent in the centre zone. Therefore, the G37R mutation caused impairments in ambulatory activity at 7 months of age and increased anxiety as indicated by their preference for the arena perimeter. These results may indicate pathological changes in their exploratory nature and their ability to adapt to new environments. Although chronic SG exposure did not influence open field activity in wild types, it influenced the time spent in the centre zone in G37R males. This observation indicates a higher level of anxiety compared to control-fed mutant males which made a comparable number of passes to the centre but spent just as much time in the centre as controls.

Open field activity for female mice were largely unimpressive with no significant changes in any of the parameters studied. This observation indicates that female mice do not show ambulatory impairments at 7 months of age due to either the mutation or chronic SG exposure. It is possible that female mice may show similar impairments at later time points.

Figure 3-9. Open field locomotion at age 7 months for G37R and wild type mice fed SG. Exploratory locomotion was measured over a 5 minute session in an automated open field environment using the Noldus tracking system with overhead camera monitoring. The total distance parameter (A) represents horizontal ambulatory locomotion. Female mice showed no significant differences in total distance traveled between groups. G37R males showed less total distance traveled than wild type littermates. Mean time spent in the central zone (B) was reduced only in G37R males fed SG. Mean number of crossings into central zone (C) was reduced only in G37R male mouse groups. Data are expressed as mean ± SEM.

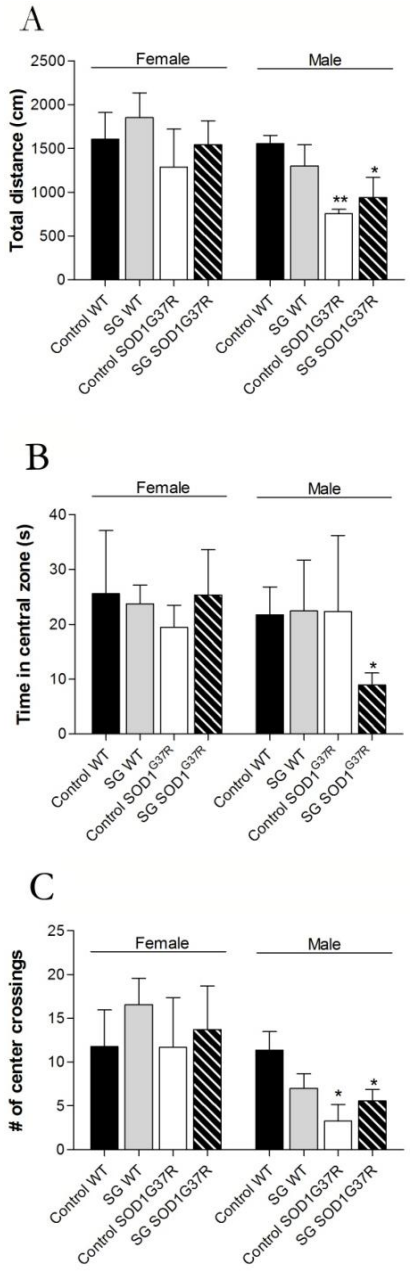

3.3.5 Motor neuron degeneration

All transgenic and non-transgenic animals were sacrificed at disease end-stage or experimental end stage, as described above in the Methods. Mice that have reached this end point were euthanized and tissues were collected. The average age of sacrifice was 366 ± 9 days for males and 378 ± 5 days for females.

The motor neuron count of cholinergic ChAT-positive cells in the anterior lumbar spinal cord is shown in Figure 3-10L. At end-stage disease and after prolonged SG exposure, in comparison with wild type controls, significant decreases in cell count were found in G37R controls ($p = 0.019$ for males, $p = 0.0017$ for females) and SG-fed G37R mice ($p = 0.0034$ for males, $p = 0.0008$ for females). However, no significant difference was found in SG-fed wild types ($p = 0.12$ for males, $p = 0.09$ for females), although the cell count was noticeably smaller in this group for both sexes (26% decrease compared to controls). A severe reduction in the number of ChAT-immunoreactive neurons in SOD1 transgenic mice was expected compared to control mice (Dalcanto & Gurney, 1994a; Dalcanto & Gurney, 1994b; Morrison et al., 1998). One-way ANOVA showed no significant main effects of the SG diet in males ($F = 2.7$, $DF = 34$, $p = 0.16$) or in females ($F = 1.7$, $DF = 40$, $p = 0.15$). Significant main effects were observed for genotype in both males ($F = 1.2$, $DF = 34$, $p = 0.002$) and females ($F = 1.04$, $DF = 40$, $p = 0.0002$). Analysis of gene × diet interaction showed no significance in males ($F = 0.27$, $DF = 1$, $p = 0.61$) and females ($F = 0.01$, $DF = 1$, $p = 0.91$). However, when all the animals from both sexes were combined, significant main effects of both diet ($p = 0.007$) and genotype ($p < 0.0001$) were found. In contrast, no significant diet × genotype interaction was observed ($p = 0.66$).

The distribution of motor neurons (Figure 3-10A, C, E, G) shows the location of motor neurons in the anterolateral portion of the ventral horn corresponding to Rexed lamina IX. Representative micrographs of ChAT-positive cells in the ventral lumbar horn are viewed at 40x and shown in Figures 3-10B, D, F, H. In the SG-fed wild type group, fewer numbers of motor neuronswere observed in this area (Fig. 3-10D) and the surviving motor neurons were located more dorsally (Fig. 3-10C) when compared to controls. Fewer surviving motor neurons were observed in G37R spinal cords with (Fig. 3-10G, H) and without (Fig. 3-10E, F) exposure to SG. The pattern of motor neuron loss in G37R animals appeared to be more uniform, and the surviving motor neurons were observed in the anterolateral horn of lumbar cord (Fig. 3-10E, G).

Representative micrographs of pathological features associated with motor neurons viewed at 100x are shown in Figures 3-10I, J, K. Some surviving motor neurons in the control and SG-fed G37R lumbar cords showed morphological features including motor neurons with "ghost cell" appearance (Fig. 3-10J) and motor neurons with shrunken somata (Fig. 3-10K) compared to normal rhomboid or round shaped cells in controls (Fig. 3-10I). The appearances and numbers of motor neurons were not significantly different betweenthe left and right ventral horns (data not shown).

Nissl staining of lumbar spinal cord sections showed that all groups exhibited morphologically abnormal cells that appeared to be undergoing degeneration among healthy cells (Fig. 3-11). Morphologically abnormal cells were observed as achromasia/chromatolysis accompanied with an eccentric nucleus and peripheral displacement of Nissl substance (Fig. 3-11F) and occasionally neurons with shrunken somata (Fig. 3-11D). Similar to those observed with ChAT immunofluorescence, a number of Nissl stained neurons exhibited a "ghost cell" appearance (Fig. 3-11H) which appeared to be the beginning stages of chromatolysis. Since morphological changes to neurons were observed in all groups, Nissl staining was used to correlate the numbers of pathologic motor neurons with their soma size in each corresponding group. Virtually all wild type control mice showed clusters of apparently normal (healthy) motor neurons with dark Nissl staining and a well-defined nucleus in the ventrolateral lumbar horn (Figure 3-11A, B). SG-fed wild type mice also showedclusters of healthy motor neurons, some with dispersed Nissl staining indicative of chromatolysis among healthy motor neurons (Figure 3-11C). G37R ventral lumbar horns showed the greatest paucity in motor neuron numbers (Figure 3-11E, G).

The graph of motor neuron number showed a normal distribution of Nissl stained neuronal diameters for malemice (Kolmogorov-Smirnov test, $p > 0.01$) while soma diameters in female mice did not show a normal distribution (Kolmogorov-Smirnov test, $p < 0.01$; Table 3-6, Fig. 3-12). Nevertheless, the data set for males and females showed a similar mean and standard deviation in soma diameter distribution (Table 3-6), and hence a normal distribution was assumed for female data. The frequency distributions of neuronal diameters within each cell morphology in wild type or G37R mice were different between males and females. The cell diameters for female and male mice are presented in Figs. 3-13 and 3-14, respectively, for direct comparison of the distributions broken down by cell morphology between experiment groups. In female mice, neurons with an apparently normal morphology have a wide distribution of cell diameters in all groups (Fig. 3-13A – D), with 18% of the motor neurons in the two wild type groups having a soma diameter between 25 and 30

μm as compared to 13% and 11% in the control- and SG-fed G37R groups, respectively. Chromatolytic motor neurons in SG-fed G37R female mice showed a small range of diameter (Fig. 3-13H), while all other groups showed a comparable wide distribution (Fig. 3-13E – G). SG-fed wild type females showed fewer chromatolytic motor neurons having a diameter between 25 and 30 μm (3% compared to 6% in controls). Female G37R groups showed a smaller range in shrunken somata diameters (Fig. 3-13K, L) compared to wild type groups (Fig. 3-13I, J). Nissl stained neurons with shrunken somata having a diameter between 25 and 30 μm were observed in similar ratios between female mouse groups. Table 3-7 summarizes the frequency of healthy (apparently normal), chromatolytic, and shrunken neurons having a soma diameter between 25 and 30 μm expressed as a percentage of total motor neurons broken down by group and sex.

Table 3-6. One-sample Kolmogorov-Smirnov test for normalityof cell diameter distribution

Female (n = 2495)			Male (n = 1700)		
Normal Parameters[1,2]	Mean	24.4946	Normal Parameters[1,2]	Mean	25.8356
	S.D.	7.08027		S.D.	7.42697
Most Extreme Differences	Absolute	0.044	Most Extreme Differences	Absolute	0.034
	Positive	0.044		Positive	0.034
	Negative	-0.036		Negative	-0.022
Kolmogorov-Smirnov Z		2.202	Kolmogorov-Smirnov Z		1.387
Asymp. Sig. (2-tailed)		**0.000**	**Asymp. Sig. (2-tailed)**		**0.043**

[1] Test distribution is Normal; [2] Calculated from data. The n value denotes the total number of Nissl stained cells counted.

Frequency distribution data showed similar trends in male mice with the main difference in apparently normal neurons. The wild type male groups showed a similar wide distribution of motor neurons with apparently normal morphology (Fig. 3-14 A, B), with approx. 20% of the motor neurons in the two wild type groups having a soma diameter between 25 and 30 μm. In the G37R male groups, the distribution for healthy neurons was skewed towards smaller diameters (Fig. 3-14C, D), with 7% of the motor neurons in the control-fed G37R group having a soma diameter between 25 and 30 μm and 3% in the SG-fed G37R group. Chromatolytic motor neurons in SG-fed G37R male mice showed a small range of diameter (Fig. 3-14H), while all other groups showed a comparable wide distribution (Fig. 3-14E – G). SG-fed wild type males showed fewer chromatolytic motor neurons having a diameter between 25 and 30 μm (2% compared to 4% in controls). Male G37R groups showed a smaller range in shrunken somata diameters (Fig. 3-14K, L) compared to

wild type groups (Fig. 3-14I, J). Nissl stained neurons with shrunken somata having a diameter between 25 and 30 μm were observed more frequently in wild type male groups than in G37R male groups (see Table 3-7).

The reduced proportion of large diameter motor neurons lumbar ventral horn of G37R and/or SG-fed groups and the consequent significant reduction in cell diameter range are further illustrated in the cumulative distribution functions (Fig. 3-15). A significant leftward shift of the cumulative distribution function in SG-fed wild type ($p < 0.001$), control-fed G37R ($p = 0.001$), and SG-fed G37R ($p < 0.001$) female mice indicates a decline in soma diameters of neurons with an apparently normal morphology (Fig. 3-15A). Chromatolytic neurons also showed significant leftward shifts in the cumulate distribution in both the SG-fed groups ($p < 0.001$, wild type SG; $p = 0.01$, G37R SG), while significant leftward shift of the control-fed G37R mice was not significant ($p = 0.328$; Fig. 3-15B). No significant shifts of the cumulative frequency histogram were observed in shrunken neurons between groups (Fig. 3-15C). Data for significant leftward shift revealed similar results in male mice, with the exception of two differences. Significant leftward shifts in the cumulative distribution of healthy neurons were greater between male groups (Fig. 3-15D) than females, and chomatolytic neurons only showed leftward shifts in the cumulative distribution of in SG-fed G37R mice (Fig. 3-15E) compared to controls. Table 3-8 summarizes multiple comparisons of cumulative frequency histograms between groups, broken down by sex and cell morphology.

Table 3-7. Ratios of Nissl stained neurons with a soma diameter between 25 and 30 μm

	Total cells	healthy	chromatolytic	shrunken
Males				
WT Control	671	20.0%	4.5%	3.6%
WT SG	564	20.6%	1.9%	2.6%
G37RControl	334	7.2%	12.6%	0.3%
G37R SG	161	3.1%	3.7%	0.6%
Females				
WT Control	1112	17.6%	6.0%	2.1%
WT SG	796	17.8%	3.3%	1.9%
G37RControl	500	13.2%	5.4%	0.8%
G37R SG	80	11.2%	5.0%	1.2%

Table 3-8. Significant differences in cumulative frequency of cell diameter

		Group A	Group B	Mean Difference (A-B)	Std. Error	Sig.
Female	Healthy	WT control	WT SG	1.90404‡	0.33439	0.000
			G37R control†	2.38695‡	0.40984	0.000
			G37R SG†	3.14666‡	0.83560	0.001
		G37R control	G37R SG	0.75971	0.87442	0.821
	Chromatolytic	WT control	WT SG†	3.86972‡	0.85381	0.000
			G37R control	1.36135	0.80405	0.328
			G37R SG†	7.51196 ‡	2.40517	0.010
		G37R control	G37R SG	6.15062	2.44841	0.059
	Shrunken	WT control	WT SG	0.91126	1.03601	0.815
			G37R control	1.23046	1.16837	0.718
			G37R SG	2.95917	2.05953	0.478
		G37R control	G37R SG	1.72871	2.20323	0.861
Male	Healthy	WT control	WT SG†	3.53183‡	0.43672	0.000
			G37R control†	6.40946‡	0.64949	0.000
			G37R SG†	6.83329‡	0.63974	0.000
		G37R control	G37R SG	0.42383	0.80981	0.953
	Chromatolytic	WT control	WT SG	2.62669	1.20977	0.133
			G37R control	-0.32220	0.95462	0.987
			G37R SG†	5.55371‡	1.88347	0.018
		G37R control	G37R SG	5.87590‡	1.83170	0.008
	Shrunken	WT control	WT SG	1.26020	1.01737	0.603
			G37R control	2.74375	1.74477	0.397
			G37R SG	1.08518	2.34086	0.967
		G37R control	G37R SG	-1.65857	2.70299	.928

† Indicates groups that were found to show significant leftward shift compared to WT controls.
‡Denotes significant mean difference at the 5% level. Data expressed as multiple comparison using Tukey HSD post hoc test.

Figure 3-10. Motor neuron lossobserved in the ventral lumbar horn.

Representative micrographs of ChAT immunostaining in lumbar spinal sections of control and G37R transgenic mice. A – D illustrates ChAT-positive cell distribution and number in the lumbar cord of control-fed wild type (A,B) and SG-fed wild type (C,D) mice. E – H illustrates ChAT-positive distribution and number in the lumbar cord of control-fed G37R (E, F) and SG-fed G37R (G, H) mice. In wild type controls, motor neurons are widely distributed in the left and right ventral lumbar horn (A) and have a distinct nucleus identified with Hoechst staining (B). In SG-fed wild types, motor neuron loss is noticeable from the most ventral portion of the left and right lumbar horns (C) and surviving motor neurons also have a distinct nucleus identified with Hoechst staining (D), although cell loss was not significant in this group for both sexes. The number of ChAT-positive neurons is significantly reduced in control-fed (E, F) and SG-fed (G, H) transgenic micecompared with control wild types. Motor neurons in control lumbar cords showed healthy motor neuron morphology and ChAT expression (I) while ChAT expression in "ghost cell" (J) and shrunken (K) motor neurons were observed mostly in transgenic lumbar cords.Data on graph (L) presented as ratio of motor neuron numbers compared to wild type controls ± SD. When motor neuron counts from both sexes were combined, a significant main effect was observed for both diet and genotype. Scale bars are 300 μm in the upper micrographs (10x magnification), 60 μm in the lower micrographs (40x magnification), and 30 μm in I, J, and K (100x magnification).

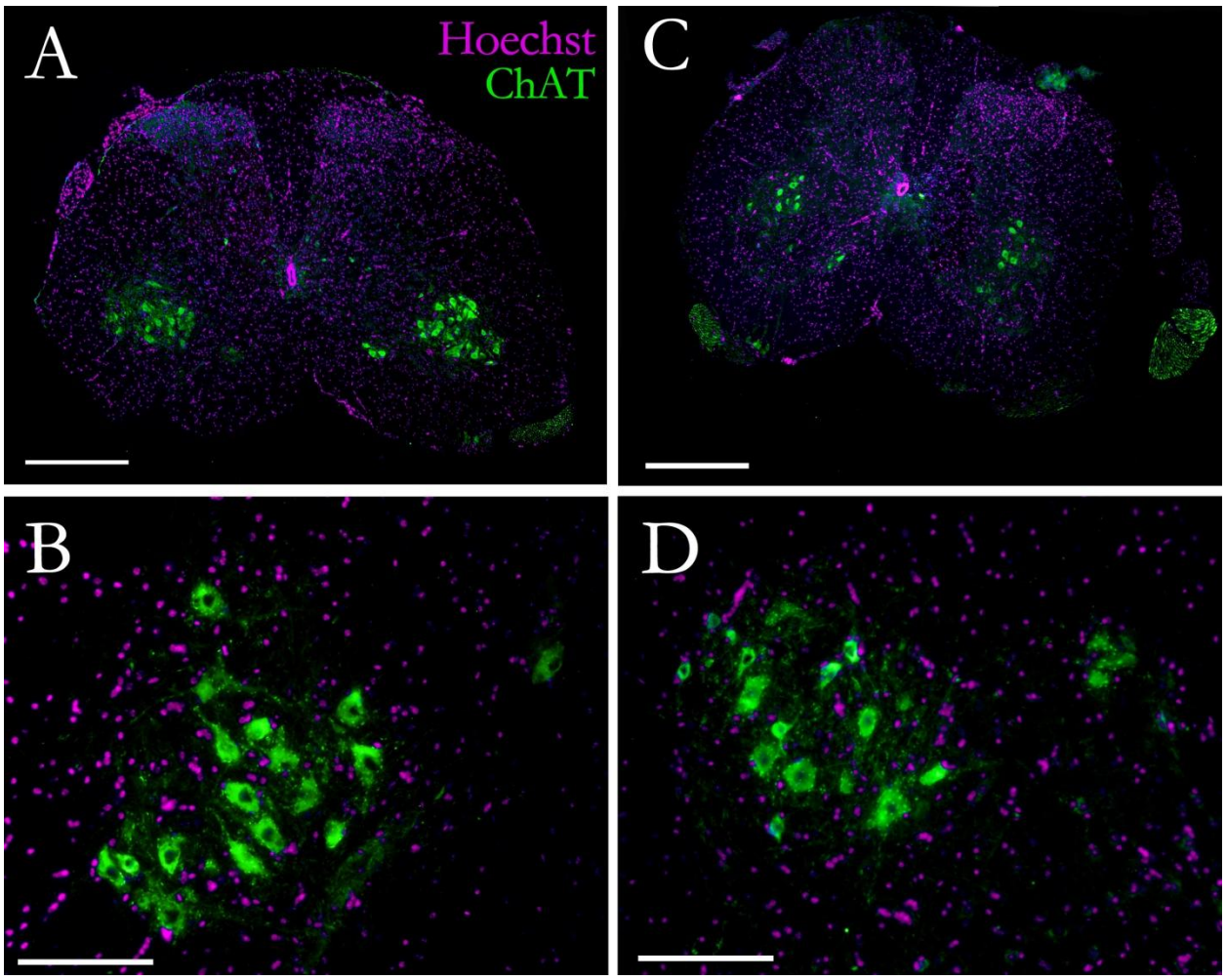
A
Hoechst
ChAT
C
B
D

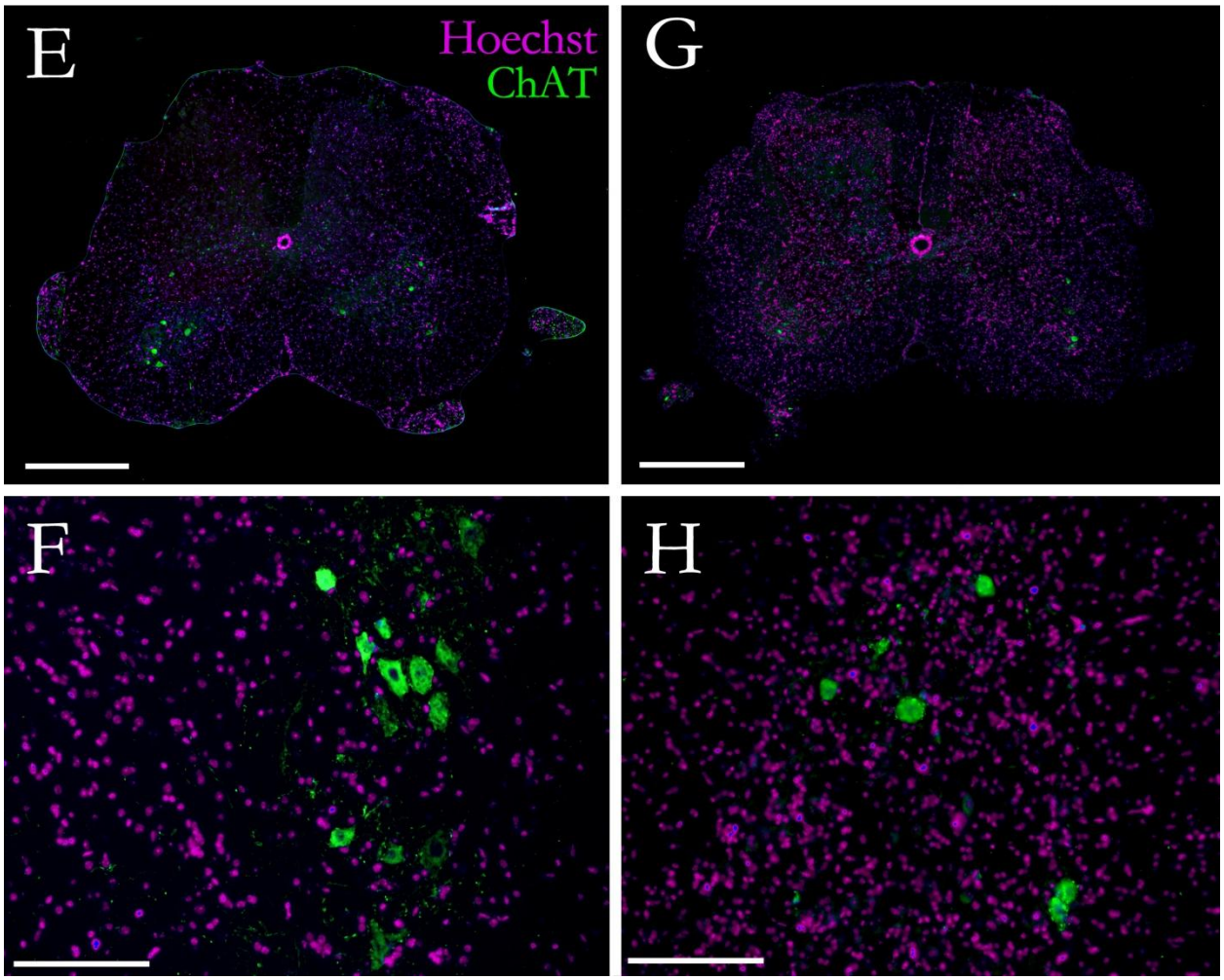
E
Hoechst
ChAT
G
F
H

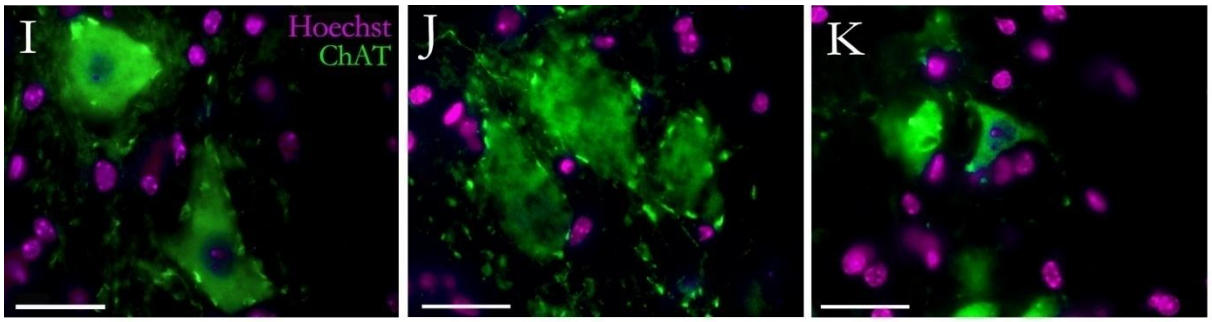
I
Hoechst
ChAT
J
K

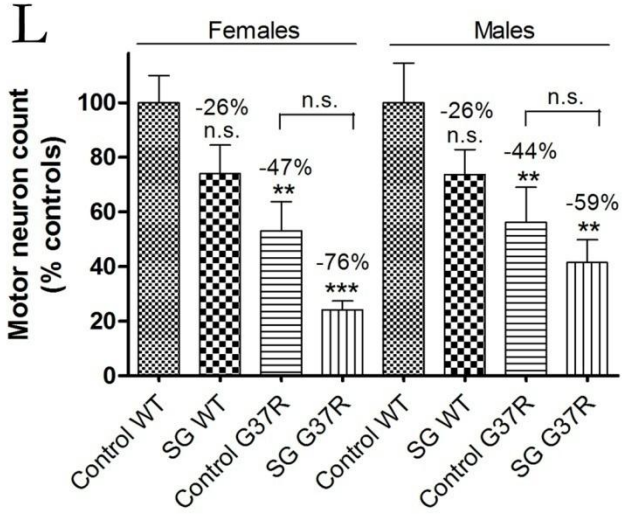
L
Females
Males
Motor neuron count (% controls)
100
80
60
40
20
0
-26%
n.s.
-47%
**
-76%
***
n.s.
-26%
n.s.
-44%
**
-59%
**
n.s.
Control WT
SG WT
Control G37R
SG G37R
Control WT
SG WT
Control G37R
SG G37R

Figure 3-11. Morphological changes in motor neurons in the ventral horn of the spinal cord. Nissl-stained sections from the ventrolateral horn of the lumbar cord enlargement of control-fed wild type (A), SG-fed wild type (C), control-fed G37R (E) and SG-fed G37R (G) mice. Neuron density in the ventral horn of the transgenic mouse (E, G) is reduced compared with the control (A). B – H are representative higher power micrographs of the ventral horn in the corresponding group of the upper panels. Morphologically abnormal cells are clearly evident at this magnification, and shrunken (D), chromatolytic (F), and ghost cell appearances (H) are observed among apparently healthy cells (B), although not limited to these corresponding experimental groups. See text for more details. Scale bars = 60 μm in upper panels, 30 μm in lower panels. (A – G original magnification 40x; B – H original magnification 100x)

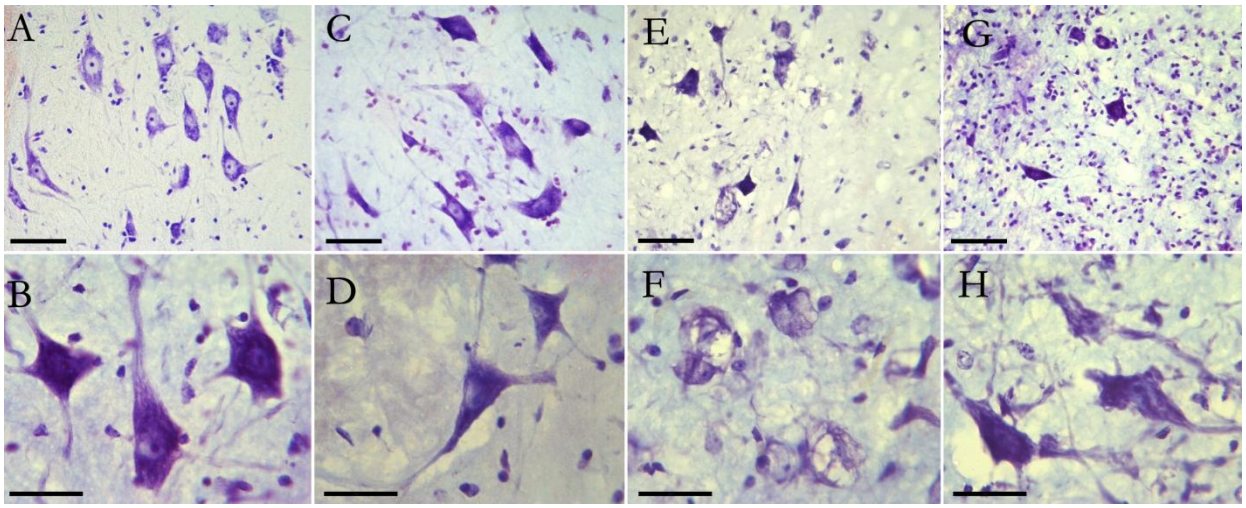

Figure 3-12. Frequency distribution of motor neuron soma diameters.

Histogram representing the distribution of Nissl stained neuronal diameters in the ventral lumbar horn of female (A) and male (B) mice. The data shows a normal distribution in the males only, and a comparable mean for both sexes (see Table 3-6 in text).

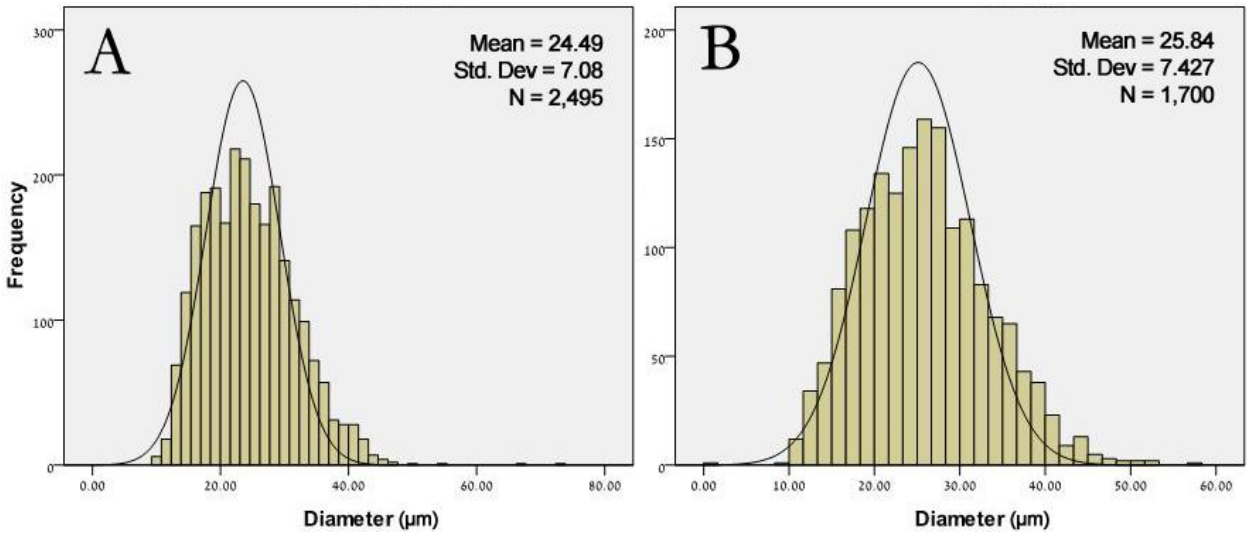

Figure 3-13. Changes in the frequency distribution of motor neuron sizes in females. All groups showed a similar wide distribution of motor neurons with apparently normal morphology; the mean soma diameter was consistently between 23 and 25 μm for each group. In the SG-fed G37R mouse the distribution was skewed toward smaller motor neuron soma diameters with chromatolytic morphology; the mean soma diameter was 23.2 μm compared to 30.8 μm for wild type controls. In the control-fed and SG-fed G37R mouse the distribution was also skewed toward smaller soma diameters with shrunken morphology; the mean soma diameter was 20.3 and 18.6 μm, respectively, compared to 21.6 μm for wild type controls.

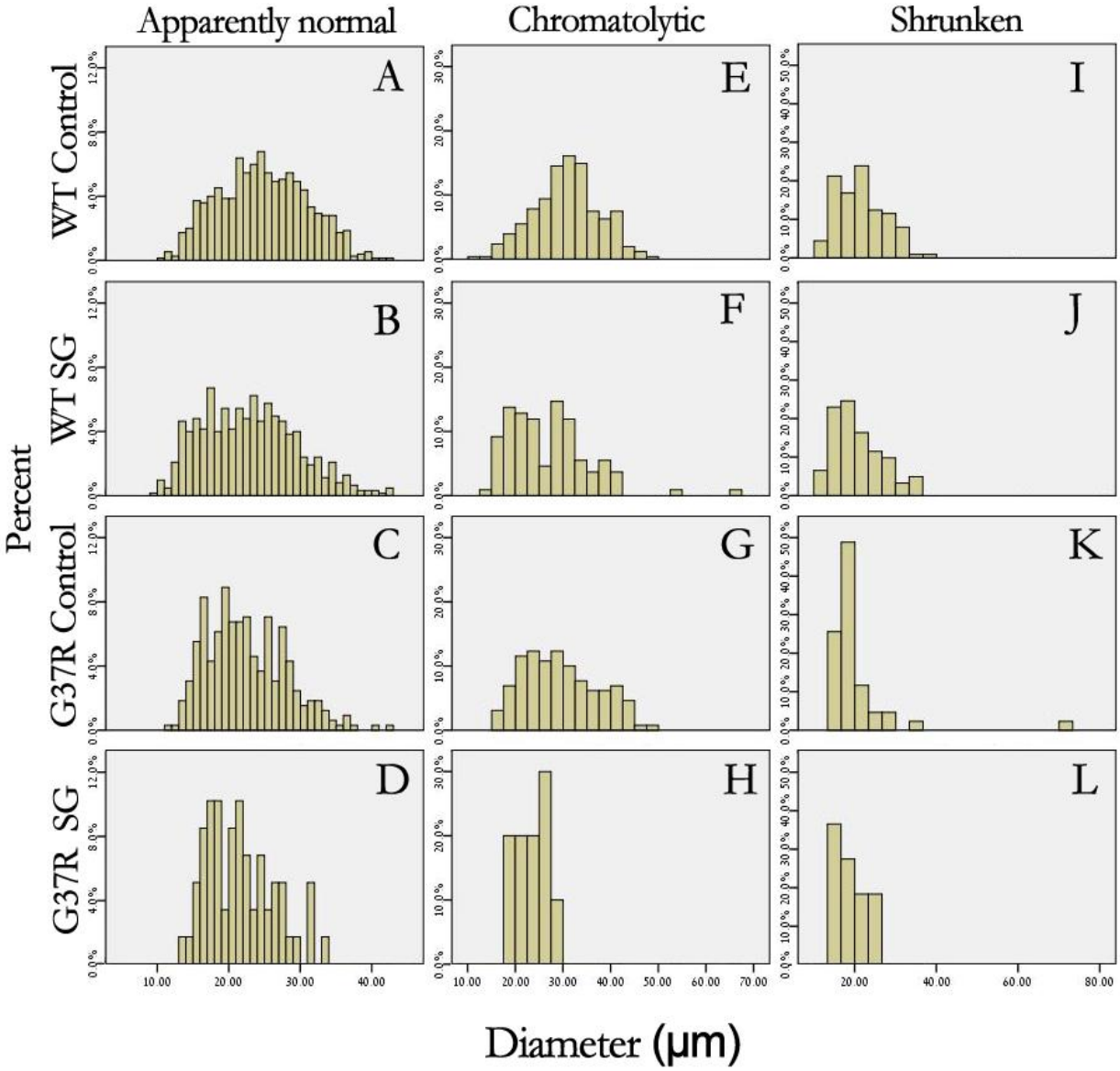
Apparently normal
Chromatolytic
Shrunken
WT Control
WT SG
G37R Control
G37R SG
Percent
A
B
C
D
E
F
G
H
I
J
K
L
Diameter (µm)

Figure 3-14. Changes in the frequency distribution of motor neuron sizes in males.

The wild type groups showed a similar wide distribution of motor neurons with apparently normal morphology; the mean soma diameter was 25.5 and 28.2μm for the control- and SG-fed wild type group, respectively. In the G37R groups, the distribution for healthy neurons was skewed towards smaller diameters; the mean diameter was approx. 21 μm for both G37R groups. In the SG-fed G37R mouse the distribution was skewed toward smaller motor neuron soma diameters with chromatolytic morphology; the mean soma diameter was 23.8μm compared to 29.3μm for wild type controls. In the control-fed and SG-fed G37R mouse the distribution was also skewed toward smaller soma diameters with shrunken morphology; the mean soma diameter was 19.6 and 21.3 μm, respectively, compared to 22.4 μm for wild type controls.

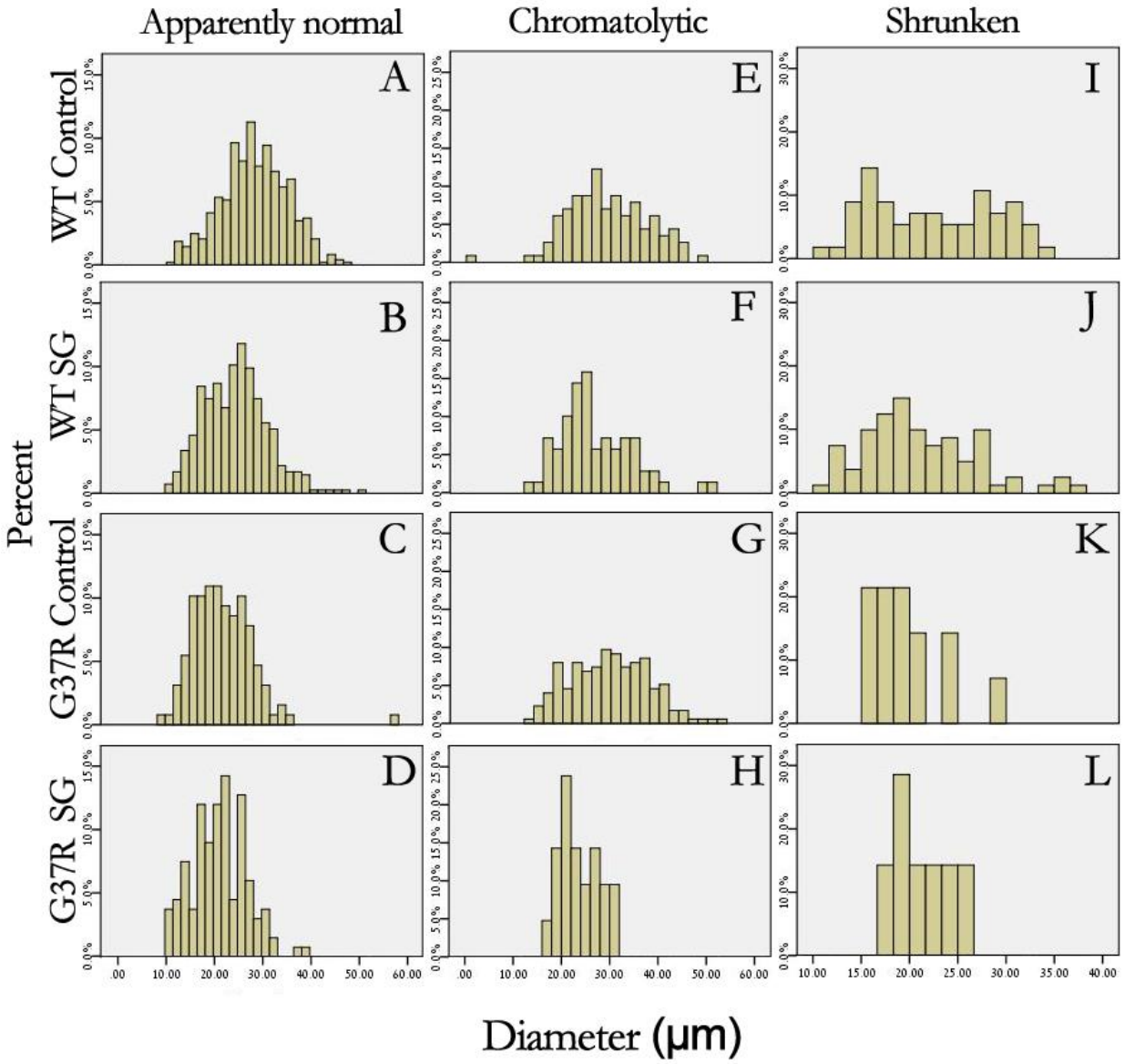
Apparently normal
Chromatolytic
Shrunken
WT Control
WT SG
G37R Control
G37R SG
A
B
C
D
E
F
G
H
I
J
K
L
Percent
Diameter (µm)

Figure 3-15. Changes in cumulative distribution of motor neuron sizes.

The changes in cell diameters of different cell morphologies between groups are illustrated by a cumulative distribution function. Data are broken down further into female (A – C) and male (D – F) mice. There was a significant leftward shift of soma diameters of healthy neurons in all experimental groups of both female ($p < 0.01$) and male ($p < 0.0001$) mice, demonstrating a reduction in soma size compared to wild type controls. A significant reduction in soma size was also observed for chromatolytic neurons of SG-fed G37R mice of both sexes ($p < 0.05$). Motor neurons with shrunken soma did not show any changes in cell size across groups.

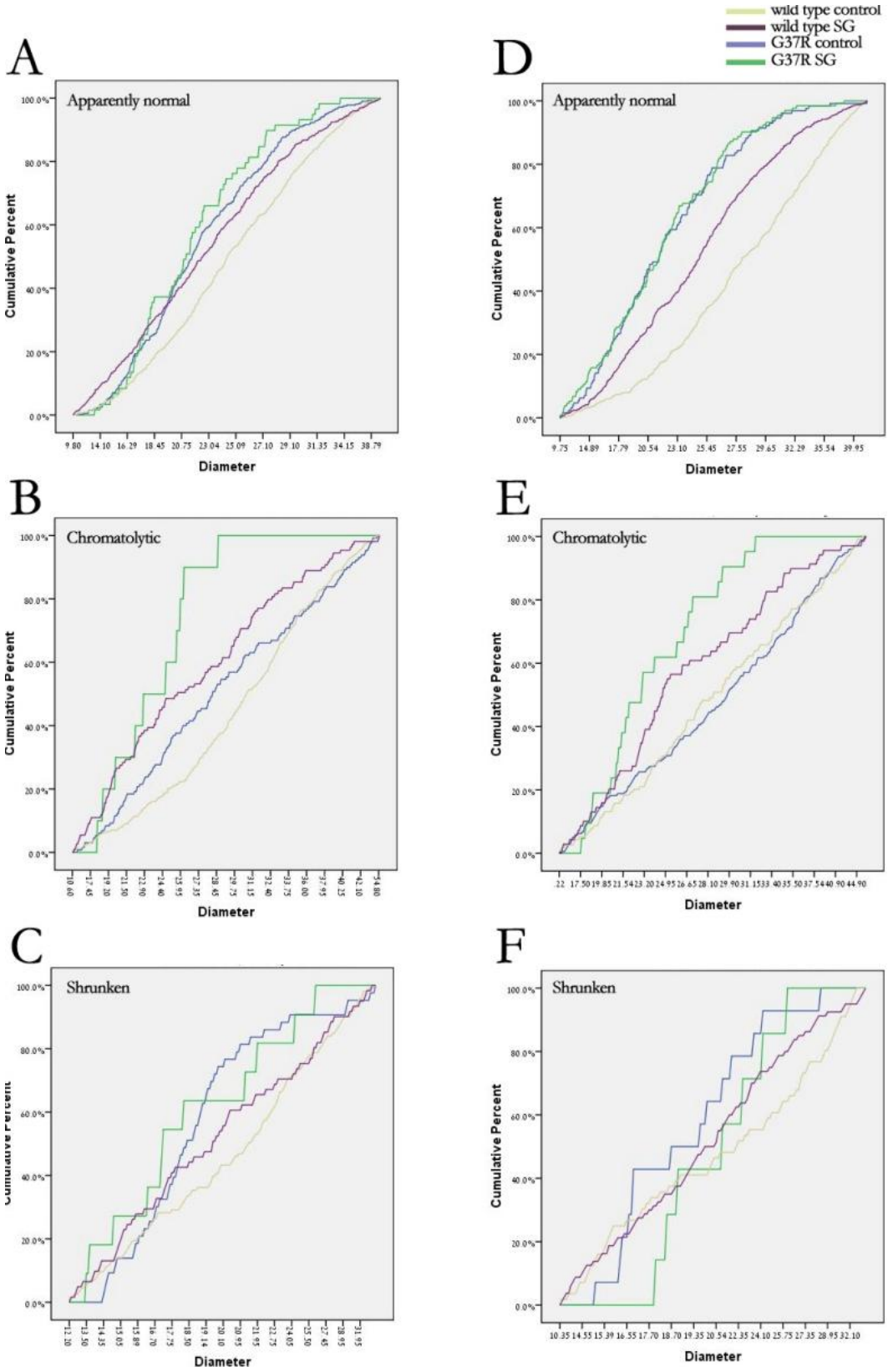
A
Apparently normal
Cumulative Percent
Diameter
B
Chromatolytic
Cumulative Percent
Diameter
C
Shrunken
Cumulative Percent
Diameter
wild type control
wild type SG
G37R control
G37R SG
D
Apparently normal
Cumulative Percent
Diameter
E
Chromatolytic
Cumulative Percent
Diameter
F
Shrunken
Cumulative Percent
Diameter

3.3.6 Astrocyte gliosis

All transgenic and non-transgenic animals were sacrificed at disease end-stage or experimental end stage, as described above in the Methods. Mice that have reached this end point were euthanized and tissues were collected. The average age of sacrifice was 366 ± 9 days for males and 378 ± 5 days for females.

Astrocyte gliosis was determined by quantifying the immunohistochemical labelling intensity of green fluorescent GFAP positive cells in the ventral horn of the lumbar spinal cord in conjunction with blue Hoechst staining (Fig. 3-16). While the focus of the quantification was in the ventral horn where motor neuron pathology is observed, the glial activation was actually apparent throughout the entire grey matter. Astrocyte distribution was sparse in the lumbar cord of wild type control (Fig. 3-16A) and SG-fed wild type (Fig. 3-16D) mice, showing occasional grouping of GFAP positive cells in the ventrolateral anterior horn. In both these groups, astrocytes were observed in their resting morphology with long, thin processes and a small cell body (Figs. 3-16C, F). Treatment with SG in wild type mice showed a significant trend for increased GFAP labelling in both females ($p = 0.037$; Fig. 3-16O) and males ($p < 0.0001$; Fig. 3-16O). G37R lumbar cords showed a marked increase in astrocyte gliosis for both sexes ($p << 0.0001$; Fig. 3-16O). Furthermore, the control-fed G37R mouse was observed to have astrocytes that were exclusively in the activated state with enlarged cell bodies and thickened, retracted processes (Fig. 3-16J, K); or astrocytes that exclusively showed increased branching of long thin processes (Fig. 3-16H, I). Treatment of SG in G37R animals did not increase astrocyte proliferation further in males ($p = 0.48$), but significantly decreased GFAP label intensity in females ($p = 0.017$; Fig.3-16O). All GFAP-positive cells in this group showed astrocytes with an activated morphology (Fig.3-16M, N).

Significant main effects of genotype on increased GFAP green fluorescence intensity was observed in males ($F = 3.69$, $DF = 222$, $p << 0.0001$) and females ($F = 2.49$, $DF = 221$, $p << 0.0001$). Interaction between diet and genotype was significant for both males ($p = 0.007$) and females ($p = 0.001$).

3.3.7 Microglial response

Microglial proliferation was described by quantifying the immunohistochemical labelling intensity of red fluorescent Iba1 positive cells in the ventral horn of the lumbar cord in conjunction with blue Hoechst staining (Fig. 3-17). As before, the spinal cord tissues were collected at end-stage

disease, when the age of the mice were 366 ± 9 days for males and 378 ± 5 days for females. While the focus of the quantification was in the ventral horn where motor neuron pathology is observed, the microglial activation was actually apparent throughout the entire grey matter.

Microglial distribution was minimal and uniform in control-fed (Fig. 3-17A, B) and SG-fed (Fig. 3-17D, E) wild type lumbar cord. In both these groups, Iba1 positive cells were observed as ramified microglia with a small round cell body (Figs. 3-17C, F) and differences in microglial label intensity were comparable in both males ($p = 0.35$) and females ($p = 0.051$; Fig. 3-17M). Control-fed G37R lumbar cords showed a marked increase in microgliosis for both sexes ($p < 0.0001$; Fig. 3-17M). Iba1-positive cells in this group were observed to have both enlarged "amoeboid-like" cell bodies with retracted processes (Figure 3-17H) and cells with remaining processes that have not yet retracted (Figure 3-17I, arrow) in the same spinal cord. The latter proportion of microglia appeared to be in transition between a quiescent ramified resting state and an activated state. Treatment of SG in G37R animals did not increase astrocyte proliferation further in females ($p = 0.28$), but significantly increased Iba1 label intensity in males ($p = 0.006$; Fig. 3-13M). Virtually all Iba1-positive cells in this group assumed an activated morphology with retracted processes and large cell body (Fig. 3-17K, L).

Significant main effects of genotype on increased Iba1 red fluorescence intensity was observed in males ($F = 3.4$, $DF = 220$, $p < 0.0001$) and females ($F = 2.75$, $DF = 220$, $p < 0.0001$). Interaction between diet and genotype was significant for both males ($p = 0.008$) and females ($p = 0.002$).

3.4 Discussion

The aim of the present study was to evaluate the potential deleterious effects of cycad toxins in a model of familial ALS. The results presented provide a detailed analysis of the progression of motor deficits in FALS mice exposed to cycad toxins at 10 weeks of age to disease end-stage. Chronic SG exposure in FALS resulted in significant diet and genotype interaction effects during motor performance testson rotarod, wire hang, and leg extension reflex. However, SG treatment had no effect on gait parameters or open field locomotion at 7 months of age. There was a non-significant trend towards motor neuron loss and increased gliosis in the lumbar ventral horn at disease end-stage, and there was significant gene × diet interaction only for measures of gliosis.

The effects of chronic cycad toxin exposure in male mice have been well characterized in behavioural (Wilson et al., 2002; Tabata et al., 2008) and histological studies (Wilson et al., 2003; Wilson et al., 2004). Motor neuron function starts to become impaired after 14 days of chronic cycad exposure in outbred adult male mice and, in parallel with decreased motor neuron numbers, show evidence of an early glutamate-mediated excitotoxicity following cycad exposure. Data has been reported for synthetic cycad toxins, where significant motor dysfunction is evident following 30 weeks of chronic treatment, and the onset of motor neuron death was observed from 15 weeks (Tabata et al., 2008). I have previously reported some parallels between the time of appearance of these pathologies and the progression of motor deficits in cycad-fed male mice (Lee et al., 2009). Here, the results confirm the motor impairments for certain behavioural measures. For example, motor coordination and grip endurance were impaired from 8 weeks of chronic SG exposure in males. Motor coordination and grip endurance in SG-fed female mice were impaired from 18 and 38 weeks, respectively. Extension reflex of wild type mice were also impaired from 26 weeks of SG exposure in females, whereas in males, extension deficits were observable by 2 weeks of SG feeding but never reached significance throughout the study. In the present studies I evaluated the onset of hindlimb dysfunction in more detail by measuring gait parameters during locomotion. Deficits observed in these behavioural tests also showed variances between sexes. Unlike the other motor behaviours previously described, gait deficits were virtually undetected in across female groups, and male groups exhibited mild impairments at 7 months of age. Within the treadmill test for gait abnormalities, digital footprint tracks showed increases in stride length in SG-fed males. Contrary results in the study by Wilson et al. (2002) might be explained by differing levels of fear or exploratory behaviour of the mice in this study. The former study used finger paint for footprint analyses instead of digital footprint. To my knowledge, this is the first report using ventral plane videography to study gait changes in cycad toxin-fed mice.

Weight loss is an accepted measurement of symptom onset (motor dysfunction) and progression in the SOD1 model of neurodegeneration (Boillee et al., 2006). Male and female mice in this study showed no significant weight loss between control and SG-fed animals. The weight measurements between wild type and mutant SOD1 animals were also comparable. The discrepancy found in weight measurements between this study and others (Knippenberg et al., 2010) using mutant SOD1 animals is due to the difference feeding paradigms. None of the animals in this study were provided with *ad libitum* amounts of food and their feeding schedules were strictly

regulated to provide a maintenance diet only. Dupuis et al. (2004) showed evidence for a disease-specific skeletal muscle hypermetabolism and increased energy expenditure in transgenic ALS mice. However, food intake is not directly related to early damage or motor neuron death. It has been demonstrated that rotarod performance is a more sensitive measure of motor function than weight loss, and comparisons between using weight loss versus motor performance have shown discrepancies in mutant SOD1 mice (Reyes et al., 2010).

Mutant SOD1 animals used in this study exhibited the stereotyped motor weakness and eventual hind limb paralysis as described previously (Dalcanto et al., 1995; DalCanto et al., 1997). The age of onset of disease reported here was delayed by about 3 months as compared to that previously described by Wong et al. (1995) describing G37R lines of transgenic mice established from four founders, i.e., 11 months versus 6 – 8 months, respectively. However, the G37R progeny described in the former study was on a mixed genetic background, and the transgenic mice from the current study have been backcrossed onto a pure C75BL/6 background. On a congenic C57BL/6 background, transgenic mice survive over a year with a median lifespan of 376 days and disease onset at 307 ± 6 days (Abou Ezzi et al., 2010). Urushitani et al. (2007) reported, in G37R line 29 mice, disease onset at 352 ± 2.45 days. Barneoud and Curet reported a delay in the onset of end stage criterion by about 20 days in a study of SOD1G93A mice, and suggested that a partial loss of the extra transgene copies caused a small shift in the genotype (Barneoud et al., 1999). It is possible that a loss in G37R transgene copies occurs as a result of continued breeding onto C57BL/6 background.

Rotarod results showed that G37R mice started to decline in performance between 37 and 40 weeks of age for female mice with and without SG exposure. Declines in rotarod performance in G37R male mice have not yet occurred by 30 weeks of age, the maximum age at which behavioural results are available for these mice, and occur at 15 weeks of age with SG exposure. The finding of late declines in rotarod performance of G37R mice is consistent with an earlier report showing a rapid decline of rotarod performance at approximately 350 days (50 weeks) of age in this mouse line (Urushitani et al., 2007). Another study reported a progressive decline in rotarod performance from 280 days (40 weeks) of age to 390 days (55.7 weeks) in this mouse line (Haenggeli et al., 2007). In contrast, preferential motor unit loss from fast-twitch muscles (Hegedus et al., 2007) and the initiation of the denervation process of motor endplates (Fischer et al., 2004) start earlier, before the onset of disease symptoms in G93A mice. Considering that SOD1 mice present marked deficits in

the compensatory sprouting capacity of their motor neurons (Hegedus et al., 2008), it is likely that these deficits lead to the presentation of locomotor dysfunction.

Hindlimb extension reflex scores showed a steady decline at 32 weeks of age in G37R female mice with and without SG exposure. Declines in reflex scores for G37R males were observed starting at 21 weeks of age. However, there were large variations of reflex score between successive test days and hence the path of progressive decline did not follow a smooth curve. A recent study in this mouse line reported declines in hindlimb reflex scores starting at 270 days (38.6 weeks) of age (Abou Ezzi et al., 2010), in contrast with an earlier report of 102 days (14.6 weeks) of age (M. Urushitani et al., 2007). Hindlimb extension in the two former studies was evaluated using a 3-point scoring method to the discretion of the experimenter. Data on reflex scores in these reports showed large standard deviations throughout the study, a reflection of possible bias or discrepancies arising from observer variability.

Similar to previous studies (Weydt et al., 2003; Miana-Mena et al., 2005), the battery of tests in the current study shows different time courses in disease progression in G37R mice. For example, the most sensitive test in terms of early detection was the rotarod. Measures of latency to fall were able to detect group differences male mice soon after commencement of SG exposure. Comparisons between male and female rotarod performance clearly delineated sex differences in that female mice showed motor coordination deficits later than males. In contrast, the open field locomotion test was least sensitive at detecting group differences in this study. Several measures (ambulatory distance, time spent in central zone, and crossing episodes) were unable to detect any group differences in females up to 7 months of age. Differences in male groups were minimal, with decreased ambulatory distances and crossing episodes only in control- and SG-fed G37R mice. These findings are in contrast with a recent study in G93A mice reporting that the open field was the most sensitive test in terms of detecting significant group differences during the pre-symptomatic stage (Hayworth et al., 2009). Detailed timeline studies of exploratory activity are not available for G37R animals, and less commonly used than rotarod, wire hang, and extension reflex for detecting early motor deficits.

This study provides novel information about the start and progression of motor deficits and gait abnormalities in G37R mice in conjunction with synthetic cycad toxin exposure. In all tests used in this study, gene × toxin interaction effects were examined in sex, litter, and age matched

groups. Furthermore, identically housed cohorts with equal numbers of males and females were compared to minimize differences due to environment. Significant interactions between genotype and SG diet were observed in the rotarod, wire hang, and hindlimb extension reflex tests for both sexes despite high variabilities in motor performance between test subjects. Male and female mice differed in the age at which group differences were observed for each test, the age at which these group differences reached significance, and the level of significance. High variabilities of progressive motor dysfunction between animals, together with sex differences, have been reported in other behavioural studies in SOD1G93A mice (Knippenberg et al., 2010). Sex differences in disease onset have been reported in both low and high copy number G93A mice with female onset as measured by hindlimb extension reflex occurring later than males (Veldink et al., 2003). Male mice are more often used in behavioural studies to eliminate the difficulty of assessing behaviour at matched times during the estrous cycle in females (Meziane et al., 2007), a factor that explains in part the high variability observed in females. It is possible that male mice are more susceptible to SG-mediated behavioural deficits than female mice (Banjo, 2009). In addition, numerous studies have shown more robust behavioural abnormalities in male animals following toxin exposure (Markowski et al., 1998; Schneider et al., 2008; Bitanihirwe et al., 2010; Salas-Ramirez et al., 2010; Mooney et al., 2011), documenting a potential protective role of female sex hormones. Lastly, mice were individually housed because of experimental considerations; however, studies have shown that individual housing can result in physiologic and behavioural changes in animals (Brain et al., 1979). The magnitude of effects of individual housing is further influenced by the strain, sex, and age of animals when they are individually housed (Voikar et al., 2005). Differences in housing arrangements can therefore partly explain discrepancies between behavioural studies.

Spinal motor neurons are at a heightened susceptibility corresponding to SOD1 ALS disease progression. Significant motor neuron loss was observed in all G37R animals (47% in females, 44% in males) and significant main effects of genotype on motor neuron loss were observed for both sexes at disease end stage. These findings are consistent with the original studies of G37R line 29 mice that described pathology restricted to motor neurons in the spinal cord (Wong et al., 1995). Loss of motor neurons in the spinal cords of G37R mice were reported as comparable to G93A mice at terminal stage (Watanabe et al., 2001). A recent study using this mouse line reported a significant decrease (approx. 44%) in the number of motor neurons at 330 days corresponding to symptomatic stage of disease (Abou Ezzi et al., 2010). In contrast, a non-significant trend toward

motor neuron loss in wild type males and females was observed subsequent to prolonged SG exposure (26% motor neuron loss in both sexes). Main effects of diet on motor neuron loss were not significant for both sexes. A non-significant reduction in surviving motor neurons following SG feeding conflicts with earlier studies reporting increased death of motor neurons exposed to cycad flour (Wilson et al., 2002) and to synthetic cycad toxins (Khabazian et al., 2002; Tabata et al., 2008; Lee et al., 2009). Differences in mouse strain (CD-1 versus C57BL/6), age at the start of feeding (5 months versus 10 weeks), and feeding duration (weeks versus months) are evident between the former studies and this current study. In a comparative study between CD-1 and C57BL/6 male mice exposed to synthetic cycad toxin, Tabata et al. (2008) reported no significant of motor deficits in C57BL/6 mice, which indicates possible strain specific effects of toxin. In the same study, the authors also showed a significant reduction in motor neurons following a 5-month washout period during which no new toxin was introduced, offering an explanation of continued CNS toxicity due to localized retention of toxin. Results from this current study do not support the idea of toxin retention, since the BL/6 mice received a comparable dose of toxin commencing at a younger age (10 weeks versus 5 months) for a longer period of time (45 weeks versus 10 weeks). Numerous other studies have also reported murine genetic background effects on the severity and/or onset of disease (Heiman-Patterson et al., 2005; Yang et al., 2005; Finn et al., 2010; Lima et al., 2010). These studies report a resilience of C57BL/6 mice to developing predicted outcomes of toxin-mediated disease.

It has recently been shown that washed cycad induces pure hallmarks of Parkinsonism in rats, in the absence of motor neuron loss or astrogliosis common to ALS (Shen et al., 2010). This finding reflects the differential expression of symptoms in animal models of ALS-PDC, which may feature signs of either purely ALS or PDC. It is possible that a separation of disorders is reproduced in toxin-fed animal models, and while some of them developed ALS, others developed PDC as the major presenting feature. Motor neuron loss and astrogliosis are not the unique and critical aspects of Parkinsonism outcomes, and including them in the quantification analysis may account for the insignificant changes observed in these measurements. The scope of research in this study did not include this possibility, as Parkinsonism behaviours and neuropathology such as substantia nigra pars compacta involvement or aberrant striatal levels of dopamine were not investigated. Finally, the detailed investigation of the late disease stage presented in this study shows only a small temporal snapshot for this age-related neurodegenerative disease. The possible profound effects of

the toxin may have dissipated by the end stage time point studied here. Perhaps the greatest limitation to this study is the sole focus on end stage of disease, although studies of end stage disease are important to elucidate long term toxin effects and the effects on survival and disease progression. Alternatively, prolonged toxin exposure may have triggered adaptation to increased toxin levels in the cellular environment. In vitro studies have shown that modulate survival signals and change the threshold at which they initiate toxin-induced death, barring significant cytotoxic damage (Boyle et al., 1997). Possible defence mechanisms include increased expression of toxin resistance genes or up regulation of receptors for neurotrophic factors.

Differentiating alpha from gamma motor neurons wasdifficult as both neuron types within a motor pool are ChAT positive (Friese et al., 2009), and neurons with the characteristic Nissl staining of motor neurons showed such a large range of soma diameter. The morphometric results in this study focused on Nissl stained neurons primarily in Rexed lamina IX, the area of the ventral horn with the greatest ratio of α motor neurons to interneurons. In addition, it was suggested that 95% of limb motor neurons are above 25 μm, while neurons less than 17.5 μm should be almost solely interneurons (Stephens et al., 2006). Interneurons are capable of surviving the loss of motorneuron targets (Lim et al., 2000). Following this size criterion for motor neurons, the results from this study are still consistent with a relative preservation of interneurons in all the experimental groups of both sexes. The results of this study showed a significant leftward shift in the cumulative histogram of soma diameter distribution in control- and SG-fed G37R cords of both sexes. Male mice showed an additional leftward shift toward smaller cell diameters following SG feeding in wild types. Studies in G93A mice reported preferential loss of the most forceful motor units paralleled by denervation of large type IIB (fast-fatigable) muscle fibres and indicate conversion to motor units innervated by smaller motor axons during the presymptomatic stage (Hegedus et al., 2008). In addition, motor neurons of fast-fatigable fibres have been shown to be selectively vulnerable to ER stress, with an aprubt unfolded protein response unique to this motor neuron subtype (Saxena et al., 2009). The transition to the unfolded protein response in fast-fatigable motor neurons occurs before peripheral denervation and is invariably accompanied by microgliosis in the lumbar spinal cord of mSOD1 mice (Saxena et al., 2009). Observations of a significant reduction in motor neuron diameter at disease end stage in this study support the possibility of activity-dependent conversion to smaller motor axons innervating type IIA (fatigue resistant) muscle fibres. Furthermore, the appearance of

morphological changes in surviving motor neurons accompanied by microglial activation following chronic SG exposure indicates the involvement of ER stress-induced pathology.

Prolonged dietary exposure to SG elicited asignificant astrocytic response in the ventral lumbar horn of both sexes that was more pronounced in males than females (58% increase in males compared to 20% in females). This finding is consistent with previous studies of toxin administration to male mice (Wilson et al., 2002; Lee et al., 2009), and provide novel data for glial response in females. G37R expression elicited a prominent microglial and astroglial response, some of which showed morphological changes reminiscent of activation. Prominent hypertrophic astrocytes and irregular amoeboid shaped microglia are predominantly located in the anterior horn of symptomatic G37R mice (Kriz et al., 2002; Graber et al., 2010). Enhanced gliosis as measured by increased microglial cell numbers and GFAP staining intensity was observed in other studies of this line of symptomatic G37R mouse (Abou Ezzi et al., 2010). Prolonged SG exposure in G37R mice showed similar widespread distribution of microglia and astrocytes, all of which became hypertrophic with retracted processes. This is a novel finding demonstrating that SG targets the type of glia (resting or activated) even in the absence significant increases in gliosis, as in the case of the microglial response. Although the effects of SG on eliciting a glial response are small compared to the genetic effects, significant diet × genotype interactions were observed in both sexes.

In conclusion, I show that significant interactions between the G37R genotype and SG diet result in clinically detectable motor deficits at differing ages of onset between male and female G37R mice. My results provide convincing evidence that reduction in soma diameter of surviving motor neurons and associated activation of neuroglia occurs at disease end stage of G37R mice with SG exposure, in accordance to my previous findings of a spinal origin to cycad toxicity (Lee et al., 2009). The additive effects of SG on motor dysfunction behavioural tests and motor neuron loss in G37R mice support the available evidence for genetic susceptibility to neurotoxin tolerance as a multifactorial cause for the development of ALS and other neurodegenerative diseases (Bradley et al., 2009). The concept of gene-environment interactions is not new to research focused on delineating causes for neurodegeneration with no clear genetic links (van Dellen et al., 2005; Vance et al., 2010). Further study at earlier time points is required to determine mechanisms of selective motor neuron vulnerability in the context of gene-environment interactions to direct treatment strategies for degenerative disorders with a complex etiology. This is important in light of the complexity of gene-environmental interactions and the heterogeneity of the ALS motor phenotype

(Ravits et al., 2009). Nevertheless, all post-mortem studies share the same limitation of visualizing only a snapshot of a disease at one given point in time. In addition, the results of this study could be relevant to the understanding of other complex neurodegenerative diseases with uncertain etiologies but overlapping features such as sporadic Parkinson's disease and Alzheimer's with dementia. This will be a critical development because hereditary and sporadic causes of human motor neuron disease seldom occur in isolation.

Figure 3-16. Distribution and intensity of astrocytic gliosis in the lumbar spinal cord.

Representative micrographs of green fluorescent GFAP immunostaining in lumbar spinal sections of control and G37R transgenic mice. Upper micrographs (A, D, G, L) illustrate GFAP-positive cell distribution in the lumbar cord of control-fed wild type (A) SG-fed wild type (C), control-fed G37R (G) and SG-fed G37R (L) mice. Middle micrographs (B, E, H, M) illustrates GFAP-positive cell numbers in the corresponding groups. Lower micrographs (C, F, I, N) illustrate representative cell morphologies at high magnification in the corresponding groups. In wild type animals, astroglia are clustered in the left and right ventrolateral lumbar horn (B, E). In G37R mice, astroglial proliferation is uniform throughout the entire grey matter (G, L) and significantly increased compared to controls (O). Astrocyte morphology showed a small cell body and long thin processes in control-fed wild type (C) and SG-fed wild type (F) mice. The control-fed G37R mouse either showedactivated astrocyte morphology (K) with widespread proliferation (J) or cells with increased branching of thin processes (I). Treatment with SG in mutant animals did not change the intensity ofastrogliosis (O; compare H – J with M), but all astrocytes assumed the activated morphology (N). Data on graph (O) presented as percent of green fluorescent GFAP labelling compared to wild type controls ± S.E.M. Both sexes showed significant main effects of genotype on GFAP proliferation and a significant diet × genotype interaction. Scale bars are 300 μm in the upper micrographs (10x magnification), 60 μm in the middle micrographs (40x magnification), and 30 μm in the lower micrographs (100x magnification).

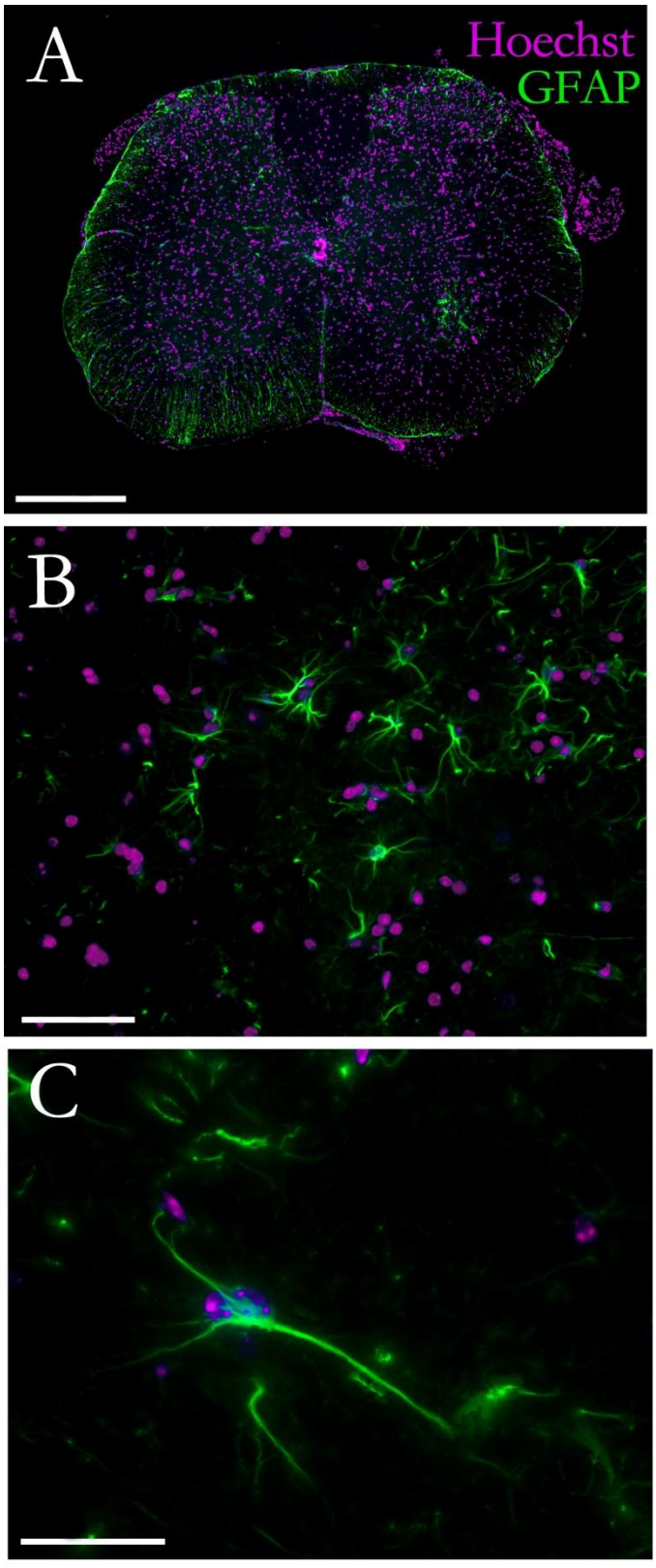
A
Hoechst
GFAP
B
C

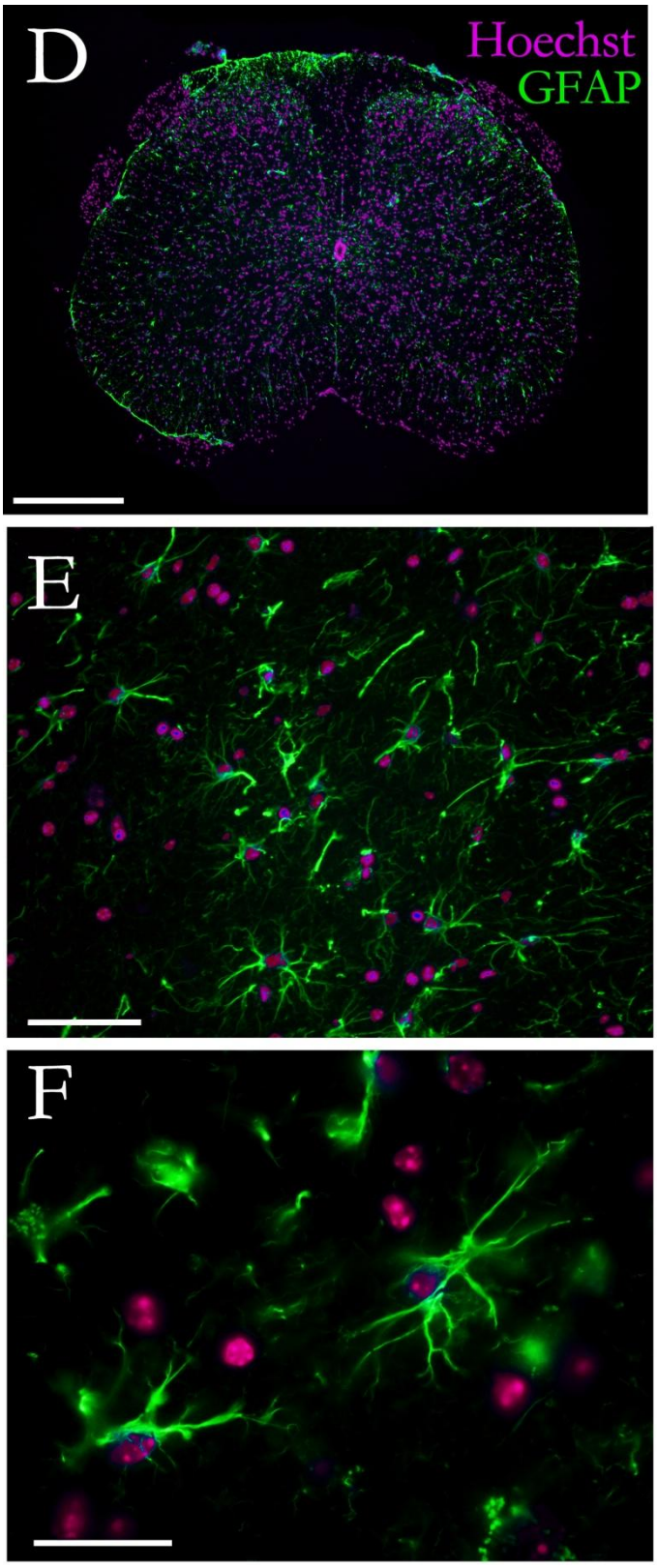
D
Hoechst
GFAP
E
F

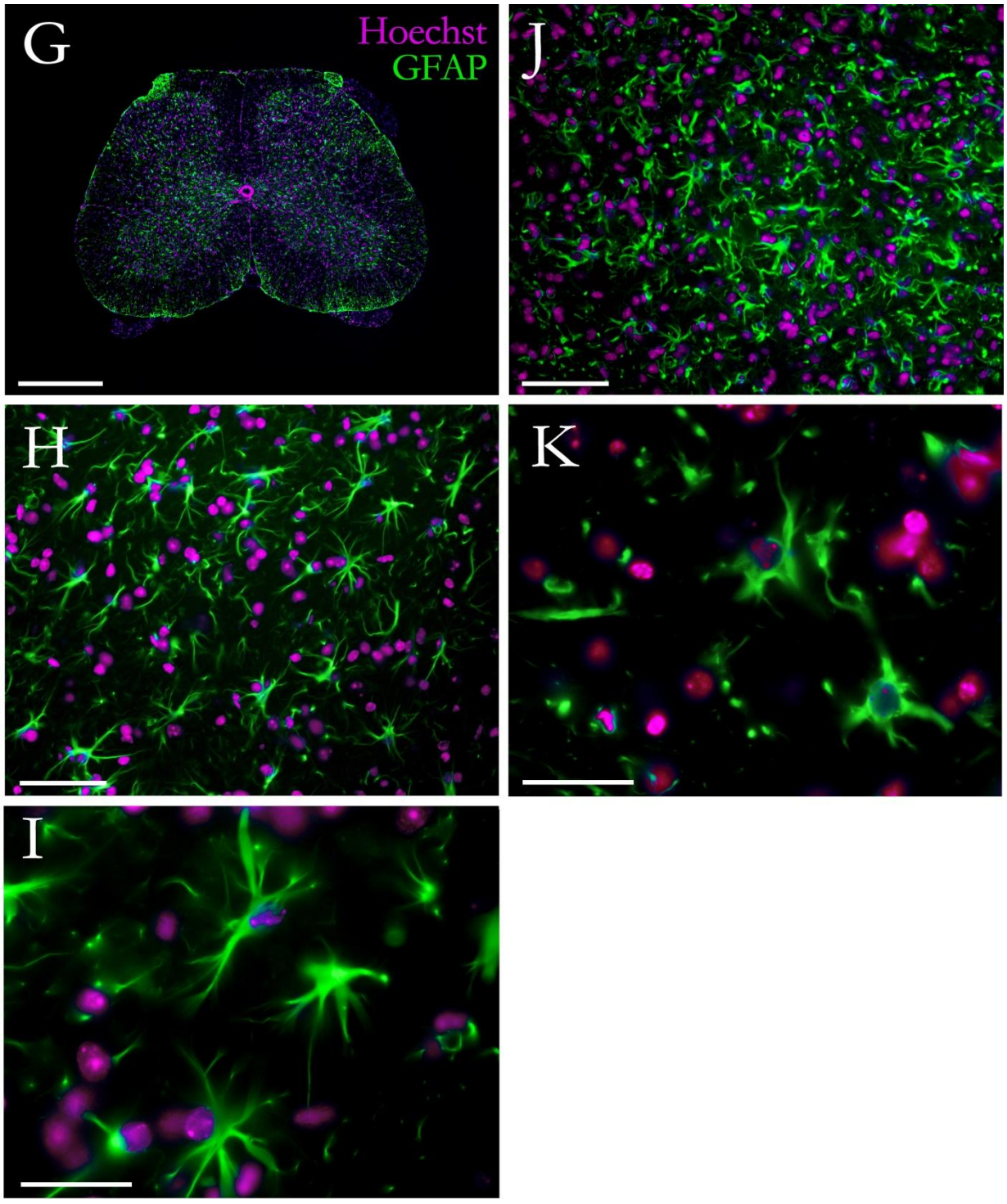
G
Hoechst
GFAP
J
H
K
I

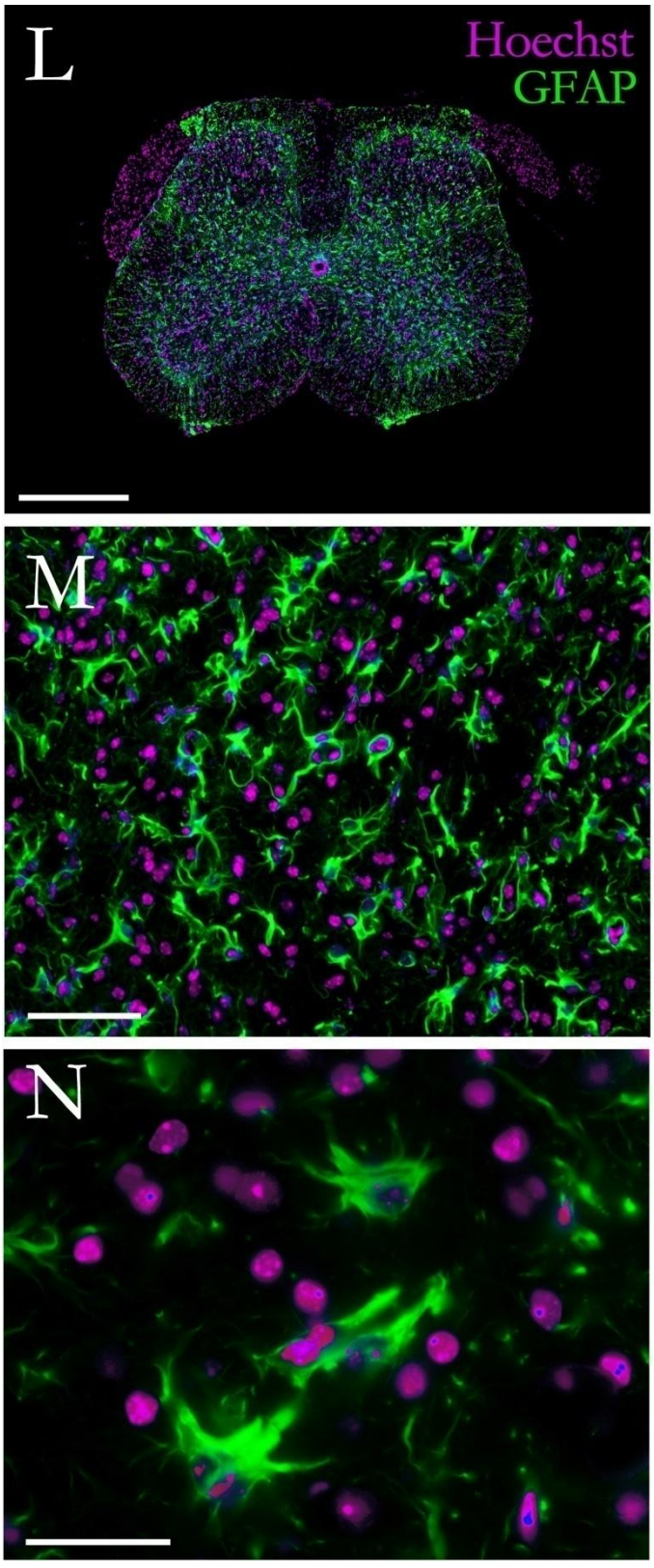
L
Hoechst
GFAP
M
N

O

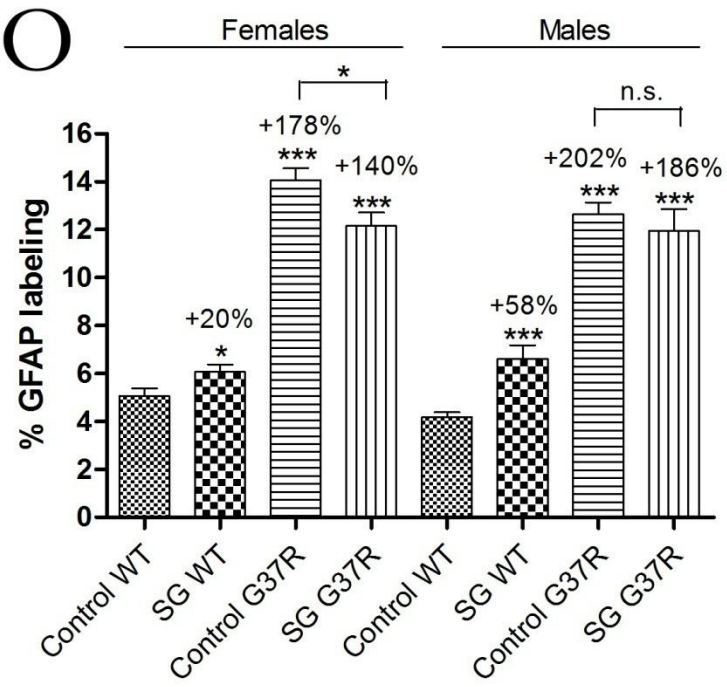
Females
Males
*
n.s.
+178%
***
+140%
***
+202%
***
+186%
***
+20%
*
+58%
***
% GFAP labeling
16
14
12
10
8
6
4
2
0
Control WT
SG WT
Control G37R
SG G37R
Control WT
SG WT
Control G37R
SG G37R

Figure 3-17. Distribution and intensity of microglial activation in lumbar spinal cord.

Representative micrographs of red fluorescent Iba1 immunostaining in lumbar spinal sections of control and G37R transgenic mice. Upper micrographs (A, D, G, J) illustrate uniform Iba1-positive cell distribution in the lumbar cord grey matter of control-fed wild type (A) SG-fed wild type (C), control-fed G37R (G) and SG-fed G37R (J) mice. Middle micrographs (B, E, H, K) illustrate Iba1-positive cell numbers in the corresponding groups. Lower micrographs (C, F, I, L) illustrate representative cell morphologies at high magnification in the corresponding groups. Iba1-positive cells in wild type control lumbar cords (B, C) and SG-fed wild types (E, F) appeared as small cell bodies with ramified processes. The labelling intensity of Iba1 between these two groups was comparable (M). Control-fed G37R mice showed a marked increase in microglia proliferation in both sexes (G, M). Microglia morphology in this group assumed bothactivated "amoeboid-like" morphologies (H) and a transition state with enlarged cell bodies and unretracted processes (I, arrow). Treatment with SG in G37R animals did not change the intensity of microgliosis (M; compare H and K), but all microgliawere observed to assume the activated morphology (L). Data on graph (M) presented as percent of red fluorescent Iba1 labelling compared to wild type controls ± S.E.M. Both sexes showed significant main effects of genotype on microglia proliferation and a significant diet × genotype interaction. Scale bars are 300 μm in the upper micrographs (10x magnification), 60 μm in the middle micrographs (40x magnification), and 30 μm in the lower micrographs (100x magnification).

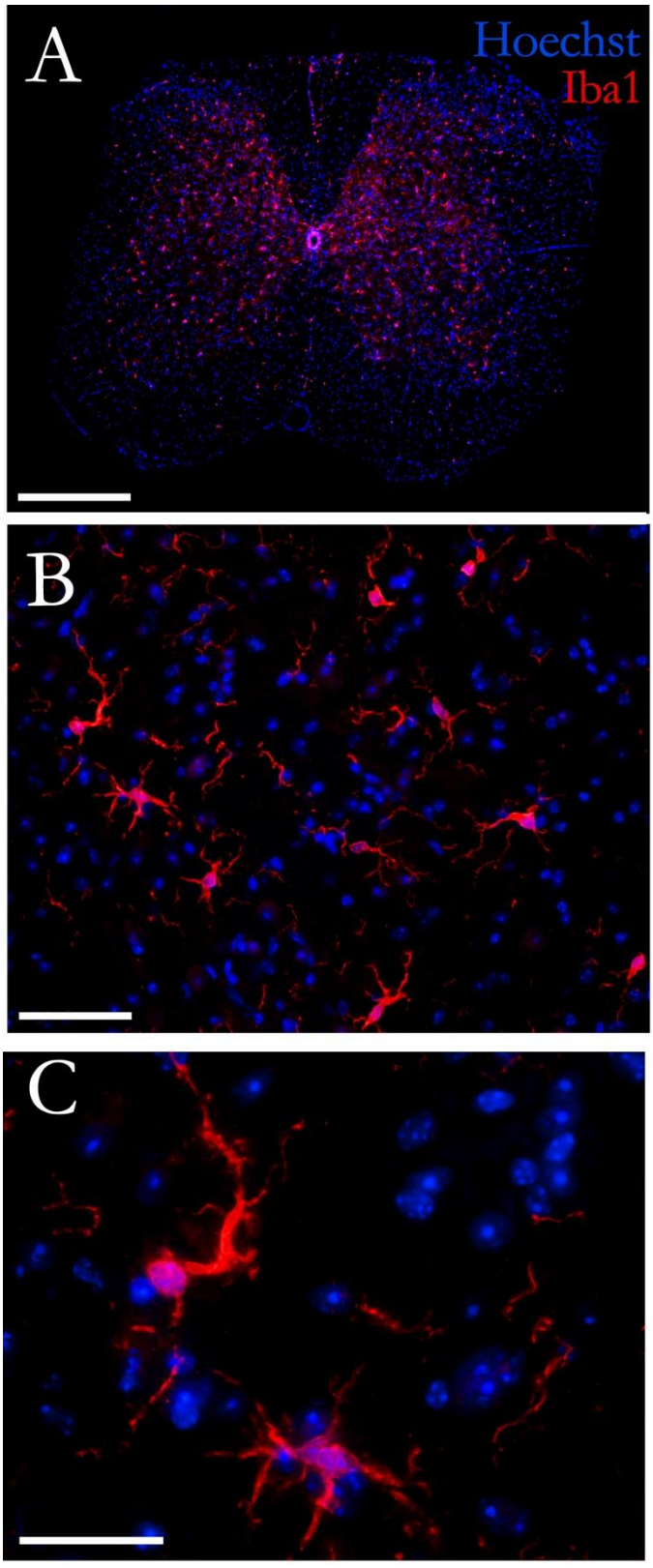
A
Hoechst
Iba1
B
C

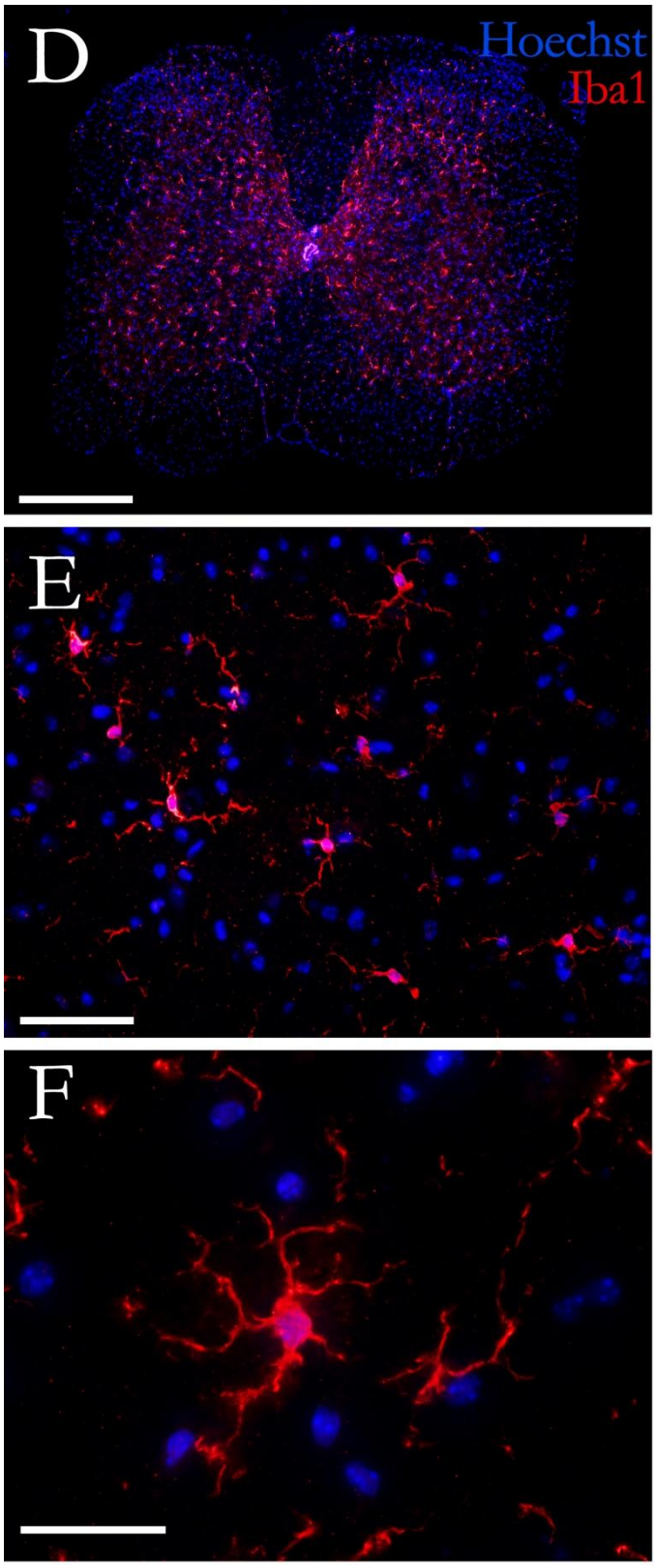
D
Hoechst
Iba1
E
F

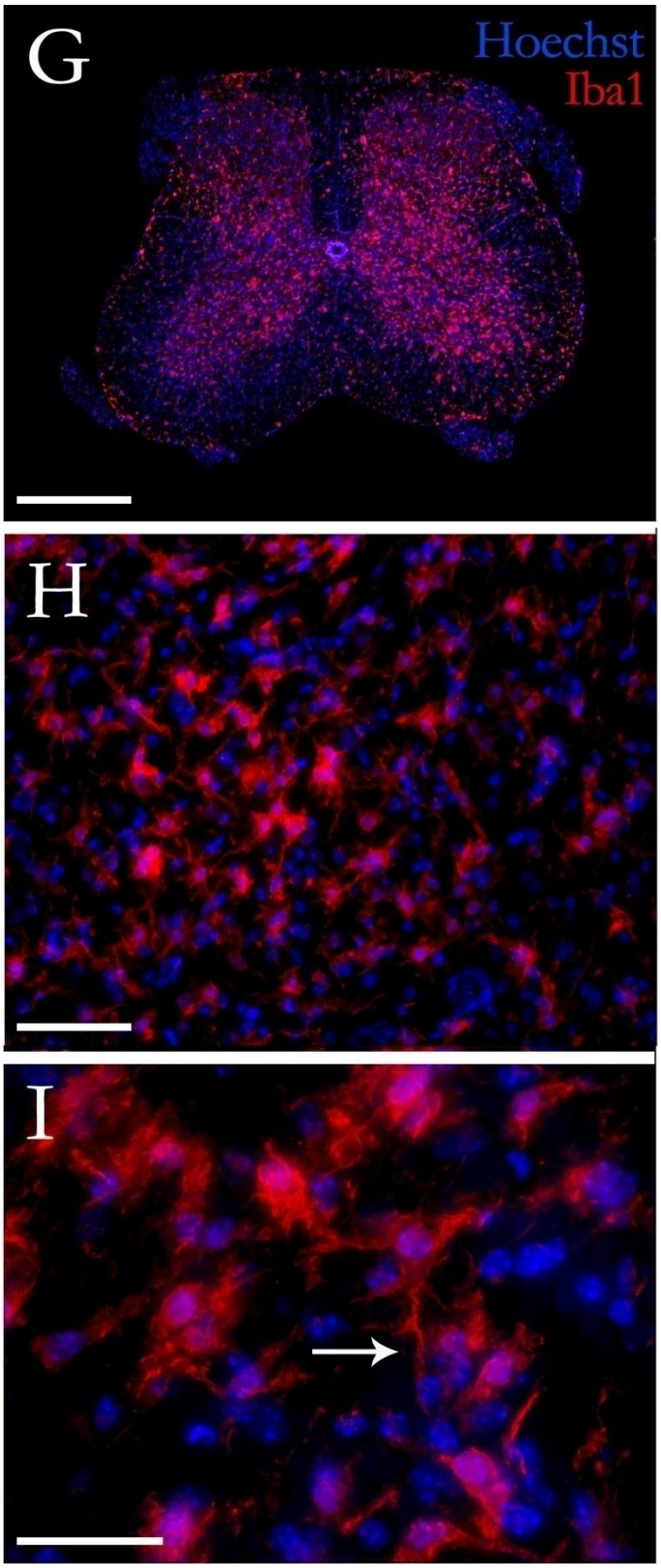
G
Hoechst
Iba1
H
I

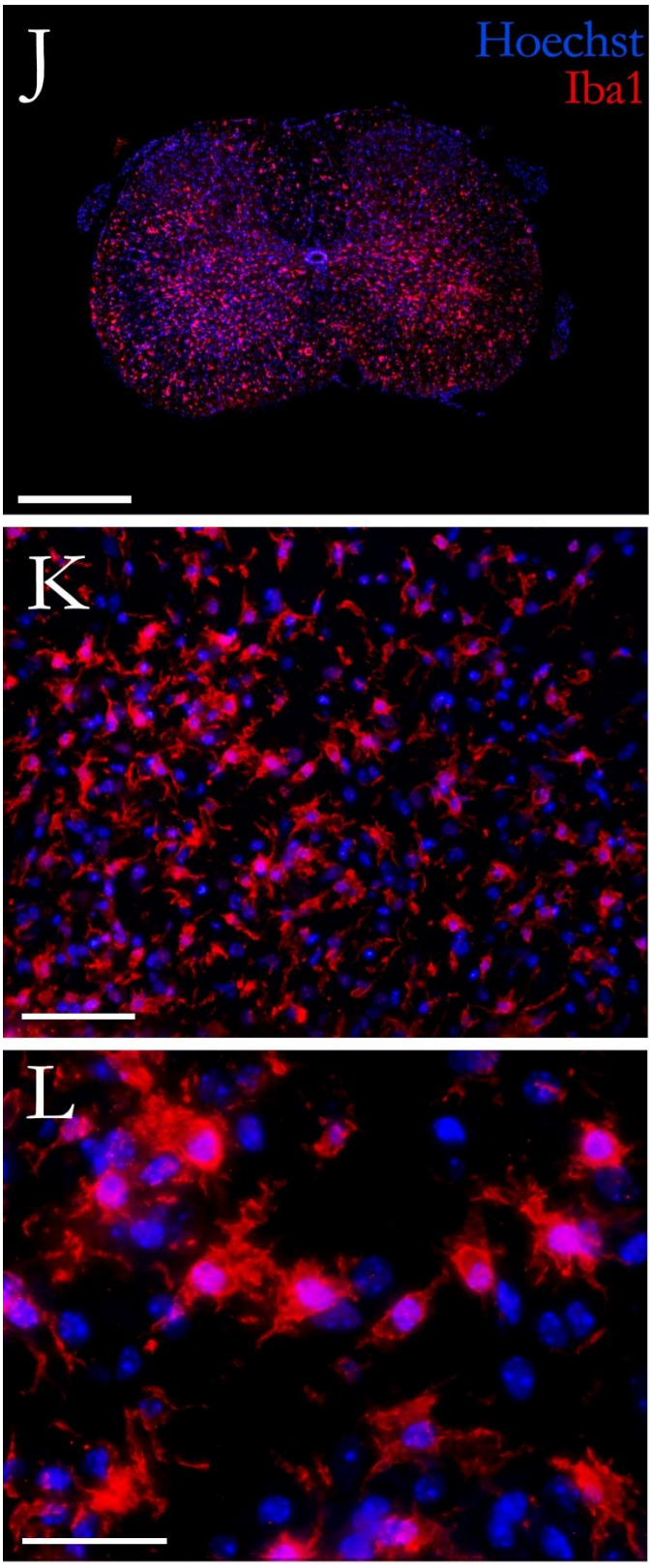
J
Hoechst
Iba1
K
L

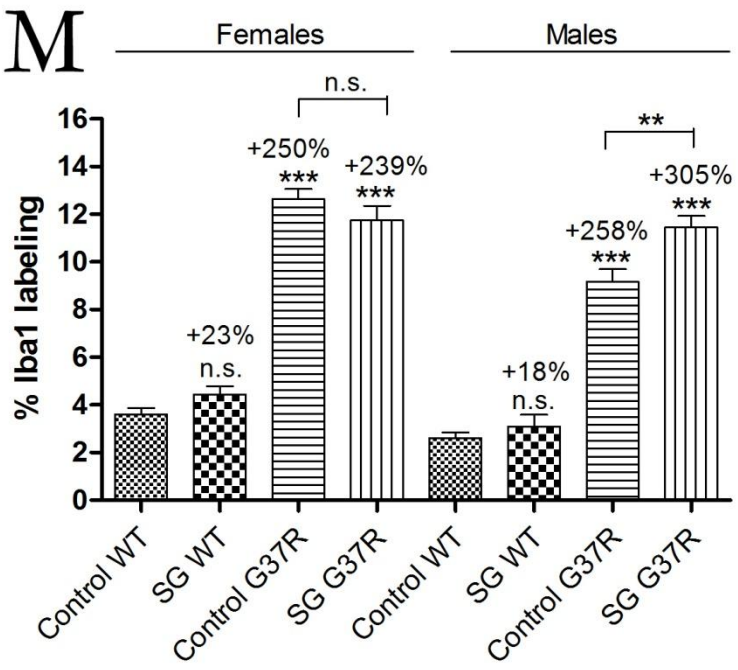
M
Females
Males
n.s.
**
% Iba1 labeling
16
14
12
10
8
6
4
2
0
+23%
n.s.
+250%
***
+239%
***
+18%
n.s.
+258%
***
+305%
***
Control WT
SG WT
Control G37R
SG G37R
Control WT
SG WT
Control G37R
SG G37R

Chapter 4. Peripheral and cortical involvement

4.1 Introduction

Quantitative morphology of motor neurons in the spinal cord and relevant motor cortical areas is of essential significance for understanding the combined environmental and transgenic effects of their demise in ALS. These studies are widely investigated in the scientific literature with respect to neurodegenerative disorders in motor neuron disease and animal models. However, an investigation of ALS which primarily targets the motor system is incomplete without considering neuropathological involvement of peripheral nerves and spinal roots. Transgenic mice that carry missense mutations in the Cu/Zn superoxide dismutase-1 gene (SOD1) remain the standard pre-clinical model for investigating ALS disease mechanisms and progression (Gurney, 1994). Congenic SOD1 mice with glycine to arginine switch at codon 37 (G37R) have been generated and display a reproducible ALS phenotype, but with delayed disease onset (Wong et al., 1995) compared to the more widely used glycine to alanine at codon 93 (G93A) SOD1 mouse. Mutant SOD1G37R mice show progressive motor function deterioration throughout a longer disease course due to the expression of lower copy numbers of the mutant SOD1 gene (Wong et al., 1995; Nguyen et al., 2000). An overwhelming number of studies in G93A mice show early (presymptomatic) loss of functional motor units with motor endplate denervation occurring well before the death of spinal motor neurons (Chiu et al., 1995; Fischer et al., 2004; Hegedus et al., 2007; Hegedus et al., 2008; Gordon et al., 2009). It is expected that motor efferents to the periphery are affected in a disease where muscle weakness and atrophy are the predominant symptoms, but it is unclear in which order (central or peripheral) the progression of degenerative changes occurs.

Loss of intact neuromuscular junctions following motor axonal retraction leaves muscle fibres denervated. Peripheral axon regeneration occurs upon muscle denervation, characterized by axon terminal sprouting from nearby intact motor neurons that form new synaptic connections with denervated muscle fibres (Son et al., 1995; Kang et al., 2003; Love et al., 2003). Studies in G93A transgenic mice have reported evidence for axon regeneration in hindlimb muscles (Fischer et al., 2004; Schaefer et al., 2005). Reinnervation in patients with ALS is thought to arise primarily through collateral sprouting (sprouting occurring at the nodes of Ranvier along the axon), and sprouts are observed to grow along pathways formed by degenerative axons (Gurney et al., 1984). However, any sprouting of intact branches to help prolong motor function is only transient due to the overwhelming pace of denervation (Gurney et al., 1994). The distal nerve may also lose its capacity to support regenerating motor axons following prolonged denervation due to an increasingly non-

permissive environment lacking essential neurotrophic factors (Hoke et al., 2002). Furthermore, anatomical studies in SOD1 ALS mouse models have demonstrated that motor axons innervating fast-twitch fatigable type IIB muscle fibres are selectively vulnerable and fail to sprout, while those innervating fast fatigue-resistant (type IIA) or slow (type I) fibres are resistant and retained their sprouting competence (Frey et al., 2000; Pun et al., 2006). According to Sobue and colleagues, the α motor neuron axons were more vulnerable compared to the γ motor neuron axons to degeneration in ALS (Sobue et al., 1981). It has been demonstrated by retrograde Fluorogold tracing that the alpha motor neurons innervating the gastrocnemius muscle are selectively lost in mutant SOD1 mice (Mohajeri et al., 1998). Studies in the mutant SOD1 mouse model and in one case study of an ALS patient have noted that axon pathology appeared to be dying back in a retrograde degenerative fashion, with intact proximal axons but with neuromuscular junction denervation (Fischer et al., 2004). Still the possibility of anterograde degeneration in ALS cannot be completely discounted (Eisen et al., 2001), and human post mortem material is almost always from end stage patients where it is difficult to study pathological changes in the neuromuscular system with any accuracy. However, neuromuscular junction vulnerability may not play a key role in all forms of ALS, as noted in a mouse model of Guamanian ALS-PDC where lower motor neuron loss and pathology preceded denervation of the neuromuscular junction (Lee et al., 2009). When taken together, these findings validate such animal models since alpha motor neuron axons and neuromuscular junctions are important pathological targets in many forms of ALS.

A growing number of studies have focussed on the importance of peripheral synapses between lower motor neurons and muscle fibres at the neuromuscular junction in disease pathogenesis of SOD1-related models of ALS (Murray et al., 2010). Synaptic and distal axonal compartments of neurons are important pathological targets, but the degree to which these non-somatic cellular components are affected compared to the somatic motor neuron component is not completely understood. In addition, neuromuscular junction vulnerability in non genetic or environmental forms of ALS that exhibit comparable symptoms of muscular weakness and paralysis at end stage has not been characterized at any great detail. The question remains whether or not motor end plate synapses and distal axons are the initial and early stages of the disease process in the less studied SALS or environmentally induced ALS. It is possible that gene-environment interactions in ALS modulate the severity of pathology at the distal motor axons. Nguyen and colleagues demonstrated in mutant SOD1 mice an early vulnerability of neuromuscular junctions to

hypoxia and oxidative stress that preceded motor neuron death (David et al., 2007). Early vulnerability of neuromuscular junctions to environmental factors such as the dietary consumption of cycad toxins may signal or contribute to the events involved in spinal motor neuron death. It is important to consider the site at which pathology originates in order to deliver meaningful therapeutic intervention in ALS.

Despite the body of work highlighting the important role of aberrant synaptic connections in ALS pathogenesis, the direct contribution of muscle to ALS pathogenesis remains controversial. One recent study demonstrated that mutant SOD1 expression in skeletal muscle has a causal role in transgenic mice, suggesting a new non-autonomous mechanism for motor neuron degeneration (Wong et al., 2010). These findings are supported by studies showing clear mitochondrial dysfunction, cell death, and increased apoptotic protein expression in muscle biopsy specimens from patients with sporadic ALS (Schoser et al., 2001; Crugnola et al., 2010). However, genetic manipulations or viral gene therapy in ALS mouse models to selectively reduce mutant SOD1 expression in muscle did not affect muscle function, disease onset or survival (Miller et al., 2006). It is possible that these conflicting results using conditional expressors and viral techniques in animal models are the result of variability in the resultant levels of mutant SOD1 and the time point at which the genetic manipulations are first introduced. Standardization of these methods is important to yield more consistent results, especially with a focus on attempts to modulate disease onset and progression presymptomatically, or at least before onset of neuromuscular junction abnormalities. It remains most likely that a complex system of interactions between genetic susceptibility in multiple cell types and harmful environmental factors introduced at different time points is required to elicit the full spectrum of ALS pathology (Coppede et al., 2006). Investigations to elucidate the details of this complex biological network are vital for the development of successfully targeted therapeutic approaches for ALS.

This study attempted to distinguish between the pathological consequences of either genetic predisposition to neurodegeneration or neurotoxin acting alone on motor axons, and the site of primary pathogenesis when both stressors act in combination. The neurotoxin used in this study was synthetic stigmasterol β-D-glucoside (SG), a known compound isolated from cycad seeds (Khabazian et al., 2002). Transgenic SOD1G37R (line 29) were bred in this study and selected for heterozygosity as previously described above. The transgenic mouse model employed in this study showed pathology restricted to motor neurons in the spinal cord and brainstem (Wong et al., 1995).

However, like other SOD1 mutations and G37R lines, this mouse model showed stereotypical muscle weakness and late disease hind limb paralysis (Dalcanto et al., 1995; DalCanto et al., 1997). The severity of hind limb degeneration validates the need for extending research beyond the spinal cord to the peripheral components of the motor system. The gastrocnemius along with the soleus muscle of the posterior hind limb is involved in plantar flexing during locomotion, actions which are selectively affected in late disease. Furthermore, profoundly impaired retrograde tracer uptake was observed in symptomatic mSOD mice while motor neuron loss was only moderate (Parkhouse et al., 2008).

Confocal imaging of neuromuscular junctions and axons in the gastrocnemius muscle in SOD1 animals revealed several distinct appearances, including axonal branches that appeared to be normal except that they did not form contact sites with muscle fibres while remaining in close proximity to end plates. In the same animals, the number of axons in the ventral nerve roots was quantified with measurements of axonal diameters, providing a size histogram of remaining myelinated axons. Furthermore, the degree of denervation at neuromuscular junctions was quantified and compared to spinal motor neuron pathology to provide a sequential view of motor neuron pathology in these animals.

4.2 Methods

4.2.1 Immunohistochemistry and apoptosis detection

To determine the fate of spinal motor neurons, immunofluorescence with ChAT was used in combination with a modified TUNEL technique (Gavrieli et al., 1992) to label fragmented DNA and the nuclear stain Hoerchst. Spinal cords (10 μm thick) were washed 3 times in PBS (5 minutes per wash) before being equilibrated in terminal deoxynucleotidal transferase (TdT) buffer (200 mM sodium cacodylate, 25 mM Tris HCl, pH 6.6, 0.25 mg/mL BSA, and 1 mM cobalt chloride). The slides were saturated with fluorescein-labelled nucleotides (Roche, Indianapolis, IN, US) and TdT, and the TUNEL reaction was performed at 37°C for one hour. The reaction was terminated by immersing sections for 15 minutes a buffer containing 300 mM sodium chloride and 30 mM sodium citrate. The slides were washed 3 times to remove unincorporated fluorescein-dUTP. Tissue sections were then blocked in 2% normal rabbit sera in PBS for 30 minutes at room temperature. This solution was replaced by blocking solution containing 1:100 anti-ChAT and slides were incubated for 1 hour at room temperature followed by overnight at 4°C. Slides were washed 3 times

in PBS and incubated for 1 hour with blocking solution containing 1:100 Alexa 546-conjugated rabbit anti-goat (Jackson ImmunoResearch). Slides were washed twice in PBS for 5 minutes each, and once in sterile distilled water for 5 minutes. Sections were stained in 1 μg/mL Hoechst 33258 and mounted in 0.2% DABCO-glycerol. In negative controls, the TdT was omitted.

4.2.2 Muscle tissue staining

To examine motor end plate integrity at end stage, slide-mounted gastrocnemius muscle sections (35 μm thick) were air dried, washed 3 times in PBS (5 minutes per wash), and incubated for 30 minutes at room temperature with 1:200 Alexa 594-conjugated α-bungarotoxin (Invitrogen, Eurgene, OR; #B13423) diluted in PBS. Muscle sections were rinsed 3 times in PBS followed by 3 times in Tris buffered saline (TBS) containing 0.4% Triton X-100. Muscles were then blocked in 5% NGS and 0.4% Triton X-100 in TBS for 2 hours at 4°C. After blocking, muscles were washed 3 times in 0.4% Triton X-100 in TBS and incubated in an antibody cocktail containing 1:200 anti-neurofilament 160 mouse monoclonal (Millipore; MAB 5254), 1:30 anti-synaptic vesicle protein 2 (Developmental Studies Hybridoma Bank, Iowa City, IA), and 5% NGS diluted in 0.4% Triton X-100 in TBS for 48 hours at 4°C. Following that, muscles were rinsed 5 times in TBS and incubated in 1:200 FITC goat anti-mouse (Jackson ImmunoResearch; #115-096-003) diluted in 0.4% Triton X-100 TBS for another 48 hours at 4°C. After washing 5 times in TBS, muscles were stained with 4 μg/ml Hoechst 33258 for 30 minutes, rinsed in TBS, and mounted in 0.2% DABCO-glycerol.

4.2.3 Cell quantification and imaging

To quantify the amount of pathological marker labelling in the CNS, every tenth transverse section of lumbar cord between L3 and L5 was assessed. This region contains motor neurons innervating the gastrocnemius muscles of the legs. Quantification after immunohistochemistry was performed blind with respect to treatment and genotype using Adobe Photoshop CS3 (Version 10.0) on images captured on a Zeiss microscope (Axiovert 200M inverted; Carl Zeiss, Thornwood, NY). Data was expressed as % fluorescent labelling to black space in the field of view. Stained muscle sections were quantified for % end plate innervation. End plates (visualized by bungarotoxin) were scored as innervated when it was observed to be completely overlapped with the axon terminal (visualized by neurofilament stain). End plates were deemed denervated if they were completely not associated with an axon, and scored as intermediately innervated if there was only

partial overlap between end plate and axon. Mean counts for each group were compared by two-way ANOVA using Prism 5.0 (GraphPad Software, Inc.).

Ventral nerve roots from L1 to L5 were dissected bilaterally and processed as described above. Cross sections (7 μm thick) were cut perpendicular to the long axis of the roots with a Leica cryostat (model CM3050 S) and were mounted on glass slides. Sections were rinsed briefly in water, and stained with toluidine blue. The transverse sections were photographed using a Motic microscope at a 100x magnification. Different areas of the cross sections of the roots were examined by simple random selection as described by Dolapchieva (Dolapchieva, 2004). The axonal diameter was measured as the length of Feret's diameter, and selected myelinated nerve fibres were used. Profiles of paranodes and merging profiles of myelinating fibres were not included.

4.2.4 Statistics

Data are presented as means ± standard error of the means (S.E.M.) as indicated.Graphs were constructed usingPrism 5 (GraphPad Software Inc., San Diego, CA). All results were analyzed to determine the effect of SG alone, G37R mutation alone, or the interaction between these two variables by ANOVA via Statistica 8.0 statistical software (StatSoft Inc., Tulsa, OK). Statistical significance between experimental and control groups for histological assessments were calculated using the Student *t*-test. Distributions of toluidine blue stained ventral roots were tested for normality using a one-sample Kolmogorov-Smirnov test, and differences between groups for each sex were detected using one-way ANOVA. Following that, a post hoc test using multiple comparison Tukey HSD test was used to find out which groups were significantly different from controls. The analysis and graphs of distribution functions were computed by SPSS version 17.0 (New York, USA). Differences were considered statistically significant at $p < 0.05$. P values were expressed as exact values except in cases where $p < 0.0001$. The statistical content and methodology was reviewed by a statistician.

4.3 Results

4.3.1 Neuromuscular junction integrity

Evaluations of end plates with rhodamine conjugated α-bungarotoxin immunofluorescence showed significant abnormalities in all G37R groups of both sexes (Fig. 4-1G). There were no detectable differences in motor end plate pathology between both sexes. Virtually all endplates

(>90%) were innervated in control-fed wild type mice in both sexes (Fig. 4-1A, G). Prolonged exposure to SG in wild type mice did not significantly change neuromuscular junction innervations in eithersex ($p = 0.75$ in males; $p = 0.066$ for females), as reported previously (Lee et al., 2009). Control-fed G37R mice showed significant end plate denervation compared with control wild types, with 82% denervation in females ($p < 0.0001$) and 65% denervation in males ($p = 0.0005$; Fig. 4-1E, G). Following treatment with SG in G37R mice, significance levels of denervation did not change (64% in females, $p = 0.0005$; 83% in males, $p < 0.0001$). Hence SG treatment did not significantly change end plate innervations in males or females. The decrease and increase in denervation for SG-fed G37R females and males, respectively, compared to control-fed G37R was not significant ($p = 0.36$ for females; $p = 0.12$ for males).

Endplates in the denervated groups were observed in the absence of neurofilament immunolabelling (Fig. 4-1E, F). Neuromuscular junctions showing terminal axons but no end plate overlap were labelled as intermediate (Fig. 4-1C, D) and represented approximately 10% of the population in all G37R groups and the SG-fed wild type group (Fig. 4-1G). Intermediate end plates represented <10% of the population in wild type controls. Where innervation was observed, the axon entering each neuromuscular junction was thick and variegated in diameter, terminal branches were uniform in width and acetylcholine receptor-rich sites on each muscle fibre were closely apposed to terminal branches (Fig. 4-1A, B). The slightly more proximal parts of each terminal branch were all indistinguishable (compare Fig.4-1A to Fig. 4-1C), indicating that the abnormality is initially confined to the most distal parts of the axons.

4.3.2 Pathological changes in ventral roots

The axon diameter distribution histogram showed a normal distribution of toluidine blue stained motor axon diameters for the control-fed wild types (Kolmogorov-Smirnov test, $p > 0.01$) while distribution of axonal diameters for other groups did not show a normal distribution (Kolmogorov-Smirnov test, $p < 0.01$; Fig. 4-2). In the ventral roots of all mice, the minimal axonal diameter that could be measured accurately was 1 μm (Fig. 4-3). In wild type mice, the average axonal diameter ranged between 1 μm and 14 μm (Fig. 4-3E, F), while the range for G37R mice was between 1 μm and 12 μm (Fig. 4-3G, H). A peak of 6 μm, representing the diameter of the majority of axon fibres, appeared in the WT controls (Fig. 4-3E). A bimodal distribution was visualized in

SG-fed WT mice (Fig. 4-3F). The values of the main modality ranged between 5 μm and 10 μm, and peaked at 7 μm. A smaller peak was observed in the WT SG group at 2 μm.

The frequency distributions of axon diameters were different between wild type and G37R mice (Fig. 4-4). In wild type controls, motor axons have a wide distribution of axon diameters, with the greatest number of axons having a diameter between 6 and 9 μm. SG-fed wild type mice showed a comparable wide distribution of axon diameters, with the greatest number of axons having a diameter between 6 and 10 μm. SG-fed wild types also showed a greater number of motor axons <10 μm in diameter than the controls. Both G37R groups showed a similar wide distribution range, although skewed toward smaller axon diameters compared to wild types.

The reduced proportion of large diameter motor axons inthe lumbar ventral root of both G37R groups and the consequent significant reduction in axon diameter range are further illustrated in the cumulative distribution functions (Fig. 4-5). A significant leftward shift of the cumulative distribution function in SG-fed G37R ($p < 0.05$), control-fed G37R ($p < 0.05$) indicates a decline in axon calibre in these groups. No significant shifts of the cumulative frequency histogram were observed in SG-fed wild types compared to controls ($p > 0.05$). In addition to a leftward shift in the normal distribution for G37R groups, a steeper slope for the smallest diameters was observed for these groups. This observation is consistent with the frequency distribution histogram which shows greater numbers of axons in the smaller diameter ranges.

4.3.3 Motor cortex pathology

Motor cortex pathology was unremarkable, showing no significant differences between groups. Treatment with SG did not affect the cellular distribution in the primary cortex in wild type animals (Fig. 4-6C) compared to controls (Fig. 4-6A). Neuronal morphology in layer V of M1 was comparable between these two groups (Fig.4-6B, D) as observed by Nissl staining. G37R primary motor cortex showed a laminar distribution and morphology comparable to wild type motor cortex (Fig. 4-6E, I). A fraction of G37R animals showed cellular morphologies reminiscent of chromalysis in layer V (Fig.4-6G, H), but the laminar distribution of cells in these animals was comparable to controls (Fig. 4-6F). Primary motor cortex in SG-fed G37R animals was comparable to control-fed G37R mice (Fig.4-6J-L). Histology of the supplementary motor cortex (M2) was also comparable to controls with respects to laminar distribution and cellular pathology as observed by Nissl staining and H&E (data not shown).

4.3.4 Apoptosis detection

Fluorescent labelling with TUNEL showed the presence of apoptotic cells in all groups studied (Fig. 4-7). The distribution of TUNEL labelling between groups was comparable to controls. Hoechst staining revealed a 1:1 ratio of TUNEL positive cells with apoptotic nuclei. TUNEL labelling was absent in negative control sections in which TdT was omitted from the reaction mixture. Double fluorescent labelling with TUNEL and anti-ChAT showed that the identity of apoptotic cells in all were not motor neurons. The occurrence of TUNEL positive and ChAT positive labelling represented only a small fraction of motor neurons with pathologic morphology (Fig. 4-7C, D arrows), indicating that other cellular population(s) were undergoing apoptosis.

4.4 Discussion

In the present study, the results demonstrate for the first time the contribution of SG to neurodegenerative processes of ALS in the peripheral motor axon and motor cortex caused by mutant SOD1G37R. At disease end stage, when degenerative changes in motor neurons and cell death are well underway, marked synaptic loss in motor endplates and reduction in axon calibre occur in mice with low mutant SOD1G37R burden. Chronic treatment with SG had no effect on furthering these degenerative changes in peripheral motor components in G37R mice. Although *in vitro* studies have shown that synthetic cycad sterols act directly on neural cells (Khabazian et al., 2002; Ly et al., 2007), SG appears to be primarily involved in inflammatory reactions and motor neuron pathology in the spinal cord. Chronic dietary administration of SG also induced significant reductions in motor function during behavioural tests. The fact that SG-mediated neuropathology was only noted in the spinal cord where neuronal cell death mainly occurs indicates that it could contribute to cell dysfunction leading to neurodegeneration in SOD1 mutant mice. It is possible that environmental toxins initiate neural pathogenesis by triggering inflammation-mediated neurodegeneration.

Synaptic loss at motor end plates of the gastrocnemius muscle of mutant SOD1 mice was consistent with the remarkable decline in motor function and paralysis of the hind limbs. Numerous other studiesshow early vulnerability of fast-type neuromuscular synapses and functional motor unit losses (Frey et al., 2000; Pun et al., 2006; Hegedus et al., 2007) in SOD1 ALS models. Atkin and colleagues reported no detectable muscle pathology in presymptomatic SOD1 G93A mice and

selective denervation of a subset of fast twitch muscle fibres at disease end stage (Atkin et al., 2005). Other studies detected skeletal muscle denervation in SOD1 G93A mice as early as 47 days (Fischer et al., 2004; Zhang et al., 2008b), and still other studies reported denervation occurring later at 10 weeks (Zhang et al., 2008b). The diagnosis of neuromuscular junction pathology is not limited to denervation, and may include other individual features such as neurofilament accumulation, pathological involvement of terminal Schwann cells and/or their neighbouring neuromuscular junction capping cells, or pathology of the postsynaptic components of the neuromuscular junction that includes motor end plates. Hence an important question is what features should be considered as essential or relevant aspects of synaptic pathology of the human condition. The features and time course of neuromuscular junction pathology is important in the development of therapeutic strategies, and studies into neuromuscular junction structure and function in affected muscles from ALS patients are required.

The 'intermediate' neuromuscular junctionscorrespond to junctions as being in the process of either denervation or reinnervation, and were observed in all wild type and G37R groups. Other studies in mutant SOD1 mouse gastrocnemius muscle using similar histochemical techniques also reported intermediate innervations of motor end plates in conjunction with marked denervation (Fischer et al., 2004; Abou Ezzi et al., 2010). Using time-lapse imaging of nerve terminals in double transgenic SOD1G93A and motor axons labelling with yellow fluorescent protein, Schaeffer and colleagues revealed two distinct motor neuron types; vulnerable motor units with junctions in the process of denervation having unique appearance of fragmented branches and compensatory motor units that are protected from degenerative changes and have thin reinnervating branches. It is possible that the immunofluorescence technique on cryosectionsused herewas not sensitive enough to observe fragmentation to differentiate between denervation (vulnerable) and reinnervation (compensatory). Tam et al. (2001) described clear histochemical evaluations of sprouting in partially denervated muscles differentiated in cryostat muscle sections. However, the authors used very thick tissue sections (100 μm) and were able to visualize entire motor units and hence minimize errors on identifying intermediate innervation. In addition, changes in innervation states at individual neuromuscular junctions may not, on its own, be the sole determinant of pathology of the associated motor neuron. Progressive motor neuron loss maybe clinically masked by the reinnervation process, and hence an estimation of the number of surviving motor units is more meaningful in separating motor neuron loss from reinnervation. Therefore, it will be of interest to examine changes in motor

unit number following prolonged SG exposure and comparing the results in mutant SOD1 mice. Cycad steryls are toxic to motor neurons and the consequences of their neurotoxicity on motor unit remodelling has not been examined and therefore cannot be ruled out. This study also does not take into account electrophysiologic parameters of surviving motor neurons. Abnormal electrical conductances have been described in numerous studies of various mutant SOD1mice, favouring hyperexcitability changes in spinal motor neurons (Kuo et al., 2004; Pambo-Pambo et al., 2009; Sunico et al., 2011). Correlation of the morphological parameters with the elctrophysiologic parameters would help differentiate between the 'sick motor neuron' hypothesis and the hypothesis stating that loss of a threshold number of motor neurons leads to the phenotype.

Another major finding demonstrated here is a significant reduction in motor axon calibre in G37R mice that is unaffected by chronic SG dietary administration. The numbers of large calibre axons is significantly lower in G37R ventral roots compared with wild types, while the number of small calibre axons is increased. This finding is consistent with increased numbers of small axon fibres and greater frequency of axonal degeneration in the ventral spinal root of ALS patients (Hanyu et al., 1982). Other studies in the same line of G37R mice reported significant reductions in axonal proteins before disease onset and massive axonal loss in L5 ventral roots at disease end stage (Kriz et al., 2002; Farah et al., 2003; Abou Ezzi et al., 2010). Large myelinated fibres undergo atrophy, while myelin sheaths increase in thickness and show various irregularities (Thomas et al., 1981). In addition, significant decreases in large fibres in the G37R groups are comparable to the loss of large myelinated fibres in the L4 ventral roots described in old animals (Ansved et al., 1990), consistent with the classification of ALS as an age-related disease. The degree of demyelination (or abnormalities in myelination) has not been described in this G37R mouse line, but it is possible that mutant SOD1 triggers an advanced aging process on the large fibres of spinal motor neurons. A marked increase in small calibre axons at disease end stage may indicate new growth rather than persistent axons, occurring in the form of thin branches that emanate primarily from axons as opposed to terminal sprouts. Motor neurons innervating type I and type IIA muscle fibres retain sprouting competence compared to the loss of sprouting competence in motor neurons innervating the fast-type-fatigable type IIB fibres (Frey et al., 2000; Pun et al., 2006). Sobue and colleagues, in a study of ALS patients, reported that ventral root atrophy eventually resulted from preferential degeneration of large myelinated axons with relative sparing of small fibres at late stage disease (Sobue et al., 1981). The SOD1G37R line 29 mice used in this study is a milder model of ALS, and

therefore it is plausible that some sprouting, although expectedly rare, is still occurring at end stage disease in a subset of axons innervating slow-type muscle fibres. However, in this study it is impossible to distinguish between thin axons that are refractory to degeneration from new (reinnervating) thin axons that are compensatory. Alternatively, the identity of these small calibre axons may be gamma efferent fibres that innervate the intrafusal muscle fibres.

Even though G37R expression resulted in marked synapse and large axonal loss, it is noteworthy that cortico-motorneurons were not affected in the G37R mice, with or without prolonged SG exposure. In the G37R line 29 mice, pathology was shown to be restricted to motor neurons in spinal cord and brainstem (Wong et al., 1995; Wong et al., 2002), which may in part explain why an overt pathology was not observed in the motor cortex. The restriction of neuropathology to lower motor neurons in different mutant SOD1 mouse models points to a primary action on lower motor neurons. When taken together, this combined gene-environment model of ALS is insufficient at modeling the human condition specifically for studying the motor cortex, since it has long been known that degeneration and paucity of the human Betz cells are features of ALS (Brownell et al., 1970; Hammer et al., 1979), and transgenic mice do not represent the complete human ALS phenotype. However, studies of motor cortex neuropathology are confounding because cortical changes are relatively minimal compared to pathogenesis caudal to the medulla (Smith, 1960; Brownell et al., 1970), and abnormal features such as neuronal inclusions in Betz cells may be an age-related non-specific degenerative change, since they appeared more frequently in elderly individuals (Sasaki et al., 2001). Perhaps neuropathological studies of the motor cortex must look beyond changes detectable only by immunocytochemical or ultrastructural methods. For example, combined structural and functional connectivity studies using diffusion tensor imaging (DTI) and functional magnetic resonance imaging (fMRI) demonstrates evidence of intracranial degeneration of the corticospinal tract and motor network deterioration in ALS (Verstraete et al., 2010). However, a recent *in vivo* study of the motor cortex in presymptomatic G93A mice failed to find any evidence of histopathological lesions, including those of motor neuron loss or increased gliosis (Spalloni et al., 2011). Using neuronal subtype-specific markers, Ozdinler and colleagues distinguished corticospinal motor neurons from subcerebral projection neurons and reported early presymptomatic degeneration of corticospinal motor neurons in mutant SOD1 G93A mice followed by corticospinal tract degeneration later in disease progression (Oezdinler et al., 2011). Application of rigorous methodology in other animal models of ALS is valuable to

demonstrate the specificity of corticospinal motor neuron degeneration in layer V of motor cortex, a feature that would mirror the cortical pathology found in human ALS. In the current study, the methodologies used to identify degeneration of cortical motor neurons provided only a limited analysis. Although the methodology used in this study does not allow detailed cellular and molecular investigation of the pathology of cortical motor neurons in G37R mice, it was included to identify apparent pathological changes, such as a paucity of motor cortical cells or changes in the distinctive large morphology of cortical motor neurons, due to the SOD1 mutation or exposure to SG. Cresyl violet labeled corticospinal motor neurons were confirmed in this study to reside in layer V of the motor cortex by their distinct morphology with a large pyramidal cell body and a long apical dendrite.

There are still conflicting reports on whether the cell death of motor neurons in ALS occurs through apoptosis or necrosis. My results demonstrate TUNEL-positive cells with occasional overlap with ChAT-positive motor neurons in G37R lumbar cord. In agreement with this study, Yamazaki and colleagues reported occasional TUNEL-positive motor neurons in the spinal cord of ALS patients with a shrunken or atrophic morphology inconsistent with apoptosis (Yamazaki et al., 2005). Other studies also failed to report evidence for an apoptotic mode of neuronal death in ALS (Kihira et al., 1998; He et al., 2000; Tomik et al., 2005). Conclusive evidence of apoptosis may be difficult to detect in a progressive neurodegenerative disease such as ALS, given the rapidity of the apoptotic cell death process compared to the relatively slow disease time course. It is generally accepted that programmed cell death does occur in ALS but its role as the major mechanism of cell death is unknown (Sathasivam et al., 2001). The results of this study support the hypothesis that apoptosis is not the major mechanism of cell death in spinal cord of the G37R line 29 model of ALS. However, different SOD1 mutations present varying levels of clinical severity, since G93Amice exhibited significantly increased cell death and number of TUNEL-positive cells (Patel et al., 2002). Morphological studies of surviving motor neurons in this study suggest a mechanism of cell death presenting as chromatolysis, atrophy, and pyknotic nuclei. These vacuolation observed hereresembles a non-apoptotic form of cell death, pointing towards the necrosis side of the apoptosis-necrosis morphological continuum.

Figure 4-1. Neuromuscular junction and end plate pathology in gastrocnemius muscle.

Motor end plates were identified with rhodamine conjugated α-bungarotoxin (red) and axons were identified with neurofilament and SV2 (green). Virtually all motor end plates in wild type controls were innervated (A), showing clear overlap between red and green fluorescence labelling (B). Intermediate filaments represented >10% of wild type control mice and approximately 10% of the other groups, showing an axon in the vicinity of a motor end plate but with no overlap (C, D). All G37R groups showed significant increases in denervation of motor end plates visualized by empty motor end plates (E, F). Graph in (G) expressed as mean ± S.D. Numbers in parentheses indicates the number of neuromuscular junction that was counted in that group. Scale bar 40 μm. (** $p < 0.001$; *** $p < 0.0001$).

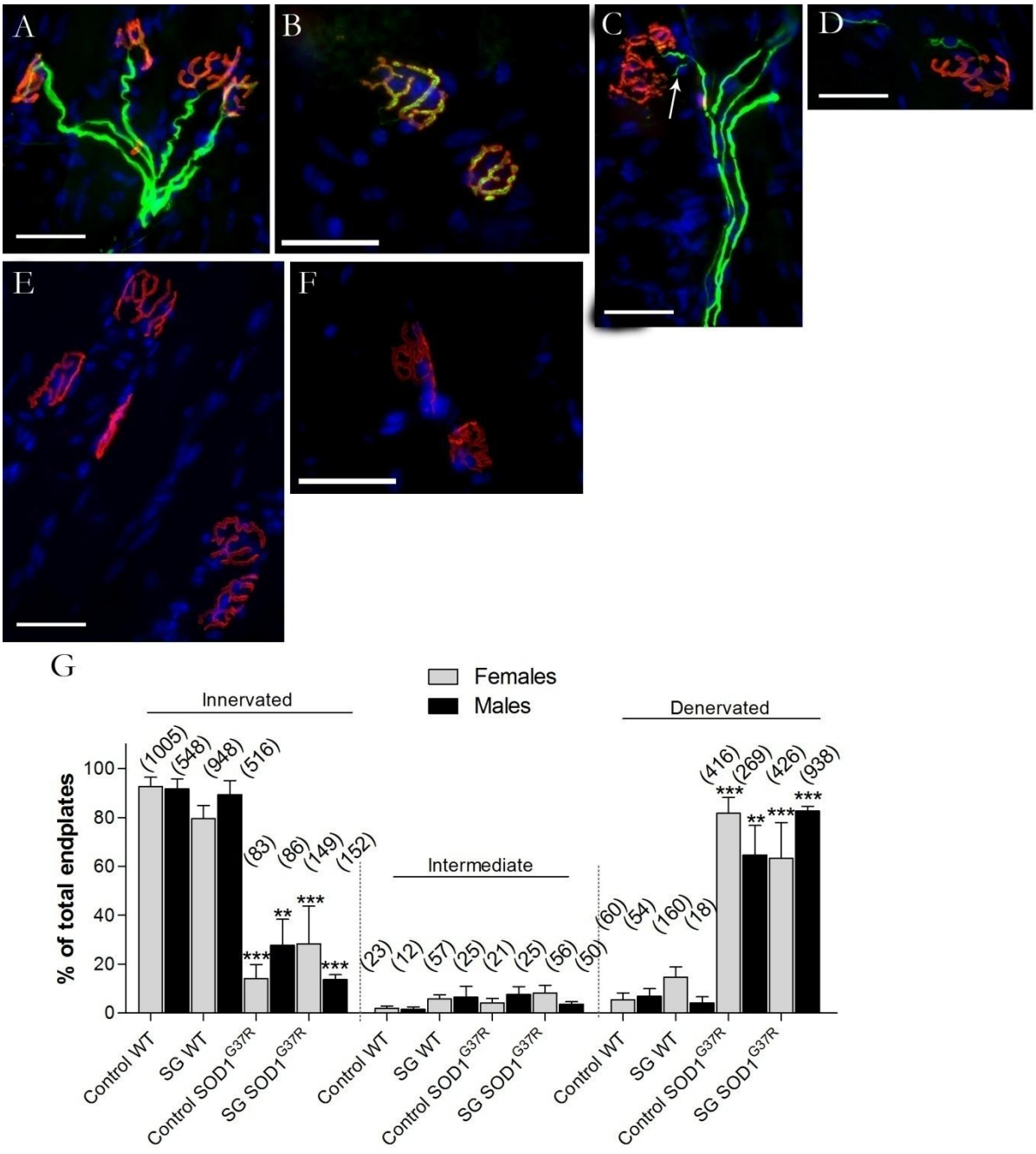
A
B
C
D
E
F
G
Females
Males
Innervated
Intermediate
Denervated
% of total endplates
100
80
60
40
20
0
(1005)
(548)
(948)
(516)
(83)
(86)
(149)
(152)
(23)
(12)
(57)
(25)
(21)
(25)
(56)
(50)
(60)
(54)
(160)
(18)
(416)
(269)
(426)
(938)
***
**
***
***
**
***
***
Control WT
SG WT
Control SOD1G37R
SG SOD1G37R
Control WT
SG WT
Control SOD1G37R
SG SOD1G37R
Control WT
SG WT
Control SOD1G37R
SG SOD1G37R

Figure 4-2. Frequency distribution of motor axon diameters.

Histogram representing the distribution of toluidine blue stained axon diameters in the ventral root of lumbar cord of control-fed wild type (A), SG-fed wild type (B), control-fed G37R (C), and SG-fed G37R (D) mice. The data shows a normal distribution in the wild type controls only (A), and a comparable mean for SG-fed wild types (B). The value of N is the number of motor axons counted in each group, and data from male and female mice were combined.

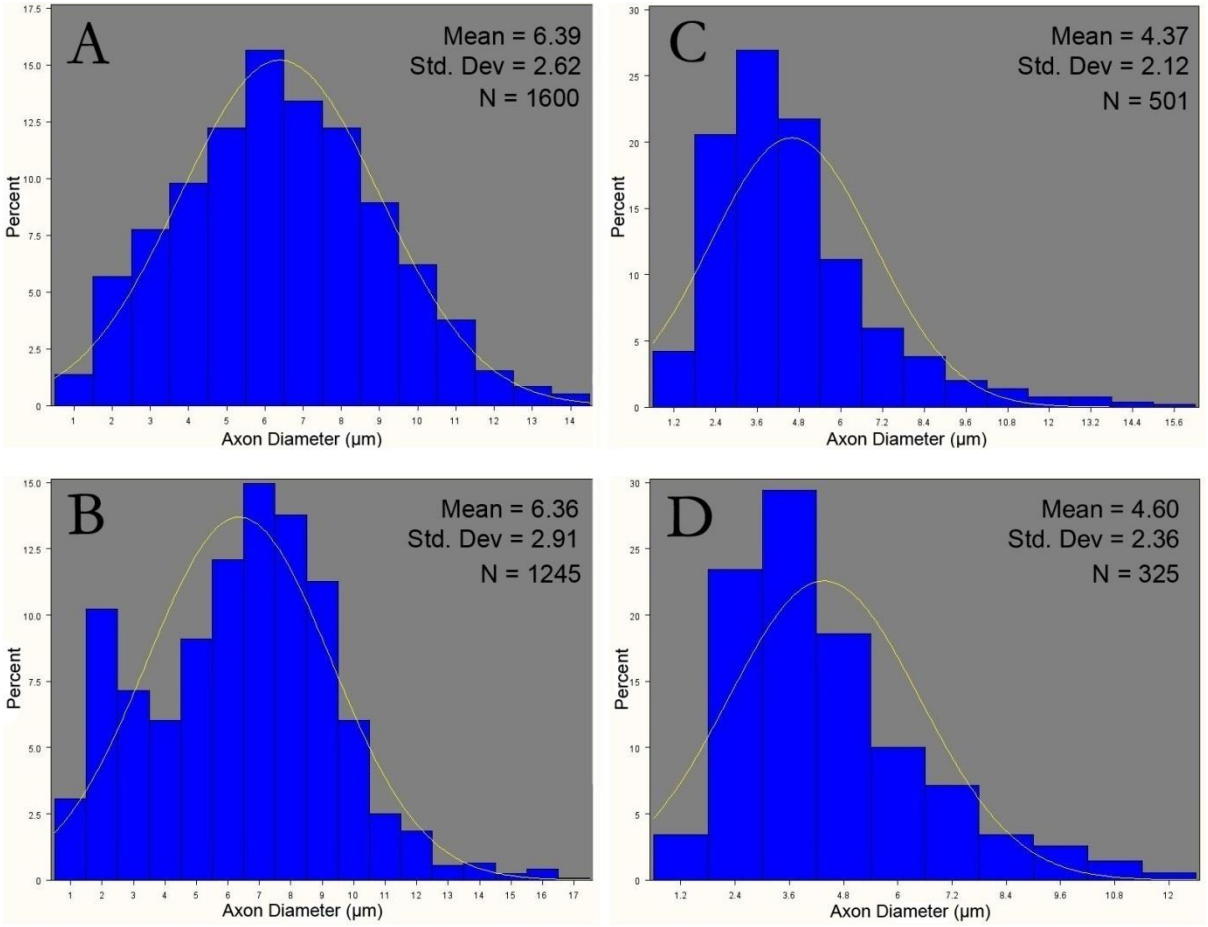

Figure 4-3. Axon size and frequency in ventral root of lumbar spinal cord.

Transverse sections of ventral roots in control-fed wild type (A), SG-fed wild type (B), control-fed G37R (C), and SG-fed G37R (D) mice were stained with toluidine blue and visualized using light microscopy. Wild type control ventral roots show a normal distribution with a peak at 6 μm and a maximum diameter of 14 μm (E). SG-fed wild type ventral roots show a bimodal distribution with peaks at 2 and 7 μm, and a maximum diameter of 14 μm. Ventral roots of G37R mice show a reduced mean diameter, with a maximum diameter of 12 μm and a peak at 3-4 μm for control-fed G37R and 4 μm for SG-fed G37R (F). The value of N is the number of motor axons counted in each group and data from male and female mice were combined. Scale bar 60 μm.

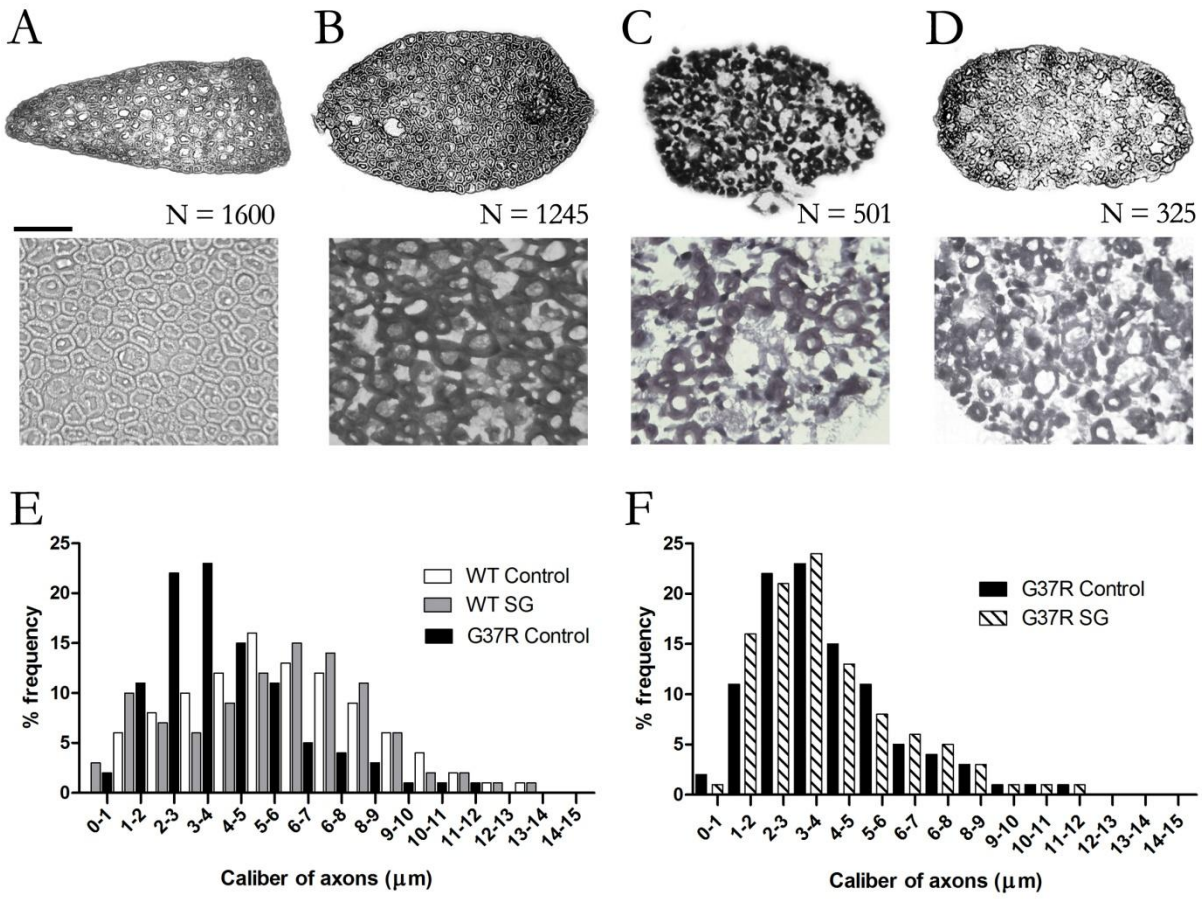

Figure 4-4. Changes in the frequency distribution of motor axon diameters.

All groups showed a similar wide distribution of motor axon diameters. The mean axon diameter was 6.4 μm for both wild type groups, with SG-fed wild types showing a greater number of small diameter axons. In the G37R mouse groups, the distribution was skewed toward smaller axon diameters. The mean axon diameter was 4.4 and 4.6 μm for SG- and control-fed G37R groups, respectively. Data from male and female mice were combined.

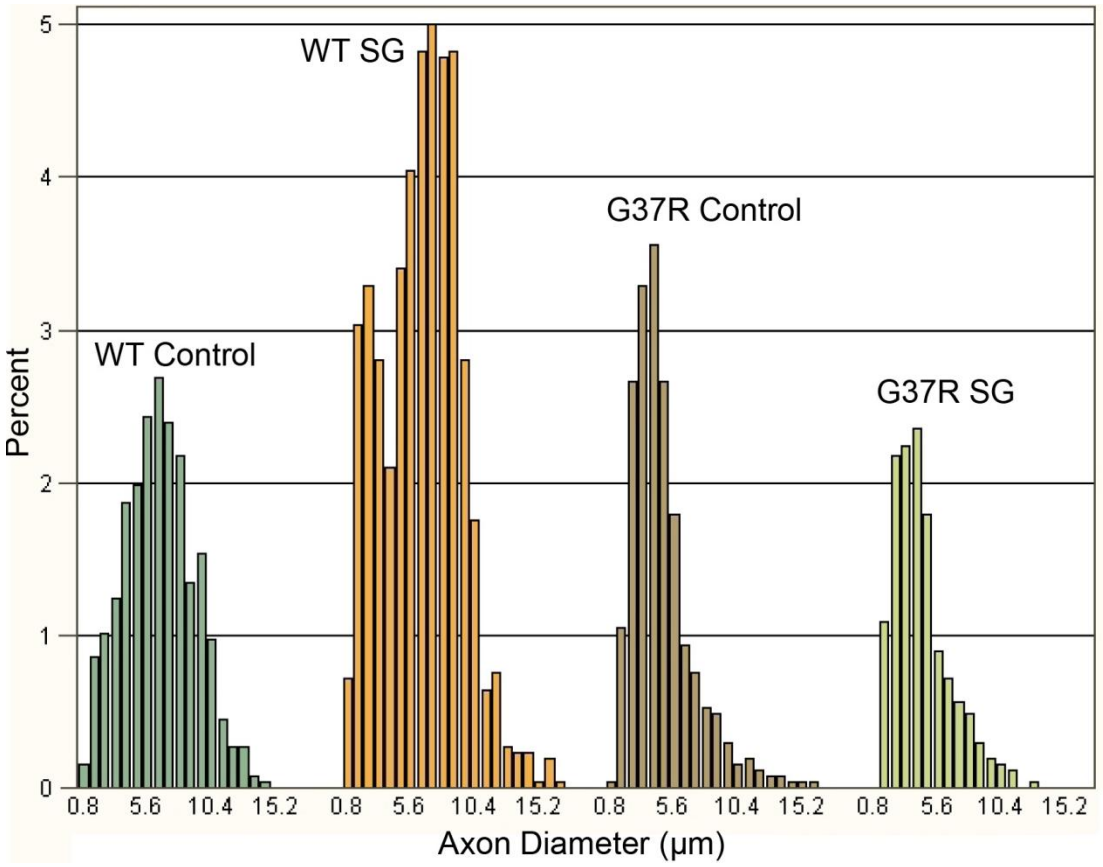

Figure 4-5. Changes in cumulative distribution of motor axon diameter.

The changes in axon calibres between groups are illustrated by a cumulative distribution function. There was a significant leftward shift of axon diameters in G37R groups ($p < 0.05$), demonstrating a reduction in axon calibre compared to wild type controls. The steeper initial slope of the histogram corresponding to both G37R groups shows greater numbers of motor axons belonging to the smallest diameter range. Motor axons from SG-fed wild types did not show any changes in diameter compared to wild type controls. Data from male and female mice were combined.

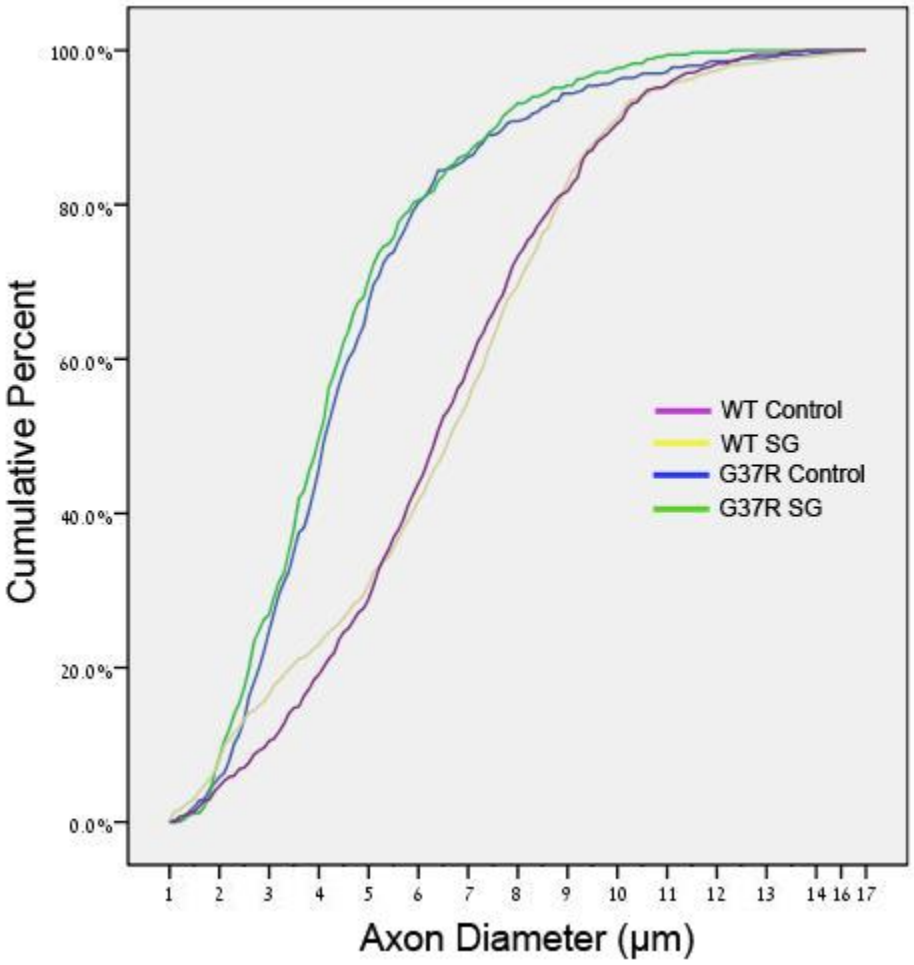

Figure 4-6. Neuronal cell changes in primary motor cortex (M1).

Distribution of neuronal cells in layer V of M1 in control-fed wild typeanimals (A) is comparable to the distribution in SG-fed wild type animals (C). Pyramidal cells in layer V of control-fed wild types appear healthy with large darkly stained cell bodies and dendritic processes (B), and those in SG-fed wild types are comparable to controls (D). Distribution of neuronal cells in M1 of control-fed (E) and SG-fed (I) G37R animals is also comparable to controls. Higher magnification of E and I shows healthy pyramidal cells comparable to controls among a relatively smaller population of chromatolytic cells (F and J, respectively). A fraction of control-fed (G) and SG-fed (K) show a reduced density of darkly stained pyramidal cells in layer V of M1. Higher magnification in this subset shows few healthy cells among a relatively larger population of chromatolytic cells (H and L, respectively). (M) Cross section of M1 showing the laminar layers. Male and female mice show similar distribution cortical cells, and hence the data for neuronal cell changes in the motor cortex have been pooled together. Scale bar 40 μm in A – L, and 100 μm in M.

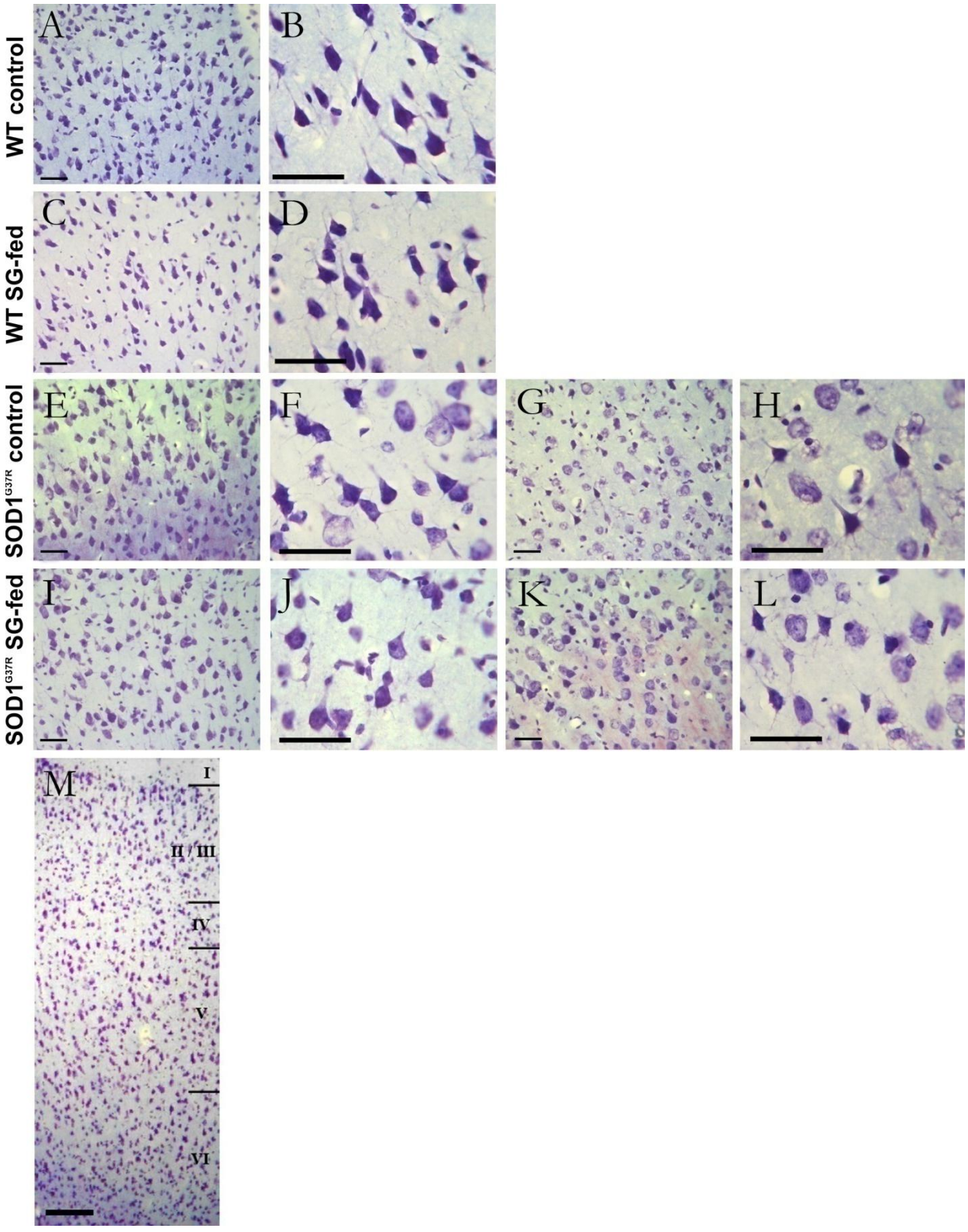
WT control
WT SG-fed
SOD1G37R control
SOD1G37R SG-fed
A
B
C
D
E
F
G
H
I
J
K
L
M
I
II / III
IV
V
VI

Figure 4-7. Double TUNEL and ChAT immunofluorescence in lumbar spinal cord.

TUNEL positive cells are observed in the lumbar ventral horn of wild type control (A), SG-fed wild type (B), G37R control (C) and SG-fed G37R (D) mice. Male and female mice show similar distribution of TUNNEL-positive cells, and hence the data for TUNEL and ChAT immunofluorescence have been pooled together. The distribution of TUNEL labelling in the ventral horn is indicated by the asterisks. Occasional TUNEL positive ChAT positive motor neurons are observed in the G37R groups (arrows in C, D), but the majority of surviving motor neurons are TUNEL negative despite the appearance of pathologic morphology. Scale bar 100 μm.

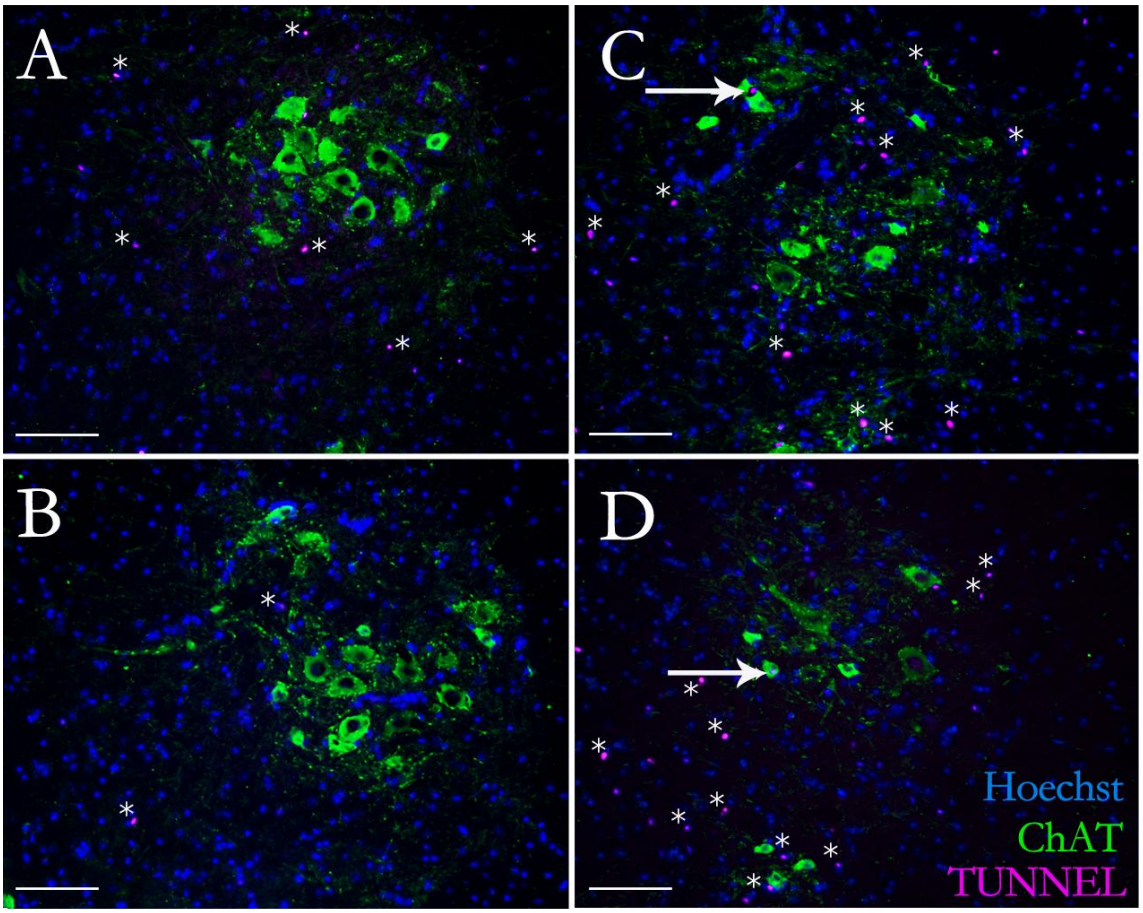

Chapter 5. General Discussion

Gene-environment interactions are suspected when one or more environmental risk factors modulate the risk for disease in subjects with a genetic susceptibility. For example, observation of marked neurofilament accumulation in the brains and spinal cords of Chamorros with ALS-PDC in Guam, where consumption of cycad material was vital for sustenance, may lead to the hypothesis that for a specific subpopulation of Guamanians with a genetic predisposition to neurofilament accumulation, exposure to cycad toxins may be more harmful. Identification of environmental risk factors involved in gene-environmental interactions is difficult, because ALS is a heterogeneous disease and a specific exposure to an environmental neurotoxin may result in only a small or negligible increase in risk. In addition, there are many toxins in the environment, making it difficult to identify the putative toxin causing ALS. Furthermore, as discussed previously, the pathogenic mechanisms of motor neuron degeneration in ALS are numerous and act through various pathways. It is possible that different genes responsible for familial ALS may interact with different environmental triggers. It is also possible that the critical environmental and gene-environment interactions may occur well before the onset of clinical manifestations and remain undetected until years later. Thus, the most feasible approach the study gene-environment interaction in ALS is to evaluate the additional (deleterious) effect of environmental toxins on specific mutations in genes causing ALS. This is especially true if the neurodegenerative changes in ALS are the result of additive or synergistic effects of multiple exposures to a neurotoxin(s) and these effects become compounded by increased vulnerability of the aging motor neurons to toxic injury. Determination of disease progression in gene-environment interaction models is important, because characterization of exogenous influences on the course of the disease will help find ways to prevent disease in individuals at risk.

Several lines of evidence are consistent with a significant contribution of environmental risk factors to the pathogenesis of ALS. Epidemiological studies have found an association between increased risk of ALS and exposure to toxic agents in both the occupational and non-vocational settings (Govoni et al., 2005; Furby et al., 2010). Experimental *in vivo* studies have shown that neurotoxic treatments are capable of reproducing a pathology resembling neurodegenerative disease in a rodents and monkeys (Dastur, 1964; Wilson et al., 2002; Lee et al., 2009; Shen et al., 2010). Recent genetic approaches to the study of ALS have resulted in new insights into the etiology of

neurodegneration. As discussed in Chapter 1, recent advancements in genetic discoveries, namely TDP-43 and FUS, have led to a better understanding of ALS pathogenesis. Although much work is necessary for understanding the precise mechanism of TDP-43 and FUS-mediated pathology, the relevance of these proteins to ALS and other neurodegenerative diseases has become evident. Ubiquitinated TDP-43 and FUS positive intracytoplasmic inclusions are significant components of round and skein-like neural and glial inclusions typically observed in the CNS of patients with sporadic ALS (Arai et al., 2006; Vance et al., 2009). Aberrant localization of these proteins in cytoplasmic inclusions is likely to underlie the development of the clinical manifestations ranging from motor weakness to upper motor neuron involvement, as studies introducing human forms of these proteins were demonstrated to be sufficient to cause progressive neurodegenerative symptoms in mice (Stallings et al., 2010). However, the loss of motor neurons in the more common SALS is still largely unexplained. It is likely that the etiology is multifactorial, involving gene-environment interactions. Thus, identifying genes that predispose ALS pathogenesis could help elucidate possible toxic events that may lead to motor neuron degeneration. More importantly, studies of the mechanisms of harmful environmental agents might help to identify specific genes that modulate neurodegeneration. In this thesis I have followed the leads provided initially by the observations on post-war Guam to search for clues about genetic susceptibility and environmental triggers for neurodegeneration that may potentially lead to preventative strategies identifying individuals at risk while limiting exposure to harmful agents.

Using an established mutant SOD1 G37R mouse model of ALS, I have tested the hypothesis that pathogenesis in motor system compartmentsexpressing mutant SOD1 occurs with greater severity following prolongedexposure to an exogenously administered toxin. In these transgenic animals, the genetic susceptibility to neurodegeneration is associated with a delayed phenotype of ALS expressing at 11 months of age, and pathology preferentially targeting lower motor neurons. Subsequently, I explored the collective effects of mutant SOD1 and toxin on motor axons at the ventral root and terminals at neuromuscular junctions to find evidence pointing to the tissue(s) of primary importance in ALS pathogenesis. In this chapter I will discuss the strengths and weaknesses of my findings in light of other current and ongoing research in the field of neurodegeneration in ALS. I will also discuss the relevance of my findings in the context of other studies of the molecular mechanisms considered important in contributing to motor neuron

degeneration. I will end with my suggestions for future research to contribute to a successful search for therapeutic interventions for at risk patients with a genetic susceptibility to ALS.

5.1 Summary

The results of this study demonstrate significant interaction between synthetic cycad toxin and mutant SOD1G37R genotypeon the progression of motor deficits, evidenced by SG-affected outcomes of reduced latencies to fall from the rotarod and wire hang and reduced extension reflex scores. Reduced motor neuron numbers in the lumbar anterior horn was observed in G37R mice, and introduction of SG showed a nonsignificant trend toward further motor neuron loss. Chronic SG treatment in both wild type and G37R mice resulted in a leftward shift toward smaller motor neuron soma diameters with apparently normal and chromatolytic morphologies. The interplay between genetic and environmental factors had a significant effect on increased gliosis in the lumbar spinal grey matter, with marked expression of an activated glial morphology. In studies of peripheral components of the motor system, G37R mice showed a marked reduction in innervated motor end platesand a significant shift toward smaller motor axon calibres, which was unchanged with SG treatment. Marked lumbar cord and peripheral nerve pathology in G37R mice is observed with only minimal changes in the motor cortex. The deleterious effects of chronic SG exposure are localized to cord, and indicate that the CNS response to such environmental factors is spinal in origin.

5.2 Molecular mechanisms of motor neuron degeneration

Amyotrophic lateral sclerosis is a late onset neurodegenerative disease characterized by progressive muscle weakness and eventual paralysis, paralleled by death of large motor neurons in the cortex, brainstem and spinal cord (Julien, 2001). The results of my initial studies on the occurrence of motor neuron loss and atrophy with concurrent soma size changes are consistent with human ALS cases. For example, astudy in human ALS spinal cord shows a paucity of alpha motor neurons in conjunction with an increase in interneuron numbers and small diameter motor neurons (Stephens et al., 2006). The degree of motor neuron death is variable between ALS patients as evidenced by post mortem analysis and literature on animal models of disease. One possible explanation for this inconsistency is that the initial neuronal population affected varies between individual patients since ALS affects both upper and lower motor neurons and exhibits heterogeneous sites of onset. Supporting this hypothesis is the observation of differing susceptibilities among motor neuron groups at different levels of the CNS throughout the progression of the disease. In the lumbar spinal cords of the mutant SOD1 G37R mouse model

used in this study, anterior motor neuron loss, atrophy and neuropathology of surviving cells, and gliosis are the hallmark features. Transgenic mice overexpressing SOD1 mutations develop some, but not all, of the symptoms and pathology of the human disease (Gurney, 1994; Wong et al., 1995; Julien et al., 2006). SOD1 mutant mice show the same inflammatory changes that are observed in sporadic ALS including the presence of abundant activated microglia and astrocytes (Barbeito et al., 2004; Sargsyan et al., 2005). Excitotoxicity due to astrocyte dysfunction and inflammation from astrocyte activation are other events likely to be involved in the propagation of the neurodegenerative process (Hall et al., 1998; Hirano, 1998). The development of these inflammatory changes coincides with disease onset and increases in intensity with disease progression (McGeer et al., 2002). These pathologic features are also mirrored in the lumbar cords of animals exposed to SG in the absence of SOD1 mutations, although to a lesser extent.Mohajeri and colleagues demonstrated preservation of the small gamma motor neurons in symptomatic mutant SOD1 mice compared to wild type counterparts (Mohajeri et al., 1998). However, their cell counts of small motor neurons may have included both gamma motor neurons and surviving alpha motor neurons that have atrophied. The method used in this study is a detailed size distribution analysis of motor neuron populations and demonstrates a shift from large to small motor neurons in transgenic and SG-fed mice. In addition, these methods account for the morphological indications of atrophic alpha motor neurons and thus represent a more accurate representation of motor neuron numbers in different subclasses.

It also seems likely that motor neuron pathology mediated by SG and mutant SOD1 G37R occurred through comparable modes of degeneration. Vacuolization of large motor neuron cell bodies is indicative of degeneration and appears as chromatolysis in light microscopy. The results presented in this study demonstrated chromatolysis and atrophy in a subset of anterior horn cells in all experimental groups studied. Central chromatolysis of anterior horn cells is one of the typical pathological findings of ALS along with extensive neuronal loss and cytoplasmic neuronal inclusion bodies (Mizusawa et al., 1991; Kusaka et al., 1988). Chromatolytic motor neurons in wild type controls of both sexes were shown to have larger cell diameters than chromatolytic neurons in all the other experimental groups. This finding is consistent with a pronounced reduction in soma size of chromalytic neurons of ALS patients compared to neurons showing central chromatolysis in control subjects (Sasaki et al., 1996). An ultrastructural study of chromatolytic motor neurons in ALS reported features of diminished synaptic function (reduced number and lengh of individual

synapses) in these pathologic neurons (Sasaki et al., 1996). Taken together with the findings of the present study, an increase in smaller diameter chromatolytic neurons represents pathologic interneurons that may be inhibitory or excitatory. In G37R mutants, glutamate-mediated excitotoxicity is one plausible mechanism contributing to motor neuron death. One mechanism of excitotoxicity includes reduction of the astroglial glutamate transporter EAAT2 (Rothstein et al., 1995). Earlier studies in G37R mice reported that the expression of high levels of mutant human SOD1G37R in large spinal motor neurons does not cause neurodegeneration, supporting the involvement of non-neural cells such as glia in excitotoxicity (Pramatarova et al., 2001; Ilieva et al., 2009). Thus, SG and mutant SOD1G37R may share a common mechanism of modulating the overall excitability of spinal cord motor neurons. Aberrant control of motor neuronal excitability is possible, since hyperexcitability has been described in the motor cortex and spinal cord of ALS patients (Sasabe et al., 2010). The molecular mechanisms governing aberrant excitability in motor neurons (aberrant glutamate transport, Ca^{2+} permeability of AMPA receptors, excitatory/inhibitory synaptic imbalance) also render motor neurons susceptible to excitotoxic degeneration or death (Bogaert et al., 2010a; Finn et al., 2010; Grosskreutz et al., 2010). The subsequent increase in intracellular Ca^{2+} due to excitotoxicity may then lead to vulnerability to mitochondria-mediated apoptosis andoxidative stress from reactive oxygen species production, which represents a self-perpetuating vicious cycle of cell demise.

Motor neuron degeneration mechanisms implicated by chromatolysis were not the only indicators of pathogenesis in this gene-environment model of ALS. As discussed in Chapter 2, shrunken or atrophic motor neurons observed in the anterior lumbar spinal cord may indicate a different molecular mechanism of degeneration. Oyanagi and colleagues observed shrunken anterior horn cells in both ALS patients and controls, but only shrunken cells in ALS patients showed endoplasmic reticula with abnormal distended cisternae and decreased ribosomal detachment from rough endoplasmic reticulum (Oyanagi et al., 2008). Moreover, their findings of endoplasmic reticulum (ER) stress were unique to shrunken cells (chromatolytic cells were excempt). ER stress induces accumulation of misfolded secreted or membrane proteins in the ER lumen (Sasaki, 2010). Therefore, there may be a disrupted transport of newly synthesized proteins and an accumulation of misfolded proteins in the motor neurons of this gene-environment model of ALS. The accumulation of damaged proteins in the cytoplasm may subsequently lead to impairment of the ubiquitin-proteasome degradation system, yielding the intracellular inclusions (skein-like inclusions,

Lewy body-like hyaline inclusions) characteristic of ALS. A recent study using mutant SOD1 human neuroblastoma cells reported ER stress-induced Lewy body-like hyaline inclusions subsequently leading to activation of the apoptotic pathway (Koyama et al., 2010). These Lewy body-like hyaline inclusions are composed of ER and exhibit SOD1 and ubiquitin immunoreactivity, which ultimately leads to cell death. The authors suggested that ER stress in their model of FALS increases vulnerability to ER stress and causes mutant SOD1 aggregation. Similarly, ultrastructural analysis of transgenic mice showed vacuolization and cytoplasmic filamentous inclusions in affected motor neurons (Dalcanto & Gurney, 1994a). Furthermore, the influences of ER stress are not limited to inclusion formation and also affect motor neuron survival, gliosis, motor dysfunction, disease onset, and survival (Shimazawa 2010). Shimazawa et al. (2010) identified a small molecule with a protective effect on ER stress-induced pathogenesis in transgenic mice via induction of VGH nerve growth factor inducible. In their study, the authors reported slowed disease progression, prolonged survival, and increased motor neuron survival following chronic subcutaneous administration of this VGF inducer. Although motor neuron loss was found to be a remarkable feature of this gene-environment model of ALS, TUNEL-positive motor neuron labelling in experimental groups were comparable to controls and pathologic motor neurons did not exhibit the characteristic features of apoptosis such as plasma membrane blebbing or nuclear condensation. This indicates that apoptosis was not the key mechanism of cell death at disease end stage. It is possible that the window for apoptotic cell death had already passed, and cell dysfunction rather than overt cell death plays a more significant role in the late disease stage studied here. Various upstream caspases in the apoptotic cascade were reported to be activated by ER stress at an early stage of disease prior to any hindlimb paralysis (Wootz et al., 2004). Furthermore, displacement of cytoskeletal elements by vacuoles from degenerating mitochondria have been implicated in the generation of central chromatolysis in mutant SOD1 mice, leading to cytoplasmic accumulation of phosphorylated neurofilament (Wong et al., 1995). Thus, mitochondrial dysfunction in this mouse model studied may not lead directly to programmed cell death, but may have an insidious effect on neurons and their ability to maintain metabolic homeostasis, exerting a synergistic effect with other pathological molecular pathways. The role of chromatolytic and shrunken motor neurons in control animals is unclear, but pathologic motor neurons in neurodegenerative disease show aberrant characteristics (smaller soma and rough ER dysfunction) that are not described in pathological-appearing motor neurons of controls.

The gene-environment model of ALS presented in this study reveals a mode of motor neuron vulnerability involving remarkable vacuolar changes indicative of mitochondria dysfunctionat disease end stage. Neuronal vacuolation in SOD1 transgenic mice is due to the swelling of ER and mitochondria (Dalcanto & Gurney, 1994a), but ER pathology in G37R lines is not a prominent characteristic (Wong et al., 1995). That surviving motor neurons did not show morphological evidence for apoptotic death and *in situ* labelling of DNA breaks did not reveal increased apoptosis is in agreement with earlier studies of SOD1 transgenic mice (Chiu et al., 1995; Dalcanto et al., 1995). The loss of neurons, reduction of large diameter myelinated axons, and denervation of muscle all take place at disease end stage in this gene-environment mouse model. The preservation of some large diameter cells in the population of surviving motor neurons argues against the hypothesis that a large calibre (and hence greater metabolic demand) renders motor neurons more vulnerable in ALS. This finding is supported by another study reporting that the large calibre and high neurofilament content of α motor neuron axons did not account for the selective vulnerability of motor neurons in ALS (Nguyen et al., 2000).

5.3 Pathogenesis of peripheral motor components

Recently, there is an emerging hypothesis that skeletal muscle is a primary site of pathogenesis in ALS, presenting evidence forretrograde degeneration in motor neuron disease. A recent study involving skeletal muscle-restricted expression of G37R and G93A mutant SOD1 demonstrated pathologic ALS phenotypes and distal axonopathy in spinal motor neurons leading to accumulation of ubiquitinated inclusions and degeneration through apoptosis (Wong et al., 2010). Fischer et al. (2004) proposed the theory of distal axonopathy in which lumbar spinal motor neuron degeneration occurs in a retrograde fashion. During the presymptomatic stage, motor neuron nerve terminals start to die back followed by a symptomatic phase of rapid cell death. As motor neurons progressively degenerate in this retrograde fashion, they no longer stimulate their postsynaptic muscle targets resulting in muscle atrophy and paralysis. Studies in mutant SOD1G93A mouse models have shown preferential presymptomatic (~P45) denervation of fast-fatigable type IIA muscle fibres (Frey et al., 2000; Pun et al., 2006). These findings are consistent with electrophysiological studies showing early loss of the most forceful functional motor units (Hegedus et al., 2007). Another study suggested that muscle fibre atrophy and weakness might not be a simple collateral damage of LMN degeneration, but instead that muscle fibres may be the site of crucial

pathogenic events in these diseases and hence a worthy target for treatments or a preferential route for targeting motor neurons (Dupuis et al., 2010).

The results from my study demonstrate that neuromuscular junctions are vulnerable to SOD1-mediated disease triggers, and that exposure to SG in this cohort produces no further changes in end plate synaptic vulnerability at end stage of disease. These findings indicate a spinal origin of SG effects, and are consistent with my earlier report in non-transgenic mice (Lee et al., 2009). Since motor end plate synapses were shown to be particularly vulnerable in G37R mice, it is possible that other types of synapses in the motor system of the brain and spinal cord are also vulnerable. Synaptic connections at sites other than the neuromuscular junction such as at interneurons (Stephens et al., 2006) and upper motor neurons (Eisen et al., 1996) were reported to be affected in ALS, both of which make synaptic contact with lower motor neurons. Examination of the time course of synaptic loss in mutant SOD1 mice revealed an early symptomatic reduction in inhibitory but not excitatory inputs onto motor neurons (Sunico et al., 2011). A reduction in the number of synapses onto normal-appearing anterior horn cells have been reported in ALS patients (Sasaki et al., 1995). The results of my study show significant synaptic and spinal motor neuron loss in the absence of overt motor cortex pathology, supporting the arguments for retrograde (die back) degeneration at least in the G37R mouse model of ALS. Nevertheless, therapeutic studies designed to intercept synaptic loss or to preserve remaining synaptic function may be required to develop successful therapeutic interventions for ALS.

Synaptic dysfunction, as demonstrated in the motor axon terminals in this study, may lead to a number of abnormal cellular processes. Disturbances in cellular energy and oxidative damage have been widely investigated as potential contributors to neuronal cell dysfunction and death in ALS (Jung et al., 2002; Mattiazzi et al., 2002; Dupuis et al., 2004; Emerit et al., 2004). Supporting this hypothesis are studies of various features of mitochondria dysfunction from the spinal cords of transgenic mice and patients with ALS, pointing to a convergence of multiple pathological pathways onto mitochondria (Jung et al., 2002; Mattiazzi et al., 2002). It is possible that the natural metabolic resilience of motor neurons to cope with excitotoxic challenges may be compromised, thereby aberrantly modifying associated intracellular signalling pathways that would otherwise be harmless.

5.4 Evaluation of the SG-fed SOD1G37R mouse model

In light of the mutant gene dosage-dependent motor phenotypes in mouse models expressing mutant SOD1, the general outcome appears to be that too much transgene and the resulting phenotype shows severe abnormalities affecting other neuronal populations (Chiu et al., 1995; Dalcanto et al., 1995). This overly severe phenotype differs in pathology as compared to human ALS. Cleveland and colleagues suggested that an acceleration of the pathogenic process in mice by increasing the rate of mutant SOD1-mediated damage with increased abundance of mutant protein is one reason behind the contrasting pathologies (Chiu et al., 1995). Conversely, too little transgene expression and the disease is weakly penetrant and less synchronous among mice from that transgenic line (Wong et al., 1995). The original founder transgenic G37R line 29 mice showed clinical signs of motor neuron disease between 6 – 8 months of age (Wong et al., 1995). Repeated breeding of mutant SOD1 G37R progeny results in delayed clinical disease onset, as evidenced by the initial results of this study where the first signs of motor neuron disease occurred at 11 months of age. In addition, changes in the timing of disease onset are further influenced by the genetic strain of the mating parent. This finding illustrates the importance of controlling synchrony in transgenic mice to produce reliable data, and is supported by studies that demonstrate inter-species, gender, and parental variability on survival times and disease onset when using transgenic animals (Ramasubbu et al., 2002; Heiman-Patterson et al., 2005). In addition, research on the pathological alterations in the cortex of mutant SOD1 mice fail to demonstrate a unifying feature of corticomotorneuron degeneration. When taken together, it seems that mutant SOD1 transgenic mice are insufficient, or at least incomplete, models of the complete human ALS disease spectrum. Nevertheless, the aberrant property of mutant SOD1 G37R is sufficient to cause progressive motor neuron disease, and thus is useful in identifying pathogenic mechanisms in SOD1-related FALS and facilitates rapid testing of potential therapeutic approaches for this ALS subtype.

Genetic abnormalities in human ALS rarely act in isolation, as evidenced by numerous studies suggesting that the genetic background of ALS differs between populations, countries and regions (Origone et al., 2009; Rabe et al., 2010; van Es et al., 2010). The observation of differing human disease phenotypes with the same SOD1 mutation, a phenomenon described as polygenetic traits, prompted researchers to suggest an epigenetic pattern of inheritance (Felbecker et al., 2010). It is likely that an environmental factor(s) are involved to regulate the disease phenotype, as phenotypic variations between ALS patients are thus far not explained by pure genetics and there is

strong evidence that neurotoxins are sufficient etiological agents (Shaw et al., 2008). Hence SG neurotoxin exposure to low expressor mutant SOD1 mice is a more concrete model of a pathological system resembling the human condition. However, investigations involving SG neurotoxicity must also be cautious about species variability to cycad and other toxins. For example, a recent study of prolonged cycad feeding produced a purely Parkinsonism phenotype in rats (Shen et al., 2010) that is in stark contrast with the strong ALS phenotype in cycad and SG-fed mice.

Finally, mutant SOD1 mouse models do not take into consideration epigenetic mechanisms (DNA methylation, histone modifications, chromatin remodelling) that may be involved in the etiology of complex human neurodegenerative diseases like ALS. The sporadic forms of ALS produce a disease phenotype often without detectable mutations or changes in the underlying DNA sequence that could be correlated to disease causation. Furthermore, it is possible that epigenetic mechanisms may be the molecular interface mediating dynamic gene-environment interactions that modulate the latency, initiation, and progression of disease. Only very recently has an epigenetic focus merged with ALS research, which provided evidence of altered DNA methylation in SALS patients (Morahan et al., 2009). The paucity of epigenetic studies in the context of ALS indicates an urgent need to explore this young field.

5.5 Final note on pathogenic directionality

The question of which tissue constitutes the primary pathological target in ALS remains fundamental to our understanding of disease pathogenesis. Most research to date has focused on the role of mutant SOD1 in muscle and spinal cord motor neurons, although it is likely that other cell types such as glia or upper motor neurons will also uncover novel mechanisms of SOD1-mediated neurotoxicity. The normal expression of SOD1 is in spinal motor neurons, interneurons, pyramidal cells of the cortex, and neurons of the hippocampus (Pardo et al., 1995). This study has demonstrated that motor neurons, nerve, and muscle components undergo clear pathological alterations in the SOD1 G37R model of ALS. However, the results do not reveal whether increased mutant SOD1 levels have a direct effect on neuromuscular junction pathology, or whether end plate denervation occurs indirectly due to corresponding changes in lower motor neurons. Furthermore, it is possible that the presence of exogenous SG acting on motor neurons shifts the primary pathogenic target away from neuromuscular junctions and towards CNS targets even in the presence of mutant SOD1. This hypothesis is likely given the detection of SG-mediated increased gliosis and motor neuron pathology presented in this study in the absence of significant motor end plate

denervation. Similar studies performed at earlier presymptomatic time points are needed to clarify these speculations.

The observation of marked spinal cord and peripheral pathology with only minimal motor cortex changes supports a retrograde 'dying back' degeneration for this mouse model. How this finding translates to human ALS is unclear, especially given the shortcomings of such animal models as discussed above. Conflicting findings of disease directionality in different neuronal populations and methodology make interpretation difficult. For example, a study of degeneration of proximal and distal axons of respiratory motor neurons in mutant SOD1 rats failed to show indications of a retrograde or anterograde degeneration (Llado et al., 2006). On one hand, studies in axonal transport defects in transgenic mice report an impairment of axonal retrograde transport (Bilsland et al., 2010; Shi, Stroem et al., 2010) and indicate a dying back degenerative process. On the other hand, electrophysiological studies in ALS patients report a more prominent abnormality in corticomotorneurons (inhibition/excitation imbalance, reduced postsynaptic potentials) compared to lower motor neurons (Nakajima et al., 1996; Attarian et al., 2009) and support anterograde degeneration.

5.6 Suggestions for future research

This thesis addresses the potential interactive effects of an environmental toxin on genetic susceptibility to motor neuron disease and the comparative pathology arising from each stressor acting alone. However, it does not address how the genetic susceptibility of SOD1 may potentially affect toxin handling, absorption, or interaction with the handling of related molecules. It will be important to identify potential changes in detoxifying SOD1 enzyme function upon SG exposure. Cleveland and colleagues reported mutant G37R SOD1 retains full enzyme activity and forms heterodimers with wild type subunits (Borchelt et al., 1994), and suggested that mutant SOD1 may acquire properties detrimental to motor neurons. Therefore, it will be interesting to see if enzyme function is altered in the presence of a neurotoxic environmental factor. Results from such a study will be crucial in comparing the neuronal cell death pathways between environmental factors and mutant SOD1, and clarify the potential involvement increased oxidative stress as a mechanism of SG-mediated neurotoxicity. SOD1 activity gels will be a valuable tool for analyzing specific activity of the enzyme following SG exposure. Identification of putative transport proteins responsible for absorption of SG will also be necessary to demonstrate the efficacy of environmental neurotoxicity. The present model is advantageous for such a study as SG is shown to have deleterious effects

directly on the highly vascularised spinal cord, indicating that it crosses the blood brain barrier and is capable of escaping exclusion from the body by intestinal epithelium and biliary excretion. Finally, it will be important to study the interaction between mutant SOD1 and the handling of SG-related molecules such as cholesterol. Delineating potential perturbations in cholesterol metabolism could indicate a molecular mechanism for how such environmental factors increase the risk of ALS for individuals with genetic susceptibility (Dupuis et al., 2008).

Since environmental agents are involved in ALS and TDP-43 positive or FUS positive ubiquitinated intracytoplasmic inclusions are a key feature of the disease, it will be important to investigate if there is a relationship between toxicant exposure and pathological proteins. A potential link may be found in future investigations observing changes in proteinopathy in response to toxic challenges. For example, experiments designed to measure potential increases in cytoplasmic levels of TDP-43 following repeated exposures to SG in mice may provide valuable clues to potential synergistic pathological effects of environmental factors and genetic predisposition. Since SOD1 FALS is unlikely a TDP-43 proteinopathy (Mackenzie et al., 2007), mislocalization and/or phosphorylated expression neurons and glia would support a toxicant-mediated pathogenesis. Similarly, investigations delineating pathologic changes in TDP-43 proteinopathy following a single or limited dose of SG may provide clues to the potency of toxicant-induced effects. These toxicant-induced effects are particularly relevant as enhanced levels of TDP-43 may promote a gain of toxic function of this protein. Mislocalizaton and elevated TDP-43 concentrations have been shown to induce neural toxicity in a gain of toxic function mechanism (Barmada et al., 2010).

Research into gene-environmental interactions and neuronal dysfunction in neurodegenerative diseases extend beyond ALS cases and subtypes. Environmental stimulation through enrichment has been described to delay the onset and progression of motor and cognitive defects in Huntington's disease by a mechanism associated with enhanced synaptic signalling and hence improved protein trafficking (van Dellen et al., 2005). This finding demonstrates the critical role that the environment plays on even the most genetically based disorders. It is likely that the beneficial effects of enrichment described in Huntington's disease are applicable to other neurodegenerative diseases like ALS given the role for altered synaptic plasticity in ALS. The current state of knowledge of the benefits of environmental stimulation in ALS is lacking compared to studies in Huntington's disease. The present study contributes to environmental studies in ALS

employing an ingested agent capable of crossing the blood brain barrier. When taken together, it is possible that environmental factors need not be directly invasive to the CNS to exert its effects, but may rather be sufficient through indirect modulating mechanisms that represent a different level of gene-environment interplay. Further studies are required to understand the complex interplay between environmental factors and endogenous macromolecules in degeneration.Learning more about the role of the specific environmental factors and the specific neuropathological (or beneficial) pathways they initiate will provide insight into causation of SALS which, in turn, will help refine therapeutic strategies.

5.7 Concluding remarks

The findings presented in this thesis demonstrate an additive effect of SG in conjunction with the mutant SOD1G37R genotype, particularly in affecting the progression of motor behavioural deficits and pathological changes in spinal motor neurons. The accessibility of this model to experimental manipulations and its focus on gene-environmental interactions make it a more concrete model of the human condition. The lower expression levels of mutant SOD1G37R and hence the increased disease duration facilitates the study of toxins with long incubation periods and allows implementation of studies at various presymptomatic time points. In addition, the disease duration in this model is not unreasonable for rapid testing of therapeutic strategies involving new compounds designed to alter the cellular fate of surviving motor neurons. The alternate SOD1 G93A mouse is by far the more widely used model for studying motor neuron disease, and thus available experimental data on the G37R transgenic lines are more limited. It will be interesting to see if there are phenotypic variances in ALS patients from different regions with the G37R SOD1 mutation. The G37R SOD1 mutation in FALS patients is associated with a long survival time (Syriani et al., 2009), which would be an appropriate focus for clinical gene-environmental studies. However, may fundamental questions concerning the factors regulating motor neuron cell death and survival remain to be answered in the gene-environment model of ALS. What triggers the denervation of muscle fibres and what is the relationship between neuromuscular junction denervation and the observed increase in small calibre axons? Can higher doses of SG decrease disease duration or bring about pathogenesis in the motor cortex in the presence of the SOD1 mutation? What is the significance of atrophic and chromatolyic motor neurons in controls, and how does their formation differ from those in experimental groups? How can the results from such gene-environmental interaction studies be translated to human disease?

How can we identify putative environmental risk factors in the absence of disease clusters as in the majority of SALS cases? The model developed in this thesis may be important to provide the answers to these and other unanswered questions, and the results from such future studies are important to the expanding the current understanding of pathology in the ALS disease spectrum.

References

1. Abou Ezzi, S., Lariviere, R., Urushitani, M., & Julien, J. (2010). Neuronal over-expression of chromogranin A accelerates disease onset in a mouse model of ALS. *Journal of Neurochemistry, 115*(5), 1102-1111. doi:10.1111/j.1471-4159.2010.06979.x

2. Alim, M. A., Ma, Q. L., Takeda, K., Aizawa, T., Matsubara, M., Nakamura, M., Asada, A., Saito, T., Kaji, H., Yoshii, M., Hisanaga, S., & Ueda, K. (2004). Demonstration of a role for alpha-synuclein as a functional microtubule-associtated protein. *Journal of Alzheimers Disease, 6*(4), 435-442.

3. Aman, P., Panagopoulos, I., Lassen, C., Fioretos, T., Mencinger, M., Toresson, H., Hoglund, M., Forster, A., Rabbitts, T. H., Ron, D., Mandahl, N., & Mitelman, F. (1996). Expression patterns of the human sarcoma-associated genes FUS and EWS and the genomic structure of FUS. *Genomics, 37*(1), 1-8.

4. Amende, I., Kale, A., McCue, S., Glazier, S., Morgan, J. P., & Hampton, T. G. (2005). Gait dynamics in mouse models of parkinson's disease and huntington's disease. *Journal of Neuroengineering and Rehabilitation, 2*, 20. doi:10.1186/1743-0003-2-20

5. Andersen, P. M., Restagno, G., Stewart, H. G., & Chio, A. (2004). Disease penetrance in amyotrophic lateral sclerosis associated with mutations in the SOD1 gene. *Annals of Neurology, 55*(2), 298-299. doi:10.1002/ana.10850

6. Andreadou, E., Kapaki, E., Kokotis, P., Paraskevas, G. P., Katsaros, N., Libitaki, G., Petropoulou, O., Zis, V., Sfagos, C., & Vassilopoulos, D. (2008). Plasma glutamate and glycine levels in patients with amyotrophic lateral sclerosis. *In Vivo, 22*(1), 137-141.

7. Ansved, T., & Larsson, L. (1990). Quantitative and qualitative morphological properties of the soleus motor-nerve and the L5 ventral root in young and old rats - relation to the number of soleus muscle-fibers. *Journal of the Neurological Sciences, 96*(2-3), 269-282.

8. Arai, T., Hasegawa, M., Akiyama, H., Ikeda, K., Nonaka, T., Mori, H., Mann, D., Tsuchiya, K., Yoshida, M., Hashizume, Y., & Oda, T. (2006). TDP-43 is a component of ubiquitin-positive tau-negative inclusions in frontotemporal lobar degeneration and amyotrophic lateral sclerosis. *Biochemical and Biophysical Research Communications, 351*(3), 602-611. doi:10.1016/j.bbrc.2006.10.093

9. Armon, C. (2007). Sports and trauma in amyotrophic lateral sclerosis revisited. *Journal of the Neurological Sciences, 262*(1-2), 45-53. doi:10.1016/j.jns.2007.06.021

10. Arnold, A., Edgren, D. C., & Palladino, V. S. (1953). Amyotrophic lateral sclerosis: Fifty cases observed on Guam. *The Journal of Nervous and Mental Disease, 117*(2), 135-139.

11. Atkin, J. D., Scott, R. L., West, J. M., Lopes, E., Quah, A. K. J., & Cheema, S. S. (2005). Properties of slow- and fast-twitch muscle fibres in a mouse model of amyotrophic lateral sclerosis. *Neuromuscular Disorders, 15*(5), 377-388. doi:10.1016/j.nmd.2005.02.005

12. Attarian, S., Pouget, J., & Schmied, A. (2009). Changes in cortically induced inhibition in amyotrophic lateral sclerosis with time. *Muscle & Nerve, 39*(3), 310-317. doi:10.1002/mus.21137

13. Attarian, S., Vedel, J., Pouget, J., & Schmied, A. (2008). Progression of cortical and spinal dysfunctions over time in amyotrophic lateral sclerosis. *Muscle & Nerve, 37*(3), 364-375. doi:10.1002/mus.20942

14. Ayala, Y. M., Pantano, S., D'Ambrogio, A., Buratti, E., Brindisi, A., Marchetti, C., Romano, M., & Baralle, F. E. (2005). Human, drosophila, and C-elegans TDP43: Nucleic acid binding properties and splicing regulatory function. *Journal of Molecular Biology, 348*(3), 575-588. doi:10.1016/j.jmb.2005.02.038

15. Banjo, O. C. (2009). *A phenotypic and neuropathological assessment of the impact of fetal and secondary adult re-exposures to steryl glucosides in mice*. (Master of Science - MSc, University of British Columbia).

16. Barbeito, L., Pehar, M., Cassina, P., Vargas, M., Peluffo, H., Viera, L., Estevez, A., & Beckman, J. (2004). A role for astrocytes in motor neuron loss in amyotrophic lateral sclerosis. *Brain Research Reviews, 47*(1-3), 263-274. doi:10.1016/j.brainresrev.2004.05.003

17. Barmada, S. J., & Finkbeiner, S. (2010). Pathogenic TARDBP mutations in amyotrophic lateral sclerosis and frontotemporal dementia: Disease-associated pathways. *Reviews in the Neurosciences, 21*(4), 251-272.

18. Barneoud, P., & Curet, O. (1999). Beneficial effects of lysine acetylsalicylate, a soluble salt of aspirin, on motor performance in a transgenic model of amyotrophic lateral sclerosis. *Experimental Neurology, 155*(2), 243-251.

19. Batulan, Z., Shinder, G. A., Minotti, S., He, B. P., Doroudchi, M., Nalbantoglu, J., Strong, M. J., & Durham, H. D. (2003). High threshold for induction of the stress response in motor neurons is associated with failure to activate HSF1. *Journal of Neuroscience, 23*(13), 5789-5798.

20. Belzil, V. V., Valdmanis, P. N., Dion, P. A., Daoud, H., Kabashi, E., Noreau, A., Gauthier, J., Hince, P., Desjarlais, A., Bouchard, J., Lacomblez, L., Salachas, F., Pradat, P. -., Camu, W., Meininger, V., Dupre, N., Rouleau, G. A., & S2D Team. (2009). Mutations in FUS cause FALS and SALS in french and french Canadian populations. *Neurology, 73*(15), 1176-1179. doi:10.1212/WNL.0b013e3181bbfeef

21. Bergeron, C., Petrunka, C., & Weyer, L. (1996). Copper/zinc superoxide dismutase expression in the human central nervous system - correlation with selective neuronal vulnerability. *American Journal of Pathology, 148*(1), 273-279.

22. Bilsland, L. G., Sahai, E., Kelly, G., Golding, M., Greensmith, L., & Schiavo, G. (2010). Deficits in axonal transport precede ALS symptoms in vivo. *Proceedings of the National Academy of Sciences of the United States of America, 107*(47), 20523-20528. doi:10.1073/pnas.1006869107

23. Bitanihirwe, B. K. Y., Peleg-Raibstein, D., Mouttet, F., Feldon, J., & Meyer, U. (2010). Late prenatal immune activation in mice leads to behavioral and neurochemical abnormalities relevant to the

negative symptoms of schizophrenia. *Neuropsychopharmacology, 35*(12), 2462-2478. doi:10.1038/npp.2010.129

24. Bogaert, E., d'Ydewalle, C., & Van Den Bosch, L. (2010a). Amyotrophic lateral sclerosis and excitotoxicity: From pathological mechanism to therapeutic target. *Cns & Neurological Disorders-Drug Targets, 9*(3), 297-304.

25. Bogaert, E., Van Damme, P., Poesen, K., Dhondt, J., Hersmus, N., Kiraly, D., Scheveneels, W., Robberecht, W., & Van Den, B. L. (2010b). VEGF protects motor neurons against excitotoxicity by upregulation of GluR2. *Neurobiology of Aging, 31*(12), 2185-2191. doi:10.1016/j.neurobiolaging.2008.12.007

26. Boillee, S., Yamanaka, K., Lobsiger, C. S., Copeland, N. G., Jenkins, N. A., Kassiotis, G., Kollias, G., & Cleveland, D. W. (2006). Onset and progression in inherited ALS determined by motor neurons and microglia. *Science, 312*(5778), 1389-1392. doi:10.1126/science.1123511

27. Borchelt, D. R., Lee, M. K., Slunt, H. S., Guarnieri, M., Xu, Z. S., Wong, P. C., Brown, R. H., Price, D. L., Sisodia, S. S., & Cleveland, D. W. (1994). Superoxide-dismutase-1 with mutations linked to familial amyotrophic-lateral-sclerosis possesses significant activity. *Proceedings of the National Academy of Sciences of the United States of America, 91*(17), 8292-8296.

28. Borchelt, D. R., Wong, P. C., Becher, M. W., Pardo, C. A., Lee, M. K., Xu, Z. S., Thinakaran, G., Jenkins, N. A., Copeland, N. G., Sisodia, S. S., Cleveland, D. W., Price, D. L., & Hoffman, P. N. (1998). Axonal transport of mutant superoxide dismutase 1 and focal axonal abnormalities in the proximal axons of transgenic mice. *Neurobiology of Disease, 5*(1), 27-35.

29. Bosco, D. A., Lemay, N., Ko, H. K., Zhou, H., Burke, C., Kwiatkowski, T. J., Jr., Sapp, P., McKenna-Yasek, D., Brown, R. H., Jr., & Hayward, L. J. (2010a). Mutant FUS proteins that cause amyotrophic lateral sclerosis incorporate into stress granules. *Human Molecular Genetics, 19*(21), 4160-4175. doi:10.1093/hmg/ddq335

30. Bosco, D. A., Morfini, G., Karabacak, N. M., Song, Y., Gros-Louis, F., Pasinelli, P., Goolsby, H., Fontaine, B. A., Lemay, N., McKenna-Yasek, D., Frosch, M. P., Agar, J. N., Julien, J. -., Brady, S. T., & Brown, R. H., Jr. (2010b). Wild-type and mutant SOD1 share an aberrant conformation and a common pathogenic pathway in ALS. *Nature Neuroscience, 13*(11), 1396-U133. doi:10.1038/nn.2660

31. Boyle, C. C., & Hickman, J. A. (1997). Toxin-induced increase in survival factor receptors: Modulation of the threshold for apoptosis. *Cancer Research, 57*(12), 2404-2409.

32. Bradley, W. G., & Mash, D. C. (2009). Beyond Guam: The cyanobacteria/BMAA hypothesis of the cause of ALS and other neurodegenerative diseases. *Amyotrophic Lateral Sclerosis, 10*, 7-20.

33. Brain, P., & Benton, D. (1979). Interpretation of physiological correlates of differential housing in laboratory rats. *Life Sciences, 24*(2), 99-115. doi:10.1016/0024-3205(79)90119-X

34. Brody, J. A., Stanhope, J. M., & Kurland, L. T. (1975). Patterns of amyotrophic lateral sclerosis and parkinsonism-dementia on Guam. *Contemporary Neurology Series, 12*, 45-70.

35. Brownell, B., Oppenhei.Dr, & Hughes, J. T. (1970). Central nervous system in motor neurone disease. *Journal of Neurology Neurosurgery and Psychiatry, 33*(3), 338-&.

36. Bruijn, L. I., Becher, M. W., Lee, M. K., Anderson, K. L., Jenkins, N. A., Copeland, N. G., Sisodia, S. S., Rothstein, J. D., Borchelt, D. R., Price, D. L., & Cleveland, D. W. (1997). ALS-linked SOD1 mutant G85R mediates damage to astrocytes and promotes rapidly progressive disease with SOD1-containing inclusions. *Neuron, 18*(2), 327-338.

37. Bruijn, L. I., Houseweart, M. K., Kato, S., Anderson, K. L., Anderson, S. D., Ohama, E., Reaume, A. G., Scott, R. W., & Cleveland, D. W. (1998). Aggregation and motor neuron toxicity of an ALS-linked SOD1 mutant independent from wild-type SOD1. *Science, 281*(5384), 1851-1854.

38. Buee, L., PerezTur, J., Leveugle, B., BueeScherrer, V., Mufson, E. J., Loerzel, A. J., ChartierHarlin, M. C., Perl, D. P., Delacourte, A., & Hof, P. R. (1996). Apolipoprotein E in Guamanian amyotrophic lateral sclerosis Parkinsonism dementia complex: Genotype analysis and relationships to neuropathological changes. *Acta Neuropathologica, 91*(3), 247-253.

39. Buratti, E., Brindisi, A., Giombi, M., Tisminetzky, S., Ayala, Y. M., & Baralle, F. E. (2005). TDP-43 binds heterogeneous nuclear ribonucleoprotein A/B through its C-terminal tail - an important region for the inhibition of cystic fibrosis transmembrane conductance regulator exon 9 splicing. *Journal of Biological Chemistry, 280*(45), 37572-37584. doi:10.1074/jbc.M505557200

40. Butterfield, D. A., Castegna, A., Drake, J., Scapagnini, G., & Calabrese, V. (2002). Vitamin E and neurodegenerative disorders associated with oxidative stress. *Nutritional Neuroscience, 5*(4), 229-239. doi:10.1080/10284150290028954

41. Callahan, L. M., Wylen, E. L., Messer, A., & Mazurkiewicz, J. E. (1991). Neurofilament distribution is altered in the mnd (motor-neuron degeneration) mouse. *Journal of Neuropathology and Experimental Neurology, 50*(4), 491-504.

42. Carriedo, S. G., Sensi, S. L., Yin, H. Z., & Weiss, J. H. (2000). AMPA exposures induce mitochondrial Ca2+ overload and ROS generation in spinal motor neurons in vitro. *Journal of Neuroscience, 20*(1), 240-250.

43. Cermelli, C., Vinceti, M., Beretti, F., Pietrini, V., Nacci, G., Pietrosemoli, P., Bartoletti, A., Guidetti, D., Sola, P., Bergomi, M., Vivoli, G., & Portolani, M. (2003). Risk of sporadic amyotrophic lateral sclerosis associated with seropositivity for herpesviruses and echovirus-7. *European Journal of Epidemiology, 18*(2), 123-127.

44. Chen, X., Xia, Y., Gresham, L. S., Molgaard, C. A., Thomas, R. G., Galasko, D., Wiederholt, W. C., & Saitoh, T. (1996). ApoE and CYP2D6 polymorphism with and without parkinsonism-dementia complex in the people of chamorro, Guam. *Neurology, 47*(3), 779-784.

45. Chio, A., Mora, G., Calvo, A., Mazzini, L., Bottacchi, E., Mutani, R., & PARALS. (2009). Epidemiology of ALS in Italy A 10-year prospective population-based study. *Neurology, 72*(8), 725-731. doi:10.1212/01.wnl.0000343008.26874.d1

46. Chiu, A. Y., Zhai, P., Dalcanto, M. C., Peters, T. M., Kwon, Y. W., Prattis, S. M., & Gurney, M. E. (1995). Age-dependent penetrance of disease in a transgenic mouse model of familial amyotrophic-lateral-sclerosis. *Molecular and Cellular Neuroscience, 6*(4), 349-362.

47. Chou, S. M., Wang, H. S., & Komai, K. (1996). Colocalization of NOS and SOD1 in neurofilament accumulation within motor neurons of amyotrophic lateral sclerosis: An immunohistochemical study. *Journal of Chemical Neuroanatomy, 10*(3-4), 249-258.

48. Clement, A. M., Nguyen, M. D., Roberts, E. A., Garcia, M. L., Boillee, S., Rule, M., McMahon, A. P., Doucette, W., Siwek, D., Ferrante, R. J., Brown, R. H., Julien, J. P., Goldstein, L. S. B., & Cleveland, D. W. (2003). Wild-type nonneuronal cells extend survival of SOD1 mutant motor neurons in ALS mice. *Science, 302*(5642), 113-117.

49. Cleveland, D. W., & Liu, J. (2000). Oxidation versus aggregation - how do SOD1 mutants cause ALS? *Nature Medicine, 6*(12), 1320-1321.

50. Cookson, M. R., Menzies, F. M., Manning, P., Eggett, C. J., Figlewicz, D. A., McNeil, C. J., & Shaw, P. J. (2002). Cu/Zn superoxide dismutase (SOD1) mutations associated with familial amyotrophic lateral sclerosis (ALS) affect cellular free radical release in the presence of oxidative stress. *Amyotrophic Lateral Sclerosis and Other Motor Neuron Disorders, 3*(2), 75-85.

51. Cooper, A. A., Gitler, A. D., Cashikar, A., Haynes, C. M., Hill, K. J., Bhullar, B., Liu, K., Xu, K., Strathearn, K. E., Liu, F., Cao, S., Caldwell, K. A., Caldwell, G. A., Marsischky, G., Kolodner, R. D., LaBaer, J., Rochet, J., Bonini, N. M., & Lindquist, S. (2006). Alpha-synuclein blocks ER-golgi traffic and Rab1 rescues neuron loss in parkinson's models. *Science, 313*(5785), 324-328. doi:10.1126/science.1129462

52. Coppede, F., Mancuso, M., Siciliano, G., Migliore, L., & Murri, L. (2006). Genes and the environment in neurodegeneration. *Bioscience Reports, 26*(5), 341-367. doi:10.1007/s10540-006-9028-6

53. Corrado, L., Del Bo, R., Castellotti, B., Ratti, A., Cereda, C., Penco, S., Soraru, G., Carlomagno, Y., Ghezzi, S., Pensato, V., Colombrita, C., Gagliardi, S., Cozzi, L., Orsetti, V., Mancuso, M., Siciliano, G., Mazzini, L., Comi, G. P., Gellera, C., Ceroni, M., D'Alfonso, S., & Silani, V. (2010). Mutations of FUS gene in sporadic amyotrophic lateral sclerosis. *Journal of Medical Genetics, 47*(3), 190-194. doi:10.1136/jmg.2009.071027

54. Costa, L. M., Pereira, J. E., Filipe, V. M., Couto, P. A., Magalhaes, L. G., Bulas-Cruz, J., Mauricio, A. C., Geuna, S., & Varejao, A. S. P. (2010). The effect of gait speed on three-dimensional analysis of hindlimb kinematics during treadmill locomotion in rats. *Reviews in the Neurosciences, 21*(6), 487-497.

55. Crugnola, V., Lamperti, C., Lucchini, V., Ronchi, D., Peverelli, L., Prelle, A., Sciacco, M., Bordoni, A., Fassone, E., Fortunato, F., Corti, S., Silani, V., Bresolin, N., Di Mauro, S., Comi, G. P., & Moggio, M.

(2010). Mitochondrial respiratory chain dysfunction in muscle from patients with amyotrophic lateral sclerosis. *Archives of Neurology, 67*(7), 849-854.

56. Cruz-Aguado, R., Winkler, D., & Shaw, C. A. (2006). Lack of behavioral and neuropathological effects of dietary beta-methylamino-L-alanine (BMAA) in mice. *Pharmacology, Biochemistry, and Behavior, 84*(2), 294-299. doi:10.1016/j.pbb.2006.05.012

57. Cudkowicz, M. E., McKennaYasek, D., Sapp, P. E., Chin, W., Geller, B., Hayden, D. L., Schoenfeld, D. A., Hosler, B. A., Horvitz, H. R., & Brown, R. H. (1997). Epidemiology of mutations in superoxide dismutase in amyotrophic lateral sclerosis. *Annals of Neurology, 41*(2), 210-221.

58. Culotta, V. C., Yang, M., & O'Halloran, T. V. (2006a). Activation of superoxide dismutases: Putting the metal to the pedal. *Biochimica et Biophysica Acta-Molecular Cell Research, 1763*(7), 747-758. doi:10.1016/j.bbamcr.2006.05.003

59. Culotta, V. C., Yang, M., & O'Halloran, T. V. (2006b). Activation of superoxide dismutases: Putting the metal to the pedal. *Biochimica et Biophysica Acta-Molecular Cell Research, 1763*(7), 747-758. doi:10.1016/j.bbamcr.2006.05.003

60. Cutler, R. G., Pedersen, W. A., Camandola, S., Rothstein, J. D., & Mattson, M. P. (2002). Evidence that accumulation of ceramides and cholesterol esters mediates oxidative stress-induced death of motor neurons in amyotrophic lateral sclerosis. *Annals of Neurology, 52*(4), 448-457. doi:10.1002/ana.10312

61. Dalcanto, M. C., & Gurney, M. E. (1994a). Development of central-nervous-system pathology in a murine transgenic model of human amyotrophic-lateral-sclerosis. *American Journal of Pathology, 145*(6), 1271-1279.

62. Dalcanto, M. C., & Gurney, M. E. (1994b). Development of central-nervous-system pathology in a murine transgenic model of human amyotrophic-lateral-sclerosis. *American Journal of Pathology, 145*(6), 1271-1279.

63. Dalcanto, M. C., & Gurney, M. E. (1995). Neuropathological changes in 2 lines of mice carrying a transgene for mutant human Cu,Zn SOD, and in mice overexpressing wild-type human sod - a model of familial amyotrophic-lateral-sclerosis (fals). *Brain Research, 676*(1), 25-40.

64. DalCanto, M. C., & Gurney, M. E. (1997). A low expressor line of transgenic mice carrying a mutant human Cu,Zn superoxide dismutase [SOD1] gene develops pathological changes that most closely resemble those in human amyotrophic lateral sclerosis. *Acta Neuropathologica, 93*(6), 537-550.

65. DalCanto, M. C., Mourelatos, Z., Stieber, A., Gurney, M. E., & Gonatas, N. K. (1996). The golgi apparatus is affected early in a transgenic model of familial amyotrophic lateral sclerosis (FALS). *Journal of Neuropathology and Experimental Neurology, 55*(5), 223-223.

66. Dastur, D. K. (1964). Cycad toxicity in monkeys - clinical pathological + biochemical aspects. *Federation Proceedings, 23*(6P1), 1368-&.

67. Dastur, D. K., & Palekar, R. S. (1966). Effect of boiling and storing on cycasin content of cycas circinalis L. *Nature, 210*(5038), 841-&.

68. David, G., Nguyen, K., & Barrett, E. F. (2007). Early vulnerability to ischemia/reperfusion injury in motor terminals innervating fast muscles of SOD1-G93A mice. *Experimental Neurology, 204*(1), 411-420. doi:10.1016/j.expneurol.2006.12.021

69. de Jong, A., Plat, J., & Mensink, R. P. (2003). Metabolic effects of plant sterols and stanols (review). *Journal of Nutritional Biochemistry, 14*(7), 362-369. doi:10.1016/S0955-2863(03)00002-0

70. de la Corte, F. (1875). Memoria descriptiva e histórica de las islas marianas.

71. de Viana, A. V. (2004). Filipino natives in seventeenth century marianas: Their role in the establishment of the spanish mission in the islands. *Micronesian Journal of the Humanities and Social Sciences, 3*(1-2), 19-25.

72. Deng, H. X., Hentati, A., Tainer, J. A., Iqbal, Z., Cayabyab, A., Hung, W. Y., Getzoff, E. D., Hu, P., Herzfeldt, B., Roos, R. P., Warner, C., Deng, G., Soriano, E., Smyth, C., Parge, H. E., Ahmed, A., Roses, A. D., Hallewell, R. A., Pericakvance, M. A., & Siddique, T. (1993). Amyotrophic-lateral-sclerosis and structural defects in Cu,Zn superoxide-dismutase. *Science, 261*(5124), 1047-1051.

73. Di Giorgio, F. P., Carrasco, M. A., Siao, M. C., Maniatis, T., & Eggan, K. (2007). Non-cell autonomous effect of glia on motor neurons in an embryonic stem cell-based ALS model. *Nature Neuroscience, 10*(5), 608-614. doi:10.1038/nn1885

74. Dolapchieva, S. (2004). Computer-assisted morphometric study on the postnatal growth of axon size and myelin thickness in the ventral and dorsal roots of the rabbit. *Annals of Anatomy-Anatomischer Anzeiger, 186*(1), 61-68.

75. Dormann, D., Rodde, R., Edbauer, D., Bentmann, E., Fischer, I., Hruscha, A., Than, M. E., Mackenzie, I. R. A., Capell, A., Schmid, B., Neumann, M., & Haass, C. (2010a). ALS-associated fused in sarcoma (FUS) mutations disrupt transportin-mediated nuclear import. *Journal, 29*(16), 2841-2857. doi:10.1038/emboj.2010.143

76. Dormann, D., Rodde, R., Edbauer, D., Bentmann, E., Fischer, I., Hruscha, A., Than, M. E., Mackenzie, I. R. A., Capell, A., Schmid, B., Neumann, M., & Haass, C. (2010b). ALS-associated fused in sarcoma (FUS) mutations disrupt transportin-mediated nuclear import. *Journal, 29*(16), 2841-2857. doi:10.1038/emboj.2010.143

77. Duchen, L. W., & Strich, S. J. (1968). An hereditary motor neurone disease with progressive denervation of muscle in mouse - mutantwobbler. *Journal of Neurology Neurosurgery and Psychiatry, 31*(6), 535-&.

78. Duncan, M. W., Kopin, I. J., Garruto, R. M., Lavine, L., & Markey, S. P. (1988). 2-amino-3 (methylamino)-propionic acid in cycad-derived foods is an unlikely cause of amyotrophic lateral sclerosis parkinsonism. *Lancet, 2*(8611), 631-632.

79. Duncan, M. W., Steele, J. C., Kopin, I. J., & Markey, S. P. (1990). 2-amino-3-(methylamino)-propanoic acid (BMAA) in cycad flour: An unlikely cause of amyotrophic lateral sclerosis and parkinsonism-dementia of Guam. *Neurology, 40*(5), 767-772.

80. Duncan, M. W., Villacreses, N. E., Pearson, P. G., Wyatt, L., Rapoport, S. I., Kopin, I. J., Markey, S. P., & Smith, Q. R. (1991). 2-amino-3-(methylamino)-propanoic acid (BMAA) pharmacokinetics and blood-brain barrier permeability in the rat. *The Journal of Pharmacology and Experimental Therapeutics, 258*(1), 27-35.

81. Dupuis, L., Corcia, P., Fergani, A., De Aguilar, J. -. G., Bonnefont-Rousselot, D., Bittar, R., Seilhean, D., Hauw, J. -., Lacomblez, L., Loeffler, J. -., & Meininger, V. (2008). Dyslipidemia is a protective factor in amyotrophic lateral sclerosis. *Neurology, 70*(13), 1004-1009.

82. Dupuis, L., & Echaniz-Laguna, A. (2010). Skeletal muscle in motor neuron diseases: Therapeutic target and delivery route for potential treatments. *Current Drug Targets, 11*(10), 1250-1261.

83. Dupuis, L., Oudart, H., Rene, F., de Aguilar, J., & Loeffler, J. (2004). Evidence for defective energy homeostasis in amyotrophic lateral sclerosis: Benefit of a high-energy diet in a transgenic mouse. *Proceedings of the National Academy of Sciences of the United States of America, 101*(30), 11159-11164. doi:10.1073/pnas.0402026101

84. Echaniz-Laguna, A., Zoll, J., Ponsot, E., N'Guessan, B., Tranchant, C., Loeffler, J. P., & Larnpert, E. (2006). Muscular mitochondrial function in amyotrophic lateral sclerosis is progressively altered as the disease develops: A temporal study in man. *Experimental Neurology, 198*(1), 25-30. doi:10.1016/j.expneurol.2005.07.020

85. Eisen, A., EntezariTaher, M., & Stewart, H. (1996). Cortical projections to spinal motoneurons: Changes with aging and amyotrophic lateral sclerosis. *Neurology, 46*(5), 1396-1404.

86. Eisen, A., Kim, S., & Pant, B. (1992). Amyotrophic-lateral-sclerosis (ALS) - a phylogenetic disease of the corticomotoneuron. *Muscle & Nerve, 15*(2), 219-224.

87. Eisen, A., & Weber, M. (2001). The motor cortex and amyotrophic lateral sclerosis. *Muscle & Nerve, 24*(4), 564-573.

88. Elizan, T. S., Hirano, A., Abrams, B. M., Need, R. L., Vannuis, C., & Kurland, L. T. (1966). Amyotrophic lateral sclerosis and parkinsonism-dementia complex of Guam. *Archives of Neurology, 14*(4), 356-&.

89. Emerit, J., Edeas, A., & Bricaire, F. (2004). Neurodegenerative diseases and oxidative stress. *Biomedicine & Pharmacotherapy, 58*(1), 39-46. doi:10.1016/j.biopha.2003.11.004

90. EnterzariTaher, M., Eisen, A., Stewart, H., & Nakajima, M. (1997). Abnormalities of cortical inhibitory neurons in amyotrophic lateral sclerosis. *Muscle & Nerve, 20*(1), 65-71.

91. Estevez, A. G., Crow, J. P., Sampson, J. B., Reiter, C., Zhuang, Y. X., Richardson, G. J., Tarpey, M. M., Barbeito, L., & Beckman, J. S. (1999). Induction of nitric oxide-dependent apoptosis in motor neurons by zinc-deficient superoxide dismutase. *Science, 286*(5449), 2498-2500.

92. Fang, D., Zhang, S., Guo, X., Zeng, Y., Yang, Y., Zhou, D., & Shang, H. (2009). Clinical and genetic features of patients with sporadic amyotrophic lateral sclerosis in south-west China. *Amyotrophic Lateral Sclerosis, 10*(5-6), 350-354. doi:10.3109/17482960802668646

93. Fang, F., Quinlan, P., Ye, W., Barber, M. K., Umbach, D. M., Sandler, D. P., & Kamel, F. (2009). Workplace exposures and the risk of amyotrophic lateral sclerosis. *Environmental Health Perspectives, 117*(9), 1387-1392. doi:10.1289/ehp.0900580

94. Farah, C. A., Nguyen, M. D., Julien, J. P., & Leclerc, N. (2003). Altered levels and distribution of microtubule-associated proteins before disease onset in a mouse model of amyotrophic lateral sclerosis. *Journal of Neurochemistry, 84*(1), 77-86.

95. Felbecker, A., Camu, W., Valdmanis, P. N., Sperfeld, A., Waibel, S., Steinbach, P., Rouleau, G. A., Ludolph, A. C., & Andersen, P. M. (2010). Four familial ALS pedigrees discordant for two SOD1 mutations: Are all SOD1 mutations pathogenic? *Journal of Neurology Neurosurgery and Psychiatry, 81*(5), 572-577. doi:10.1136/jnnp.2009.192310

96. Figlewicz, D. A., Garruto, R. M., Krizus, A., Yanagihara, R., & Rouleau, G. A. (1994). The Cu/Zn superoxide-dismutase gene in ALS and parkinsonism-dementia of Guam. *Neuroreport, 5*(5), 557-560.

97. Finn, R., Kovacs, A. D., & Pearce, D. A. (2010). Altered sensitivity to excitotoxic cell death and glutamate receptor expression between two commonly studied mouse strains. *Journal of Neuroscience Research, 88*(12), 2648-2660. doi:10.1002/jnr.22433

98. Fischer, L. R., Culver, D. G., Tennant, P., Davis, A. A., Wang, M., Castellano-Sanchez, A., Khan, J., Polak, M. A., & Glass, J. D. (2004). Amyotrophic lateral sclerosis is a distal axonopathy: Evidence in mice and man. *Experimental Neurology, 185*(2), 232-240.

99. Forman, M. S., Trojanowski, J. Q., & Lee, V. M. (2007). TDP-43: A novel neurodegenerative proteinopathy. *Current Opinion in Neurobiology, 17*(5), 548-555. doi:10.1016/j.conb.2007.08.005

100. Frey, D., Schneider, C., Xu, L., Borg, J., Spooren, W., & Caroni, P. (2000). Early and selective loss of neuromuscular synapse subtypes with low sprouting competence in motoneuron diseases. *Journal of Neuroscience, 20*(7), 2534-2542.

101. Fridovich, I. (1995). Superoxide radical and superoxide dismutases. *Annual Review of Biochemistry, 64*, 97-112.

102. Friese, A., Kaltschmidt, J. A., Ladle, D. R., Sigrist, M., Jessell, T. M., & Arber, S. (2009). Gamma and alpha motor neurons distinguished by expression of transcription factor Err3. *Proceedings of the National Academy of Sciences of the United States of America, 106*(32), 13588-13593. doi:10.1073/pnas.0906809106

103. Fujita, Y., Okamoto, K., Sakurai, A., Amari, M., Nakazato, Y., & Gonatas, N. K. (1999). Fragmentation of the golgi apparatus of betz cells in patients with amyotrophic lateral sclerosis. *Journal of the Neurological Sciences, 163*(1), 81-85.

104. Furby, A., Beauvais, K., Kolev, I., Rivain, J., & Sebille, V. (2010). Rural environment and risk factors of amyotrophic lateral sclerosis: A case-control study. *Journal of Neurology, 257*(5), 792-798. doi:10.1007/s00415-009-5419-5

105. Galasko, D., Salmon, D., Craig, U. K., Perl, D. P., & Schellenberg, G. (2002). Clinical features and changing patterns of neurodegenerative disorders on Guam, 1997-2000. *Neurology, 59*(7), 1121-1121.

106. Garruto, R. M., Yanagihara, R., & Gajdusek, D. C. (1985). Disappearance of high-incidence amyotrophic lateral sclerosis and parkinsonism-dementia on Guam. *Neurology, 35*(2), 193.

107. Garruto, R. M., Yanagihara, R., & Gajdusek, D. C. (1988). Cycads and amyotrophic lateral sclerosis parkinsonism dementia. *Lancet, 2*(8619), 1079-1079.

108. Gavrieli, Y., Sherman, Y., & Bensasson, S. A. (1992). Identification of programmed cell-death in situ via specific labeling of nuclear-dna fragmentation. *Journal of Cell Biology, 119*(3), 493-501.

109. Geser, F., Winton, M. J., Kwong, L. K., Xu, Y., Xie, S. X., Igaz, L. M., Garruto, R. M., Perl, D. P., Galasko, D., Lee, V. M. -., & Trojanowski, J. Q. (2008). Pathological TDP-43 in parkinsonism-dementia complex and amyotrophic lateral sclerosis of Guam. *Acta Neuropathologica, 115*(1), 133-145. doi:10.1007/s00401-007-0257-y

110. Gil, J., Funalot, B., Verschueren, A., Danel-Brunaud, V., Camu, W., Vandenberghe, N., Desnuelle, C., Guy, N., Camdessanche, J. P., Cintas, P., Carluer, L., Pittion, S., Nicolas, G., Corcia, P., Fleury, M. -., Maugras, C., Besson, G., Le Masson, G., & Couratier, P. (2008). Causes of death amongst french patients with amyotrophic lateral sclerosis: A prospective study. *European Journal of Neurology, 15*(11), 1245-1251. doi:10.1111/j.1468-1331.2008.02307.x

111. Goetz, C. G. (2000). Amyotrophic lateral sclerosis: Early contributions of jean-martin charcot. *Muscle & Nerve, 23*(3), 336-343.

112. Goetz, C. G. (2002). Jean-Martin Charcot and the aging brain. *Archives of Neurology, 59*(11), 1821-1824.

113. Goetz, C. G. (2005). Jean-Martin Charcot (1825-1893). *Journal of Neurology, 252*(3), 374-375. doi:10.1007/s00415-005-0776-1

114. Goldacre, M. J., Duncan, M., Griffith, M., & Turner, M. R. (2010). Trends in death certification for multiple sclerosis, motor neuron disease, parkinson's disease and epilepsy in english populations 1979-2006. *Journal of Neurology, 257*(5), 706-715. doi:10.1007/s00415-009-5392-z

115. Gordon, T., Ly, V., & Tyreman, N. (2009). Early detection of denervated muscle fibers in hindlimb muscles after sciatic nerve transection in wild type mice and in the G93A mouse model of amyotrophic lateral sclerosis. *Neurological Research, 31*(1), 28-42. doi:10.1179/174313208X332977

116. Govoni, V., Granieri, E., Fallica, E., & Casetta, F. (2005). Amyotrophic lateral sclerosis, rural environment and agricultural work in the local health district of Ferrara, Italy, in the years 1964-1998. *Journal of Neurology, 252*(11), 1322-1327. doi:10.1007/s00415-005-0859-z

117. Gowing, G., Philips, T., Van Wijmeersch, B., Audet, J., Dewil, M., Van Den Bosch, L., Billiau, A. D., Robberecht, W., & Julien, J. (2008). Ablation of proliferating microglia does not affect motor neuron degeneration in amyotrophic lateral sclerosis caused by mutant superoxide dismutase. *Journal of Neuroscience, 28*(41), 10234-10244. doi:10.1523/JNEUROSCI.3494-08.2008

118. Graber, D. J., Hickey, W. F., & Harris, B. T. (2010). Progressive changes in microglia and macrophages in spinal cord and peripheral nerve in the transgenic rat model of amyotrophic lateral sclerosis. *Journal of Neuroinflammation, 7*, 8. doi:10.1186/1742-2094-7-8

119. Gredal, O., Pakkenberg, H., Karlsborg, M., & Pakkenberg, B. (2000). Unchanged total number of neurons in motor cortex and neocortex in amyotrophic lateral sclerosis: A stereological study. *Journal of Neuroscience Methods, 95*(2), 171-176.

120. Grille, S., Zaslawski, A., Thiele, S., Plat, J., & Warnecke, D. (2010). The functions of steryl glycosides come to those who wait: Recent advances in plants, fungi, bacteria and animals. *Progress in Lipid Research, 49*(3), 262-288. doi:10.1016/j.plipres.2010.02.001

121. Grosskreutz, J., Van Den Bosch, L., & Keller, B. U. (2010). Calcium dysregulation in amyotrophic lateral sclerosis. *Cell Calcium, 47*(2), 165-174. doi:10.1016/j.ceca.2009.12.002

122. Gurney, M. E. (1994). Mutant mice, Cu,Zn superoxide-dismutase, and motor-neuron degeneration - reply. *Science, 266*(5190), 1587-1587.

123. Gurney, M. E. (1997). Transgenic animal models of familial amyotrophic lateral sclerosis. *Journal of Neurology, 244*, S15-S20.

124. Gurney, M. E., Belton, A. C., Cashman, N., & Antel, J. P. (1984). Inhibition of terminal axonal sprouting by serum from patients with amyotrophic lateral sclerosis. *New England Journal of Medicine, 311*(15), 933-939.

125. Gurney, M. E., Cutting, F. B., Zhai, P., Doble, A., Taylor, C. P., Andrus, P. K., & Hall, E. D. (1996). Benefit of vitamin E, riluzole, and gabapentin in a transgenic model of familiar amyotrophic lateral sclerosis. *Annals of Neurology, 39*(2), 147-157.

126. Gurney, M. E., Liu, R., Althaus, J. S., Hall, E. D., & Becker, D. A. (1998). Mutant CuZn superoxide dismutase in motor neuron disease. *Journal of Inherited Metabolic Disease, 21*(5), 587-597.

127. Gurney, M. E., Pu, H. F., Chiu, A. Y., Dalcanto, M. C., Polchow, C. Y., Alexander, D. D., Caliendo, J., Hentati, A., Kwon, Y. W., Deng, H. X., Chen, W. J., Zhai, P., Sufit, R. L., & Siddique, T. (1994). Motor-neuron degeneration in mice that express a human Cu, Zn superoxide-dismutase mutation. *Science, 264*(5166), 1772-1775.

128. Haenggeli, C., Julien, J., Mosley, R. L., Perez, N., Dhar, A., Gendelman, H. E., & Rothstein, J. D. (2007). Therapeutic immunization with a glatiramer acetate derivative does not alter survival in G93A and G37R SOD1 mouse models of familial ALS. *Neurobiology of Disease, 26*(1), 146-152. doi:10.1016/j.nbd.2006.12.013

129. Hall, E. D., Andrus, P. K., Oostveen, J. A., Fleck, T. J., & Gurney, M. E. (1998). Relationship of oxygen radical-induced lipid peroxidative damage to disease onset and progression in a transgenic model of familial ALS. *Journal of Neuroscience Research, 53*(1), 66-77.

130. Hammer, R. P., Tomiyasu, U., & Scheibel, A. B. (1979). Degeneration of the human Betz cell due to amyotrophic lateral sclerosis. *Experimental Neurology, 63*(2), 336-346.

131. Hanyu, N., Oguchi, K., Yanagisawa, N., & Tsukagoshi, H. (1982). Degeneration and regeneration of ventral root motor fibers in amyotrophic lateral sclerosis - morphometric studies of cervical ventral roots. *Journal of the Neurological Sciences, 55*(1), 99-115.

132. Harwood, C. A., Mcdermott, C. J., & Shaw, P. J. (2009). Physical activity as an exogenous risk factor in motor neuron disease (MND): A review of the evidence. *Amyotrophic Lateral Sclerosis, 10*(4), 191-204. doi:10.1080/17482960802549739

133. Hasegawa, M., Arai, T., Akiyama, H., Nonaka, T., Mori, H., Hashimoto, T., Yamazaki, M., & Oyanagi, K. (2007a). TDP-43 is deposited in the Guam parkinsonism-dementia complex brains. *Brain, 130*, 1386-1394. doi:10.1093/brain/awm065

134. Hasegawa, M., Arai, T., Akiyama, H., Nonaka, T., Mori, H., Hashimoto, T., Yamazaki, M., & Oyanagi, K. (2007b). TDP-43 is deposited in the Guam parkinsonism-dementia complex brains. *Brain, 130*, 1386-1394. doi:10.1093/brain/awm065

135. Hattori, A. P. (2006). 'The cry of the little people of Guam': American colonialism, medical philanthropy, and the susana hospital for chamorro women, 1898-1941. *Health and History, 8*(1), 4-26.

136. Hayworth, C. R., & Gonzalez-Lima, F. (2009). Pre-symptomatic detection of chronic motor deficits and genotype prediction in congenic B6.Sod1(G93A) ALS mouse model. *Neuroscience, 164*(3), 975-985. doi:10.1016/j.neuroscience.2009.08.031

137. He, B. P., & Strong, M. J. (2000). Motor neuronal death in sporadic amyotrophic lateral sclerosis (ALS) is not apoptotic. A comparative study of ALS and chronic aluminium chloride neurotoxicity in new zealand white rabbits. *Neuropathology and Applied Neurobiology, 26*(2), 150-160.

138. Hegedus, J., Putman, C. T., & Gordon, T. (2007). Time course of preferential motor unit loss in the SODIG93A mouse model of amyotrophic lateral sclerosis. *Neurobiology of Disease, 28*(2), 154-164. doi:10.1016/j.nbd.2007.07.003

139. Hegedus, J., Putman, C. T., Tyreman, N., & Gordon, T. (2008). Preferential motor unit loss in the SOD1(G93A) transgenic mouse model of amyotrophic lateral sclerosis. *Journal of Physiology-London, 586*(14), 3337-3351. doi:10.1113/jphysiol.2007.149286

140. Heiman-Patterson, T. D., Deitch, J. S., Blankenhorn, E. P., Erwin, K. L., Perreault, M. J., Alexander, B. K., Byers, N., Toman, I., & Alexander, G. M. (2005). Background and gender effects on survival in the TgN(SOD1-G93A) 1 gur mouse model of ALS. *Journal of the Neurological Sciences, 236*(1-2), 1-7. doi:10.1016/j.jns.2005.02.006

141. Hezel, F. X. (1982). From conversion to conquest: The early Spanish mission in the Marianas. *The Journal of Pacific History, 17*(3), 115-137.

142. Hirano, A., Kurland, L. T., Krooth, R. S., & Lessell, S. (1961a). Parkinsonism-dementia complex, an endemic disease on the island of Guam: I. clinical features. *Brain, 84*(4), 642.

143. Hirano, A., Malamud, N., Elizan, T. S., & Kurland, L. T. (1966). Amyotrophic lateral sclerosis and parkinsonism-dementia complex on Guam: Further pathologic studies. *Archives of Neurology, 15*(1), 35.

144. Hirano, A. (1991). *Neuronal pathology, amyotrophic-lateral-sclerosis (ALS) and parkinsonism-dementia complex (pdc) on Guam*

145. Hirano, A. (1998). Neuropathology of familial amyotrophic lateral sclerosis patients with superoxide dismutase 1 gene mutation. *Neuropathology, 18*(4), 363-369.

146. Hirano, A., Arumugasamy, N., & Zimmerman, H. M. (1967a). Amyotrophic lateral sclerosis. A comparison of Guam and classical cases. *Archives of Neurology, 16*(4), 357-363.

147. Hirano, A., Kurland, L. T., & Sayre, G. P. (1967b). Familial amyotrophic lateral sclerosis - a subgroup characterized by posterior and spinocerebellar tract involvement and hyaline inclusions in anterior horn cells. *Archives of Neurology, 16*(3), 232-&.

148. Hirano, A., Malamud, N., & Kurland, L. T. (1961b). Parkinsonism-dementia complex, an endemic disease on island of Guam .2. pathological features. *Brain, 84*(4), 662-&.

149. Hof, P. R., Nimchinsky, E. A., Bueescherrer, V., Buee, L., Nasrallah, J., Hottinger, A. F., Purohit, D. P., Loerzel, A. J., Steele, J. C., Delacourte, A., Bouras, C., Morrison, J. H., & Perl, D. P. (1994). Amyotrophic-lateral-sclerosis parkinsonism-dementia complex of Guam - quantitative neuropathology, immunohistochemical analysis of neuronal vulnerability, and comparison with related neurodegenerative disorders. *Acta Neuropathologica, 88*(5), 397-404.

150. Hoffman, P. M., Chen, K. M., Gajdusek, C. D., & Brody, J. A. (1976). Amyotrophic lateral sclerosis-parkinsonian dementia of Guam - current status in research. *Neurology, 26*(4), 398-398.

151. Hoke, A., Gordon, T., Zochodne, D. W., & Sulaiman, O. A. R. (2002). A decline in glial cell-line-derived neurotrophic factor expression is associated with impaired regeneration after long-term schwann cell denervation. *Experimental Neurology, 173*(1), 77-85. doi:10.1006/exnr.2001.7826

152. Ignatius, S. H., Wu, F., Harrich, D., Garciamartinez, L. F., & Gaynor, R. B. (1995). Cloning and characterization of a novel cellular protein, tdp-43, that binds to human-immunodeficiency-virus type-1 tar dna-sequence motifs. *Journal of Virology, 69*(6), 3584-3596.

153. Ilieva, H., Polymenidou, M., & Cleveland, D. W. (2009). Non-cell autonomous toxicity in neurodegenerative disorders: ALS and beyond. *Journal of Cell Biology, 187*(6), 761-772. doi:10.1083/jcb.200908164

154. Ince, P. G., & Wharton, S. B. (2007). Cytopathology of the motor neuron. In A. Eisen, & P. J. Shaw (Eds.), (pp. 89-119) Elsevier.

155. Ince, P. G., Tomkins, J., Slade, J. Y., Thatcher, N. M., & Shaw, P. J. (1998). Amyotrophic lateral sclerosis associated with genetic abnormalities in the gene encoding Cu/Zn superoxide dismutase: Molecular pathology of five new cases, and comparison with previous reports and 73 sporadic cases of ALS. *Journal of Neuropathology and Experimental Neurology, 57*(10), 895-904.

156. Isaac, J. T. R., Ashby, M., & McBain, C. J. (2007). The role of the GluR2 subunit in AMPA receptor function and synaptic plasticity. *Neuron, 54*(6), 859-871. doi:10.1016/j.neuron.2007.06.001

157. Jaiswal, M. K., & Keller, B. U. (2009). Cu/Zn superoxide dismutase typical for familial amyotrophic lateral sclerosis increases the vulnerability of mitochondria and perturbs Ca2+ homeostasis in SOD1(G93A) mice. *Molecular Pharmacology, 75*(3), 478-489. doi:10.1124/mol.108.050831

158. Jimenez-Jimenez, F. J., Hernanz, A., Medina-Acebron, S., de Bustos, F., Zurdo, J. M., Alonso, H., Puertas, I., Barcenilla, B., Sayed, Y., & Cabrera-Valdivia, F. (2005). Tau protein concentrations in cerebrospinal fluid of patients with amyotrophic lateral sclerosis. *Acta Neurologica Scandinavica, 111*(2), 114-117. doi:10.1111/j.1600-0404.2005.00370.x

159. Johnson, J. O., Mandrioli, J., Benatar, M., Abramzon, Y., Van Deerlin, V. M., Trojanowski, J. Q., Gibbs, J. R., Brunetti, M., Gronka, S., Wuu, J., Ding, J., McCluskey, L., Martinez-Lage, M., Falcone, D., Hernandez, D. G., Arepalli, S., Chong, S., Schymick, J. C., Rothstein, J., Landi, F., Wang, Y., Calvo, A., Mora, G., Sabatelli, M., Monsurro, M. R., Battistini, S., Salvi, F., Spataro, R., Sola, P., Borghero, G., Galassi, G., Scholz, S. W., Taylor, J. P., Restagno, G., Chio, A., & Traynor, B. J. (2010). Exome sequencing reveals VCP mutations as a cause of familial ALS. *Neuron, 68*(5), 857-864.

160. Jones, C. T., Brock, D. J. H., Chancellor, A. M., Warlow, C. P., & Swingler, R. J. (1993). Cu/zn superoxide-dismutase (Sod1) mutations and sporadic amyotrophic-lateral-sclerosis. *Lancet, 342*(8878), 1050-1051.

161. Julien, J., & Kriz, J. (2006). Transgenic mouse models of amyotrophic lateral sclerosis. *Biochimica Et Biophysica Acta-Molecular Basis of Disease, 1762*(11-12), 1013-1024. doi:10.1016/j.bbadis.2006.03.006

162. Julien, J. (2001). Amyotrophic lateral sclerosis: Unfolding the toxicity of the misfolded. *Cell, 104*(4), 581-591. doi:10.1016/S0092-8674(01)00244-6

163. Jung, C. W., Higgins, C. M. J., & Xu, Z. S. (2002). Mitochondrial electron transport chain complex dysfunction in a transgenic mouse model for amyotrophic lateral sclerosis. *Journal of Neurochemistry, 83*(3), 535-545.

164. Kabashi, E., Valdmanis, P. N., Dion, P., Spiegelman, D., McConkey, B. J., Velde, C. V., Bouchard, J., Lacomblez, L., Pochigaeva, K., Salachas, F., Pradat, P., Camu, W., Meininger, V., Dupre, N., & Rouleau, G. A. (2008). TARDBP mutations in individuals with sporadic and familial amyotrophic lateral sclerosis. *Nature Genetics, 40*(5), 572-574. doi:10.1038/ng.132

165. Kakulas, B. A., Masters, C. L., Garruto, R. M., Gajdusek, D. C., Gibbs, C. J., & Chen, K. M. (1980). Clinicopathological correlations in parkinsonism-dementia complex and amyotrophic lateral sclerosis of Guam. *Journal of Neuropathology and Experimental Neurology, 39*(3), 366-366.

166. Kamel, F., Umbach, D. M., Munsat, T. L., Shefner, J. M., & Sandler, D. P. (1999). Association of cigarette smoking with amyotrophic lateral sclerosis. *Neuroepidemiology, 18*(4), 194-202.

167. Kang, H., Tian, L., & Thompson, W. (2003). Terminal Schwann cells guide the reinnervation of muscle after nerve injury. *Journal of Neurocytology, 32*(5-8), 975-985. doi:10.1023/B:NEUR.0000020636.27222.2d

168. Kang, J. H., Yim, H. S., Kwak, H. S., Chock, P. B., Stadtman, E. R., & Yim, M. B. (1996). A gain-of-function of an amyotrophic lateral sclerosis-associated Cu,Zn-superoxide dismutase mutant. *Faseb Journal, 10*(6), 1422-1422.

169. Karlsborg, M., Rosenbaum, S., Wiegell, M. R., Simonsen, H., Larsson, H. B. W., Werdelin, L. M., & Gredal, O. (2004). Corticospinal tract degeneration and possible pathogenesis in ALS evaluated by MR diffusion tensor imaging. *Amyotrophic Lateral Sclerosis and Other Motor Neuron Disorders, 5*(3), 136-140.

170. Karlsson, O., Lindquist, N. G., Brittebo, E. B., & Roman, E. (2009). Selective brain uptake and behavioral effects of the cyanobacterial toxin BMAA (beta-N-methylamino-L-alanine) following neonatal administration to rodents. *Toxicological Sciences, 109*(2), 286-295. doi:10.1093/toxsci/kfp062

171. Kasarskis, E. J., Lindquist, J. H., Coffman, C. J., Grambow, S. C., Feussner, J. R., Allen, K. D., Oddone, E. Z., Kamins, K. A., Horner, R. D., & ALS Gulf War Clinical Review Team. (2009). Clinical aspects of ALS in Gulf war veterans. *Amyotrophic Lateral Sclerosis, 10*(1), 35-41. doi:10.1080/17482960802351029

172. Kato, S., & Hirano, A. (1992). Involvement of the brain-stem reticular-formation in familial amyotrophic-lateral-sclerosis. *Clinical Neuropathology, 11*(1), 41-44.

173. Kawahara, Y., Kwak, S., Sun, H., Ito, K., Hashida, H., Aizawa, H., Jeong, S. Y., & Kanazawa, I. (2003). Human spinal motoneurons express low relative abundance of GluR2 mRNA: An implication for excitotoxicity in ALS. *Journal of Neurochemistry, 85*(3), 680-689. doi:10.1046/j.1471-4159.2003.01703.x

174. Keith-Rokosh, J., & Ang, L. C. (2008). Progressive supranuclear palsy: A review of co-existing neurodegeneration. *Canadian Journal of Neurological Sciences, 35*(5), 602-608.

175. Khabazian, I., Bains, J. S., Williams, D. E., Cheung, J., Wilson, J. M., Pasqualotto, B. A., Pelech, S. L., Andersen, R. J., Wang, Y. T., Liu, L., Nagai, A., Kim, S. U., Craig, U. K., & Shaw, C. A. (2002). Isolation of various forms of sterol beta-D-glucoside from the seed of cycas circinalis: Neurotoxicity and implications for ALS-parkinsonism dementia complex. *Journal of Neurochemistry, 82*(3), 516-528.

176. Kiernan, J. A., & Hudson, A. J. (1991). Changes in sizes of cortical and lower motor neurons in amyotrophic-lateral-sclerosis. *Brain, 114*, 843-853.

177. Kihira, T., Yoshida, S., Hironishi, M., Wakayama, I., & Yase, Y. (1998). Neuronal degeneration in amyotrophic lateral sclerosis is mediated by a possible mechanism different from classical apoptosis. *Neuropathology, 18*(3), 301-308.

178. Knippenberg, S., Thau, N., Dengler, R., & Petri, S. (2010). Significance of behavioural tests in a transgenic mouse model of amyotrophic lateral sclerosis (ALS). *Behavioural Brain Research, 213*(1), 82-87. doi:10.1016/j.bbr.2010.04.042

179. Kobayashi, Z., Tsuchiya, K., Kubodera, T., Shibata, N., Arai, T., Miura, H., Ishikawa, C., Kondo, H., Ishizu, H., Akiyama, H., & Mizusawa, H. (2011). FALS with Gly72Ser mutation in SOD1 gene: Report of a family including the first autopsy case. *Journal of the Neurological Sciences, 300*(1-2), 9-13. doi:10.1016/j.jns.2010.10.030

180. Koerner, D. R. (1952). Amyotrophic lateral sclerosis on Guam: A clinical study and review of the literature. *Annals of Internal Medicine, 37*(6), 1204.

181. Kowalska, A., Konagaya, M., Sakai, M., Hashizume, Y., & Tabira, T. (2003). Familial amyotrophic lateral sclerosis and parkinsonism-d dementia complex - tauopathy without mutations in the tau gene? *Folia Neuropathologica, 41*(2), 59-64.

182. Koyama, T., Hiratsuka, T., Matsuzaki, S., Yamagishi, S., Kato, S., Katayama, T., & Tohyama, M. (2010). Familiar amyotrophic lateral sclerosis (FALS)-linked SOD1 mutation accelerates neuronal cell death by activating cleavage of caspase-4 under ER stress in an *in vitro* model of FALS. *Neurochemistry International,* 51, 838-843.

183. Kriz, J., Nguyen, M., & Julien, J. (2002). Minocycline slows disease progression in a mouse model of arnyotrophic lateral sclerosis. *Neurobiology of Disease, 10*(3), 268-278. doi:10.1006/nbdi.2002.0487

184. Kuo, J. J., Schonewille, M., Siddique, T., Schults, A. N. A., Fu, R. G., Bar, P. R., Anelli, R., Heckman, C. J., & Kroese, A. B. A. (2004). Hyperexcitability of cultured spinal motoneurons from presymptomatic ALS mice. *Journal of Neurophysiology, 91*(1), 571-575. doi:10.1152/jn.00665.2003

185. Kurland, L. T., & Fields, W. S. (1958). Pathogenesis and treatment of parkinsonism. *Charles C Thomas: Springfield, IL,*

186. Kurland, L. T., & Mulder, D. W. (1954). Epidemiologic investigations of amyotrophic lateral sclerosis. 1. preliminary report on geographic distribution, with special reference to the Mariana islands, including clinical and pathologic observations. *Neurology, 4*(5), 355-378.

187. Kusaka, H., Imai, T., Hashimoto, S., Yamamoto, T., Maya, K., & Yamasaki, M. (1988). Ultrastructural-study of chromatolytic neurons in an adult-onset sporadic case of amyotrophic lateral sclerosis. *Acta Neuropathologica, 75*(5), 523-528.

188. Kwak, S., & Kawahara, Y. (2005). Deficient RNA editing of GluR2 and neuronal death in amyotropic lateral sclerosis. *Journal of Molecular Medicine-Jmm, 83*(2), 110-120. doi:10.1007/s00109-004-0599-z

189. Kwiatkowski, T. J., Jr., Bosco, D. A., LeClerc, A. L., Tamrazian, E., Vanderburg, C. R., Russ, C., Davis, A., Gilchrist, J., Kasarskis, E. J., Munsat, T., Valdmanis, P., Rouleau, G. A., Hosler, B. A., Cortelli, P., de Jong, P. J., Yoshinaga, Y., Haines, J. L., Pericak-Vance, M. A., Yan, J., Ticozzi, N., Siddique, T., McKenna-Yasek, D., Sapp, P. C., Horvitz, H. R., Landers, J. E., & Brown, R. H., Jr. (2009). Mutations in the FUS/TLS gene on chromosome 16 cause familial amyotrophic lateral sclerosis. *Science, 323*(5918), 1205-1208. doi:10.1126/science.1166066

190. Kwong, L. K., Neumann, M., Sampathu, D. M., Lee, V. M. -., & Trojanowski, J. Q. (2007). TDP-43 proteinopathy: The neuropathology underlying major forms of sporadic and familial frontotemporal lobar degeneration and motor neuron disease. *Acta Neuropathologica, 114*(1), 63-70. doi:10.1007/s00401-007-0226-5

191. Lagier-Tourenne, C., & Cleveland, D. W. (2009). Rethinking ALS: The FUS about TDP-43. *Cell, 136*(6), 1001-1004. doi:10.1016/j.cell.2009.03.006

192. Lalonde, R., Bensoula, A. N., & Filali, M. (1995). Rotorod sensorimotor learning in cerebellar mutant mice. *Neuroscience Research, 22*(4), 423-426.

193. Lee, M., & McGeer, P. L. (2011). Weak BMAA toxicity compares with that of the dietary supplement beta-alanine. *Neurobiology of Aging, (in press)*

194. Lee, G., Chu, T., & Shaw, C. A. (2009). The primary locus of motor neuron death in an ALS-PDC mouse model. *Neuroreport, 20*(14), 1284-1289. doi:10.1097/WNR.0b013e32833037ae

195. Leigh, P. N. (2007). Amyotrophic lateral sclerosis. In A. Eisen, & P. J. Shaw (Eds.), *Handbook of clinical neurology* (pp. 249-278) Elsevier.

196. Lepore, A. C., Dejea, C., Carmen, J., Rauck, B., Kerr, D. A., Sofroniew, M. V., & Maragakis, N. J. (2008). Selective ablation of proliferating astrocytes does not affect disease outcome in either acute or chronic models of motor neuron degeneration. *Experimental Neurology, 211*(2), 423-432. doi:10.1016/j.expneurol.2008.02.020

197. Li, T. M., Alberman, E., & Swash, M. (1988). Comparison of sporadic and familial disease amongst 580 cases of motor neuron disease. *Journal of Neurology Neurosurgery and Psychiatry, 51*(6), 778-784.

198. Lim, S. M. C., Guiloff, R. J., & Navarrete, R. (2000). Interneuronal survival and calbindin-D28K expression following motoneuron degeneration. *Journal of the Neurological Sciences, 180*(1-2), 46-51.

199. Lima, B. L., Santos, E. J. C., Fernandes, G. R., Merkel, C., Mello, M. R. B., Gomes, J. P. A., Soukoyan, M., Kerkis, A., Massironi, S. M. G., Visintin, J. A., & Pereira, L. V. (2010). A new mouse model for Marfan syndrome presents phenotypic variability associated with the genetic background and overall levels of Fbn1 expression. *Plos One, 5*(11), e14136. doi:10.1371/journal.pone.0014136

200. Lino, M. M., Schneider, C., & Caroni, P. (2002). Accumulation of SOD1 mutants in postnatal motoneurons does not cause motoneuron pathology or motoneuron disease. *Journal of Neuroscience, 22*(12), 4825-4832.

201. Liu, H., Sanelli, T., Horne, P., Pioro, E. P., Strong, M. J., Rogaeva, E., Bilbao, J., Zinman, L., & Robertson, J. (2009). Lack of evidence of Monomer/Misfolded superoxide dismutase-1 in sporadic amyotrophic lateral sclerosis. *Annals of Neurology, 66*(1), 75-80. doi:10.1002/ana.21704

202. Llado, J., Haenggeli, C., Pardo, A., Wong, V., Benson, L., Coccia, C., Rothstein, J. D., Shefner, J. M., & Maragakis, N. J. (2006). Degeneration of respiratory motor neurons in the SOD1 G93A transgenic rat model of ALS. *Neurobiology of Disease, 21*(1), 110-118. doi:10.1016/j.nbd.2005.06.019

203. Lloyd, C. M., Richardson, M. P., Brooks, D. J., Al-Chalabi, A., & Leigh, P. N. (2000). Extramotor involvement in ALS: PET studies with the GABA(A) ligand [C-11]flumazenil. *Brain, 123*, 2289-2296.

204. Love, F., Son, Y., & Thompson, W. (2003). Activity alters muscle reinnervation and terminal sprouting by reducing the number of Schwann cell pathways that grow to link synaptic sites. *Journal of Neurobiology, 54*(4), 566-576. doi:10.1002/neu.10191

205. Lowe, J., Lennox, G., Jefferson, D., Morrell, K., Mcquire, D., Gray, T., Landon, M., Doherty, F. J., & Mayer, R. J. (1988). A filamentous inclusion body within anterior horn neurons in motor neuron disease defined by immunocytochemical localization of ubiquitin. *Neuroscience Letters, 94*(1-2), 203-210.

206. Lu, M. H., Tang, N., & Ali, S. F. (2000). Effects of single injection of methylazoxymethanol at postnatal day one on cell proliferation in different brain regions of male rats. *Neurotoxicology, 21*(6), 1145-1151.

207. Luquin, N., Yu, B., Trent, R. J., Morahan, J. M., & Pamphlett, R. (2008). An analysis of the entire SOD1 gene in sporadic ALS. *Neuromuscular Disorders, 18*(7), 545-552. doi:10.1016/j.nmd.2008.04.013

208. Ly, P. T. T., Singh, S., & Shaw, C. A. (2007). Novel environmental toxins: Steryl glycosides as a potential etiological factor for age-related neurodegenerative diseases. *Journal of Neuroscience Research, 85*(2), 231-237. doi:10.1002/jnr.21147

209. Machida, Y., Tsuchiya, K., Anno, M., Haga, C., Ito, T., Shimo, Y., Wakeshima, T., & Iritani, S. (1999). Sporadic amyotrophic lateral sclerosis with multiple system degeneration: A report of an autopsy case without respirator administration. *Acta Neuropathologica, 98*(5), 512-515.

210. Mackenzie, I. R. A., Bigio, E. H., Ince, P. G., Geser, F., Neumann, M., Cairns, N. J., Kwong, L. K., Forman, M. S., Ravits, J., Stewart, H., Eisen, A., Mcclusky, L., Kretzschmar, H. A., Monoranu, C. M.,

Highley, J. R., Kirby, J., Siddique, T., Shaw, P. J., Lee, V. M., & Trojanowski, J. Q. (2007). Pathological TDP-43 distinguishes sporadic amyotrophic lateral sclerosis from amyotrophic lateral sclerosis with SOD1 mutations. *Annals of Neurology, 61*(5), 427-434. doi:10.1002/ana.21147

211. Magrane, J., Hervias, I., Henning, M. S., Damiano, M., Kawamata, H., & Manfredi, G. (2009). Mutant SOD1 in neuronal mitochondria causes toxicity and mitochondrial dynamics abnormalities. *Human Molecular Genetics, 18*(23), 4552-4564. doi:10.1093/hmg/ddp421

212. Marchetto, M. C. N., Muotri, A. R., Mu, Y., Smith, A. M., Cezar, G. G., & Gage, F. H. (2008). Non-cell-autonomous effect of human SOD1(G37R) astrocytes on motor neurons derived from human embryonic stem cells. *Cell Stem Cell, 3*(6), 649-657. doi:10.1016/j.stem.2008.10.001

213. Markowski, V. P., Cox, C., & Weiss, B. (1998). Prenatal cocaine exposure produces gender-specific motor effects in aged rats. *Neurotoxicology and Teratology, 20*(1), 43-53.

214. Marler, T. E., Lee, V., & Shaw, C. A. (2005a). Spatial variation of steryl glucosides in cycas micronesica plants: Within- and among-plant sampling procedures. *HortScience, 40*(6), 1607-1611.

215. Marler, T. E., Lee, V., & Shaw, C. A. (2005b). Cycad toxins and neurological diseases in Guam: Defining theoretical and experimental standards for correlating human disease with environmental toxins. *HortScience, 40*(6), 1598-1606.

216. Marler, T. E., & Shaw, C. A. (2009a). Phenotypic characteristics as predictors of phytosterols in mature cycas micronesica seeds. *HortScience : A Publication of the American Society for Horticultural Science, 44*(3), 725-729.

217. Martyn, C. N., & Osmond, C. (1992). The environment in childhood and risk of motor-neuron disease. *Journal of Neurology Neurosurgery and Psychiatry, 55*(11), 997-1001.

218. Maruyama, H., Morino, H., Ito, H., Izumi, Y., Kato, H., Watanabe, Y., Kinoshita, Y., Kamada, M., Nodera, H., Suzuki, H., Komure, O., Matsuura, S., Kobatake, K., Morimoto, N., Abe, K., Suzuki, N., Aoki, M., Kawata, A., Hirai, T., Kato, T., Ogasawara, K., Hirano, A., Takumi, T., Kusaka, H., Hagiwara, K., Kaji, R., & Kawakami, H. (2010). Mutations of optineurin in amyotrophic lateral sclerosis. *Nature, 465*(7295), 223-U109. doi:10.1038/nature08971

219. Mash, D., Pablo, J., Banack, S. A., Cox, P. A., Johnson, T. E., Papapetropoulos, S., & Bradley, W. (2008). Neurotoxic nonprotein amino acid BMAA in brain from patients dying with ALS and Alzheimer's disease. *Neurology, 70*(11), A329-A329.

220. Matsumoto, H., & Higa, H. H. (1966). Studies on methylazoxymethanol, the aglycone of cycasin: Methylation of nucleic acids in vitro. *Biochemical Journal, 98*(2), 20C-22C.

221. Mattiazzi, M., D'Aurelio, M., Gajewski, C. D., Martushova, K., Kiaei, M., Beal, M. F., & Manfredi, G. (2002). Mutated human SOD1 causes dysfunction of oxidative phosphorylation in mitochondria of transgenic mice. *Journal of Biological Chemistry, 277*(33), 29626-29633. doi:10.1074/jbc.M203065200

222. McDonald, M. P., Miller, K. M., Li, C., Deng, C., & Crawley, J. N. (2001). Motor deficits in fibroblast growth factor receptor-3 null mutant mice. *Behavioural Pharmacology, 12*(6-7), 477-486.

223. McGeer, P., & McGeer, E. (2002). Inflammatory processes in amyotrophic lateral sclerosis. *Muscle & Nerve, 26*(4), 459-470. doi:10.1002/mus.10191

224. McOmish, C. E., & Hannan, A. J. (2007a). Environments: Exploring gene-environment interactions to identify therapeutic targets for brain disorders. *Expert Opinion on Therapeutic Targets, 11*(7), 899-913. doi:10.1517/14728222.11.7.899

225. McOmish, C. E., & Hannan, A. J. (2007b). Environments: Exploring gene-environment interactions to identify therapeutic targets for brain disorders. *Expert Opinion on Therapeutic Targets, 11*(7), 899-913. doi:10.1517/14728222.11.7.899

226. Meziane, H., Ouagazzal, A. -., Aubert, L., Wietrzych, M., & Krezel, W. (2007). Estrous cycle effects on behavior of C57BL/6J and BALB/cByJ female mice: Implications for phenotyping strategies. *Genes Brain and Behavior, 6*(2), 192-200. doi:349736347,12,1

227. Miana-Mena, F., Munos, M., Yague, G., Mendez, M., Moreno, M., Ciriza, J., Zaragoza, P., & Osta, R. (2005). Optimal methods to characterize the G93A mouse model of ALS. *Amyotrophic Lateral Sclerosis and Other Motor Neuron Disorders, 6*(1), 55-62. doi:10.1080/14660820510026162

228. Miller, R. G., Mitchell, J. D., Lyon, M., & Moore, D. H. (2007). Riluzole for amyotrophic lateral sclerosis (ALS)/motor neuron disease (MND). *Cochrane Database of Systematic Reviews,* (1), CD001447. doi:10.1002/14651858.CD001447.pub2

229. Miller, T. M., Kim, S. H., Yamanaka, K., Hester, M., Umapathi, P., Arnson, H., Rizo, L., Mendell, J. R., Gage, F. H., Cleveland, D. W., & Kaspar, B. K. (2006). Gene transfer demonstrates that muscle is not a primary target for non-cell-autonomous toxicity in familial amyotrophic lateral sclerosis. *Proceedings of the National Academy of Sciences of the United States of America, 103*(51), 19546-19551. doi:10.1073/pnas.0609411103

230. Mizusawa, H., Nakamura, H., Wakayama, I., Yen, S. H. C., & Hirano, A. (1991). Skein-like inclusions in the anterior horn cells in motor-neuron disease. *Journal of the Neurological Sciences, 105*(1), 14-21.

231. Mizutani, T., Sakamaki, S., Tsuchiya, N., Kamei, S., Kohzu, H., Horiuchi, R., Ida, M., Shiozawa, R., & Takasu, T. (1992). Amyotrophic-lateral-sclerosis with ophthalmoplegia and multisystem degeneration in patients on long-term use of respirators. *Acta Neuropathologica, 84*(4), 372-377.

232. Mohajeri, M. H., Figlewicz, D. A., & Bohn, M. C. (1998). Selective loss of alpha motoneurons innervating the medial gastrocnemius muscle in a mouse model of amyotrophic lateral sclerosis. *Experimental Neurology, 150*(2), 329-336.

233. Moisse, K., Mepham, J., Volkening, K., Welch, I., Hill, T., & Strong, M. J. (2009a). Cytosolic TDP-43 expression following axotomy is associated with caspase 3 activation in NFL-/- mice: Support for a

role for TDP-43 in the physiological response to neuronal injury. *Brain Research, 1296*, 176-186. doi:10.1016/j.brainres.2009.07.023

234. Moisse, K., Volkening, K., Leystra-Lantz, C., Welch, I., Hill, T., & Strong, M. J. (2009b). Divergent patterns of cytosolic TDP-43 and neuronal progranulin expression following axotomy: Implications for TDP-43 in the physiological response to neuronal injury. *Brain Research, 1249*, 202-211. doi:10.1016/j.brainres.2008.10.021

235. Montine, T. J., Li, K., Perl, D. P., & Galasko, D. (2005). Lack of beta-methylamino-L-alanine in brain from controls, AD, or Chamorros with PDC. *Neurology, 65*(5), 768-769.

236. Mooney, S. M., & Varlinskaya, E. I. (2011). Acute prenatal exposure to ethanol and social behavior: Effects of age, sex, and timing of exposure. *Behavioural Brain Research, 216*(1), 358-364. doi:10.1016/j.bbr.2010.08.014

237. Morahan, J. M., Yu, B., Trent, R. J., & Pamphlett, R. (2009). A genome-wide analysis of brain DNA methylation identifies new candidate genes for sporadic amyotrophic lateral sclerosis. *Amyotrophic Lateral Sclerosis, 10*(5-6), 418-U247. doi:10.3109/17482960802635397

238. Morrison, B. M., Janssen, W. G., Gordon, J. W., & Morrison, J. H. (1998). Time course of neuropathology in the spinal cord of G86R superoxide dismutase transgenic mice. *Journal of Comparative Neurology, 391*(1), 64-77.

239. Mourelatos, Z., Gonatas, N. K., Stieber, A., Gurney, M. E., & DalCanto, M. C. (1996). The golgi apparatus of spinal cord motor neurons in transgenic mice expressing mutant Cu,Zn superoxide dismutase becomes fragmented in early, preclinical stages of the disease. *Proceedings of the National Academy of Sciences of the United States of America, 93*(11), 5472-5477.

240. Mulder, D. W. (1957). The clinical syndrome of amyotrophic lateral sclerosis. *Proceedings of the Staff Meetings.Mayo Clinic, 32*(17), 427-436.

241. Mulder, D. W., Kurland, L. T., & Iriarte, L. L. (1954). Neurologic diseases on the island of Guam. *United States Armed Forces Medical Journal, 5*(12), 1724-1739.

242. Munoz, D. G., Neumann, M., Kusaka, H., Yokota, O., Ishihara, K., Terada, S., Kuroda, S., & Mackenzie, I. R. (2009). FUS pathology in basophilic inclusion body disease. *Acta Neuropathologica, 118*(5), 617-627. doi:10.1007/s00401-009-0598-9

243. Murayama, S., Mori, H., Ihara, Y., Bouldin, T. W., Suzuki, K., & Tomonaga, M. (1990). Immunocytochemical and ultrastructural studies of lower motor neurons in amyotrophic lateral sclerosis. *Annals of Neurology, 27*(2), 137-148.

244. Murray, L. M., Talbot, K., & Gillingwater, T. H. (2010). Review: Neuromuscular synaptic vulnerability in motor neurone disease: Amyotrophic lateral sclerosis and spinal muscular atrophy. *Neuropathology and Applied Neurobiology, 36*(2), 133-156. doi:10.1111/j.1365-2990.2009.01061.x

245. Nagabhushana, A., Chalasani, M. L., Jain, N., Radha, V., Rangaraj, N., Balasubramanian, D., & Swarup, G. (2010). Regulation of endocytic trafficking of transferrin receptor by optineurin and its impairment by a glaucoma-associated mutant. *Bmc Cell Biology, 11*, 4. doi:10.1186/1471-2121-11-4

246. Nagai, M., Re, D. B., Nagata, T., Chalazonitis, A., Jessell, T. M., Wichterle, H., & Przedborski, S. (2007). Astrocytes expressing ALS-linked mutated SOD1 release factors selectively toxic to motor neurons. *Nature Neuroscience, 10*(5), 615-622. doi:10.1038/nn1876

247. Naini, A., Mehrazin, M., Lu, J., Gordon, P., & Mitsumoto, H. (2007). Identification of a novel D109Y mutation in Cu/Zn superoxide dismutase (sod1) gene associated with amyotrophic lateral sclerosis. *Journal of the Neurological Sciences, 254*(1-2), 17-21. doi:10.1016/j.jns.2006.12.009

248. Nair, G., Carew, J. D., Usher, S., Lu, D., Hu, X. P., & Benatar, M. (2010). Diffusion tensor imaging reveals regional differences in the cervical spinal cord in amyotrophic lateral sclerosis. *NeuroImage, 53*(2), 576-583. doi:10.1016/j.neuroimage.2010.06.060

249. Nakajima, M., Eisen, A., McCarthy, R., Olney, R. K., & Aminoff, M. J. (1996). Reduced corticomotoneuronal excitatory postsynaptic potentials (EPSPs) with normal ia afferent EPSPs in amyotrophic lateral sclerosis. *Neurology, 47*(6), 1555-1561.

250. Nakano, I. (2001). Pyramidal tract pathology in amyotrophic lateral sclerosis - axon staining reveals degeneration undisclosed on myelin staining. *Molecular Mechanism and Therapeutics of Amyotrophic Lateral Sclerosis, 1221*, 3-11.

251. Nakano, I., Shibata, T., & Uesaka, Y. (1993). On the possibility of autolysosomal processing of skein-like inclusions - electron-microscopic observation in a case of amyotrophic-lateral-sclerosis. *Journal of the Neurological Sciences, 120*(1), 54-59.

252. Neumann, M., Sampathu, D. M., Kwong, L. K., Truax, A. C., Micsenyi, M. C., Chou, T. T., Bruce, J., Schuck, T., Grossman, M., Clark, C. M., McCluskey, L. F., Miller, B. L., Masliah, E., Mackenzie, I. R., Feldman, H., Feiden, W., Kretzschmar, H. A., Trojanowski, J. Q., & Lee, V. M. -. (2006). Ubiquitinated TDP-43 in frontotemporal lobar degeneration and amyotrophic lateral sclerosis. *Science, 314*(5796), 130-133. doi:10.1126/science.1134108

253. Nguyen, M. D., D'Aigle, T., Gowing, G. V., Julien, J. P., & Rivest, S. (2004). Exacerbation of motor neuron disease by chronic stimulation of innate immunity in a mouse model of amyotrophic lateral sclerosis. *Journal of Neuroscience, 24*(6), 1340-1349. doi:10.1523/JNEUROSCI.4786-03.2004

254. Nguyen, M. D., Lariviere, R. C., & Julien, J. P. (2000). Reduction of axonal caliber does not alleviate motor neuron disease caused by mutant superoxide dismutase 1. *Proceedings of the National Academy of Sciences of the United States of America, 97*(22), 12306-12311.

255. Niebroj-Dobosz, I., & Janik, P. (1999). Amino acids acting as transmitters in amyotrophic lateral sclerosis (ALS). *Acta Neurologica Scandinavica, 100*(1), 6-11.

256. Nihei, K., Mckee, A. C., & Kowall, N. W. (1993). Patterns of neuronal degeneration in the motor cortex of amyotrophic-lateral-sclerosis patients. *Acta Neuropathologica, 86*(1), 55-64.

257. Nishida, K., Kobayashi, A., & Nagahama, T. (1955). Studies on cycasin, a new toxic glycoside, of cycas revoluta thun. *Bulletin of the Agricultural Chemical Society of Japan, 19*(3), 172-177.

258. Nishihira, Y., Tan, C., Toyoshima, Y., Yonemochi, Y., Kondo, H., Nakajima, T., & Takahashi, H. (2009). Sporadic amyotrophic lateral sclerosis: Widespread multisystem degeneration with TDP-43 pathology in a patient after long-term survival on a respirator. *Neuropathology, 29*(6), 689-696. doi:10.1111/j.1440-1789.2008.00999.x

259. Oezdinler, P. H., Benn, S., Yamamoto, T. H., Guezel, M., Brown, R. H., Jr., & Macklis, J. D. (2011). Corticospinal motor neurons and related subcerebral projection neurons undergo early and specific neurodegeneration in hSOD1(G93A) transgenic ALS mice. *Journal of Neuroscience, 31*(11), 4166-4177. doi:10.1523/JNEUROSCI.4184-10.2011

260. Okamoto, K., Fujita, Y., Aizawa, H., Kusaka, H., & Mihara, B. (2001). Basophilic cytoplasmic inclusions in amyotrophic lateral sclerosis. *Molecular Mechanism and Therapeutics of Amyotrophic Lateral Sclerosis, 1221*, 21-26.

261. Okamoto, K., Hirai, S., Amari, M., Watanabe, M., & Sakurai, A. (1993). Bunina bodies in amyotrophic-lateral-sclerosis immunostained with rabbit anti-cystatin-C serum. *Neuroscience Letters, 162*(1-2), 125-128.

262. Okamoto, K., Kihira, T., Kondo, T., Kobashi, G., Washio, M., Sasaki, S., Yokoyama, T., Miyake, Y., Sakamoto, N., Inaba, Y., & Nagai, M. (2007). Nutritional status and risk of amyotrophic lateral sclerosis in Japan. *Amyotrophic Lateral Sclerosis, 8*(5), 300-304. doi:10.1080/17482960701472249

263. Olsen, M. K., Roberds, S. L., Ellerbrock, B. R., Fleck, T. J., McKinley, D. K., & Gurney, M. E. (2001). Disease mechanisms revealed by transcription profiling in SOD1-G93A transgenic mouse spinal cord. *Annals of Neurology, 50*(6), 730-740.

264. Ono, S., Takahashi, K., Fukuoka, Y., Jinnai, K., Kanda, F., & Nagao, K. (1997). Amyotrophic lateral sclerosis with prolonged survival and degeneration of the spinocerebellar tracts, substantia nigra and dentatorubral system. *Neuropathology, 17*(4), 352-357.

265. Orban, P., Devon, R. S., Hayden, M. R., & Leavitt, B. R. (2007). Juvenile amyotrophic lateral sclerosis. In A. Eisen, & P. J. Shaw (Eds.), *Handbook of clinical neurology* (pp. 301-312) Elsevier.

266. Origone, P., Caponnetto, C., Mascolo, M., & Mandich, P. (2009). Heterozygous D90A-SOD1 mutation in an Italian ALS patient with atypical presentation. *Amyotrophic Lateral Sclerosis, 10*(5-6), 492-492. doi:10.3109/17482960903055966

267. Orrell, R. W. (2000). Amyotrophic lateral sclerosis: Copper/zinc superoxide dismutase (SOD1) gene mutations. *Neuromuscular Disorders, 10*(1), 63-68.

268. Orrell, R. W., Habgood, J. J., Malaspina, A., Mitchell, J., Greenwood, J., Lane, R. J. M., & deBelleroche, J. S. (1999). Clinical characteristics of SOD1 gene mutations in UK families with ALS. *Journal of the Neurological Sciences, 169*(1-2), 56-60.

269. Ostlund, R. E., Jr. (2007). Phytosterols, cholesterol absorption and healthy diets. *Lipids, 42*(1), 41-45. doi:10.1007/s11745-006-3001-9

270. Oyanagi, K., Makifuchi, T., Ohtoh, T., Chen, K. M., Gajdusek, D. C., Chase, T. N., & Ikuta, F. (1994b). The neostriatum and nucleus-accumbens in parkinsonism-dementia complex of Guam - a pathological comparison with Alzheimers-disease and progressive supranuclear palsy. *Acta Neuropathologica, 88*(2), 122-128.

271. Oyanagi, K., Makifuchi, T., Ohtoh, T., Chen, K. M., Vanderschaaf, T., Gajdusek, D. C., Chase, T. N., & Ikuta, F. (1994a). Amyotrophic-lateral-sclerosis of guam - the nature of the neuropathological findings. *Acta Neuropathologica, 88*(5), 405-412.

272. Oyanagi, K., & Wada, M. (1999). Neuropathology of parkinsonism-dementia complex and amyotrophic lateral sclerosis of Guam: An update. *Journal of Neurology, 246*, 19-27.

273. Oyanagi, K., Yamazaki, M., Takahashi, H., Watabe, K., Wada, M., Komori, T., Morita, T., & Mizutani, T. (2008). Spinal anterior horn cells in sporadic amyotrophic lateral sclerosis show ribosomal detachment from, and cisternal distention of the rough endoplasmic reticulum. *Neuropathology and Applied Neurobiology, 34*(6), 650-658. doi:10.1111/j.1365-2990.2008.00941.x

274. Pambo-Pambo, A., Durand, J., & Gueritaud, J. (2009). Early excitability changes in lumbar motoneurons of transgenic SOD1(G85R) and SOD1(G93A-low) mice. *Journal of Neurophysiology, 102*(6), 3627-3642. doi:10.1152/jn.00482.2009

275. Pamphlett, R., Kril, J., & Hng, T. M. (1995). Motor-neuron disease - a primary disorder of corticomotoneurons. *Muscle & Nerve, 18*(3), 314-318.

276. Pardo, C. A., Xu, Z. S., Borchelt, D. R., Price, D. L., Sisodia, S. S., & Cleveland, D. W. (1995). Superoxide-dismutase is an abundant component in cell-bodies, dendrites, and axons of motor-neurons and in a subset of other neurons. *Proceedings of the National Academy of Sciences of the United States of America, 92*(4), 954-958.

277. Parkhouse, W. S., Cunningham, L., Mcfee, I., Miller, J. M. L., Whitney, D., Pelech, S. L., & Krieger, C. (2008). Neuromuscular dysfunction in the mutant superoxide dismutase mouse model of amyotrophic lateral sclerosis. *Amyotrophic Lateral Sclerosis, 9*(1), 24-34. doi:10.1080/17482960701725646

278. Pastula, D. M., Coffman, C. J., Allen, K. D., Oddone, E. Z., Kasarskis, E. J., Lindquist, J. H., Morgenlander, J. C., Norman, B. B., Rozear, M. P., Sams, L. A., Sabet, A., & Bedlack, R. S. (2009). Factors associated with survival in the national registry of veterans with ALS. *Amyotrophic Lateral Sclerosis, 10*(5-6), 332-338. doi:10.3109/17482960802320545

279. Patel, Y., Moraes, Y. C., Latchman, D., Coffin, R., & de Belleroche, J. (2002). Neuroprotective effects of copper/zinc-dependent superoxide dismutase against a wide variety of death-inducing stimuli and proapoptotic effect of familial amyotrophic lateral sclerosis mutations. *Molecular Brain Research, 109*(1-2), 189-197.

280. Pedrini, S., Sau, D., Guareschi, S., Bogush, M., Brown, R. H., Jr., Naniche, N., Kia, A., Trotti, D., & Pasinelli, P. (2010). ALS-linked mutant SOD1 damages mitochondria by promoting conformational changes in bcl-2. *Human Molecular Genetics, 19*(15), 2974-2986. doi:10.1093/hmg/ddq202

281. Peng, L. C., Kawagoe, Y., Hogan, P., & Delmer, D. (2002). Sitosterol-beta-glucoside as primer for cellulose synthesis in plants. *Science, 295*(5552), 147-150.

282. Perl, D. P., Hirano, A., & Kurland, L. T. (1997). Guam ALS/PDC: Model of age-related neurodegeneration. *Brain Pathology, 7*(4), 1171-1172.

283. Perry, T. L., Bergeron, C., Biro, A. J., & Hansen, S. (1989). Beta-N-methylamino-L-alanine. chronic oral administration is not neurotoxic to mice. *Journal of the Neurological Sciences, 94*(1-3), 173-180.

284. Petri, S., Krampfl, K., Hashemi, F., Grothe, C., Hori, A., Dengler, R., & Bufler, J. (2003). Distribution of GABA(A) receptor mRNA in the motor cortex of ALS patients. *Journal of Neuropathology and Experimental Neurology, 62*(10), 1041-1051.

285. Petri, S., Kollewe, K., Grothe, C., Hori, A., Dengler, R., Bufler, J., & Krampfl, K. (2006). GABA(A)-receptor mRNA expression in the prefrontal and temporal cortex of ALS patients. *Journal of the Neurological Sciences, 250*(1-2), 124-132. doi:10.1016/j.jns.2006.08.005

286. Petrik, M. S., Wilson, J. M., Grant, S. C., Blackband, S. J., Tabata, R. C., Shan, X., Krieger, C., & Shaw, C. A. (2007). Magnetic resonance microscopy and immunohistochemistry of the CNS of the mutant SOD murine model of ALS reveals widespread neural deficits. *Neuromolecular Medicine, 9*(3), 216-229.

287. Piao, Y. S., Wakabayashi, K., Kakita, A., Yamada, M., Hayashi, S., Morita, T., Ikuta, F., Oyanagi, K., & Takahashi, H. (2003). Neuropathology with clinical correlations of sporadic amyotrophic lateral sclerosis: 102 autopsy cases examined between 1962 and 2000. *Brain Pathology, 13*(1), 10-22.

288. Piironen, V., Lindsay, D. G., Miettinen, T. A., Toivo, J., & Lampi, A. M. (2000). Plant sterols: Biosynthesis, biological function and their importance to human nutrition. *Journal of the Science of Food and Agriculture, 80*(7), 939-966.

289. Plaitakis, A., & Constantakakis, E. (1993). Altered metabolism of excitatory amino-acids, N-acetyl-aspartate and N-acetyl-aspartyl-glutamate in amyotrophic-lateral-sclerosis. *Brain Research Bulletin, 30*(3-4), 381-386.

290. Plato, C. C., Garruto, R. M., Galasko, D., Craig, U. K., Plato, M., Gamst, A., Torres, J. M., & Wiederholt, W. (2003). Amyotrophic lateral sclerosis and parkinsonism-dementia complex of Guam: Changing incidence rates during the past 60 years. *American Journal of Epidemiology, 157*(2), 149-157.

291. Poorkaj, P., Tsuang, D., Wijsman, E., Steinbart, E., Garruto, R. M., Craig, U. K., Chapman, N. H., Anderson, L., Bird, T. D., Plato, C. C., Perl, D. P., Weiderholt, W., Galasko, D., & Schellenberg, G. D.

(2001). TAU as a susceptibility gene for amyotropic lateral sclerosis-parkinsonism dementia complex of Guam. *Archives of Neurology, 58*(11), 1871-1878.

292. Powell, E., Anch, A., Dyche, J., Bloom, C., & Richter, R. (1999). The splay angle:: A new measure for assessing neuromuscular dysfunction in rats. *Physiology & Behavior, 67*(5), 819-821.

293. Pramatarova, A., Laganiere, J., Roussel, J., Brisebois, K., & Rouleau, G. A. (2001). Neuron-specific expression of mutant superoxide dismutase 1 in transgenic mice does not lead to motor impairment. *Journal of Neuroscience, 21*(10), 3369-3374.

294. Pun, S., Santos, A. F., Saxena, S., Xu, L., & Caroni, P. (2006). Selective vulnerability and pruning of phasic motoneuron axons in motoneuron disease alleviated by CNTF. *Nature Neuroscience, 9*(3), 408-419. doi:10.1038/nn1653

295. Qureshi, M. M., Hayden, D., Urbinelli, L., Ferrante, K., Newhall, K., Myers, D., Hilgenberg, S., Smart, R., Brown, R. H., Jr., & Cudkowicz, M. E. (2006). Analysis of factors that modify susceptibility and rate of progression in amyotrophic lateral sclerosis (ALS). *Amyotrophic Lateral Sclerosis, 7*(3), 173-182. doi:10.1080/14660820600640596

296. Rabe, M., Felbecker, A., Waibel, S., Steinbach, P., Winter, P., & Ludolph, A. C. (2010). The epidemiology of CuZn-SOD mutations in germany: A study of 217 families. *Journal of Neurology, 257*(8), 1298-1302. doi:10.1007/s00415-010-5512-9

297. Rafalowska, J., & Podlecka, A. (1998). Does the pathological factor in amyotrophic lateral sclerosis (ALS) damage also astrocytes? *Folia Neuropathologica, 36*(2), 87-93.

298. Rakhit, R., Crow, J. P., Lepock, J. R., Kondejewski, L. H., Cashman, N. R., & Chakrabartty, A. (2004). Monomeric Cu,Zn-superoxide dismutase is a common misfolding intermediate in the oxidation models of sporadic and familial amyotrophic lateral sclerosis. *Journal of Biological Chemistry, 279*(15), 15499-15504. doi:10.1074/jbc.M313295200

299. Rakhit, R., Cunningham, P., Furtos-Matei, A., Dahan, S., Qi, X. F., Crow, J. P., Cashman, N. R., Kondejewski, L. H., & Chakrabartty, A. (2002). Oxidation-induced misfolding and agagaregation of superoxide dismutase and its implications for amyotrophic lateral sclerosis. *Journal of Biological Chemistry, 277*(49), 47551-47556. doi:10.1074/jbc.M207356200

300. Rakhit, R., Robertson, J., Vande Velde, C., Horne, P., Ruth, D. M., Griffin, J., Cleveland, D. W., Cashman, N. R., & Chakrabartty, A. (2007). An immunological epitope selective for pathological monomer-misfolded SOD1 in ALS. *Nature Medicine, 13*(6), 754-759. doi:10.1038/nm1559

301. Ramasubbu, J., Buradagunta, S., Thompson, K., Gerstmayr, E., Sadasivan, S., Vieira, F., Keefe, K., Gupta, M., Theodoss, J., Mayan, K., Sichello, C., Wieman, L., Clark, J., Guleria, I., Scott, S., Menon, K., Manes, L. V., Heywood, J. A., & Ramesh, T. M. (2002). Complexities in the design and analysis of drug effects using the Sod1 G93a mouse model for amyotrophic lateral sclerosis. *Society for Neuroscience Abstract Viewer and Itinerary Planner, 2002*, AbstratNo.789.9.

302. Ravits, J. M., & La Spada, A. R. (2009). ALS motor phenotype heterogeneity, focality, and spread deconstructing motor neuron degeneration. *Neurology, 73*(10), 805-811. doi:10.1212/WNL.0b013e3181b6bbbd

303. Ravits, J., Paul, P., & Jorg, C. (2007). Focality of upper and lower motor neuron degeneration at the clinical onset of ALS. *Neurology, 68*(19), 1571-1575.

304. Reed, D., Plato, C., Elizan, T., & Kurland, L. T. (1966). Amyotrophic lateral Sclerosis/parkinsonism-dementia complex - a 10-year follow-up on Guam .I. epidemiologic studies. *American Journal of Epidemiology, 83*(1), 54-&.

305. Reed, D. M., & Brody, J. A. (1975). Amyotrophic lateral sclerosis and parkinsonism-dementia on Guam, 1945-1972: I. descriptive epidemiology. *American Journal of Epidemiology, 101*(4), 287-301.

306. Reyes, N. A., Fisher, J. K., Austgen, K., VandenBerg, S., Huang, E. J., & Oakes, S. A. (2010). Blocking the mitochondrial apoptotic pathway preserves motor neuron viability and function in a mouse model of amyotrophic lateral sclerosis. *Journal of Clinical Investigation, 120*(10), 3673-3679. doi:10.1172/JCI42986

307. Riggs, N. V. (1956). Glucosyloxyazoxymethane, a constituent of the seeds of cycas-circinalis L. *Chemistry & Industry,* (35), 926-926.

308. Roberts, G. W. (1988). Immunocytochemistry of neurofibrillary tangles in dementia pugilistica and alzheimers-disease - evidence for common genesis. *Lancet, 2*(8626-7), 1456-1458.

309. Robertson, J., Sanelli, T., Xiao, S., Yang, W., Horne, P., Hammond, R., Pioro, E. P., & Trong, M. J. S. (2007b). Lack of TDP-43 abnormalities in mutant SOD1 transgenic mice shows disparity with ALS. *Neuroscience Letters, 420*(2), 128-132. doi:10.1016/j.neulet.2007.03.066

310. Rogers, R. F. (1995). *Destiny's landfall : A history of Guam*. Honolulu: University of Hawaii Press.

311. Rosen, D. R., Siddique, T., Patterson, D., Figlewicz, D. A., Sapp, P., Hentati, A., Donaldson, D., Goto, J., Oregan, J. P., Deng, H. X., Rahmani, Z., Krizus, A., Mckennayasek, D., Cayabyab, A., Gaston, S. M., Berger, R., Tanzi, R. E., Halperin, J. J., Herzfeldt, B., Vandenbergh, R., Hung, W. Y., Bird, T., Deng, G., Mulder, D. W., Smyth, C., Laing, N. G., Soriano, E., Pericakvance, M. A., Haines, J., Rouleau, G. A., Gusella, J. S., Horvitz, H. R., & Brown, R. H. (1993). Mutations in Cu/Zn superoxide-dismutase gene are associated with familial amyotrophic-lateral-sclerosis. *Nature, 362*(6415), 59-62.

312. Rothstein, J. D., Martin, L. J., & Kuncl, R. W. (1992). Decreased glutamate transport by the brain and spinal-cord in amyotrophic-lateral-sclerosis. *New England Journal of Medicine, 326*(22), 1464-1468.

313. Rothstein, J. D., Vankammen, M., Levey, A. I., Martin, L. J., & Kuncl, R. W. (1995). Selective loss of glial glutamate transporter glt-1 in amyotrophic-lateral-sclerosis. *Annals of Neurology, 38*(1), 73-84.

314. Rutherford, N. J., Zhang, Y., Baker, M., Gass, J. M., Finch, N. A., Xu, Y., Stewart, H., Kelley, B. J., Kuntz, K., Crook, R. J. P., Sreedharan, J., Vance, C., Sorenson, E., Lippa, C., Bigio, E. H., Geschwind, D. H., Knopman, D. S., Mitsumoto, H., Petersen, R. C., Cashman, N. R., Hutton, M., Shaw, C. E., Boylan,

K. B., Boeve, B., Graff-Radford, N. R., Wszolek, Z. K., Caselli, R. J., Dickson, D. W., Mackenzie, I. R., Petrucelli, L., & Rademakers, R. (2008). Novel mutations in TARDBP(TDP-43) in patients with familial amyotrophic lateral sclerosis. *Plos Genetics, 4*(9), e1000193. doi:10.1371/journal.pgen.1000193

315. Sahlender, D. A., Roberts, R. C., Arden, S. D., Spudich, G., Taylor, M. J., Luzio, J. P., Kendrick-Jones, J., & Buss, F. (2005). Optineurin links myosin VI to the golgi complex and is involved in golgi organization and exocytosis. *Journal of Cell Biology, 169*(2), 285-295. doi:10.1083/jcb.200501162

316. Salas-Ramirez, K. Y., Frankfurt, M., Alexander, A., Luine, V. N., & Friedman, E. (2010). Prenatal cocaine exposure increases anxiety, impairs cognitive function and increases dendritic spine density in adult rats: Influence of sex. *Neuroscience, 169*(3), 1287-1295. doi:10.1016/j.neuroscience.2010.04.067

317. Salen, G., Shore, V., Tint, G. S., Forte, T., Shefer, S., Horak, I., Horak, E., Dayal, B., Nguyen, L., & Batta, A. K. (1989). Increased sitosterol absorption, decreased removal, and expanded body pools compensate for reduced cholesterol synthesis in sitosterolemia with xanthomatosis. *Journal of Lipid Research, 30*(9), 1319.

318. Salerno, A., & Georgesco, M. (1998). Double magnetic stimulation of the motor cortex in amyotrophic lateral sclerosis. *Electroencephalography and Clinical Neurophysiology, 107*(2), 133-139.

319. Sanelli, T., Xiao, S., Horne, P., Bilbao, J., Zinman, L., & Robertson, J. (2007). Evidence that TDP-43 is not the major ubiquitinated target within the pathological inclusions of amyotrophic lateral sclerosis. *Journal of Neuropathology and Experimental Neurology, 66*(12), 1147-1153.

320. Sargsyan, S., Monk, P., & Shaw, P. (2005). Microglia as potential contributors to motor neuron injury in amyotrophic lateral sclerosis RID C-6155-2008 RID A-5215-2009. *Glia, 51*(4), 241-253. doi:10.1002/glia.20210

321. Sasabe, J., & Aiso, S. (2010). Aberrant control of motoneuronal excitability in amyotrophic lateral sclerosis: Excitatory Glutamate/D-serine vs. inhibitory Glycine/gamma-aminobutanoic acid (GABA). *Chemistry & Biodiversity, 7*(6), 1479-1490.

322. Sasaki, S., & Iwata, M. (1995). Synaptic loss in the proximal axon of anterior horn neurons in motor-neuron disease. *Acta Neuropathologica, 90*(2), 170-175.

323. Sasaki, S., & Iwata, M. (1996). Ultrastructural study of the synapses of central chromatolytic anterior horn cells in motor neuron disease. *Journal of Neuropathology and Experimental Neurology, 55*(8), 932-939.

324. Sasaki, S., & Iwata, M. (1999a). Motor neuron disease with predominantly upper extremity involvement: A clinicopathological study. *Acta Neuropathologica, 98*(6), 645-650.

325. Sasaki, S., & Iwata, M. (1999b). Atypical form of amyotrophic lateral sclerosis. *Journal of Neurology Neurosurgery and Psychiatry, 66*(5), 581-585.

326. Sasaki, S., & Iwata, M. (2001). Ultrastructural study of betz cells in the primary motor cortex of the human brain. *Journal of Anatomy, 199*, 699-708.

327. Sasaki, S., & Maruyama, S. (1993). Ultrastructural-study of bunina bodies in the anterior horn neurons of patients with amyotrophic-lateral-sclerosis. *Neuroscience Letters, 154*(1-2), 117-120.

328. Sasaki, S., & Maruyama, S. (1994). Immunocytochemical and ultrastructural studies of the motor cortex in amyotrophic-lateral-sclerosis. *Acta Neuropathologica, 87*(6), 578-585.

329. Sasaki, S. (2010). Endoplasmic reticulum stress in motor neurons of the spinal cord in sporadic amyotrophic lateral sclerosis. *Journal of Neuropathology and Experimental Neurology, 69*(4), 346-355. doi:10.1097/NEN.0b013e3181d44992

330. Sasaki, S., & Iwata, M. (2007). Mitochondrial alterations in the spinal cord of patients with sporadic amyotrophic lateral sclerosis. *Journal of Neuropathology and Experimental Neurology, 66*(1), 10-16.

331. Sathasivam, S., Ince, P. G., & Shaw, P. J. (2001). Apoptosis in amyotrophic lateral sclerosis: A review of the evidence. *Neuropathology and Applied Neurobiology, 27*(4), 257-274.

332. Schaefer, A., Sanes, J., & Lichtman, J. (2005). A compensatory subpopulation of motor neurons in a mouse model of amyotrophic lateral sclerosis. *Journal of Comparative Neurology, 490*(3), 209-219. doi:10.1002/cne.20620

333. Schaller, H. (2003). The role of sterols in plant growth and development. *Progress in Lipid Research, 42*(3), 163-175.

334. Schiffer, D., Attanasio, A., Chio, A., Migheli, A., & Pezzulo, T. (1994). Ubiquitinated dystrophic neurites suggest corticospinal derangement in patients with amyotrophic-lateral-sclerosis. *Neuroscience Letters, 180*(1), 21-24.

335. Schiffer, D., & Fiano, V. (2004). Astrogliosis in ALS: Possible interpretations according to pathogenetic hypotheses. *Amyotrophic Lateral Sclerosis and Other Motor Neuron Disorders, 5*(1), 22-25.

336. Schmalbruch, H., Jensen, H. J. S., Bjaerg, M., Kamieniecka, Z., & Kurland, L. (1991). A new mouse mutant with progressive motor neuronopathy. *Journal of Neuropathology and Experimental Neurology, 50*(3), 192-204.

337. Schmied, A., & Attarian, S. (2008). Enhancement of single motor unit inhibitory responses to transcranial magnetic stimulation in amyotrophic lateral sclerosis. *Experimental Brain Research, 189*(2), 229-242. doi:10.1007/s00221-008-1420-y

338. Schneider, T., Roman, A., Basta-Kaim, A., Kubera, M., Budziszewska, B., Schneider, K., & Przewtocki, R. (2008). Gender-specific behavioral and immunological alterations in an animal model of autism induced by prenatal exposure to valproic acid. *Psychoneuroendocrinology, 33*(6), 728-740. doi:10.1016/j.psyneuen.2008.02.011

339. Schoser, B. G. H., Wehling, S., & Blottner, D. (2001). Cell death and apoptosis-related proteins in muscle biopsies of sporadic amyotrophic lateral sclerosis and polyneuropathy. *Muscle & Nerve, 24*(8), 1083-1089.

340. Schulz, J. D., Wilson, J. M. B., & Shaw, C. A. (2003). A murine model of ALS-PDC with behavioral and neuropathological features of parkinsonism. *Parkinson's Disease: The Life Cycle of the Dopamine Neuron, 991*, 326-329.

341. Seawright, A. A., Ng, J. C., Oelrichs, P. B., Sani, Y., Nolan, C. C., Lister, A. T., Holton, J., Ray, D. E., & Osborne, R. (1999). In Chen C. J. (Ed.), *Recent toxicity studies in animals using chemical derived from cycads*. BEIJING; 137 CHAONEI DAJIE, BEIJING 100010, PEOPLES R CHINA: WORLD PUBLISHING CORPORATION.

342. Seltzer, Z., & Dorfman, R. (2004). Identifying genetic and environmental risk factors for chronic orofacial pain syndromes: Human models. *Journal of Orofacial Pain, 18*(4), 311-317.

343. Shan, X., Vocadlo, D., & Krieger, C. (2009). Mislocalization of TDP-43 in the G93A mutant SOD1 transgenic mouse model of ALS. *Neuroscience Letters, 458*(2), 70-74. doi:10.1016/j.neulet.2009.04.031

344. Shaw, C. A., Wilson, J. M. B., Cruz-Aguado, R., Singh, S., Hawkes, E. L., Lee, V., & Marler, T. (2006). Cycad-induced neurodegeneration in a mouse model of ALS–PDC: Is the culprit really BMAA or is a novel toxin to blame. *Botanical Review,*

345. Shaw, C. E., Arechavala-Gomeza, V., & Al-Chalabi, A. (2007). Familial amyotrophic lateral sclerosis. In A. Eisen, & P. J. Shaw (Eds.), *Handbook of clinical neurology* (pp. 279-300) Elsevier.

346. Shaw, C. A., & Hoglinger, G. U. (2008). Neurodegenerative diseases: Neurotoxins as sufficient etiologic agents? *Neuromolecular Medicine, 10*(1), 1-9. doi:10.1007/s12017-007-8016-8

347. Shaw, C. A., & Wilson, J. M. B. (2003). Analysis of neurological disease in four dimensions: Insight from ALS-PDC epidemiology and animal models. *Neuroscience and Biobehavioral Reviews, 27*(6), 493-505. doi:10.1016/j.neubiorev.2003.08.001

348. Shen, W. B., McDowell, K. A., Siebert, A. A., Clark, S. M., Dugger, N. V., Valentino, K. M., Jinnah, H. A., Sztalryd, C., Fishman, P. S., Shaw, C. A., Jafri, M. S., & Yarowsky, P. J. (2010). Environmental neurotoxin-induced progressive model of parkinsonism in rats. *Annals of Neurology, 68*(1), 70-80. doi:10.1002/ana.22018

349. Shi, P., Gal, J., Kwinter, D. M., Liu, X., & Zhu, H. (2010). Mitochondrial dysfunction in amyotrophic lateral sclerosis. *Biochimica et Biophysica Acta-Molecular Basis of Disease, 1802*(1), 45-51. doi:10.1016/j.bbadis.2009.08.012

350. Shi, P., Stroem, A., Gal, J., & Zhu, H. (2010). Effects of ALS-related SOD1 mutants on dynein- and KIF5-mediated retrograde and anterograde axonal transpor. *Biochimica et Biophysica Acta-Molecular Basis of Disease, 1802*(9), 707-716. doi:10.1016/j.bbadis.2010.05.008

351. Shimazawa, M., Tanaka, H., Ito, Y., Morimoto, N., Tsuruma, K., Kadokura, M., Tamura, S., Inoue, T., Tamada, M., Takahashi, H., Warita, H., Aoki, M., & Hara H. (2010). An inducer of VGF protects cells against ER-stress induced cell death and prolongs survival in the mutant SOD1 animal models of familial ALS. *PLOS One,* 5(12), 1-15.

352. Shiotsuki, H., Yoshimi, K., Shimo, Y., Funayama, M., Takamatsu, Y., Ikeda, K., Takahashi, R., Kitazawa, S., & Hattori, N. (2010). A rotarod test for evaluation of motor skill learning. *Journal of Neuroscience Methods, 189*(2), 180-185. doi:10.1016/j.jneumeth.2010.03.026

353. Shoesmith, C. L., Findlater, K., Rowe, A., & Strong, M. J. (2007). Prognosis of amyotrophic lateral sclerosis with respiratory onset. *Journal of Neurology Neurosurgery and Psychiatry, 78*(6), 629-631. doi:10.1136/jnnp.2006.103564

354. Siddique, T., Figlewicz, D. A., Pericakvance, M. A., Haines, J. L., Rouleau, G., Jeffers, A. J., Sapp, P., Hung, W. Y., Bebout, J., Mckennayasek, D., Deng, G., Horvitz, H. R., Gusella, J. F., Brown, R. H., & Roses, A. D. (1991). Linkage of a gene causing familial amyotrophic-lateral-sclerosis to chromosome-21 and evidence of genetic-locus heterogeneity. *New England Journal of Medicine, 324*(20), 1381-1384.

355. Small, D. H. (1998). The role of the amyloid protein precursor (APP) in Alzheimer's disease: Does the normal function of APP explain the topography of neurodegeneration? *Neurochemical Research, 23*(5), 795-806.

356. Smith, D. W. (1966). Mutagenicity of cycasin aglycone (methylazoxymethanol), a naturally occurring carcinogen. *Science (New York, N.Y.), 152*(726), 1273-1274.

357. Smith, M. C. (1960). Nerve fibre degeneration in the brain in amyotrophic lateral sclerosis. *Journal of Neurology Neurosurgery and Psychiatry, 23*(4), 269-282.

358. Snyder, L. R., Cruz-Aguado, R., Sadilek, M., Galasko, D., Shaw, C. A., & Montine, T. J. (2009a). Lack of cerebral bmaa in human cerebral cortex. *Neurology, 72*(15), 1360-1361. doi:10.1212/WNL.0b013e3181a0fed1

359. Snyder, L. R., Cruz-Aguado, R., Sadilek, M., Galasko, D., Shaw, C. A., & Montine, T. J. (2009b). Parkinson-dementia complex and development of a new stable isotope dilution assay for BMAA detection in tissue. *Toxicology and Applied Pharmacology, 240*(2), 180-188. doi:10.1016/j.taap.2009.06.025

360. Sobue, G., Matsuoka, Y., Mukai, E., Takayanagi, T., & Sobue, I. (1981). Pathology of myelinated fibers in cervical and lumbar ventral spinal roots in amyotrophic lateral sclerosis. *Journal of the Neurological Sciences, 50*(3), 413-421.

361. Son, Y. J., & Thompson, W. J. (1995). Schwann-cell processes guide regeneration of peripheral axons. *Neuron, 14*(1), 125-132. doi:10.1016/0896-6273(95)90246-5

362. Spalloni, A., Origlia, N., Sgobio, C., Trabalza, A., Nutini, M., Berretta, N., Bernardi, G., Domenici, L., Ammassari-Teule, M., & Longone, P. (2011). Postsynaptic alteration of NR2A subunit and defective

autophosphorylation of alphaCaMKII at threonine-286 contribute to abnormal plasticity and morphology of upper motor neurons in presymptomatic SOD1(G93A) mice, a murine model for amyotrophic lateral sclerosis. *Cerebral Cortex, 21*(4), 796-805. doi:10.1093/cercor/bhq152

363. Spatz, M. (1969). Toxic and carcinogenic alkylating agents from cycads. *Annals of the New York Academy of Sciences, 163*(Biological Effects of Alkylating Agents), 848-859.

364. Spencer, P. S. (1987). Guam ALS parkinsonism-dementia - a long-latency neurotoxic disorder caused by slow toxin(s) in food. *Canadian Journal of Neurological Sciences, 14*(3), 347-357.

365. Spencer, P. S., Kisby, G. E., & Ludolph, A. C. (1991). Slow toxins, biologic markers, and long-latency neurodegenerative disease in the western Pacific region. *Neurology, 41*(5), 62-68.

366. Spencer, P. S., Nunn, P. B., Hugon, J., Ludolph, A. C., Ross, S. M., Roy, D. N., & Robertson, R. C. (1987). Guam amyotrophic-lateral-sclerosis parkinsonism dementia linked to a plant excitant neurotoxin. *Science, 237*(4814), 517-522.

367. Spink, A. J., Tegelenbosch, R. A. J., Buma, M. O. S., & Noldus, L. P. J. J. (2001). The EthoVision video tracking system - A tool for behavioral phenotyping of transgenic mice. *Physiology & Behavior, 73*(5), 731-744.

368. Stallings, N. R., Puttaparthi, K., Luther, C. M., Burns, D. K., & Elliott, J. L. (2010). Progressive motor weakness in transgenic mice expressing human TDP-43. *Neurobiology of Disease, 40*(2), 404-414. doi:10.1016/j.nbd.2010.06.017

369. Stanhope, J. M., Brody, J. A., & Morris, C. E. (1972). Epidemiologic features of amyotropic lateral sclerosis and parkinsonism-dementia in Guam, Mariana Islands. *International Journal of Epidemiology, 1*(3), 199-210.

370. Steele, J. C. (2005). Parkinsonism-dementia complex of Guam. *Movement Disorders : Official Journal of the Movement Disorder Society, 20 Suppl 12*, S99-S107. doi:10.1002/mds.20547

371. Steele, J. C., Olszewski, J., & Richardson, J. C. (1964). Progressive supranuclear palsy - heterogeneous degeneration involving brain stem basal ganglia + cerebellum with vertical gaze + pseudobulbar palsy nuchal dystonia + dementia. *Archives of Neurology, 10*(4), 333-&.

372. Stephens, B., Guiloff, R. J., Navarrete, R., Newman, P., Nikhar, N., & Lewis, P. (2006). Widespread loss of neuronal populations in the spinal ventral horn in sporadic motor neuron disease. A morphometric study. *Journal of the Neurological Sciences, 244*(1-2), 41-58. doi:10.1016/j.jns.2005.12.003

373. Stieber, A., Gonatas, J. O., & Gonatas, N. K. (2000). Aggregates of mutant protein appear progressively in dendrites, in periaxonal processes of oligodendrocytes, and in neuronal and astrocytic perikarya of mice expressing the SOD1(G93A) mutation of familial amyotrophic lateral sclerosis. *Journal of the Neurological Sciences, 177*(2), 114-123.

374. Strong, M., & Rosenfeld, J. (2003). Amyotrophic lateral sclerosis: A review of current concepts. *Amyotrophic Lateral Sclerosis and Other Motor Neuron Disorders, 4*(3), 136-143.

375. Strong, M. J. (2010). The evidence for altered RNA metabolism in amyotrophic lateral sclerosis (ALS). *Journal of the Neurological Sciences, 288*(1-2), 1-12. doi:10.1016/j.jns.2009.09.029

376. Strong, M. J., Volkening, K., Hammond, R., Yang, W., Strong, W., Leystra-Lantz, C., & Shoesmith, C. (2007). TDP43 is a human low molecular weight neurofilament (hNFL) mRNA-binding protein. *Molecular and Cellular Neuroscience, 35*(2), 320-327. doi:10.1016/j.mcn.2007.03.007

377. Sunico, C. R., Dominguez, G., Manuel Garcia-Verdugo, J., Osta, R., Montero, F., & Moreno-Lopez, B. (2011). Reduction in the motoneuron Inhibitory/Excitatory synaptic ratio in an early-symptomatic mouse model of amyotrophic lateral sclerosis. *Brain Pathology, 21*(1), 1-15. doi:10.1111/j.1750-3639.2010.00417.x

378. Sutedja, N. A., Veldink, J. H., Fischer, K., Kromhout, H., Heederik, D., Huisman, M. H. B., Wokke, J. H. J., & van den Berg, L. H. (2009). Exposure to chemicals and metals and risk of amyotrophic lateral sclerosis: A systematic review. *Amyotrophic Lateral Sclerosis, 10*(5-6), 302-U90. doi:10.3109/17482960802455416

379. Swarup, G., & Nagabhushana, A. (2010). Optineurin, a multifunctional protein involved in glaucoma, amyotrophic lateral sclerosis and antiviral signalling. *Journal of Biosciences, 35*(4), 501-505. doi:10.1007/s12038-010-0056-9

380. Syriani, E., Morales, M., & Gamez, J. (2009). The p.E22G mutation in the Cu/Zn superoxide-dismutase gene predicts a long survival time. *Journal of the Neurological Sciences, 285*(1-2), 46-53. doi:10.1016/j.jns.2009.05.011

381. Tabata, R. C., Wilson, J. M. B., Ly, P., Zwiegers, P., Kwok, D., Van Kampen, J. M., Cashman, N., & Shaw, C. A. (2008). Chronic exposure to dietary sterol glucosides is neurotoxic to motor neurons and induces an ALS-PDC phenotype. *Neuromolecular Medicine, 10*(1), 24-39. doi:10.1007/s12017-007-8020-z

382. Tam, S., Archibald, V., Jassar, B., Tyreman, N., & Gordon, T. (2001). Increased neuromuscular activity reduces sprouting in partially denervated muscles. *Journal of Neuroscience, 21*(2), 654-667.

383. Tamaoka, A., Odaka, A., Ishibashi, Y., Usami, M., Sahara, N., Suzuki, N., Nukina, N., Mizusawa, H., Shoji, S., Kanazawa, I., & Mori, H. (1994). App717 missense mutation affects the ratio of amyloid-beta protein species (A-beta-1-42/43 and A-beta-1-40) in familial Alzheimers-disease brain. *Journal of Biological Chemistry, 269*(52), 32721-32724.

384. Tan, C., Eguchi, H., Tagawa, A., Onodera, O., Iwasaki, T., Tsujino, A., Nishizawa, M., Kakita, A., & Takahashi, H. (2007). TDP-43 immunoreactivity in neuronal inclusions in familial amyotrophic lateral sclerosis with or without SOD1 gene mutation. *Acta Neuropathologica, 113*(5), 535-542. doi:10.1007/s00401-007-0206-9

385. Tanaka, J., Nakamura, H., Tabuchi, Y., & Takahashi, K. (1984). Familial amyotrophic lateral sclerosis - features of multisystem degeneration. *Acta Neuropathologica, 64*(1), 22-29.

386. Testa, D., Lovati, R., Ferrarini, M., Salmoiraghi, F., & Filippini, G. (2004). Survival of 793 patients with amyotrophic lateral sclerosis diagnosed over a 28-year period. *Amyotrophic Lateral Sclerosis and Other Motor Neuron Disorders, 5*(4), 208-212. doi:10.1080/14660820410021311

387. Thomas, P. K., King, R. H. M., & Sharma, A. K. (1981). Age-changes in the peripheral-nerves of the rat. *Gerontology, 27*(1-2), 116-117.

388. Toft, M. H., Gredal, O., & Pakkenberg, B. (2005). The size distribution of neurons in the motor cortex in amyotrophic lateral sclerosis. *Journal of Anatomy, 207*(4), 399-407.

389. Tomik, B., Adamek, D., Pierzchalski, P., Banares, S., Duda, A., Partyka, D., Pawlik, W., Kaluza, J., Krajewski, S., & Szczudlik, A. (2005). Does apoptosis occur in amyotrophic lateral sclerosis? TUNEL experience from human amyotrophic lateral sclerosis (ALS) tissues. *Folia Neuropathologica, 43*(2), 75-80.

390. Troost, D., Smitt, P. A. E. S., Dejong, J. M. B. V., & Swaab, D. F. (1992). Neurofilament and glial alterations in the cerebral-cortex in amyotrophic-lateral-sclerosis. *Acta Neuropathologica, 84*(6), 664-673.

391. Tsnchiya, K., Takahashi, M., Shiotsu, H., Akiyama, H., Haga, C., Watabiki, S., Taki, K., Nakan, I., & Ikeda, K. (2002). Sporadic amyotrophic lateral sclerosis with circumscribed temporal atrophy: A report of an autopsy case without dementia and with ubiquitinated intraneuronal inclusions. *Neuropathology, 22*(4), 308-316.

392. Tsuchiya, K., Arai, M., Matsuya, S., Nishimura, H., Ishiko, T., Kondo, H., Ikeda, K., & Matsushita, M. (1999). Sporadic amyotrophic lateral sclerosis resembling primary lateral sclerosis: Report of an autopsy case and a review of the literature. *Neuropathology, 19*(1), 71-76.

393. Tsuchiya, K., Shintani, S., Nakabayashi, H., Kikugawa, K., Nakano, R., Haga, C., Nakano, I., Ikeda, K., & Tsuji, S. (2000). Familial amyotrophic lateral sclerosis with onset in bulbar sign, benign clinical course, and bunina bodies: A clinical, genetic, and pathological study of a japanese family. *Acta Neuropathologica, 100*(6), 603-607.

394. Tu, P. H., Raju, P., Robinson, K. A., Gurney, M. E., Trojanowski, J. Q., & Lee, V. M. Y. (1996). Transgenic mice carrying a human mutant superoxide dismutase transgene develop neuronal cytoskeletal pathology resembling human amyotrophic lateral sclerosis lesions. *Proceedings of the National Academy of Sciences of the United States of America, 93*(7), 3155-3160.

395. Turner, B. J., Baumer, D., Parkinson, N. J., Scaber, J., Ansorge, O., & Talbot, K. (2008). TDP-43 expression in mouse models of amyotrophic lateral sclerosis and spinal muscular atrophy. *Bmc Neuroscience, 9*, 104. doi:10.1186/1471-2202-9-104

396. Turner, M. R., Cagnin, A., Turkheimer, F. E., Miller, C. C. J., & Shaw, C. E. (2004). Evidence of widespread cerebral microglial activation in amyotrophic lateral sclerosis: An [C-11](R)-PK11195

positron emission tomography study. *Neurobiology of Disease, 15*(3), 601-609. doi:10.1016/j.ndb.2003.12.012

397. Uchikado, H., DelleDonne, A., Ahmed, Z., & Dickson, D. W. (2006). Lewy bodies in progressive supranuclear palsy represent an independent disease process. *Journal of Neuropathology and Experimental Neurology, 65*(4), 387-395.

398. Urushitani, M., Kurisu, J., Tsukita, K., & Takahashi, R. (2002). Proteasomal inhibition by misfolded mutant superoxide dismutase 1 induces selective motor neuron death in familial amyotrophic lateral sclerosis. *Journal of Neurochemistry, 83*(5), 1030-1042.

399. Urushitani, M., Abou Ezzi, S., & Julien, J. (2007). Therapeutic effects of immunization with mutant superoxide dismutase in mice models of amyotrophic lateral sclerosis. *Proceedings of the National Academy of Sciences of the United States of America, 104*(7), 2495-2500. doi:10.1073/pnas.0606201104

400. Valenti, M., Pontieri, F. E., Conti, F., Altobelli, E., Manzoni, T., & Frati, L. (2005). Amyotrophic lateral sclerosis and sports: A case-control study. *European Journal of Neurology, 12*(3), 223-225.

401. Van Damme, P., Bogaert, E., Dewil, M., Hersmus, N., Kiraly, D., Scheveneels, W., Bockx, I., Braeken, D., Verpoorten, N., Verhoeven, K., Timmerman, V., Herijgers, P., Callewaert, G., Carmeliet, P., Van den Bosch, L., & Robberecht, W. (2007). Astrocytes regulate GluR2 expression in motor neurons and their vulnerability to excitotoxicity. *Proceedings of the National Academy of Sciences of the United States of America, 104*(37), 14825-14830. doi:10.1073/pnas.0705046104

402. Van Deerlin, V. M., Leverenz, J. B., Bekris, L. M., Bird, T. D., Yuan, W., Elman, L. B., Clay, D., Wood, E. M., Chen-Plotkin, A. S., Martinez-Lage, M., Steinbart, E., McCluskey, L., Grossman, M., Neumann, M., Wu, I., Yang, W., Kalb, R., Galasko, D. R., Montine, T. J., Trojanowski, J. Q., Lee, V. M., Schellenberg, G. D., & Yu, C. (2008). TARDBP mutations in amyotrophic lateral sclerosis with TDP-43 neuropathology: A genetic and histopathological analysis. *Lancet Neurology, 7*(5), 409-416. doi:10.1016/S1474-4422(08)70071-1

403. van Dellen, A., Grote, H. E., & Hannan, A. J. (2005). Gene-environment interactions, neuronal dysfunction and pathological plasticity in Huntington's disease. *Clinical and Experimental Pharmacology and Physiology, 32*(12), 1007-1019.

404. van der Graaff, M. M., de Jong, J. M. B. V., Baas, F., & de Visser, M. (2009). Upper motor neuron and extra-motor neuron involvement in amyotrophic lateral sclerosis: A clinical and brain imaging review. *Neuromuscular Disorders, 19*(1), 53-58. doi:10.1016/j.nmd.2008.10.002

405. van Es, M. A., Dahlberg, C., Birve, A., Veldink, J. H., van den Berg, L. H., & Andersen, P. M. (2010). Large-scale SOD1 mutation screening provides evidence for genetic heterogeneity in amyotrophic lateral sclerosis. *Journal of Neurology Neurosurgery and Psychiatry, 81*(5), 562-566. doi:10.1136/jnnp.2009.181453

406. Vance, C., Rogelj, B., Hortobagyi, T., De Vos, K. J., Nishimura, A. L., Sreedharan, J., Hu, X., Smith, B., Ruddy, D., Wright, P., Ganesalingam, J., Williams, K. L., Tripathi, V., Al-Saraj, S., Al-Chalabi, A., Leigh,

P. N., Blair, I. P., Nicholson, G., de Belleroche, J., Gallo, J. -., Miller, C. C., & Shaw, C. E. (2009). Mutations in FUS, an RNA processing protein, cause familial amyotrophic lateral sclerosis type 6. *Science, 323*(5918), 1208-1211. doi:10.1126/science.1165942

407. Vance, J. M., Ali, S., Bradley, W. G., Singer, C., & Di Monte, D. A. (2010). Gene-environment interactions in Parkinson's disease and other forms of Parkinsonism. *Neurotoxicology, 31*(5), 598-602. doi:10.1016/j.neuro.2010.04.007

408. Vega, A., & Bell, E. A. (1967). Alpha-amino-beta-methylaminopropionic acid a new amino acid from seeds of cycas circinalis. *Phytochemistry, 6*(5), 759-&.

409. Veldink, J., Bar, P., Joosten, E., Otten, M., Wokke, J., & van den Berg, L. (2003). Sexual differences in onset of disease and response to exercise in a transgenic model of ALS. *Neuromuscular Disorders, 13*(9), 737-743. doi:10.1016/S0960-8966(03)00104-4

410. Verstraete, E., van den Heuvel, M. P., Veldink, J. H., Blanken, N., Mandl, R. C., Pol, H. E. H., & van den Berg, L. H. (2010). Motor network degeneration in amyotrophic lateral sclerosis: A structural and functional connectivity study. *Plos One, 5*(10), e13664. doi:10.1371/journal.pone.0013664

411. Voikar, V., Polus, A., Vasar, E., & Rauvala, H. (2005). Long-term individual housing in C57BL/6J and DBA/2 mice: Assessment of behavioral consequences RID A-2015-2008. *Genes Brain and Behavior, 4*(4), 240-252. doi:349736300,12,1

412. Vucic, S., Cheah, B. C., & Kiernan, M. C. (2009). Defining the mechanisms that underlie cortical hyperexcitability in amyotrophic lateral sclerosis. *Experimental Neurology, 220*(1), 177-182. doi:10.1016/j.expneurol.2009.08.017

413. Vucic, S., & Kiernan, M. C. (2006). Novel threshold tracking techniques suggest that cortical hyperexcitability is an early feature of motor neuron disease. *Brain, 129*, 2436-2446. doi:10.1093/brain/awl172

414. Vucic, S., Nicholson, G. A., & Kiernan, M. C. (2008). Cortical hyperexcitability may precede the onset of familial amyotrophic lateral sclerosis. *Brain, 131*, 1540-1550. doi:10.1093/brain/awn071

415. Wada, M., Uchihara, T., Nakamura, A., & Oyanagi, K. (1999). Bunina bodies in amyotrophic lateral sclerosis on Guam: A histochemical, immunohistochemical and ultrastructural investigation. *Acta Neuropathologica, 98*(2), 150-156.

416. Wang, H. Y., Wang, I. F., Bose, J., & Shen, C. K. J. (2004). Structural diversity and functional implications of the eukaryotic TDP gene family. *Genomics, 83*(1), 130-139. doi:10.1016/S0888-7543(03)00214-3

417. Wang, L., Sharma, K., Grisotti, G., & Roos, R. P. (2009). The effect of mutant SOD1 dismutase activity on non-cell autonomous degeneration in familial amyotrophic lateral sclerosis. *Neurobiology of Disease, 35*(2), 234-240. doi:10.1016/j.nbd.2009.05.002

418. Wang, X. B., Chen, D. F., Niu, T. H., Wang, Z. X., Wang, L. H., Ryan, L., Smith, T., Christiani, D. C., Zuckerman, B., & Xu, X. P. (2000). Genetic susceptibility to benzene and shortened gestation: Evidence of gene-environment interaction. *American Journal of Epidemiology, 152*(8), 693-700.

419. Watanabe, M., Dykes-Hoberg, M., Culotta, V. C., Price, D. L., Wong, P. C., & Rothstein, J. D. (2001). Histological evidence of protein aggregation in mutant SOD1 transgenic mice and in amyotrophic lateral sclerosis neural tissues. *Neurobiology of Disease, 8*(6), 933-941. doi:10.1006/nbdi.2001.0443

420. Weiss, J. H., Koh, J. Y., & Choi, D. W. (1989). Neurotoxicity of beta-N-methylamino-L-alanine (BMAA) and beta-N-oxalylamino-L-alanine (BOAA) on cultured cortical neurons. *Brain Research, 497*(1), 64-71.

421. Weisskopf, M. G., O'Reilly, E., McCullough, M. L., Calle, E. E., Thun, M. J., Cudkowicz, M., & Ascherio, A. (2004). Prospective study of military service and risk of amyotrophic lateral sclerosis. *Neurology, 62*(7), A267-A268.

422. Weisskopf, M. G., O'Reilly, E. J., McCullough, M. L., Calle, E. E., Thun, M. J., Cudkowicz, M., & Ascherio, A. (2005). Prospective study of military service and mortality from ALS. *Neurology, 64*(1), 32-37.

423. Weydt, P., Hong, S., Kliot, M., & Moller, T. (2003). Assessing disease onset and progression in the SODI mouse model of ALS. *Neuroreport, 14*(7), 1051-1054. doi:10.1097/00001756-200305230-00029

424. Whiting, M. G. (1963). Toxicity of cycads. *Economic Botany, 17*(4), 270-302.

425. Williams, D. R., & Lees, A. J. (2009). Progressive supranuclear palsy: Clinicopathological concepts and diagnostic challenges. *Lancet Neurology, 8*(3), 270-279.

426. Williamson, T. L., Bruijn, L. I., Zhu, Q. Z., Anderson, K. L., Anderson, S. D., Julien, J. P., & Cleveland, D. W. (1998). Absence of neurofilaments reduces the selective vulnerability of motor neurons and slows disease caused by a familial amyotrophic lateral sclerosis-linked superoxide dismutase 1 mutant. *Proceedings of the National Academy of Sciences of the United States of America, 95*(16), 9631-9636.

427. Wilson, J. M., Khabazian, I., Wong, M. C., Seyedalikhani, A., Bains, J. S., Pasqualotto, B. A., Williams, D. E., Andersen, R. J., Simpson, R. J., Smith, R., Craig, U. K., Kurland, L. T., & Shaw, C. A. (2002). Behavioral and neurological correlates of ALS-parkinsonism dementia complex in adult mice fed washed cycad flour. *Neuromolecular Medicine, 1*(3), 207-221. doi:10.1385/NMM:1:3:207

428. Wilson, J. M., & Shaw, C. A. (2006a). Evidence for an excitotoxicity in murine model of ALS-PDC. *Journal of Neurochemistry, 96*, 87-87.

429. Wilson, J. M. B., Khabazian, I., Pow, D. V., Craig, U. K., & Shaw, C. A. (2003). Decrease in glial glutamate transporter variants and excitatory amino acid receptor down-regulation in a murine model of ALS-PDC. *Neuromolecular Medicine, 3*(2), 105-117.

430. Wilson, J. M. B., Petrik, M. S., Grant, S. C., Blackband, S. J., Lai, J., & Shaw, C. A. (2004). Quantitative measurement of neurodegeneration in an ALS-PDC model using MR microscopy. *NeuroImage, 23*(1), 336-343. doi:10.1016/j.neuroimage.2004.05.026

431. Wilson, J. M. B., Petrik, M. S., Moghadasian, M. H., & Shaw, C. A. (2005). Examining the interaction of apo E and neurotoxicity on a murine model of ALS-PDC. *Canadian Journal of Physiology and Pharmacology, 83*(2), 131-141. doi:10.1139/Y04-140

432. Wilson, J. M. B., & Shaw, C. A. (2007). Late appearance of glutamate transporter defects in a murine model of ALS-parkinsonism dementia complex. *Neurochemistry International, 50*(7-8), 1067-1077. doi:10.1016/j.neuint.2006.09.017

433. Wong, M., & Martin, L. J. (2010). Skeletal muscle-restricted expression of human SOD1 causes motor neuron degeneration in transgenic mice. *Human Molecular Genetics, 19*(11), 2284-2302. doi:10.1093/hmg/ddq106

434. Wong, P. C., Cai, H. B., Borchelt, D. R., & Price, D. L. (2002). Genetically engineered mouse models of neurodegenerative diseases. *Nature Neuroscience, 5*(7), 633-639.

435. Wong, P. C., Pardo, C. A., Borchelt, D. R., Lee, M. K., Copeland, N. G., Jenkins, N. A., Sisodia, S. S., Cleveland, D. W., & Price, D. L. (1995). An adverse property of a familial ALS-linked Sod1 mutation causes motor-neuron disease characterized by vacuolar degeneration of mitochondria. *Neuron, 14*(6), 1105-1116.

436. Wooley, C. M., Sher, R. B., Kale, A., Frankel, W. N., Cox, G. A., & Seburn, K. L. (2005). Gait analysis detects early changes in transgenic SOD1 (G93A) mice. *Muscle & Nerve, 32*(1), 43-50.

437. Wootz, H., Hansson, I., Korhonen, L., Napankangas, U., & Lindholm, D. (2004). Caspase-12 cleavage and increased oxidative stress during motoneuron degeneration in transgenic mouse model of ALS. *Biochem and Biophys Research Communications,* 322, 281-286.

438. Yamanaka, K., Boillee, S., Kollias, G., & Cleveland, D. W. (2006). Selective gene ablation of mutant SOD1 in microglia significantly slows disease progression of ALS. *Neurology, 66*(5), A197-A198.

439. Yamanaka, K., Chun, S. J., Boillee, S., Fujimori-Tonou, N., Yamashita, H., Gutmann, D. H., Takahashi, R., Misawa, H., & Cleveland, D. W. (2008). Astrocytes as determinants of disease progression in inherited amyotrophic lateral sclerosis. *Nature Neuroscience, 11*(3), 251-253. doi:10.1038/nn2047

440. Yamazaki, M., Esumi, E., & Nakano, I. (2005). Is motoneuronal cell death in amyotrophic lateral sclerosis apoptosis? *Neuropathology, 25*(4), 381-387.

441. Yamazaki, M., Hasegawa, M., Mori, O., Murayama, S., Tsuchiya, K., Ikeda, K., Chen, K. M., Katayama, Y., & Oyanagi, K. (2005). Tau-positive fine granules in the cerebral white matter: A novel finding among the tauopathies exclusive to parkinsonism-dementia complex of Guam. *Journal of Neuropathology and Experimental Neurology, 64*(10), 839-846.

442. Yang, C. D., Yu, L. Q., Li, W. P., Xu, F., Cohen, J. C., & Hobbs, H. H. (2004). Disruption of cholesterol homeostasis by plant sterols. *Journal of Clinical Investigation, 114*(6), 813-822. doi:10.1172/JCI200422186

443. Yang, T. X., Huang, Y. G., Ye, W. L., Hansen, P., Schnermann, J. B., & Briggs, J. P. (2005). Influence of genetic background and gender on hypertension and renal failure in COX-2-deficient mice. *American Journal of Physiology-Renal Physiology, 288*(6), F1125-F1132. doi:10.1152/ajprenal.00219.2004

444. Yim, M. B., Chock, P. B., & Stadtman, E. R. (1993). Enzyme function of copper, zinc superoxide-dismutase as a free-radical generator. *Journal of Biological Chemistry, 268*(6), 4099-4105.

445. Yim, M. B., Kang, J. H., Yim, H. S., Kwak, H. S., Chock, P. B., & Stadtman, E. R. (1996). A gain-of-function of an amyotrophic lateral sclerosis-associated Cu,Zn-superoxide dismutase mutant: An enhancement of free radical formation due to a decrease in K-m for hydrogen peroxide. *Proceedings of the National Academy of Sciences of the United States of America, 93*(12), 5709-5714.

446. Zanette, G., Tamburin, S., Manganotti, P., Refatti, N., Forgione, A., & Rizzuto, N. (2002). Changes in motor cortex inhibition over time in patients with amyotrophic lateral sclerosis. *Journal of Neurology, 249*(12), 1723-1728. doi:10.1007/s00415-002-0926-7

447. Zhang, H., Tan, C., Mori, F., Tanji, K., Kakita, A., Takahashi, H., & Wakabayashi, K. (2008a). TDP-43-immunoreactive neuronal and glial inclusions in the neostriatum in amyotrophic lateral sclerosis with and without dementia. *Acta Neuropathologica, 115*(1), 115-122. doi:10.1007/s00401-007-0285-7

448. Zhang, J., Zhang, G., Morrison, B., Mori, S., & Sheikh, K. A. (2008b). Magnetic resonance imaging of mouse skeletal muscle to measure denervation atrophy. *Experimental Neurology, 212*(2), 448-457. doi:10.1016/j.expneurol.2008.04.033

449. Zhang, Z. X., Anderson, D. W., Lavine, L., & Mantel, N. (1990). Patterns of acquiring parkinsonism-dementia complex on Guam. 1944 through 1985. *Archives of Neurology, 47*(9), 1019-1024.

450. Ziemann, U., Winter, M., Reimers, C. D., Reimers, K., Tergau, F., & Paulus, W. (1997). Impaired motor cortex inhibition in patients with amyotrophic lateral sclerosis - evidence from paired transcranial magnetic stimulation. *Neurology, 49*(5), 1292-1298.

451. Zoccolella, S., Beghi, E., Palagano, G., Fraddosio, A., Guerra, V., Samarelli, V., Lepore, V., Simone, I. L., Lamberti, P., Serlenga, L., Logroscino, G., & SLAP Registry. (2007). Riluzole and amyotrophic lateral sclerosis survival: A population-based study in southern Italy. *European Journal of Neurology, 14*(3), 262-268. doi:10.1111/j.1468-1331.2006.01575.x

452. Zoccolella, S., Beghi, E., Palagano, G., Fraddosio, A., Samarelli, V., Lamberti, P., Lepore, V., Serlenga, L., Logroscino, G., & SLAP Registry. (2006). Signs and symptoms at diagnosis of amyotrophic lateral sclerosis: A population-based study in southern Italy. *European Journal of Neurology, 13*(7), 789-792. doi:10.1111/j.1468-1331.2006.01384.x

453. Zuniga Ramirez, C., Matsubara, J. M., Nosnik, J. L., Diaz, S. P., Raina, G. B., & Micheli, F. (2006). Amyotrophic lateral sclerosis due to HIV infection. *Revista Ecuatoriana De Neurologia, 15*(1), 47-50.

Appendix A : A brief history of Guam

Guam was first inhabited by sea-faring people believed to have been of Indo-Malaya descent migrating from Southeast Asia (Rogers, 1995). These ancient Chamorros lived isolated and independent from other countries until its first contact with Western Europe by a crew of explorers led by Ferdinand Magellan who discovered the island serendipitously during a failed circumnavigation of the globe (de Viana, 2004). They landed on the Northwest coast of Guam and were greeted by ambitious people with a culture and values very different from their own. Unfortunately, the differences were too great and resulted in hostility that became a pattern in later Spanish-Chamorro relations as Spanish ships continued to visit Guam for rations year after year (Rogers, 1995).

Guam was officially claimed by Spain in 1565 in the name of Philip II when Miguel Lopez de Legazpi landed on Utamac Bay (Rogers, 1995; de Viana, 2004). Then called the Isles of Thieves the island served only as a stopover for galleons from Mexico coming to the Philippines (de Viana, 2004) to replenish their fresh water and food supplies (Hezel, 1982). However, its long history of Spanish colonization began in 1668, six years after Father Diego Luis de San Vitores arrived at the shores of Guam. San Vitores quickly developed an obsession while on a quest to establish a mission among the Chamorros (de Viana, 2004). His request was finally granted by issue of royal edicts with support from Queen Regent Mariana of Austria, widow to Philip IV (Hezel, 1982). In gratitude for the Queen's help, San Vitores requested that the islands be renamed Marianas in her honour (de Viana, 2004). The arrival of San Vitores was initially met by enthusiasm and acceptance of the new faith. As a result, the Spanish transformed the Chamorro way of life by introducing Western language, religion, culture, and clothing, and introducing European farming techniques. Hostilities soon arose against a resurgence of traditional Chamorro beliefs resulting in the subsequent Spanish-Chamorro Wars from 1669 to 1671 (Brody et al., 1975; Rogers, 1995). Chamorro resistance to the mission and brutal attacks on the missionaries caused the early missionaries to change their original pacifist stance to more stern approaches involving an authority system to inspire fear and restraint (Hezel, 1982). Chamorro outbreaks of violence continued, and in 1672 San Vitores was murdered in Tumon for baptising the newborn baby of Chief Mata'pang without his consent (de Viana, 2004; Hezel, 1982). Vitores's martyrdom led to Spanish retaliation and by the remainder of 1678 into 1679 Spanish soldiers swept through the remaining hostile areas of Guam, taking control of the Chamorros. Some historians reported that the Spanish sanctioned troops to break down walls of

resistance and destroy property as a deterrent for future violence. It was believed that the progression in Spanish rule from protection of the missionaries to conquest of the Chamorros resulted out of necessity only to achieve Christianization of the natives, which was the original goal of the Spanish government (Hezel, 1982). By 1680, many Chamorros gave up in embittered resignation and saw their once courageous leaders executed. Guam was divided into districts around structured Christian communities where Chamorros were forced to settle and start a new way of life (Rogers, 1995). In the years that followed, groups of rebel Chamorros launched unexpected attacks on the Spaniards and their new Spanish governor. Firearms gave the Spaniards a powerful advantage, ironically in addition to the aid of loyal Christian Chamorros. By early 1685, all organized Chamorro resistance on Guam ended and the Chamorro population was threatened again by the introduction of new European diseases (Rogers, 1995; Stanhope et al., 1972).

The loss of Chamorros by 1690 was best described as a near decimation of the Chamorro race. Obviously, warfare was one cause of the population decline, but other causes include deprivation, diseases, infertility and epidemics. The remaining Chamorros were rounded up into certain villages of Guam where they were monitored by the military, forced to attend church daily, were separated into upper and lower classes, and adopted Spanish language and customs (Rogers, 1995). The early 1700s marked a near extinction of the old generation of Chamorros from the time of San Vitores as the remaining population were threatened by epidemics of diphtheria and typhus. In 1710, an official Spanish census reported that only 3539 pure-blooded Chamorros ("Natural Indians") remained on the island of Guam (Brody et al., 1975; Hezel, 1982). The Spaniards imported Filipinos to repopulate Guam, and in 1727 the consensus reported over 400 families of Spanish and Filipinos, most of whom had wives and children of mixed ethnicity (Stanhope et al., 1972). The years between 1780 and 1816 were a demographic transition period for Guam, when Spanish consensuses showed pure-blooded Chamorros equal in numbers with non Chamorros and a growing population of hybrid neo-Chamorros was emerging (Rogers, 1995). Population declines continued and labor shortages necessitated introduction of Filipino workers, most of who remained on Guam and married Chamorrow women (Brody et al., 1975). Chamarro-Filipino intermarriages were extensive and served to save the Marianas from being completely depopulated.

The last century of Guam's long history under Spanish rule proved to be uncertain and plagued with suffering. During the 1800s, Guam was penetrated by non-Spanish traders, and the

primitive people of Guam repeatedly suffered upon contact with new civilization (Rogers, 1995). The administration of Guam was insecure as Guam witnessed 26 reassignments of governors during Spanish rule, each naively optimistic at first and worn-out as their efforts failed at improving the situation in Guam. It suffered from violent natural disasters including typhoons and earthquakes and tidal waves that caused widespread death and destruction. The island's rich vegetation attracted trade from outside Europe and introduction of uncontrollable epidemics of venereal diseases, leprosy, and influenza. Finally, the massive smallpox epidemic of 1856 decimated 60% of the entire population of Guam, bringing about political and social reforms on Guam (Rogers, 1995).

The island was handed over to the United States Government in 1898 during the Spanish-American War. Guam began a new era of political and cultural transformation and faced new disease epidemics (Rogers, 1995). In addition, Guam was being transformed eagerly by the Americans into a naval base. American's brought a new style of colonialism separating church and state, and rules concerning Guam's education system and health sector were administered by an ever changing U.S. naval governor. Positive developments occurred during this time for the first time on Guam. Health conditions began to improve with the introduction of water treatment, garbage collection, ice plants for meat storage, and the first American hospital with naval doctors providing free outpatient and surgical treatment (Hattori, 2006). Chamorro quality of life improved with the development of infrastructure, cable communications, media communications, American entertainment, new styles of homes and farming techniques. In the years following World War I, Guam's population was flourishing again, but it consisted of military personnel, their families, and non-native people in addition to the Chamorro natives. Chamorros were finally granted Guam citizenship, a bill of rights to protect them from arbitrary decrees, and the Guam Congress. In addition, the end of World War I left Guam the only island of the Micronesia not under Japanese control (Rogers, 1995). The threat of war on Guam was imminent.

In 1941, Japan invaded Guam's shores and occupied the island after World War II. American naval defences were largely insufficient, which left Guam defenceless. American survivors were taken as prisoners of war to Japan while Chamorros struggled under harsh Japanese administration, suffering many war atrocities (Rogers, 1995). The United States regained possession of Guam in 1944 during the Battle of Guam in an invasion of shattering death and destruction that surpassed the Japanese invasion. Due to its strategic position, Guam was used as a command post

for the U.S. military, and a naval government was established. In 1949, the Organic Act was finally legalized, making Guam an unincorporated territory of the United States with a civilian government instead of a naval government, and granting U.S. citizenship to the Chamorros (Rogers, 1995). The island's economy flourished following American funding to rebuild the land that was destroyed by war to first world economic standards.

A civilian hospital was opened in 1950 and christened the Guam Memorial Hospital, replacing the old Naval Hospital (Rogers, 1995). Physicians and nurses were recruited from the Philippines and accorded American credentials. Many of these Filipino professionals remained on Guam to form the main body of the island's private medical community. Research started on the local Guamanian paralyticdisease since naval medical professionals found a high incidence of deaths among the Chamorros before the war. The Chamorros recognized this illness and called it *lytico* with influence by the Spaniards. This time, with the aid of more stringent medical diagnosis, the Americans thought the disease to be ALS, which was fairly rare in the United States (Koerner, 1952). In 1956, a research office funded by the federal government opened in Guam Medical Hospital under Leonard T. Kurland and Donald Mulder, doctors from the Mayo Clinic, to study the phenomenally high frequency of ALS unique to Guam (Rogers, 1995). The National Institute of Neurological Disorders and Stroke (NINDS) Research Centre on Guam was later established in 1956, introducing more intense case findings and stringent diagnosing criteria (Plato et al., 2003). Research on the disease in Guam has continued ever since, most notably by on-island neurologists K-M Cheng and John Steele (Steele, 2005).

Appendix B : Plant steryls

Steryls are an important class of organic molecule naturally occurring in plants and animals that possess the signature structure of 4 hydrocarbon rings coupled to a hydroxyl group on one end. Cholesterol is the most familiar type of animal sterol and differs from plant sterols by the structure of the hydrocarbon tail extending from the opposite end of the hydroxyl group. Sterols from plants are called phytosterols, where the most familiar ones are campesterol, sitosterol, and stigmasterol. Perhaps the feature that is most relevant to the search for an appropriate cycad toxin is the fact that sterols are amphipathic lipids – molecules that are mostly hydrophobic but contain a hydrophilic region composed of the hydroxyl group. This accounts for a less likelihood of sterols to be eliminated from cycad following washing procedures compared to their hydrophilic amino acid derivative counterparts.

Steryl glucosides are the most common plant sterols, where the steryl (structurally referred to as the glycoside) is linked to D-glucose with a β-glycosidic linkage to the hydroxyl group. Little is known of the functions of steryl glycosides.It was suggested that certain steryl glucosides such as sitosterol-β-D-glucoside in the plasma membrane participate in cellulose synthesis in plants(Peng et al., 2002). Steryl glycosides also appear to be essential for the pathogenicity of bacteria, the cellular functions of fungi, and seed development in plants (Grille et al., 2010). Since plant sterols are amphipathic like cholesterol, they are important constituents in the plasma membrane and the membranes of mitochondria and endoplasmic reticulum. Certain sterols regulate the fluidity and permeability of the phospholipid bilayers of plant membranes in a manner similar to cholesterol in mammalian cells, while others act as plant growth hormones (Schaller, 2003). Marler et al. (2005a; 2005b) propose that steryl glucosides serve as glucose donors across membranes for cycad seed tissue development based on their observation that these sterols decline with seed age, implying metabolism of early storage pools of glucose. Steryl glucosides were found to be abundant in the outer sarcotesta tissue of cycad seeds and proposed to regulate membrane properties for surviving Guam's seasonal weather patterns.

Different plants may make many different sterols in amounts and proportions depending on the species.Generally, plants typically make sterols in the approximate range of 70% sitosterol, 20% stigmasterol, and 5% campesterol (Piironen et al., 2000). And while steryl glucosides are common to most plants, they are expressed at comparatively higher levels in cycad seeds (Shaw et al., 2006). It

has been suggested that dietary supplementation with plantsterols serves as a cholesterol reduces agent with the potential for reducing risk of coronary heart disease (Ostlund, 2007). However, there is evidence that while plant sterols can substitute for cholesterol in maintaining membrane function in mammalian cells, they can exert harmful effects by disrupting cholesterol homeostasis (Yang et al., 2004). In addition, increased levels of plasm phytosterols from the diet (since phytosterols are not synthesized endogenously) serve as markers for phytosterolemia, an inherited lipid storage disease in which patients have a very low rate of cholesterol synthesis (Salen et al., 1989). Although these phytosterols do account for a large portion of human dietary intake especially in a vegetarian diet, bodily accumulation of sterols other than cholesterol is actively prevented by intestinal epithelium and is also excreted from the liver into the bile. It is currently not understood why phytosterols are so steadily excluded from the body. The actual absorption of dietary plant sterols in humans is low (0.02-3.5%) compared to cholesterol (35-70% (de Jong et al., 2003)) and hence account for the normally low levels of plant sterols in the blood and tissues of normal mammals. However, subsistence on cycad seeds as in the case of the Chamorros may have resulted in a much higher level of steryl glucoside consumption leading to accumulation in tissues and blood plasma (Marler, 2005a; 2005b). The low levels of plant sterols in mammals make it difficult to assess their biological effects, and as a result there is no detailed evidence to date as to the effect of sterols in the central nervous system, let alone its possible mechanism(s) of entry. It has been suggested that *apo E* facilitates entry of these sterols into the CNS, since the sterols were observed to be sequestered in plasma of mice deficient in *apo E* instead of uptake into tissues (Wilson et al., 2005). Investigations into plant sterols are focused solely on their direct peripheral effects, most notably their influences on cholesterol metabolism and how they may supplement a prophylactic diet in the prevention of chronic diseases such as cardiovascular disease, diabetes, and cancer. Meanwhile, research into the role of steryl glucosides – ideally in conjunction to the possibility of genetic susceptibility factors – in the context of neurodegenerative disease etiology is severely lacking. Hence it is difficult and misleading to quote data from studies of metabolic or cardiovascular disease and relate it to neurodegenerative disease research since the biological action of plant sterols in CNS tissue is unknown.

Figure B-1. Chemical structure of isolated cycad toxins and cholesterol.

(A) β-sitosterol β-D-glucoside (BSSG). This was found to be the largest fraction of sterol glucosides in cycad

(B) Stigmasterol β-D-glucoside (SG). The only structural difference from BSSG is the presence of a double bond on the hydrocarbon tail.

(C) Campesterol β-D-glucoside. This structure also differs from BSSG by its hydrocarbon tail.

(D) Cholesterol. The cycad sterols can be described as derivatives of cholesterol.

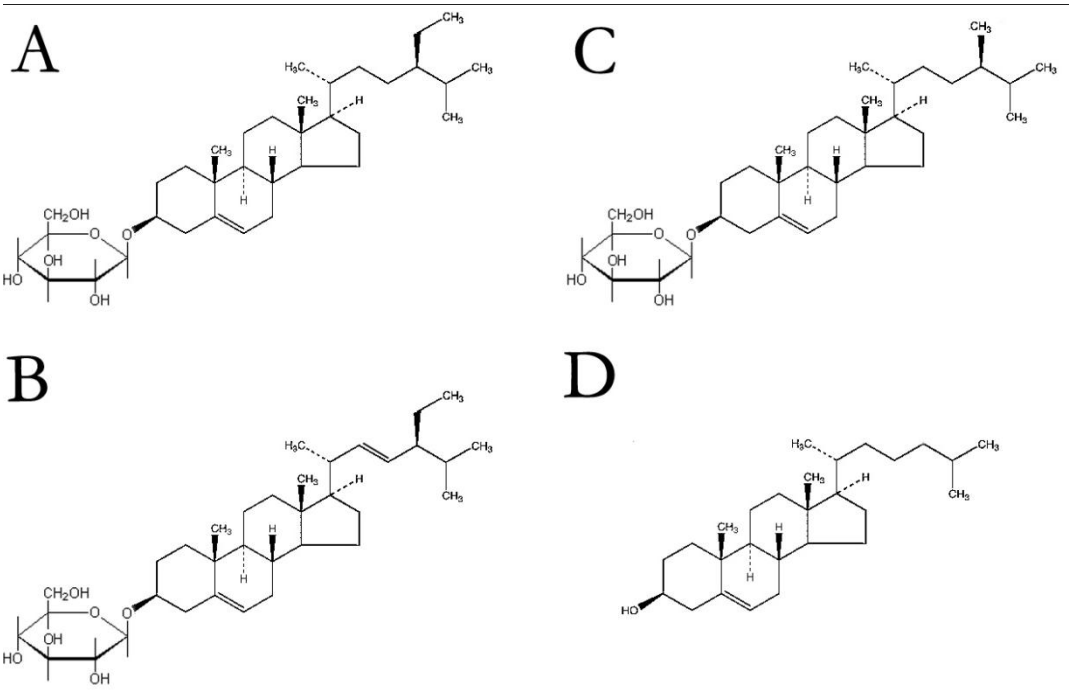

Appendix C : Comparative study in SOD1G93A mice

ALS is a progressive adult-onset neurodegenerative disorder characterized by motor neuron loss in the motor cortex, brainstem, and spinal cord. The discovery of missense mutations in the gene encoding SOD1 in subsets of familial ALS cases directed most ALS research to discovering the mechanism of motor neuron vulnerability (Rosen et al., 1993. Most widely used is the SOD1G93A transgenic mouse, whose phenotype recapitulates the clinical and histopathological features of ALS (Gurney et al., 1997; Miana-Mena et al., 2005). The mutants SOD1G93A mouse model expresses higher copy numbers of mutant SOD1 and therefore a more severe disease phenotype with shorter disease duration compared to mutant SOD1G37R (Wong et al., 1995). Transgenic animals with this mutant human SOD1 allele show many features of the human disease, including adult-onset muscle weakness, motor neuron loss, and premature death (Gurney et al., 1994).

Magnetic resonance microscopy (MRM) studies in G93A mice demonstrate widespread neuropathological changes including marked reductions in volumes of spinal grey matter, cortex, substantia nigra, and striatum (Petrik et al., 2007). These findings are comparable to earlier MRM studies in a mouse model of Guamanian ALS-PDC obtained by chronic dietary exposure to cycad flour (Wilson et al., 2004). The main difference between these two disease models is an additional reduction in spinal cord white matter volume in G93A mice that was not detected in the other model. Cycad-fed animals produce significant motor deficits and increased neuroinflammation along with motor neuron death in the spinal cord after 30 days of exposure (Lee et al., 2009). Results from my current study demonstrate similar motor deficits and increased spinal neuroinflammatory response in mutant SOD1G37R mice exposed to synthetic cycad toxin. Furthermore, significant interactions between toxic diet and G37R genotype were oberved under multiple conditions tested.

To further investigate the implication of gene-environment interactions in ALS caused by mutant SOD1, I generated and analysed SOD1G93A mice that received chronic SG exposure. Here, I report that motor neuron degeneration and increased CNS response to synthetic cycad toxins are reproducible and demonstrate predicted outcomes.

Methods

Transgenic SOD1G93A mice were bred from matings of wild type C57BL/6 dams with male heterozygous mice donated from the laboratory of Dr. Neil Cashman. In this complementary study, mutant SOD1G93A mice and wild type littermates were fed a daily diet containing 42 mg of steryl glucoside per kilogram of body weight commencing at 4 weeks of age. Age-matched transgenic animals and wild type littermates not receiving steryl glucoside were used as controls. All groups of animals were monitored for clinical motor deficits with motor behavioural testing as described above in Chapter 3. The 4 week starting point for SG feeding allowed time for sufficient baseline motor behavioural testing after weaning at 3 weeks. The 42 mg/kg body weight dose of SG corresponds approximately to those reported in Tabata et al (2008). It is important to note that the pellet containing steryl glucoside was only a part of the overall diet, with the other part consisiting of regular mouse chow. These control animals were maintained on a regular mouse chow diet of daily proportions equal in weight (and caloric value) to the diet containing toxin. Mice were considered at end stage of the disease when they were severely paralyzed and were unable to right themselves within 30 seconds when placed on their side.

All transgenic and non-transgenic animals were sacrificed at disease end-stage or experimental end stage, as described above. Animals were sacrificed by intracardial perfusion as described above in Chapter 3. The central nervous system (CNS) were dissected out and processed as described above in Chapter 3. To determine disease progression in the mouse central nervous system, immunofluorescence with cell-specific antibodies in conjunction with Hoechst (Sigma; #33258) staining was used. Refer to Table 3-1 and 3-2 for a list the antibodies used in visualizing the CNS and the secondary antibodies. Immunohistochemistry of lumbar spinal sections were performed as described in Chapter 3. In brief, sections were then blocked in PBS containing 1% BSA, 0.1% Triton X-100, 0.05% Tween-20, and 10% normal serum (NGS; Vector Labs, Burlingame, CA #S-1000) and incubated overnight at 4°C with the primary antibody diluted in PBS containing 1% BSA and 0.05% sodium azide. Sections were then rinsed 3 times in PBS and incubated for one hour at room temperature with the appropriate secondary antibody diluted in PBS. Following 3 PBS rinses, sections were stained in 4 μg/ml Hoechst 33258 for 10 minutes, rinsed in PBS, and mounted in 0.2% DABCO-glycerol. In negative controls, the primary antibody was omitted.

Quantification of immunofluorescence was performed as described in Chapter 3 on every tenth transverse section of lumbar cord between L3 and L5. Motor neurons in the ventral horn of lumbar cord were identified as ChAT-positive cells with Hoechst staining. All motor neurons were counted in the ventral horns of every tenth cord section. Astrocytes and microglia in the lumbar cord were identified as GFAP- and Iba1-positive cells with Hoechst staining, respectively. In brief, all astrocytes and microglia were counted as the number of fluorescent pixels in the standardized field of interest. Green or red pixels of GFAP- and Iba-positive cells, respectively, for each group were presented as a percentage of the total pixels, or the percent of fluorescent labelling.

Data are presented as means ± standard error of the means (S.E.M.) as indicated. Statistical significance between groups on rotarod performance, wire hang test, leg extension test, and body weight measures were analyzed using a repeated measures ANOVA via Statistica8.0 statistical software (StatSoft Inc., Tulsa, OK) and graphed using Prism 5 (GraphPad Software Inc., San Diego, CA). All results were analyzed to determine the effect of SG alone, G93A mutation alone, or the interaction between these two variables by ANOVA. Statistical significance between experimental and control groups for all other behavioural and histological assessments were calculated using the Student *t*-test. The *t* test was used when only two groups and one condition were compared, as in the case of the quantitative histological data. Differences were considered statistically significant at $p < 0.05$. P values were expessed as exact values except in cases where $p < 0.0001$.

Results and discussion

Clinical disease develops and progresses in a stereotyped fashion in mice expressing mutant SOD1 G93A. The first obserevable sign of disease is a fine tremor in either one or both hind limbs occurring between 90 to 100 days of age. The appearance of wobbling and instability occurred within one month after the first signs of tremor. The disease progresses to end stage between 120 and 140 days of age, as observed by pronounced proximal muscle weakness, marked hind limb atrophy and paralysis. In addition, end stage mice appeared thin along their flanks and extended their hind limbs either less than normal or pulled in when lifted by the tail.

The major difference between SOD1G93A and SOD1G37R mice is the more profound motor deficit observed in G93A mutants of both sexes in all behavioural tests performed (Figure 1, compare red shapes to blue shapes). This result is consistent with other studies reporting mutant gene dosage-dependent motor phenotypes in mouse models expressing different copy numbers of

mutant SOD1 (Dalcanto et al., 1995; DalCanto et al., 1997). Mutant G93A mice were distinguished as symptomatic upon hind limb trembling and loss of hind limb extension reflex, which occurred simultaneously for males and females (Figure C-1A, E). Deficits in rotarod performance (Figure C-1C, G) and grip endurance (Figure C-1B, F) in male and female G93A mutant mice were observed at much earlier time points than G37R mutants described above. In addition, weight loss in G93A mice was significant with disease progression (Figure C-1D, H).

Exposure to SG in G93A mutants had significant effect on wire hang performance in males and decreases in body weight for females (Table C-1). Significant interactions between SG diet and genotype were observed for the rotarod and wire hang for males, and body weight measurements in females. The clinical phenotype of mutant SOD1 mice with the G93A mutation is already so severe that addition of another exogenous stressor is comparable to the unlikelihood of producing additional modifications in an already saturated system. Toxins in cycad including SG are slow acting and produce a neurodegenerative disease with long latency (Spencer et al., 1991). It is possible that the incubation period in these wild type animals was insufficient given the earlier time at sacrifice in this experiment compared to the wild type mice in the G37R experiment.

Table C-1. Significant main effects of diet and genotype on motor deficits of G93A mice

Effect	Extension Reflex	Rotarod	Wire Hang	Weight
Males				
SG Diet	$p = 0.082$	$p = 0.054$	$p = 0.006$†	$p = 0.16$
G93A Genotype	$p < 0.0001$†	$p < 0.0001$†	$p < 0.0001$†	$p < 0.0001$†
Diet × Genotype	$p = 0.16$	$p = 0.03$†	$p = 0.024$†	$p = 0.45$
Females				
SG Diet	$p = 0.55$	$p = 0.94$	$p = 0.37$	$p < 0.0001$†
G93A Genotype	$p < 0.0001$†	$p < 0.0001$†	$p < 0.0001$†	$p < 0.0001$†
Diet × Genotype	$p = 0.98$	$p = 0.078$	$p = 0.54$	$p < 0.0001$†

†Denotes significance in the corresponding effect

Motor neuron loss in G93A mutant mice revealed one major difference when compared to motor neuron data for G37R mice. Wild type mice of both sexes showed significant motor neuron loss when exposed to SG (Figure C-2), whereas motor neuron loss in the G37R experiment did not reach significance in SG-fed wild type mice. In G93A male mice, significant main effects of diet ($p = 0.018$) and genotype ($p = 0.002$) on motor neuron loss were observed. However, the gene × diet interaction was not significant ($p = 0.082$). Similar data was observed in females; both diet ($p = 0.035$) and genotype ($p < 0.0001$) were influencing factors on motor neuron loss, while gene × diet

interaction was insignificant ($p = 0.064$). Since motor neuron loss occured in all wild type mice fed SG yet did not show significant motor dysfunction on behavioural tests, this finding supports the hypothesis of significant motor neuron loss occurring before an overt clinical phenotype and suggests a threshold of cell death to be reached before observation of ALS symptoms. In addition, SG-fed wild type males showed a higher level of significance than females, indicating a greater effect of SG on males. Wild type mice without SG exposure in the G37R experiment were also much older than those in this experiment, which may explain the discrepancy. Prolonged exposure to SG in G93A males and females did not produce any changes in motor neuron loss compared to control-fed mutants. A lack of SG effect on the G93A mutant background illustrates again the relatively insignificant potency of a stressor in an already saturated system.

As described above in Chapter 3, gliosis in G37R lumbar cords showed a heterogeneous expression of resting morphologies with ramified thin processes and activated morphologies with retracted processes. Treatment of SG in G37R mutants abolished this heterogeneity, and resulted in a uniform expression of the activated morphology. Expression of resting morphologies in astrocytes and microglia is absent in lumbar cords with the G93A mutation, as all GFAP-positive and Iba1-positive cells show the activated phenotype with retracted processes and large cell bodies (Figures C-3 and C-4). It is possible that the lumbar spinal cords expressing the more severe G93A mutation have a more 'toxic' or pathologic cellular environment, triggering earlier activation of glial cells. Furthermore, SG exposure to wild type animals in this G93A study showed a heterogenous morphology in microglia that was absent in SG-fed wild type animals in the G37R mutation study. This finding of heterogeneous microglial morphology in the younger SG-fed wild types of this experiment is in agreement with the hypothesis of an early 'window of opportunity' for SG-mediated neurotoxicity. Exposure to SG during this critical period triggers significant microglial proliferation and activation, which precedes astrocyte activation.

Female mice showed significant main effects of genotype ($p < 0.0001$) on increased astrocytosis, while non-significant effects were observed for diet ($p = 0.28$) and gene × diet interaction ($p = 0.22$). Male mice showed similar data with significant main effects of genotype ($p < 0.0001$) on astrocytosis, diet ($p = 0.53$) and interaction ($p = 0.63$) were not significant. These findings were different from the G37R mouse data, where significant interaction effects were observed for both sexes.

Genotype had a significant effect on increasing microgliosis in G93A females ($p < 0.0001$). However, the effects of diet ($p = 0.44$) were not significant. Interaction between the two factors was also significant ($p = 0.0009$). In males, both diet ($p = 0.041$) and genotype ($p < 0.0001$) had a significant effect on increasing microgliosis while the interaction was not significant ($p = 0.18$).

Figure C-1. Clinical motor phenotype in mutant SOD1G93A mice.

Onset of leg extension deficits distinguished symptomatic mice from presymptomatic G93A mice, and occured simultaneously in male (A) and female (E) mice. Mutant SOD1 males show deficits in grip endurance with SG exposure (B). Wild type male mice show a decline in rotarod performance after continued exposure to SG (C). Significant body weight loss was observed in male (D) and female (H) G93A mice towards end stage disease corresponding to the onset of hind limb paralysis. Neither female wild types nor G93A mutants showed changes in motor deficit following prolonged SG exposure (E-G). The overall effects of SG administration were unremarkable compared to SOD1-mediated deficits.

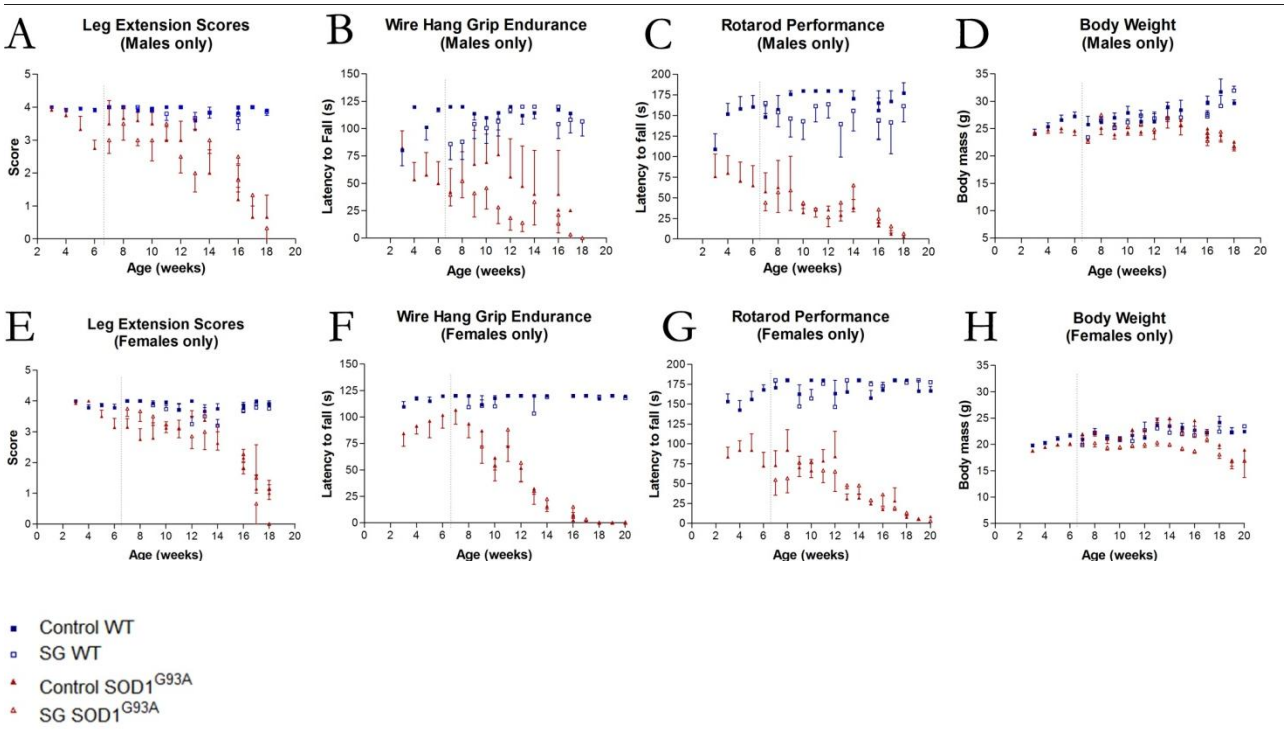

Figure C-2. Spinal motor neuron loss in G93A mice.

Top panels show distribution of ChAT-positive cells in the ventral horn of lumbar cord. Bottom panels show higher magnification of ChAT-positve anterior horn cells between L3 to L5 of spinal cord. Control-fed wild type mice of both sexes showed numerous ChAT-positive cells distributed in the ventral lumbar cord (A, E). Following exposure to SG in wild type animals (B, F), male mice showed a 46% decrease in motor neurons ($p = 0.009$) and females showed a 25% decrease ($p = 0.034$). G93A mice showed a significant motor neron loss (C, G), which was comparable between males and females ($p = 0.004$ and $p < 0.0001$, respectively). SG-mediated motor neuron loss was unremarkable in the presence of the G93A mutation (D, H) for both males ($p = 0.53$) and females ($p = 0.81$). Scale bar 200 μm.

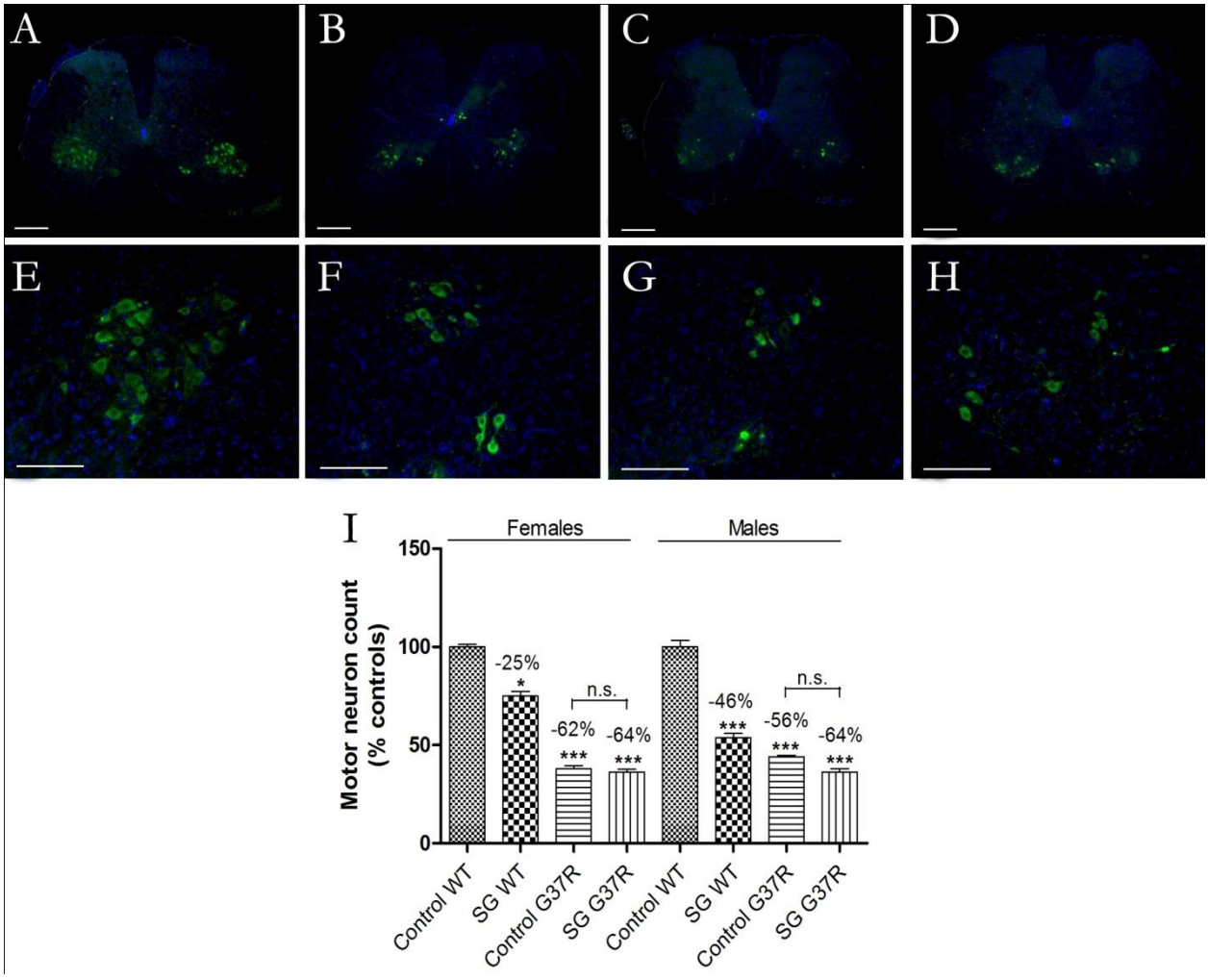

Figure C-3. Astrocytosis in the lumbar cord of G93A mice.

Top panels show distribution of GFAP-positive cells in the lmbar spinal cord. Bottom panels show higher magnification of GFAP-positve cells in the ventral horn of spinal cord between segments L3 to L5. Insets in bottom panels show the representative morphology of GFAP-labeled cell. Control-fed wild type mice show <5% GFAP labelling intensity in the lumbar cord, with astrocytes resembling a resting morphology (A, E, inset). Following exposure to SG in wild type animals (B, F), female mice showed a significant 46% increase in GFAP labelling ($p = 0.05$) and males showed a non-significant 29% increase ($p = 0.56$). Mutant G93A mice showed significant increases in GFAP labelling (C, G), representing a 142% increase in females ($p < 0.0001$) and 255% increase in males ($p < 0.0001$). Changes in astrocyte gliosis were unremarkable following SG exposure in the presence of the G93A mutation (D, H) for both females ($p = 0.92$) and males ($p = 0.34$). Scale bar 200μm in A – D, and 100μm in E – H.

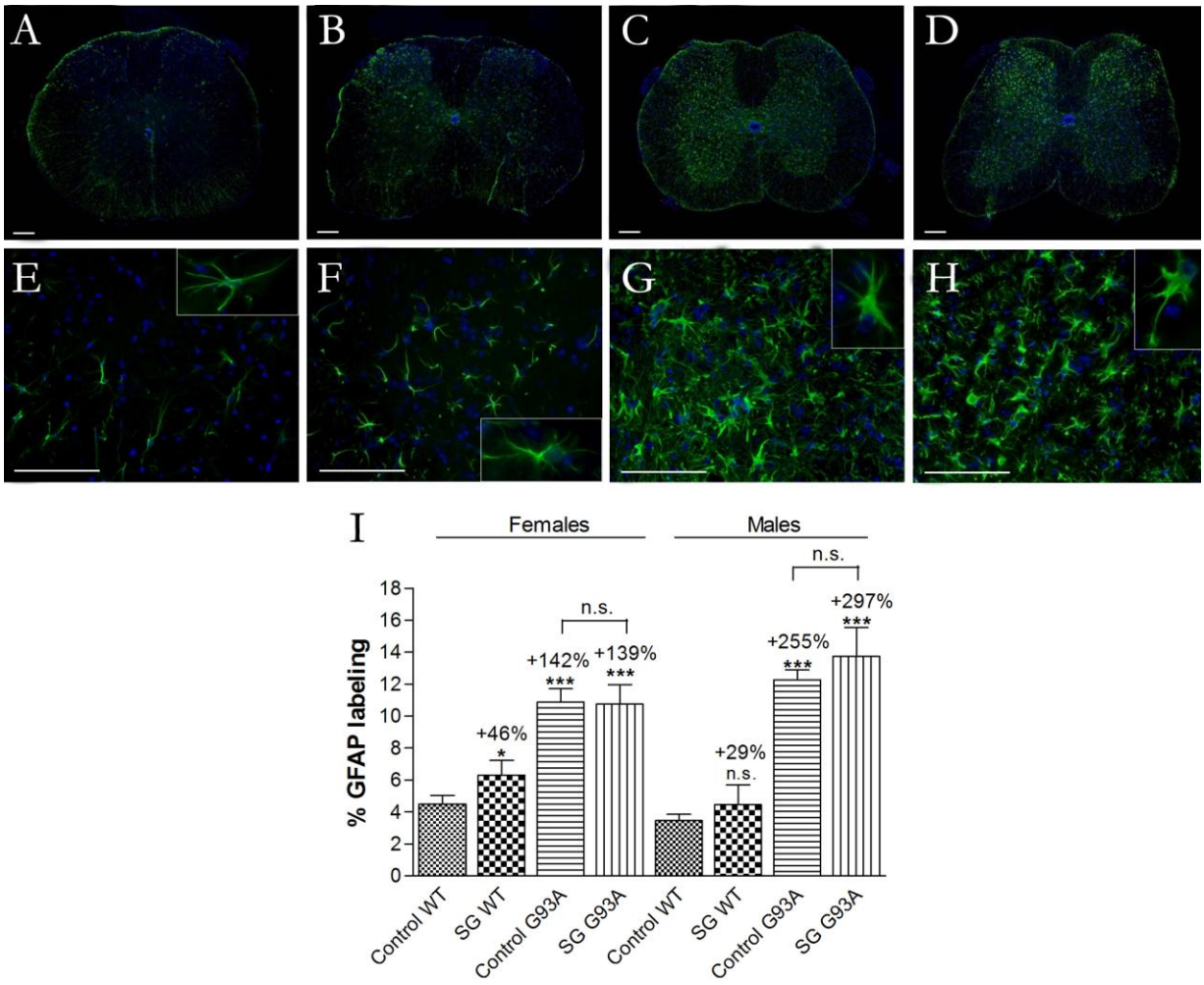

Figure C-4. Microglia activation in the lumbar spinal cord expressing mutant G93A SOD1. Top panels show distribution of Iba1-positive cells in the lmbar spinal cord. Bottom panels show higher magnification of Iba1-positve cells in the ventral horn of spinal cord between segments L3 to L5. Insets in bottom panels show the representative morphology of Iba1-labeled cell. Control-fed wild type mice show <3% Iba1 labelling intensity in the lumbar cord, with microglia resembling a resting morphology (A, E, inset). Following exposure to SG in wild type animals (B, F), female mice showed a significant 144% increase in Iba1 labelling ($p = 0.036$) and males showed a non-significant 33% increase ($p = 0.46$). Mutant G93A mice showed significant increases in Iba1 labelling (C, G), representing a 434% increase in females ($p < 0.0001$) and 194% increase in males ($p = 0.016$). Changes in microgliosis were unremarkable following SG exposure in the presence of the G93A mutation (D, H) in female and male mice ($p = 0.077$ and 0.09, respectively). Scale bar 200 μm in A – D, and 100μm in E – H.